



Provided by the author(s) and University of Galway in accordance with publisher policies. Please cite the published version when available.

Title	The use of supported photomediators in the generation of carbon radicals for synthetic purposes
Author(s)	Lohan, Mary Treasa
Publication Date	2012-11-05
Item record	http://hdl.handle.net/10379/3280

Downloaded 2024-05-06T15:43:31Z

Some rights reserved. For more information, please see the item record link above.





**The use of supported photomediators
in the generation of carbon radicals
for synthetic purposes**

Mary Treasa Lohan, B.Sc (Hons.)

**Presented for the degree of Ph.D. at the
National University of Ireland, Galway**

**School of Chemistry,
National University of Ireland, Galway**

November 2012

Supervisor: Dr. Niall W.A. Geraghty

Head of School: Prof. Paul V. Murphy

Table of Contents	i
Acknowledgements	viii
Abstract	ix
Abbreviations	x

Chapter 1 Introduction

1.0 Introduction	2
1.1 Carbon radicals	2
1.1.1 Introduction.....	2
1.1.2 Carbon radicals	2
1.1.3 Forming radicals	3
1.1.4 Factors affecting the stability of C-radicals.....	6
1.2 Polarity of radicals	7
1.3 Hydrogen abstraction as a route to carbon radicals	9
1.3.1 Thermal hydrogen abstraction	9
1.3.2 Photochemical hydrogen abstraction.....	11
1.4 Basic organic photochemistry	14
1.4.1 Photochemical and photophysical processes: the Jablonski Diagram.....	14
1.4.2 Photosensitisation	16
1.4.3 Photochemistry of the carbonyl group.....	18
1.5 Factors affecting hydrogen abstraction from CH bonds	24
1.5.1 Bond dissociation energy (BDE).....	24
1.5.2 Hydrogen donors	24
1.5.3 Stereoelectronic effects.....	28
1.5.4 The nature and energy of the photomediator's triplet state	29
1.6 General reaction mechanism	29
1.7 Other photocatalysts	32

1.8	The photochemical addition reactions of H-donors to unsaturated systems.....	33
1.8.1	The photochemical addition reactions of cycloalkanes.....	33
1.8.2	The photochemical addition reactions of cyclic ethers	41
1.8.3	The photochemical addition reactions of 1,3-dioxolanes.....	46
1.8.4	The photochemical addition reactions of alcohols	53
1.9	Supported catalysts.....	58
1.10	Molecular modelling.....	62
1.10.1	Introduction	62
1.10.2	Molecular mechanics.....	63
1.10.3	Conformational searching.....	66
1.10.4	Quantum mechanics	68
1.11	Aims of this project.....	72
 Chapter 2 Results and Discussion		
2.0	Results and discussion	74
2.1	Preparation of supported photomediators	74
2.1.1	Synthesis of 3-aminopropyl silica bound benzophenone SP1.....	74
2.1.2	Synthesis of propyl linked 4-hydroxybenzophenone silica SP2	75
2.1.3	Synthesis of the silica supported C-5 quaternary ammonium salt SP3 ...	79
2.1.4	Synthesis of silica supported C-8 quaternary ammonium salt SP4.....	83
2.1.5	Synthesis of silica supported C-12 quaternary ammonium salt SP5.....	86
2.2	Photochemical reactions using 3-aminopropyl silica bound benzophenone SP1.....	88
2.2.1	Reactions with the monosubstituted alkyne methyl propiolate using SP1	88
2.2.2	Reaction with a larger quantity of methyl propiolate using SP1	102
2.2.3	Reactions with the disubstituted alkyne DMAD using SP1	103

2.3	Photochemical reactions using propyl linked 4-hydroxybenzophenone silica SP2.....	113
2.3.1	Reactions with the monosubstituted alkyne methyl propiolate using SP2	113
2.3.2	Reactions with the disubstituted alkyne DMAD using SP2	119
2.4	Photochemical reactions using silica supported C-5 quaternary ammonium salt SP3.....	123
2.4.1	Reactions with the monosubstituted alkyne methyl propiolate using SP3	123
2.4.2	Reactions carried out using larger quantities of SP3	130
2.4.3	Reaction carried out using a smaller quantity of SP3	133
2.4.4	Reactions with the disubstituted alkyne DMAD using SP3	134
2.4.5	Reactions with monosubstituted alkenes using SP3	137
2.4.6	Reactions with disubstituted alkenes using SP3	140
2.5	Synthesis of methyl (2E)-2-[(benzyloxy)imino]propanoate.....	144
2.5.1	Synthesis of methyl (2Z)-2-(hydroxyimino)propanoate	144
2.5.2	Synthesis of methyl (2E)-2-[(benzyloxy)imino]propanoate.....	145
2.6	Photochemical reactions of methyl (2E)-2-[(benzyloxy)imino]propanoate using SP3	146
2.6.1	Photochemical reaction of benzylated oxime with 2-propanol	146
2.6.2	Photochemical reaction of benzylated oxime with THF	147
2.6.3	Photochemical reaction of benzylated oxime with 1,3-dioxolane.....	149
2.7	Photochemical reactions using silica supported C-8 quaternary ammonium salt SP4.....	150
2.7.1	Reactions with the monosubstituted alkyne methyl propiolate using SP4	150
2.7.2	Reaction with the disubstituted alkyne DMAD using SP4.....	152
2.8	Photochemical reactions using silica supported C-12 quaternary ammonium salt SP5.....	153

2.8.1	Reactions with monosubstituted alkyne methyl propiolate using SP5..	153
2.8.2	Reaction with the disubstituted alkene maleic acid using SP5.....	154
2.8.3	Reaction with methyl (2 <i>E</i>)-2-[(benzyloxy)imino]propanoate using SP5....	155
2.9	Recycling of supported photomediators	156
2.9.1	Photochemical reaction of methyl propiolate and 2-propanol using SP1 ...	156
2.9.2	Photochemical reaction of methyl propiolate and 2-propanol using SP3 ...	158
2.9.3	Photochemical reaction of methyl propiolate and 2-propanol using SP5 ...	160
2.10	Optimisation of the methyl propiolate/2-propanol reaction using SP3 .	162
2.10.1	Effect of varying the quantity of photomediator	162
2.10.2	Effect of varying the quantity of solvent.....	163
2.10.3	Effect of varying the quantity of alkyne.....	164
2.10.4	Effect of varying the quantity of H-donor.....	165
2.11	Optimisation of the methyl propiolate/THF reaction using SP3.....	166
2.11.1	Effect of varying the quantity of photomediator	166
2.11.2	Effect of varying the quantity of solvent.....	167
2.11.3	Effect of varying the quantity of photomediator using a very large excess of THF	167
2.12	Molecular modelling	169
2.12.1	Introduction	169
2.12.2	Conformational search results	171
2.13	Discussion.....	190
2.13.1	Reactivity of hydrogen donors	190
2.13.2	Reactivity of the unsaturated substrates	194
2.13.3	Reactivity of the supported photomediators.....	194

2.13.4	Stability of the supported photomediators	196
2.13.5	Summary of the reactivity of the supported photomediators.....	199
2.13.6	Rationalising the order of reactivity of the supported photomediators using molecular modelling.....	199
2.13.7	Synthetic potential of the supported photomediators	203
2.13.8	Reaction optimisation	203
2.14	Future work.....	204

Chapter 3 Experimental

3.0	Experimental	207
3.1	Preparation of supported photomediators	207
3.1.1	Synthesis of 3-aminopropyl silica bound benzophenone SP1	207
3.1.2	Synthesis of propyl linked 4-hydroxybenzophenone silica SP2.....	208
3.1.3	Synthesis of the silica supported C-5 quaternary ammonium salt SP3 ..	210
3.1.4	Synthesis of silica supported C-8 quaternary ammonium salt SP4	213
3.1.5	Synthesis of silica supported C-12 quaternary ammonium salt SP5	215
3.2	Photochemical reactions using 3-aminopropyl silica bound benzophenone SP1	217
3.2.1	Reactions with the monosubstituted alkyne methyl propiolate using SP1	217
3.2.2	Reaction with a larger quantity of methyl propiolate using SP1	223
3.2.3	Reactions with the disubstituted alkyne DMAD using SP1	223
3.3	Photochemical reactions using propyl linked 4-hydroxybenzophenone silica SP2.....	229
3.3.1	Reactions with the monosubstituted alkyne methyl propiolate using SP2	229
3.3.2	Reactions with the disubstituted alkyne DMAD using SP2	231
3.4	Photochemical reactions using silica supported C-5 quaternary ammonium salt SP3.....	233

3.4.1	Reactions with the monosubstituted alkyne methyl propiolate using SP3 ..	233
3.4.2	Reactions carried out using larger quantities of SP3	235
3.4.3	Reaction carried out using a smaller quantity of SP3	236
3.4.4	Reactions with the disubstituted alkyne DMAD using SP3	237
3.4.5	Reactions with monosubstituted alkenes using SP3	239
3.4.6	Reactions with disubstituted alkenes using SP3	240
3.5	Synthesis of methyl (2E)-2-[(benzyloxy)imino]propanoate.....	243
3.5.1	Synthesis of methyl (2Z)-2-(hydroxyimino)propanoate.....	243
3.5.2	Synthesis of methyl (2E)-2-[(benzyloxy)imino]propanoate.....	243
3.6	Photochemical reactions of methyl (2E)-2-[(benzyloxy)imino]propanoate using SP3	244
3.6.1	Photochemical reaction of benzylated oxime with 2-propanol	244
3.6.2	Photochemical reaction of the benzylated oxime with THF	245
3.6.3	Photochemical reaction of the benzylated oxime with 1,3-dioxolane... 246	
3.7	Photochemical reactions using silica supported C-8 quaternary ammonium salt SP4	247
3.7.1	Reactions with the monosubstituted alkyne methyl propiolate using SP4 ..	247
3.7.2	Reaction with the disubstituted alkyne DMAD using SP4.....	248
3.8	Photochemical reactions using silica supported C-12 quaternary ammonium salt SP5	249
3.8.1	Reactions with monosubstituted alkyne methyl propiolate using SP5..	249
3.8.2	Reactions with the disubstituted alkene maleic acid using SP5	250
3.8.3	Reaction with methyl (2E)-2[(benzyloxy)imino]propanoate using SP5	250
3.9	Recycling of supported photomediators	251
3.9.1	Photochemical reaction of methyl propiolate with 2-propanol using SP1 ..	251

3.9.2	Photochemical reaction of methyl propiolate with 2-propanol using SP3 ..	252
3.9.3	Photochemical reaction of methyl propiolate with 2-propanol using SP5 ..	253
3.10	Optimisation of the methyl propiolate/2-propanol reaction using SP3..	254
3.10.1	Effect of varying the quantity of photomediator	254
3.10.2	Effect of varying the quantity of solvent	256
3.10.3	Effect of varying the amount of alkyne	258
3.10.4	Effect of varying the amount of H-donor	259
3.11	Optimisation of the methyl propiolate/THF reaction using SP3	260
3.11.1	Effect of varying the quantity of photomediator	260
3.11.2	Effect of varying the quantity of solvent	261
3.11.3	Effect of varying the quantity of photomediator using a very large excess of THF.....	262
3.12	Photochemical reactions using benzophenone	264
3.12.1	Photochemical reaction of methyl propiolate with 2-propanol	264
3.12.2	Photochemical reaction of methyl propiolate with THF	264
3.12.3	Photochemical reaction of DMAD with 2-propanol.....	264
3.13	Conformational searching.....	265
	Bibliography.....	276
	Presentations and Publications.....	a

Acknowledgements

Abstract

Carbon-carbon bond formation is a key step in synthetic organic chemistry and there are many methods available for carrying it out, a number of which involve the use of carbon radicals. Many methods however involve the use of tin compounds and/or radical initiators such as peroxides or azo compounds and as a result are unattractive. An alternative approach, described in this thesis, involves the photochemical generation of carbon radicals using a photomediator such as an aromatic ketone, for example, benzophenone. While this method is very useful, it is hampered by the need to remove benzophenone, and/or benzpinacol, the result of ketyl radical dimerisation, from the reaction product and this requires column chromatography.

It was in light of these drawbacks that silica supported photomediators were considered for this work. It was anticipated that silica supported photomediators would be easily removed from the reaction by simple filtration. This would not only allow the rapid isolation of products without the need for column chromatography, but would also allow the photomediator to be easily recovered allowing for its possible recycling. It was envisioned that ketyl radical dimerisation might be less of a problem with supported photomediators as recombination should be less efficient for surface bound radicals.

Five supported photomediators were prepared *via* either covalent or electrostatic bonding of the photomediator to the surface. Carbon-carbon bond forming reactions involving a series of hydrogen donors, 2-propanol, cyclopentanol, 1,3-dioxolane, cyclopentane and THF, and a range of electron deficient unsaturated systems were carried out. The electrostatically bonded photomediators were more efficient than the covalently bonded photomediators. THF was the most reactive hydrogen donor while in general cyclopentane was the most unreactive hydrogen donor. Optimisations studies revealed that the amount of photomediator could be significantly reduced while the recycling studies indicated that the supported photomediators could be recycled a number of times before a decrease in reactivity was observed. A computational model of the silica linked photomediators was developed and used to explore the relationship between the reactivity and structure of the supported photomediators.

Abbreviations

AIBN	2,2-Azobisisobutyronitrile
AQ	Anthraquinone
aq.	Aqueous
Ar	Aromatic
BPSS	Benzophenone disodium disulfonate
Bn	Benzyl group (C ₆ H ₅ CH ₂)
Bp	Boiling point
BDE	Bond dissociation energy
CDMS	Chlorodimethylsilane
CPK	Corey Pauling Koltun
<i>J</i>	Coupling constant in NMR
DCM	Dichloromethane
°C	Degree Celsius
DFT	Density functional theory
DEPT	Distortionless enhancement by polarization transfer
DMAD	Dimethyl acetylenedicarboxylate
d	Doublet
dd	Double doublet
EDG	Electron donating group
<i>E</i>	Entgegen (<i>trans</i>)
eq.	Equivalent
EWG	Electron withdrawing group
GC	Gas chromatography

<i>Gem</i>	Geminal
<i>g</i>	Gram
HF	Hartree-Fock
Hz	Hertz
HOMO	Highest occupied molecular orbital
HRMS	High resolution mass spectrometry
h	Hour
IR	Infra-Red
IC	Internal conversion
ISC	Intersystem crossing
lit.	Literature
L	Litre
<i>LR</i>	Long range
LUMO	Lowest unoccupied molecular orbital
MHz	Megahertz
MP	Methyl propiolate
mp	Melting point
Me	Methyl group (CH ₃)
mg	Milligram
mL	Millilitre
min	Minute
mol	Mole
mol %	Mole percent
MM	Molecular mechanics

MP	Møller-Plesset
m	Multiplet
nm	Nanometre
NBS	<i>N</i> -Bromosuccinimide
NMR	Nuclear magnetic resonance
<i>p</i>	Para
ppm	Parts per million
QM	Quantum mechanics
q	Quartet
rt	Room temperature
SE	Semi-empirical
s	Singlet
SOMO	Singly occupied molecular orbital
SP	Supported photomediator
TBADT	Tetrabutylammonium decatungstate
THF	Tetrahydrofuran
THP	Tetrahydropyran
t	Triplet
UV	Ultraviolet
VDW	Van der Waal
VR	Vibrational relaxation
<i>Vic</i>	Vicinal
Z	Zusammen (<i>cis</i>)

Chapter 1

Introduction

1.0 Introduction

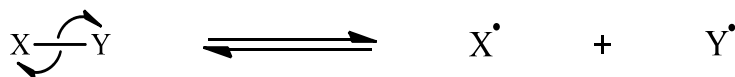
1.1 Carbon radicals

1.1.1 Introduction

The formation of carbon-carbon bonds is at the forefront of synthetic organic chemistry and this is evident looking at the vast number of methods available to carry out this process¹, most of which are ionic. The Friedel-Crafts alkylation, for example utilises a carbocation, generated from the reaction of a Lewis acid and an alkyl halide, which undergoes nucleophilic attack by an aromatic hydrocarbon, such as benzene, to generate a new carbon-carbon bond. The Michael reaction, another ionic reaction, involves attack by a carbon nucleophile on an α,β -unsaturated carbonyl compound forming a new carbon-carbon bond. Over the last number of decades, another important method that has emerged for forming such bonds involves the use of carbon radicals^{2,3}.

1.1.2 Carbon radicals

A radical is any atom or neutral molecule that contains one or more unpaired electrons⁴. Formed by homolytic cleavage of a chemical bond which leaves each new fragment with an unpaired electron, radicals are neutral reactive species (**Scheme 1**).



Scheme 1

Carbon radicals may be planar, as is the case with the corresponding carbocations, in which the carbon atom is sp^2 hybridised and the unpaired electron is in a p orbital perpendicular to the plane of the sp^2 orbital. They may also be pyramidal, the carbon atom being sp^3 hybridised with rapid interconversion of the two configurations of the pyramidal radical. Chemical methods of determining the structure of a carbon radical

normally involve the generation of a radical at an asymmetric centre and the observation of whether or not racemisation occurs; retention or inversion would argue for a pyramidal radical, whereas racemisation would indicate a planar, or a rapidly interconverting pyramidal radical⁵.

1.1.3 Forming radicals

Radicals can be formed by two general methods, fission of a single bond or single electron transfer reactions. The energy needed to homolytically cleave a bond can be provided in the form of heat or UV light, in processes termed thermolysis and photolysis, respectively.

1.1.3.1 Electron transfer reactions

Ashby defined a single electron transfer reaction as one that is initiated by a single electron transfer from a nucleophile to a substrate producing a radical intermediate⁶. Electron transfer, by definition, involves oxidation and reduction. Starting from a neutral molecule, upon adding or removing a single electron, we can produce a radical anion or radical cation, respectively. In the case of the radical cation, a weak bond results due to an electron being removed from the bonding orbital, and so fragmentation to a radical and a cation occurs readily. For the radical anion an extra electron is present in the anti-bonding orbital which again weakens the bond leading to homolytic cleavage (**Figure 1**).

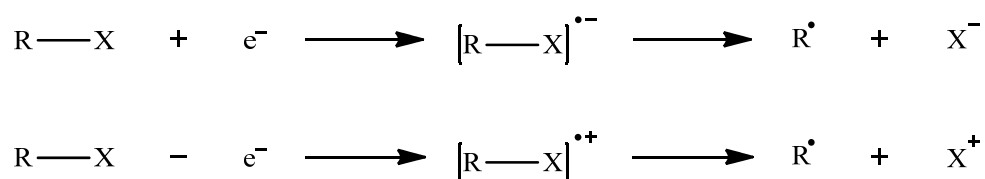


Figure 1

Charged molecules, cations and anions, can also gain or lose a single electron to form a radical species, the process being mediated by either an oxidising or a reducing agent, such as a metal ion, that changes its oxidation number by one (Figure 2).

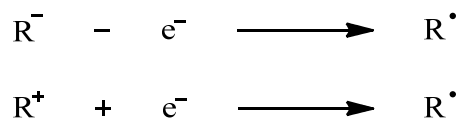
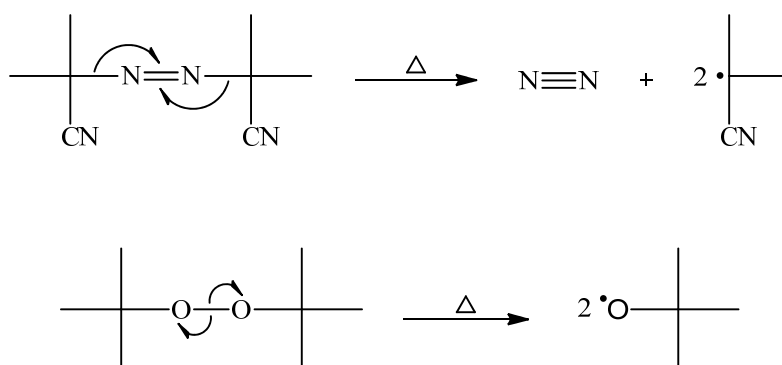


Figure 2

1.1.3.2 Thermolysis

Molecules have several vibrational energy levels and at low temperatures, most molecules occupy the lowest level. Heating a molecule increases the vibrational energy of the molecule which can be lost by collision, or fragmentation, that is homolysis of one or more bonds. Thermolysis can require temperatures as high as 800-1000 °C but thermolysis at lower temperatures (~150 °C) is possible for molecules with low bond dissociation energies (BDEs), the energy required to cleave a bond homolytically. The BDE associated with CH bonds is so large⁷, ~ 435 kJ mol⁻¹ that direct homolysis of the bond is unusual. However, certain bonds are particularly weak and so molecules with such bonds can serve as radical initiators. Azo compounds and peroxides have low BDEs and are thus used (in small quantities) to generate radicals *via* homolysis of a weak C-N or O-O bond, respectively (Scheme 2), and these can then go on to propagate a reaction.



Scheme 2

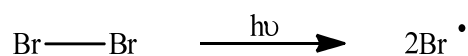
1.1.3.3 Photolysis

Photolysis uses UV light from a UV lamp, or sunlight, as a source of energy to bring about homolytic cleavage of a bond. The relationship between the wavelength of light and the energy is given by the Planck equation (**Equation 1**), where h is Planck's constant, c is the speed of light and λ is the wavelength of light measured in nanometres (nm).

$$E = hc / \lambda$$

Equation 1

Photolysis is a mild method of homolysis as high energy UV light allows the cleavage of strong bonds, which if carried out using thermolysis would require extreme temperatures. Light of 300-600 nm supplies energy of 400-200 kJ mol⁻¹ which covers the range of normal covalent BDEs. The irradiation of a molecule of bromine (BDE 192 kJ mol⁻¹) with UV light, for example, produces two bromine radicals (atoms) *via* homolysis (**Scheme 3**).



Scheme 3

An advantage of photolysis is that it can be considered to be a “clean” method of generating radicals as it avoids the use of hazardous and toxic materials, and does not leave a residue. Photolysis can also be carried out indirectly using an aromatic ketone, which can be excited by UV light to a triplet state that abstracts a hydrogen atom from a relatively weak CH bond, thus producing a carbon radical. This is the principle that underlines the work described in this thesis; it is discussed in greater detail below (**Section 1.4.3**). The photochemical intermolecular abstraction of hydrogen from CH bonds is an efficient method of generating carbon radicals that are indistinguishable from carbon radicals generated in any other way, for example using initiators. Structural factors as well as energy factors control the efficiency of hydrogen abstraction from CH bonds^{8,9} (**Sections 1.1.4 and 1.5**). In the main, once produced, radicals will react to give a more stable radical or a non-radical product.

1.1.4 Factors affecting the stability of C-radicals

A number of factors affect the stability of a radical and therefore determine the ease with which it is formed and its subsequent reactivity.

1.1.4.1 Hyperconjugation

A general stability order for radicals exists (**Figure 3**) and can be rationalised on the basis of hyperconjugation:

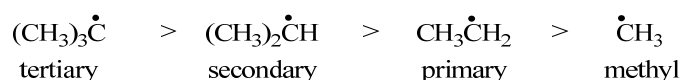
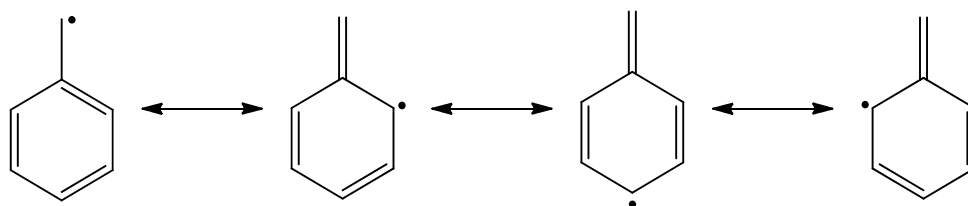


Figure 3

The singly occupied $2p$ orbital interacts with the σ and σ^* orbitals of the alkyl group next to the radical centre, the overall result being energetically favourable. When two or three alkyl groups are present, the effect is enhanced, thus accounting for the observed stability order¹⁰.

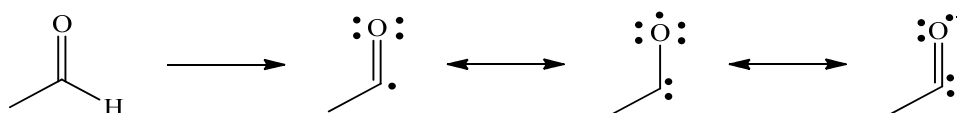
1.1.4.2 Delocalisation

When radicals are conjugated with unsaturated systems, their stability is increased. This is as a result of the delocalisation of the radical into the π system, as is the case for allylic and benzylic radicals¹¹ (**Scheme 4**). It is important to realise that, as always, an increase in stability results in a reduction in reactivity.



Scheme 4

It is also possible to have conjugation with a lone pair of a heteroatom, for example in an acyl radical, in which the carbon gains a formal negative charge, thus accounting for its reactivity (**Scheme 5**).



Scheme 5

1.1.4.3 Kinetic stability

The presence of bulky R groups can make normally reactive radicals unreactive. This is because the steric hindrance provided by the R groups prevents substrates from reaching the radical centre; such radicals are therefore kinetically stable, and are termed “persistent”. The persistent 2,4,6-tri-*tert*-butylphenyl radical (**1**) has a half-life of 0.1 s, for example, while the tris(trimethylsilyl)methyl radical (**2**) has a half-life of 200 s (**Figure 4**). The nitroxyl radical TEMPO, (2,2,6,6-Tetramethylpiperidin-1-yl)oxyl, is an example of a particularly long-lived radical.

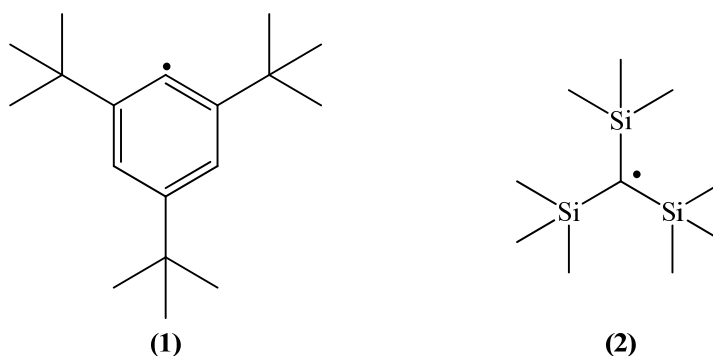
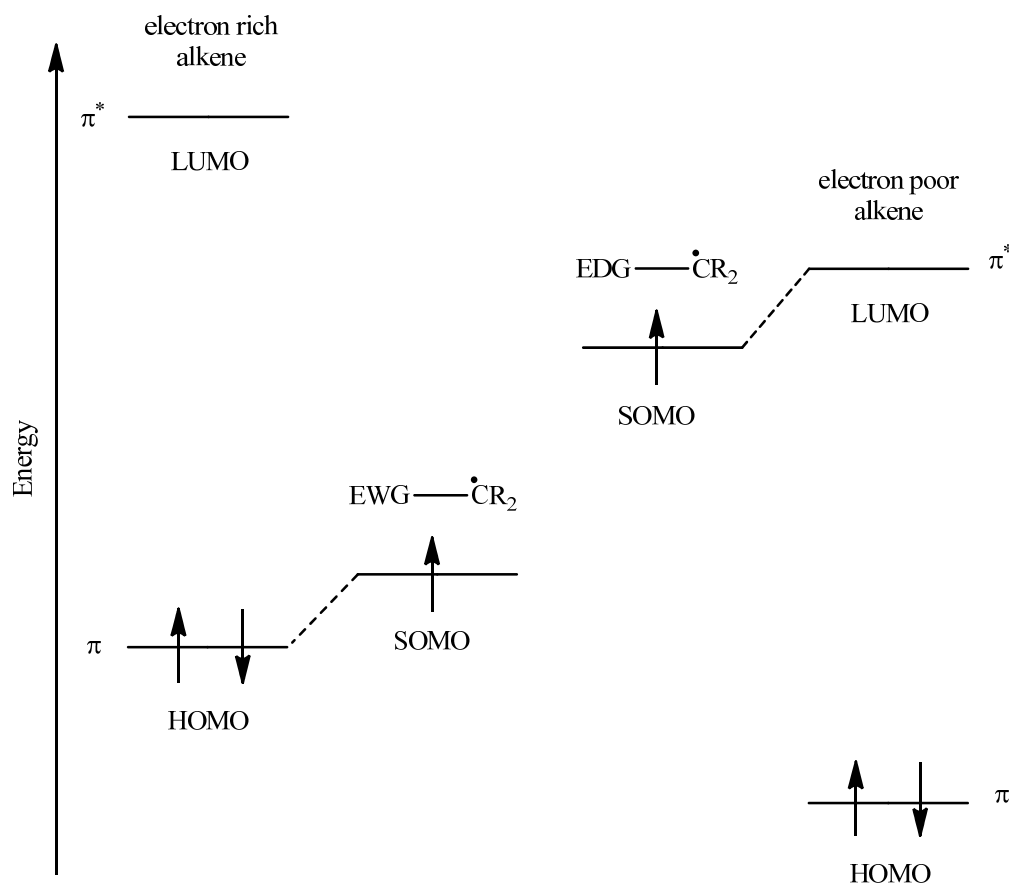


Figure 4

1.2 Polarity of radicals

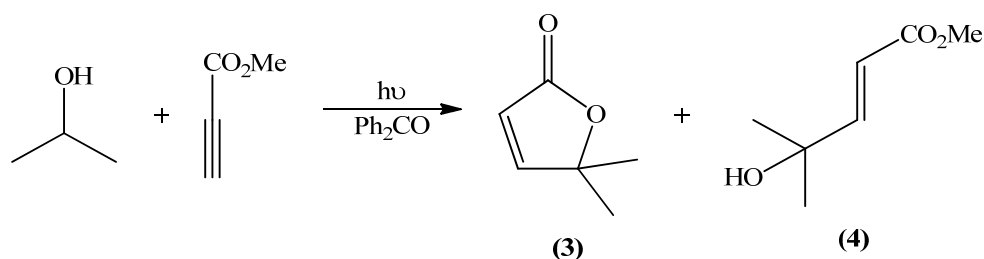
The presence of electron donating groups (EDGs) such as alkyl, amine or alcohol groups, or electron withdrawing groups (EWGs) such as carbonyl or nitrile groups, on the radical centre leads to the radical behaving as a nucleophilic or electrophilic species, respectively¹. An α -hydroxyalkyl radical is thus nucleophilic and readily reacts with electron deficient alkenes and alkynes¹². An EDG attached to a radical raises the energy of the singly occupied molecular orbital (SOMO), allowing for good interaction with the lowest unoccupied molecular orbital (LUMO) of an electron deficient alkene (**Scheme 6**). The radical is thus more likely to donate an electron than accept one, and is nucleophilic in nature. Conversely, the SOMO of a

radical attached to an EWG such as a carbonyl group, is lowered in energy, allowing for better interaction with the highest occupied molecular orbital (HOMO) of an electron rich alkene (**Scheme 6**)¹. In other words, this radical is more likely to accept an electron than to donate one, making it electrophilic.



Scheme 6

The work described in this thesis is based on the reactions of H-donor molecules such as alkanes, ethers, secondary alcohols and dioxolanes which undergo hydrogen abstraction to give nucleophilic radicals that readily attack an alkene, alkyne or C=N system which is attached to an EWG.



Scheme 7

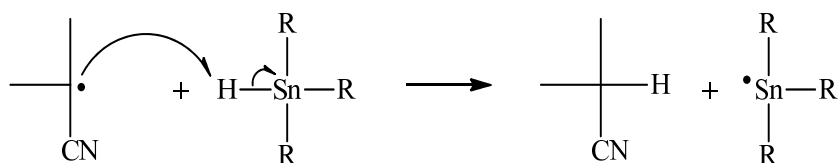
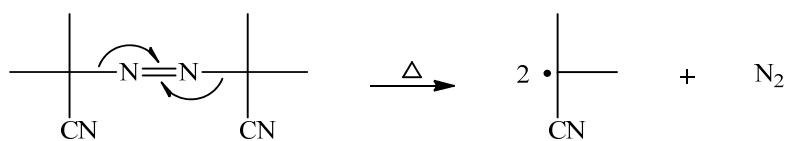
Thus the regioselective addition of an α -hydroxyalkyl radical, derived from 2-propanol, to the electron deficient β -carbon of the alkyne methyl propiolate, affords the two products (3) and (4) (Scheme 7)¹², and is an example of how polarity effects can control the outcome of a radical reaction.

1.3 Hydrogen abstraction as a route to carbon radicals

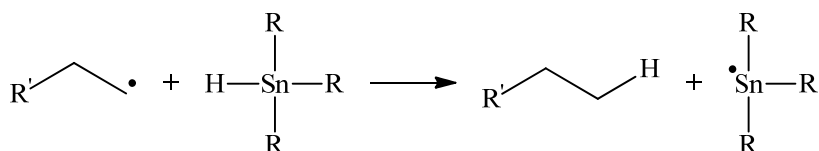
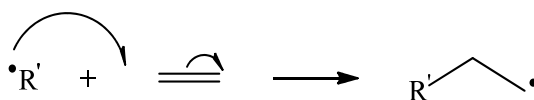
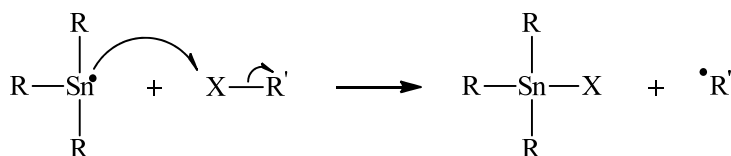
1.3.1 Thermal hydrogen abstraction

Radical reactions often occur *via* a radical chain mechanism and involve the use of an initiator as mentioned previously (Section 1.1.3.2). The first step is initiation and involves the homolytic cleavage of, for example, the C-N bonds of azobisisobutyronitrile (AIBN) with the formation of two 2-cyanopropyl radicals, and a highly stable molecule of nitrogen which provides the driving force for the reaction (Scheme 8)^{13,14}. The 2-cyanopropyl radical then abstracts a hydrogen atom from a tri-substituted tin hydride forming a tin radical, which goes on in turn to abstract a halogen from a haloalkane forming the carbon radical. Normally this radical will then react in a planned way with another reactant molecule; if not, it undergoes recombination. Overall the driving force is the formation of a tin-halogen bond, which is stronger than a tin hydride bond and is thus thermodynamically favoured.

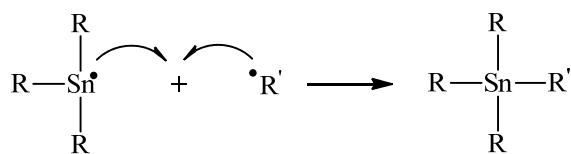
Initiation



Propagation



Termination



Scheme 8

While this type of hydrogen abstraction reaction is a well-established and useful synthetic procedure^{15,16}, there are some drawbacks. The use of tin hydrides, for example, is unattractive due to the disposal problems posed by the tin halides formed from them. The use of initiators such as peroxides in related processes is also undesirable due to the explosive properties of peroxides in general. An alternative

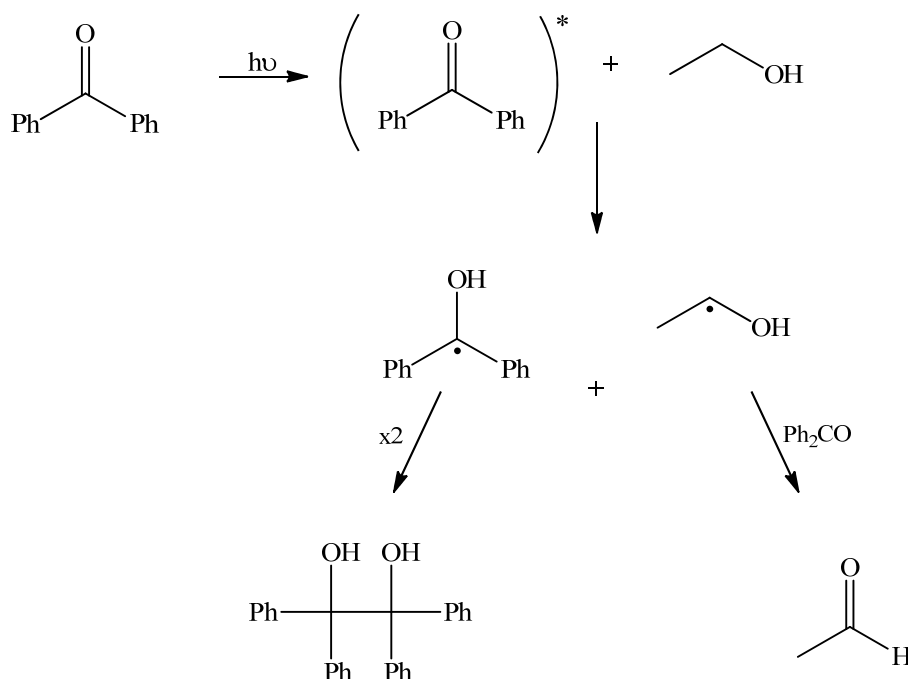
approach is the use of UV irradiation as the source of energy to promote hydrogen abstraction.

1.3.2 Photochemical hydrogen abstraction

A photochemically promoted reaction is activated by a photon of light, which is absorbed and leaves no residue, whereas catalytic methods, and those involving the use of initiators, often require the removal of reagent residues after the reaction. Photochemical reactions usually offer mild reaction conditions, while also having the advantage of high atom economy whereby all of the atoms in the reactants end up in the product. Traditional thermal methods often have a poor atom economy and may require harsh conditions¹⁷. It is also worth noting that H-abstraction techniques, both thermal and photochemical, allow molecules such as cycloalkanes and cyclic ethers, generally thought of as unreactive molecules and usually used as solvents, to act as H-donors facilitating their functionalisation¹⁸⁻²¹. Such a transformation is a rare achievement in ionic chemistry.

During a photochemical reaction, molecules may undergo chemistry which is distinct from their usual ground state behaviour, a feature that is often due to the involvement of radicals rather than ions. Take for example, 2-propanol: in a typical thermal ionic reaction, the hydrogen atom of the O-H bond is removed leaving an anion localised on the oxygen atom. However using radical chemistry, it is the methine hydrogen which is removed generating a tertiary carbon radical, as the BDE of the CH bond ($396.7 \pm 4.2 \text{ kJ mol}^{-1}$) is lower than that of the O-H bond ($438.1 \pm 4.2 \text{ kJ mol}^{-1}$)²².

Photochemical hydrogen abstraction often involves the use of an aromatic ketone such as benzophenone, the photoreduction of which in ethanol (**Scheme 9**) was first observed by Ciamician and Silber in 1900²³. It is now known that this involves photochemical hydrogen abstraction by the aromatic ketone in an ($n-\pi^*$) state.



Scheme 9

Upon irradiation with UV light, benzophenone absorbs a photon of light and is excited to a singlet excited state. From here a number of photophysical processes can occur which are best described using a Jablonski Diagram (**Section 1.4, Figure 5**). One possibility is that the ketone can end up in a triplet ($n-\pi^*$) state.

Photochemically, the ($n-\pi^*$) triplet state ketone can behave as an alkoxy radical and abstract a hydrogen atom from an appropriate molecule, usually the solvent which in this case (**Scheme 9**) is ethanol. This generates a carbon radical. The principle underpinning the work described in this thesis is that the carbon radical can be trapped using an electron deficient unsaturated system, forming a carbon-carbon bond. The key hydrogen abstraction step in these processes usually involves an agent specifically added for the purpose. As described above (**Scheme 9**), this is usually an aromatic ketone such as benzophenone. This agent has been variously described as a photosensitiser, a photomediator and a photocatalyst, and recently Albinì and Fagnoni published a comprehensive review entitled '*Photocatalysis for the formation of C-C bonds*', in which the use of the above terms is discussed¹⁷.

In the present work, the preferred term used to describe the role of benzophenone is a photomediator. Photosensitiser is unsuitable as photosensitisation does not occur. In addition, benzophenone cannot accurately be described as a photocatalyst as in most cases, it is used in quantities which are in excess of what could be described as catalytic. Thus, benzophenone is best described as a photomediator for the present work.

1.4 Basic organic photochemistry

1.4.1 Photochemical and photophysical processes: the Jablonski Diagram

Organic molecules in the ground state use their electrons, in pairs, to occupy the lowest energy orbitals available. Upon absorption of a photon of light, organic molecules enter an electronically excited state. The photochemical and photophysical processes that can occur subsequently are best described using a Jablonski Diagram (Figure 5).

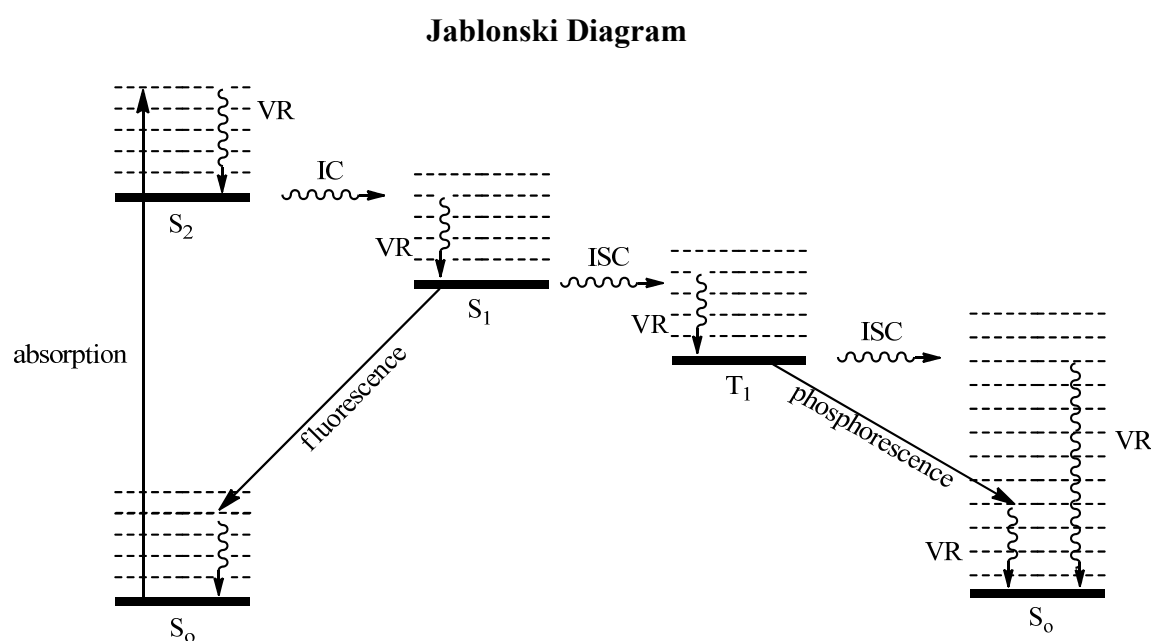


Figure 5

The main processes involved can be divided into radiative energy transfer processes (absorption, fluorescence and phosphorescence) and radiationless energy transfer processes (vibrational relaxation (VR), internal conversion (IC) and intersystem crossing (ISC)).

A molecule of, for example benzophenone, initially absorbs a photon of light and is excited from the ground state (S_0) to an upper vibrational level of an electronically excited singlet state, e.g. S_2 . This process is allowed as the multiplicity of the molecule remains unchanged and so is very rapid ($k = 10^{18} \text{ s}^{-1}$).

VR rapidly ($\sim 10^{13} \text{ s}^{-1}$) dissipates the excess vibrational energy of the excited molecule which drops to the lowest vibrational energy level of S_2 .

It can then undergo IC which is the transition of an electronically excited molecule to a lower electronic state of the same multiplicity. This again is a spin allowed process and is very efficient if the energy gap is relatively small which is always the case for electronically excited states. It occurs in the same time frame as VR. Further VR brings the molecule to the lowest vibrational energy level of S_1 . The energy gap between S_1 and S_0 is too large for IC to be efficient, but the molecule can undergo fluorescence, which is still a relatively fast allowed process ($10^6 - 10^9 \text{ s}^{-1}$), and in so doing return to S_0 .

As it involves a change in multiplicity, ISC from S_1 to T_1 is spin forbidden and is often a slow process ($10^6 - 10^9 \text{ s}^{-1}$). However, the term “forbidden” really refers to the fact that the transition is inefficient and where the energy gap between S_1 and T_1 is small, which is the case for a molecule with a carbonyl group, ISC can be very efficient; thus for example Φ (ISC) for benzophenone is approximately 1.

A carbonyl containing molecule can form both ($n-\pi^*$) and ($\pi-\pi^*$) states and the photochemistry of a particular ketone depends to a large degree on which state is lower in energy, as this will determine which will be most highly populated. In most simple ketones, the ($n-\pi^*$) state is the lower in energy.

Once occupying the lowest energy triplet state, phosphorescence, a slow forbidden process ($10^3 - 10^2 \text{ s}^{-1}$), can occur to return the molecule to the ground state. However, because this process is inefficient, as is ISC due to the large energy gap between T_1 and S_0 , the molecule can remain trapped in T_1 for a relatively long time, providing an opportunity for a chemical reaction to take place. This $S_0 \rightarrow S_2 \rightarrow S_1 \rightarrow T_1$ sequence is described as the direct population of T_1

1.4.2 Photosensitisation

It is often difficult to get a molecule “directly” into a triplet state, as unless a carbonyl group is present the energy gap between S_1 and T_1 is large, and S_1 to T_1 ISC is very inefficient. As molecules in T_1 tend to be more photochemically active due to its long lifetime, it is important to have an alternative method of populating this state. To do so efficiently, we can employ a method termed photosensitisation (**Figure 6**).

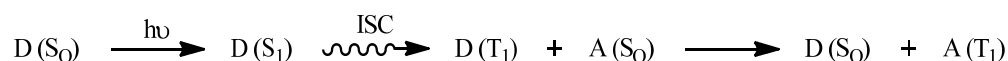


Figure 6

Photosensitisation requires the use of a donor molecule (D) that can easily access the triplet state and so this is usually a molecule containing a carbonyl group, for example benzophenone. The energy of the donor molecule in the triplet state can be transferred to an acceptor molecule (A) provided that the triplet energy of the donor is greater than that of the acceptor. In addition, the lifetime of the donor molecule in the triplet state must be sufficiently long to allow transfer of energy, which usually involves a molecular collision, to the acceptor molecule before IC or phosphorescence return $D(T_1)$ to $D(S_0)$. Ideally the photosensitiser should absorb at a different wavelength to the acceptor molecule so that there is no competition for the exciting radiation.

In summary, the donor molecule is irradiated with UV light forming $D(S_1)$ which gives $D(T_1)$ *via* ISC. At this point, the donor transfers its energy to the ground state acceptor molecule, transferring it to an excited state of the same multiplicity (T_1). In this way, the donor molecule is acting as a photosensitiser while the acceptor molecule acts as a quencher, returning the excited state donor to the ground state.

Ketones, and in particular aromatic ketones such as benzophenone, are most frequently used as photosensitisers due to their relatively long triplet lifetime; benzophenone has a triplet lifetime of 6×10^{-3} s. Ketones can occupy the triplet state very easily due to the non-bonding electrons in the n orbital on the oxygen atom and the π electrons in the double bond. Upon absorption of a photon of light, one of these

electrons can be promoted to a π^* or σ^* orbital, transitions described as ($n-\pi^*$), ($n-\sigma^*$) or ($\pi-\pi^*$) (**Figure 7**)²⁴.

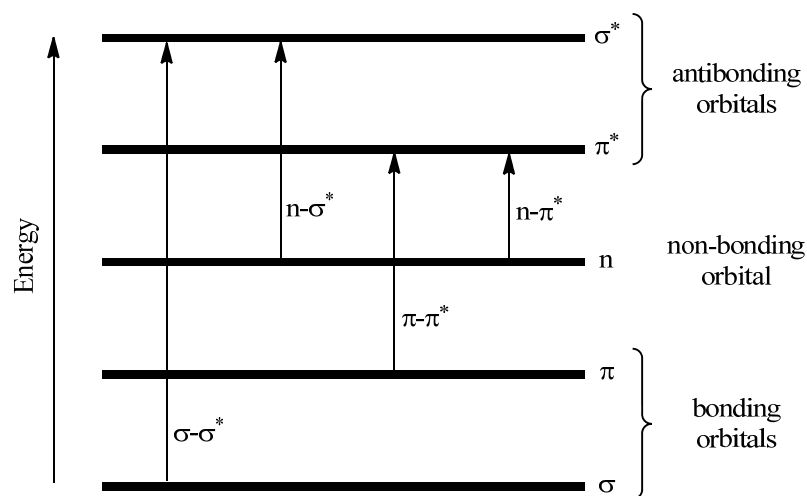


Figure 7

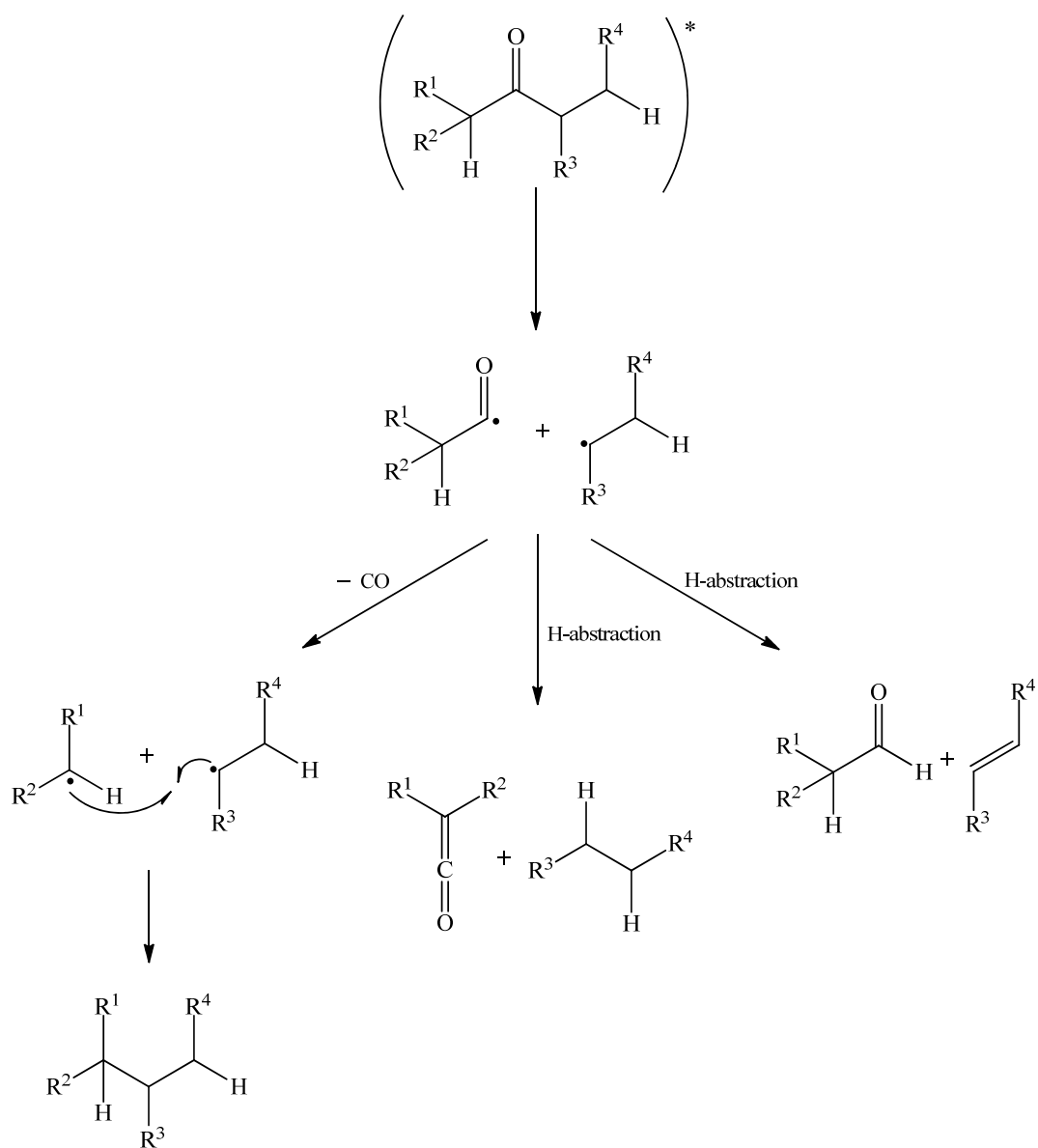
Due to the small energy gap between the n orbital and the π^* antibonding orbital, the ($n-\pi^*$) transition is the most likely transition for molecules containing n , σ and π orbitals. Both the ($n-\pi^*$) and the ($\pi-\pi^*$) transitions are achievable using low energy UV light either from medium pressure mercury vapour lamps, or sunlight, whereas a wavelength of less than 200 nm is generally required for ($\sigma-\sigma^*$) and ($n-\sigma^*$) transitions, something that would be problematic from a practical aspect.

The excitation of an electron from an n to a π^* orbital transfers electron density to the carbon and leaves a single electron in an n orbital on the oxygen atom. This localisation of spin density on the O-atom in the ($n-\pi^*$) state gives benzophenone, and all other ketones, the alkoxy radical character that is essential for hydrogen abstraction²⁵. Ketones for which the lowest triplet state is of the ($\pi-\pi^*$) type do not have alkoxy radical character²⁶ and so are not suitable as photomediators.

1.4.3 Photochemistry of the carbonyl group

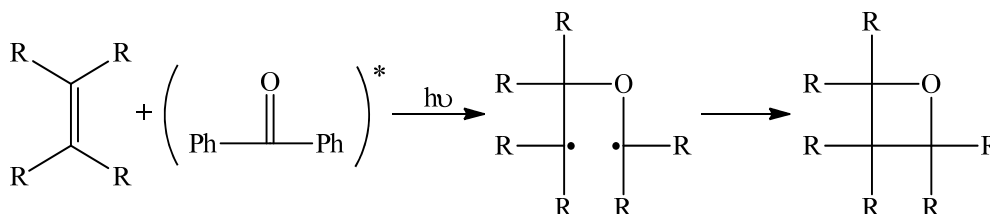
The three main classes of reaction for the excited states of carbonyl compounds are homolytic cleavage of the carbonyl group's α -bond (Norrish Type 1 Reaction) (**Scheme 10**), addition to multiple carbon-carbon bonds (Paterno-Buchi Reaction) (**Scheme 11**), or hydrogen abstraction by the carbonyl group which can occur intramolecularly (Norrish Type 2 Reaction) (**Scheme 13**) or intermolecularly (photoreduction) (**Scheme 14**).

In the case of a Norrish Type 1 Reaction, the α -bond is cleaved predominantly as it is the bond with the lower BDE. A number of secondary processes can occur following α -cleavage (**Scheme 10**). In the first instance, the loss of carbon monoxide leaves two carbon radicals, which can recombine to give a new carbon-carbon bond. Alternatively, an α -hydrogen may be abstracted from the carbonyl containing fragment, yielding a ketene and a saturated hydrocarbon. Finally, abstraction of a β -hydrogen by the carbonyl containing radical fragment produces an alkene and an aldehyde.



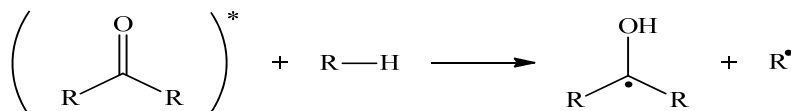
Scheme 10

The Paterno-Buchi Reaction involves the excitation of a carbonyl substrate (aldehyde or ketone) to a singlet state which undergoes ISC to a triplet state and can then undergo cycloaddition to a substituted alkene, most often one which is electron rich. Upon addition of the carbonyl to the alkene substrate, a 1,4-biradical species is formed which ring closes to form an oxetane (**Scheme 11**).



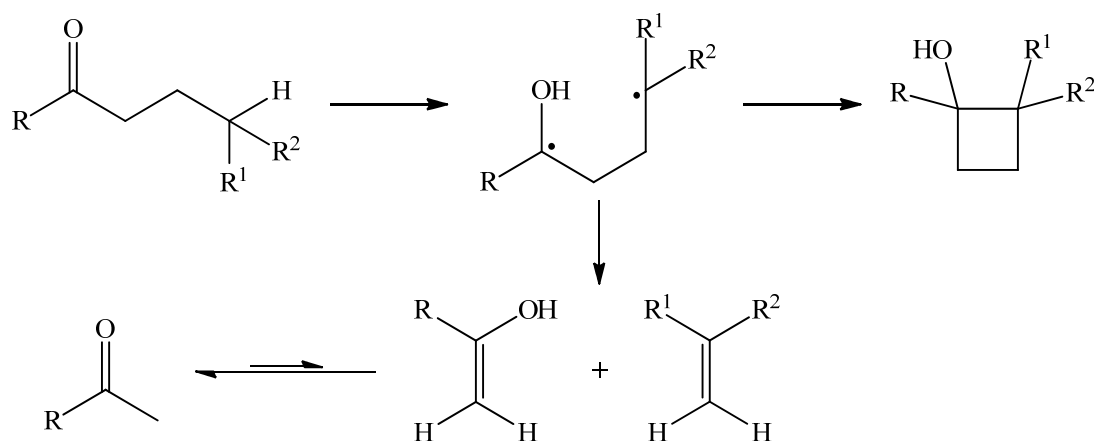
Scheme 11

Hydrogen abstraction by the carbonyl group forms the basis of the work discussed in this thesis (**Scheme 12**).



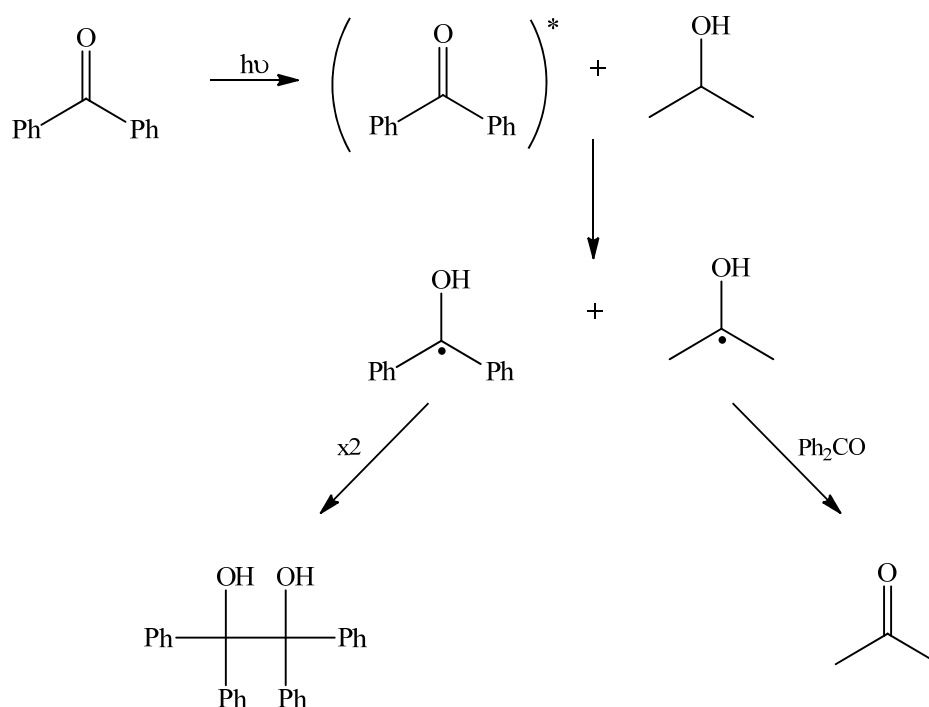
Scheme 12

When hydrogen abstraction by the carbonyl group occurs intramolecularly, this is known as a Norrish Type 2 Reaction (**Scheme 13**). It involves the abstraction of a γ -hydrogen by an excited state carbonyl to form a 1,4-biradical. This biradical can then react further to form a cyclobutane *via* radical recombination, or it may fragment forming an alkene and an enol.



Scheme 13

The photoreduction of benzophenone to benzpinacol in the presence of 2-propanol²³ was one of the reactions that paved the way for the development of organic photochemistry (**Scheme 14**).

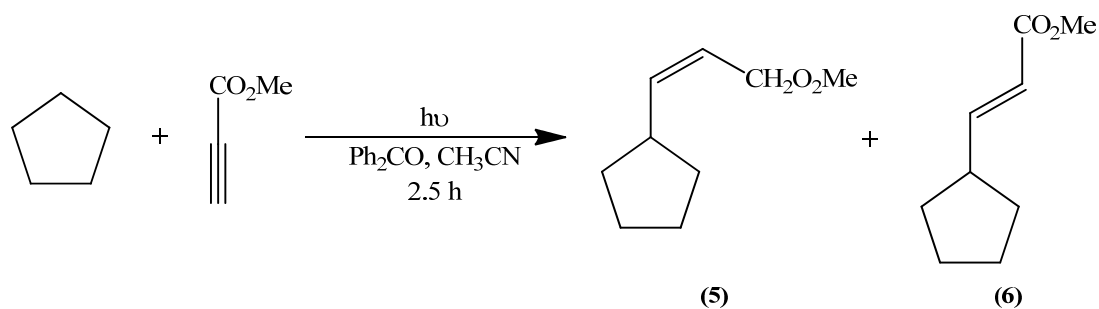


Scheme 14

Upon irradiation of benzophenone, excitation to a singlet excited state is followed by ISC and relaxation to the lowest ($n-\pi^*$) triplet state. It is in this long lived excited state that hydrogen abstraction from the relatively weak α -CH bond of the alcohol occurs, generating an α -hydroxyalkyl radical as well as a ketyl radical. This ketyl radical undergoes dimerisation to form benzpinacol while hydrogen atom transfer

from the α -hydroxyalkyl radical to a ground state benzophenone generates another ketyl radical and acetone.

As pointed out above, the formation of carbon radicals *via* photochemical hydrogen abstraction using a photoexcited carbonyl compound forms the basis of the work outlined in this thesis (**Scheme 12**). An example of the reactions involved is that between the monosubstituted alkyne methyl propiolate and cyclopentane, mediated by benzophenone, which is complete in 2.5 h and gives two products, **(5)** and **(6)**, in a 1:1.7 ratio and a combined yield of 95% (GC)²⁰ (**Scheme 15**).



Scheme 15

1.5 Factors affecting hydrogen abstraction from CH bonds

The work outlined in this thesis deals with the functionalisation of molecules using reactions which involve carbon radicals generated by photochemical hydrogen abstraction. Hydrogen abstraction from a relatively weak CH bond in a hydrogen donor, such as 2-propanol or cyclopentane, forms a nucleophilic carbon radical that can then attack an alkene or alkyne with an electron-withdrawing substituent, creating a new carbon-carbon bond. A discussion of the effect of the CH bond strength on the rate of hydrogen abstraction is therefore necessary.

1.5.1 Bond dissociation energy (BDE)

BDE is crucial in determining the outcome of a radical reaction. The size of this energy is governed by the thermodynamic stability of the product radical(s). Thus the greater the stability of the radicals formed, the lower is the BDE and the faster the rate of hydrogen abstraction. The strength of the bond formed also greatly influences the rate of abstraction as is demonstrated in the abstraction of a hydrogen atom by a halogen radical.

Bond	H-F	H-Cl	H-Br	H-I
BDE (kJ mol ⁻¹)	565	431	364	297

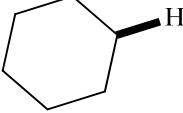
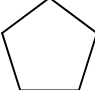
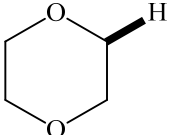
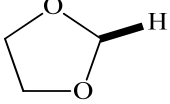
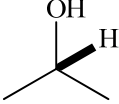
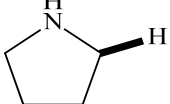
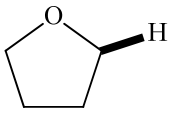
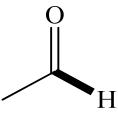
Table 1: BDEs of various hydrogen-halogen bonds

The BDE decreases as we move from HF to HI (**Table 1**) explaining why the rate of hydrogen abstraction by the respective halogen radicals increases as we ascend the halogen group. The importance of BDE in terms of identifying potential H-donors for the hydrogen abstraction generation of carbon radicals is discussed below (**Section 1.5.2**).

1.5.2 Hydrogen donors

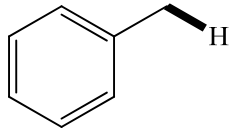
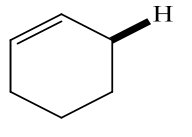
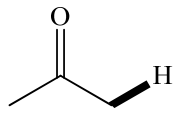
The Evans-Polanyi relationship²⁷ suggests that as the BDE decreases, the rate constant for hydrogen abstraction increases. Based on a consideration of the BDE of

CH bonds, suitable H-donors for hydrogen abstraction can thus be identified (Table 2).

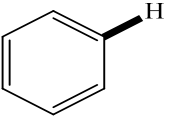
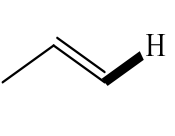
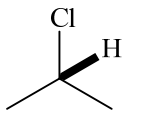
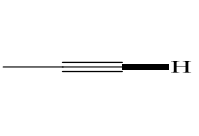
H-donor	BDE ^a	H-donor	BDE ^a
	416		400
	401		381
	396		377
	385		374

^a kJ mol⁻¹

Table 2: Suitable H-donors for hydrogen abstraction

H-donor			
BDE	376	342	402

^a kJ mol⁻¹**Table 3: H-donors which produce non-nucleophilic C-radicals**

H-donor				
BDE	472	465	423	545

^a kJ mol⁻¹**Table 4: Molecules unsuitable as H-donors due to a large BDE**

Nonetheless, BDE is not the only factor that determines the suitability of a molecule as a source of nucleophilic carbon radicals. Many CH systems with relatively small BDEs are unsuitable, as the carbon radicals generated from them have low energy SOMOs that do not interact with the LUMO of an alkene (**Table 3**). The low energy of the SOMO is generally due to resonance and such radicals are non-nucleophilic. There are thus relatively few examples of the addition of a benzylic radical to an electron deficient alkene^{28,29}. On the other hand, the efficiency of H-abstraction from an aldehyde is due to resonance, an effect which also accounts for the nucleophilicity of the radical generated (**Scheme 5**). Many molecules are also unsuitable as H-donors on a thermodynamic level due to large BDEs which prevent H-abstraction (**Table 4**).

Relationships between the regioselectivity of hydrogen abstraction and the strength of the various CH bonds in a molecule also become clear from a consideration of the relevant BDEs. The reaction of alcohols with the disubstituted alkyne dimethyl acetylenedicarboxylate (DMAD)¹² (**Scheme 16**) provides an insight into the BDE

advantage is balanced by the larger number of the other CH bonds present. Consequently, relatively small H-donor molecules, which for reasons of symmetry or reactivity have just one abstractable H-atom, are most useful from a synthetic point of view. The requirement for a large excess of H-donor means that those of relatively high volatility must be used so that they can be easily removed by distillation after the reaction has reached completion.

1.5.3 Stereoelectronic effects

Stereoelectronic effects refer to the manner in which the orientation of orbitals determines the outcome of a reaction. It has been shown^{31,32} that the rate of hydrogen abstraction from a carbon atom adjacent to a nitrogen or oxygen is far more rapid than hydrogen abstraction from the corresponding hydrocarbon. Griller³¹ determined rate constants for the abstraction of a hydrogen atom from amines and noted that abstraction was most rapid when the α -CH bond to be cleaved was eclipsed with the nitrogen lone pair. It was determined that when a dihedral angle of 60° was involved (**Figure 8**), the CH bond was less easily cleaved.

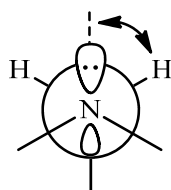


Figure 8

In keeping with this, Ingold³² showed that in the case of ethers, an accelerated rate of hydrogen abstraction was achieved when the dihedral angle between the CH bond of interest and the p -type lone pair orbital of the adjacent oxygen atom was less than 30° . A dihedral angle of 0° led to the fastest rate of abstraction, while an angle of 90° led to the slowest rate of hydrogen abstraction.

The observed reactivity can be rationalised in terms of the resonance forms available to ethers following hydrogen abstraction. A single electron effectively moves from the lone pair on the oxygen atom to the carbon radical, generating a carbanion and an oxygen radical cation (**Figure 9**). A similar explanation accounts for the accelerating effect of a nitrogen atom.

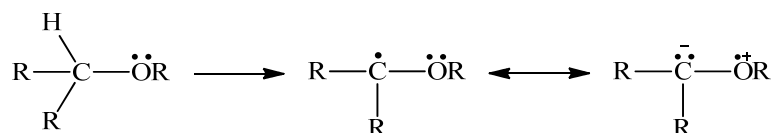


Figure 9

1.5.4 The nature and energy of the photomediator's triplet state

The energy of a singlet excited state can be obtained by using fluorescence emission spectra where the shortest wavelength band corresponds to the excited state energy. In the same way, phosphorescence emission spectra can be used to determine triplet state energies. The energy of a photomediator's triplet state plays a role in determining the efficiency of the hydrogen abstraction process because the lower the energy, the slower the rate of hydrogen abstraction (**Table 6**)³³.

Photomediator	Excited state	Triplet energy ^a
Benzophenone	$n-\pi^*$	290
Acetone	$n-\pi^*$	325
<i>p</i> -Methoxyacetophenone	$n-\pi^*$	330

^a kJ mol⁻¹

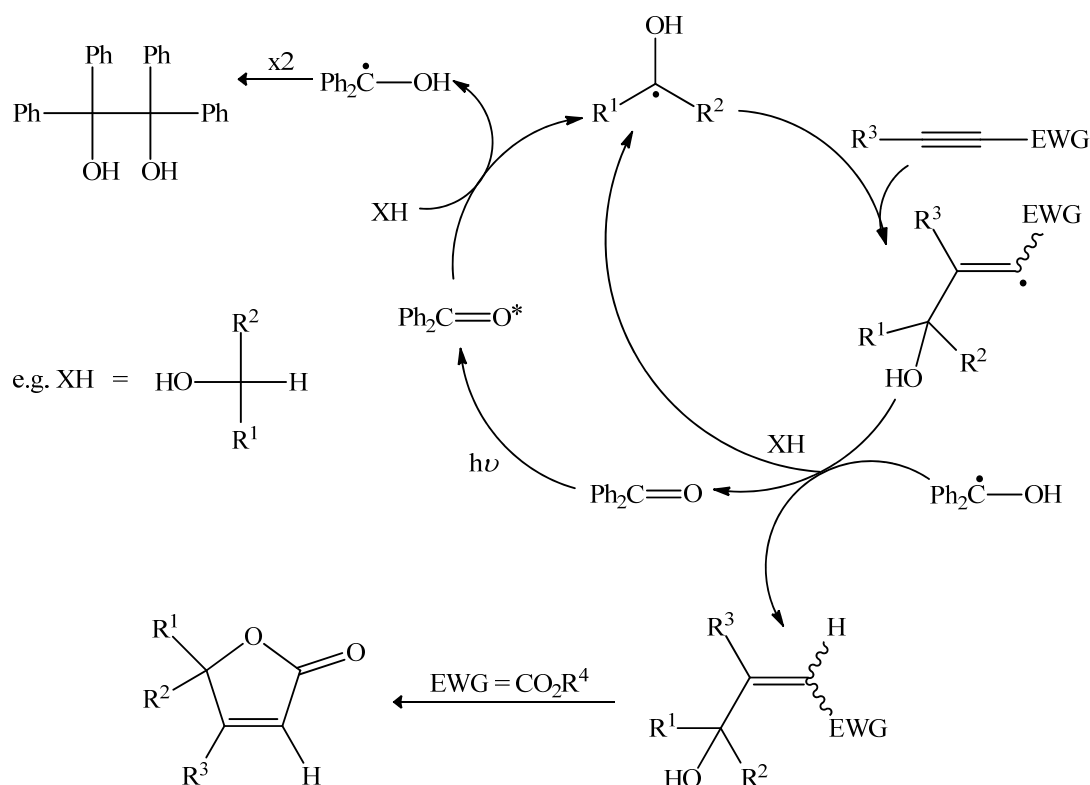
Table 6: Triplet energy of various photomediators

It is also important to consider the nature of the triplet state involved as hydrogen abstraction is only feasible when an ($n-\pi^*$) triplet excited state is formed (**Section 1.4.2**), as is the case for benzophenone or acetone²⁶.

1.6 General reaction mechanism

The work described in this thesis involves the photomediated generation of a carbon radical and its reaction with an electron deficient alkene or alkyne forming a C-C bond. A typical example is the addition of alcohols to DMAD (**Scheme 16**).

The main features of the reaction mechanism involved in this reaction are common to all reactions of this type (**Scheme 17**).



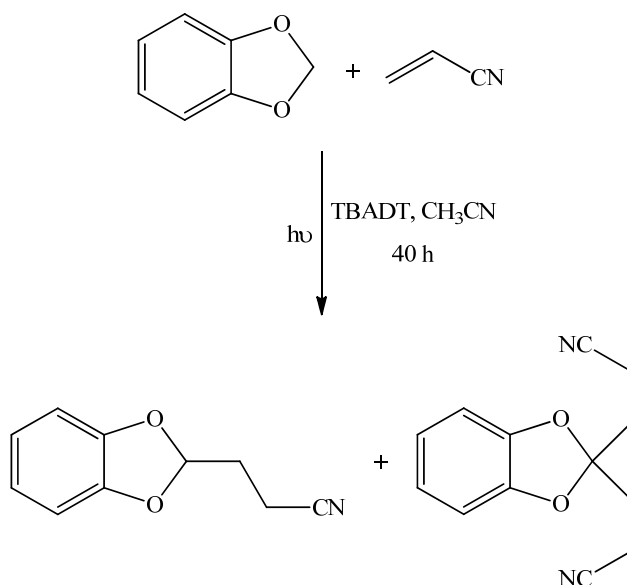
The photomediator, for example benzophenone, in the presence of UV light is initially excited to an ($n-\pi^*$) triplet state. As detailed earlier (**Section 1.4.2**) it is in this excited state that the carbonyl group behaves as an alkoxy radical²⁵ and can abstract a hydrogen from a relatively weak CH bond, for example the CH bond in a secondary alcohol such as 2-propanol. The excited state benzophenone is reduced to a ketyl radical, which is required further on in the reaction cycle but may also undergo dimerisation to generate a pinacol. If this reaction is important for a particular system, stoichiometric quantities of the photomediator will be required. Also produced is an α -hydroxyalkyl radical which, in the presence of a mono- or disubstituted electron deficient alkyne, undergoes addition forming a carbon-carbon bond and generating an alkenyl radical. This radical then has two options. It may undergo back hydrogen transfer from the ketyl radical formed earlier, regenerating benzophenone and forming the alkene product. The second option is for the alkenyl radical to react with another molecule of the H-donor, again forming a molecule of product but this time, generating another α -hydroxyalkyl radical which can go on to react with a molecule of the unsaturated substrate in a chain mechanism. Although

the potential of being able to operate *via* a chain mechanism is considerable there is little evidence that this is a viable possibility³⁴. However, in 2007, Fagnoni reported the photocatalysed addition of a series of aldehydes to electron deficient alkenes generating unsymmetrical ketones using tetrabutylammonium decatungstate (TBADT)³⁵. It was found that TBADT could be used in catalytic amounts (2 mol%), suggesting that perhaps a chain mechanism was in operation. It has also been shown that the reaction of 2-methyldioxolane with DMAD occurs with a quantum yield of 4.8³⁶. This means that for every photon of light absorbed, 4.8 molecules of product are formed, confirming that a chain mechanism is in operation.

As the alkenyl radical product undergoes rapid *E/Z* equilibration³⁷, the reaction produces an approximately 50/50 mixture of (*E*)- and (*Z*)- alkenes, the latter cyclising to form a γ -lactone. It is clear from reactions of this style that the addition of carbon radicals to alkenes is not competitive with that to alkynes as the addition of two molecules of hydrogen donor to an alkyne is rarely observed.

1.7 Other photocatalysts

A variety of inorganic ions have also been used as photocatalyst, an example being the decatungstate anion, $W_{10}O_{32}^{4-}$, which has been used in the form of the acetonitrile soluble TBADT³⁸. Although similar to benzophenone in that it absorbs light in the 300-350 nm region, it has been shown in certain cases^{35,39} to be efficient in catalytic amounts (2 mol%). This is rarely the case for benzophenone which frequently requires stoichiometric amounts to be effective. Fagnoni³⁸ exploited this feature of TBADT in a series of reactions involving 1,3-benzodioxole (**Scheme 18**) and some of its derivatives.

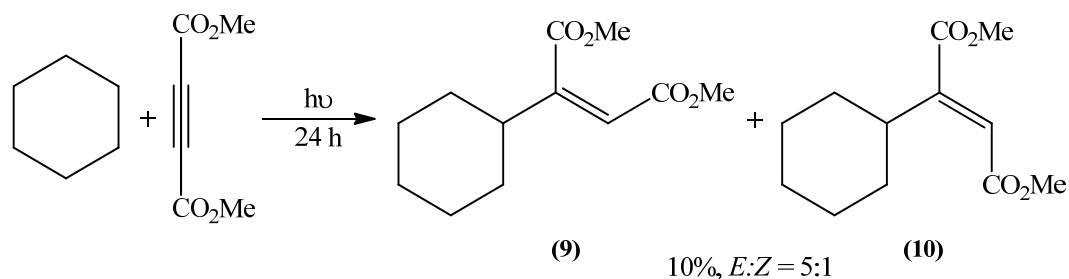


Scheme 18

1.8 The photochemical addition reactions of H-donors to unsaturated systems

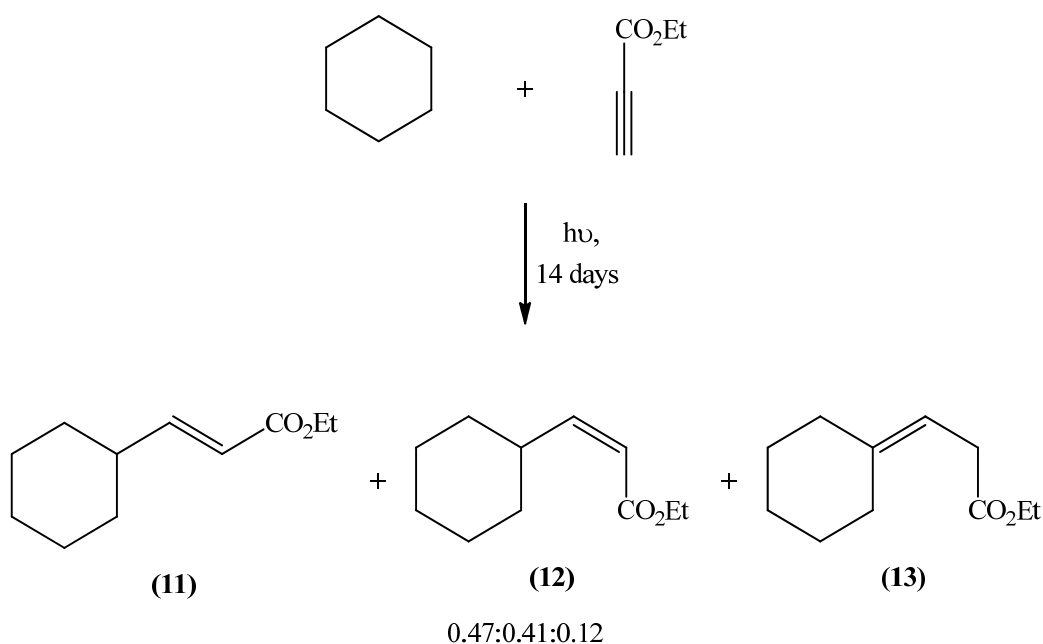
1.8.1 The photochemical addition reactions of cycloalkanes

The photomediated reaction of a cycloalkane with an electron-deficient unsaturated system, such as an alkene or an alkyne, with one or two electron withdrawing groups, is very valuable from a synthetic point of view. It provides a means of functionalising an unactivated system. The early work published was not, however, very promising. In 1969, Grovenstein reported the photochemical reactions of DMAD and benzene, and DMAD and naphthalene⁴⁰. A solution of DMAD and naphthalene in cyclohexane was irradiated in a quartz cell for 24 h at room temperature (rt) leading to the formation of two addition products, **(9)** and **(10)**, in a 5:1 ratio (**Scheme 19**). The source of irradiation was a 1000 W medium-pressure mercury lamp (200-600 nm), however a Pyrex sheet was inserted between the lamp and the quartz cell to eliminate any irradiation below 300 nm.



Scheme 19

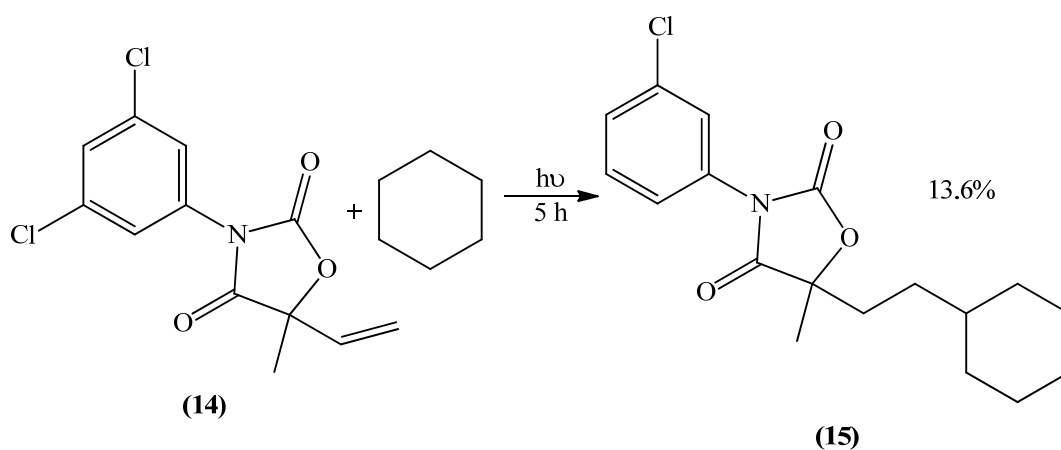
In the same year, Buchi carried out the reaction of ethyl propiolate and cyclohexane and three products were obtained (**Scheme 20**)⁴¹. The *trans* and the *cis* isomers, **(11)** and **(12)**, were the major products, with the non-conjugated product **(13)** being formed in smaller quantities.



Scheme 20

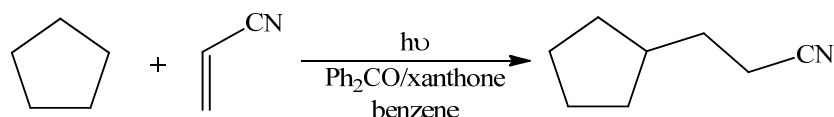
Both reactions required lengthy irradiation and no photomediator was used, leading to the conclusion that the cyclohexyl radical was generated *via* hydrogen abstraction by an excited ynoate molecule.

A more recent example involves the herbicide vinclozolin (14) which upon irradiation in cyclohexane produces a monochloro cyclohexyl product (15) (Scheme 21). Although the manner by which the cyclohexyl radical is generated is uncertain, the reaction is one of the few examples of the addition of a photochemically generated cyclohexyl radical to an alkene with no EWG⁴². Understandably the yield of the product obtained is very low.



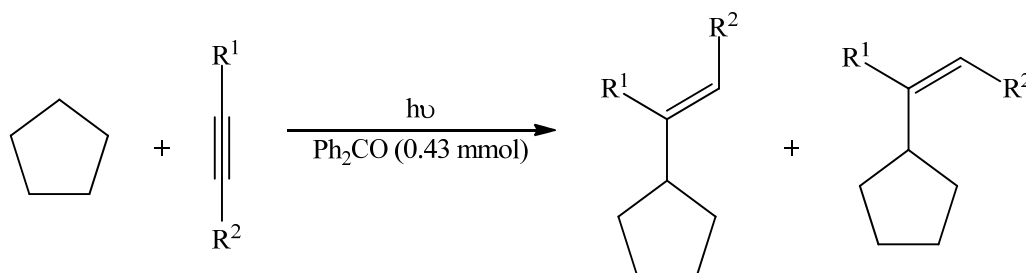
Scheme 21

As indicated, these reactions are examples of the ‘direct’ generation of carbon radicals and do not involve a specifically added photomediator. An example of the photomediated addition of cyclohexyl radicals to alkenes was provided by Fagnoni in 2001⁴³. This involved benzophenone or xanthone mediated H-abstraction from a cyclic hydrocarbon and the reaction of the resulting carbon radical with an α,β -unsaturated nitrile, leading to the formation of a β -cycloalkylnitrile (**Scheme 22**). The photomediator was used in equimolar amounts with respect to the alkene. The need for such large amounts of photomediators is a major drawback from a synthetic perspective as it greatly complicates product isolation which usually requires column chromatography.



Scheme 22

Work carried out by Geraghty, involving the benzophenone mediated addition of cycloalkanes to electron deficient alkynes (**Scheme 23, Table 7**), showed that as little as 0.15 eq. of benzophenone (relative to the alkyne) was effective and that a dramatic decrease in the rate of reaction, but not the yield, was observed when 0.09 eq. benzophenone was used in the reaction of methyl propiolate and cyclopentane²¹ (**Table 8**).



Scheme 23

R ¹	R ²	Time (h)	Yield ^a (Z, E) (%)	Ratio ^b (Z:E)
H	CO ₂ Me	2.75	37, 22	1:1.5
H	CO ₂ Et	2.5	40, 30	1:1.5

H	CN	1.3	- ^c ,16	1.5:1
H	CO ₂ H	1.5	24, - ^c	1:1.8
CO ₂ Me	CO ₂ Me	2.5	50, - ^c	45:1
CO ₂ Bu ⁱ	CO ₂ Bu ⁱ	1.5	46, 3	30:1

^a Isolated yield, ^b GC ratio, ^c Product could not be satisfactorily isolated

Table 7: The benzophenone mediated addition of cyclopentane to electron deficient alkynes

Ph ₂ CO (M) ^a	Time (h)	Yield ^b (%)	Ratio ^c (E:Z)
0.15	2.75	86	1.46:1
0.10	3	93	1.3:1
0.05	3	92	1.33:1
0.022	3	95	1.32:1
0.014	102	91	1.27:1

^a Cyclopentane solution of the alkyne (0.15 M) containing the photomediator (mmol), ^b combined GC yield, ^c GC ratio

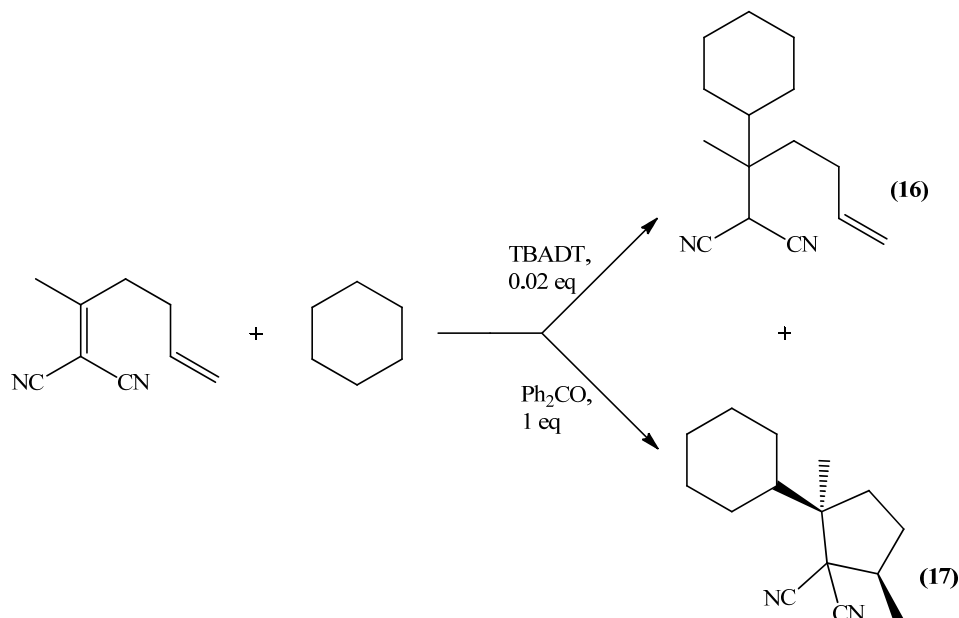
Table 8: The benzophenone mediated reaction of methyl propiolate and cyclopentane

It is difficult to deduce a pattern of reactivity for the cycloalkanes in terms of ring size. However, it is clear that cyclopentane is the most reactive with alkynes, and that cycloalkanes larger than cyclohexane do not react with DMAD²¹; surprisingly however, 2-cyclopentenone reacts with cyclododecane⁴⁴.

The requirement for up to stoichiometric quantities of a photomediator in many reactions of this type is of course due to the fact that the ketyl radical dimerises in a competitive reaction to form a pinacol which effectively removes the photomediator from the reaction. This is one of the factors which suggested the work described in this thesis relating to supported photomediators. The polyoxometallate TBADT has also been used⁴⁵ in reactions of cycloalkanes with electron deficient alkenes (**Section 1.7**)^{46,47}, but unlike benzophenone, it is effective in catalytic quantities relative to the alkene⁴⁴. The faster rate of back hydrogen transfer associated with TBADT is thought to be the key factor responsible for the observed activity³⁹.

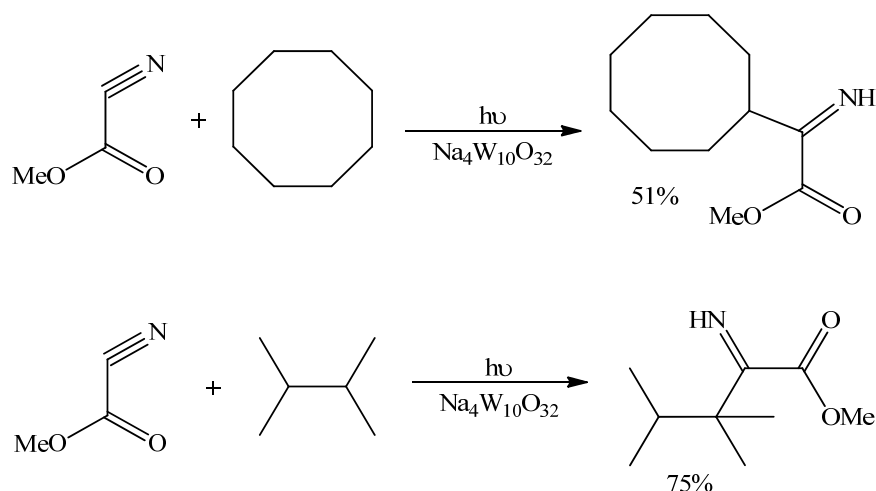
In some cases the reaction outcome can be controlled by choosing a suitable photomediator. The cyclohexyl radical generated using TBADT adds to the electron deficient double bond in 1-methyl-pent-4-en-1-ylidene malononitrile (**Scheme 24**), forming an alkyl radical which then undergoes very rapid back hydrogen transfer from the reduced decatungstate molecule generating (**16**) in a 45% yield. When

benzophenone is used, back hydrogen transfer is slower and cyclisation of the initially formed alkyl radical species onto the terminal alkene accounts for the product **(17)**, which is obtained in 28% yield^{43,46}.



Scheme 24

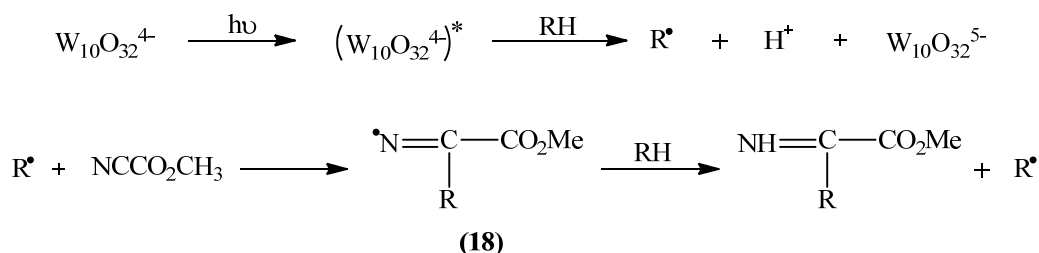
There appears to be only one instance of the addition of photochemically generated carbon radicals to C≡N bonds⁴⁸. This is due to Hill who has described the use of TBADT as a photocatalyst in the reactions of hydrocarbons such as octane and 2,3-dimethylbutane with methyl cyanoformate⁴⁸ (**Scheme 25**).



Conditions: $h\nu > 280$ nm (pyrex), MeCN, 0.006 eq. polyoxotungstate relative to methyl cyanoformate, rt, yields based on a methyl cyanoformate conversion of approximately 15%.

Scheme 25

The key step is H-atom abstraction from the alkane by an electronically excited decatungstate ion, followed by the formation of a radical chain in which the key intermediate is the iminyl radical **(18)** (Scheme 26).



Scheme 26

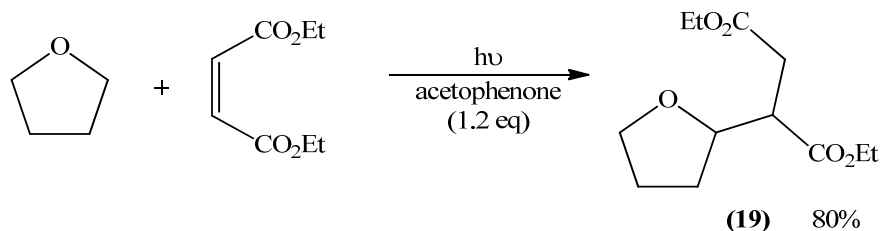
The mechanistic interpretation of this reaction is different to that used to account for the behaviour of TBADT previously (Scheme 24) where direct transfer of a H-atom from the alkane to the decatungstate ion, followed by back hydrogen transfer is thought to be involved. In the cyanoformate reactions, single electron transfer to the decatungstate produces an alkyl radical and a proton (Scheme 26). At room temperature, competitive breakdown of the iminyl radical to a nitrile is minimal (1-2%) whereas at 90 °C this becomes the major process. This work by Hill demonstrates the potential of polyoxotungstates as photomediators while also presenting a rare example of the functionalisation of an acyclic hydrocarbon. Furthermore, in keeping with the previous discussion (Section 1.1.4.2), it was noted

that the benzylic radical underwent recombination rather than addition to the unsaturated substrate⁴⁸.

1.8.2 The photochemical addition reactions of cyclic ethers

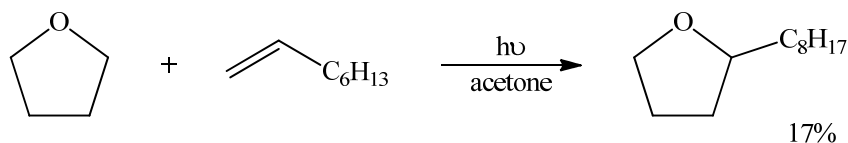
Cyclic ethers, which like the cycloalkanes of the previous section (**Section 1.8.1**) are more often thought of as solvent molecules, can also participate in photomediated addition reactions with electron deficient unsaturated substrates. As discussed earlier (**Section 1.5.3**), stereoelectronic effects are apparent for H-abstractions from the α -carbon^{31,32} in an ether, such as tetrahydrofuran (THF), and due to this effect we can expect a faster rate for photochemical hydrogen abstraction from cyclic ethers than from the corresponding cycloalkanes.

Early work by Rosenthal involved the addition of THF to the electron deficient alkene diethyl maleate, affording a single product (**19**)⁴⁹ (**Scheme 27**).



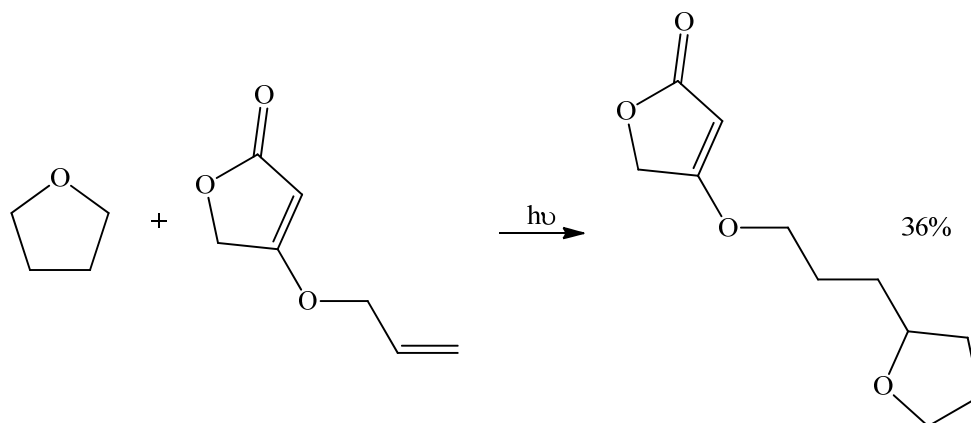
Scheme 27

In the same year, THF was also reported⁴⁹ to add to a terminal alkene at the less electrophilic site (**Scheme 28**). The addition presumably occurs at the terminal carbon as this is the less sterically hindered site. This implies that steric factors, as well as electrophilicity, determine the site of addition to an alkene in reactions of this type.



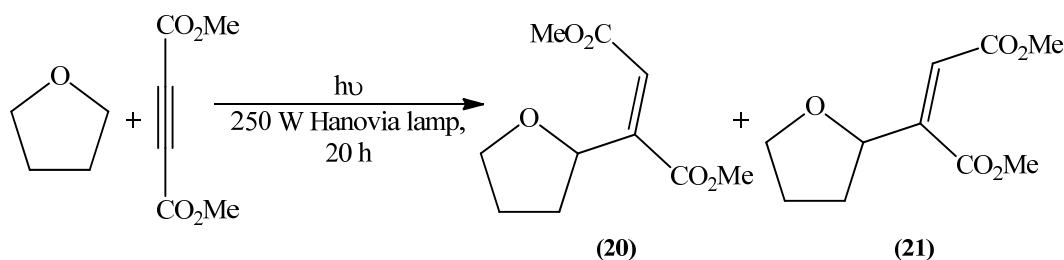
Scheme 28

This is further demonstrated in the reaction of THF with an α,β -unsaturated lactone which gives a single product that results from the addition of the tetrahydrofuranyl radical to a sterically unhindered centre rather than to the most electrophilic centre⁵⁰ (**Scheme 29**).



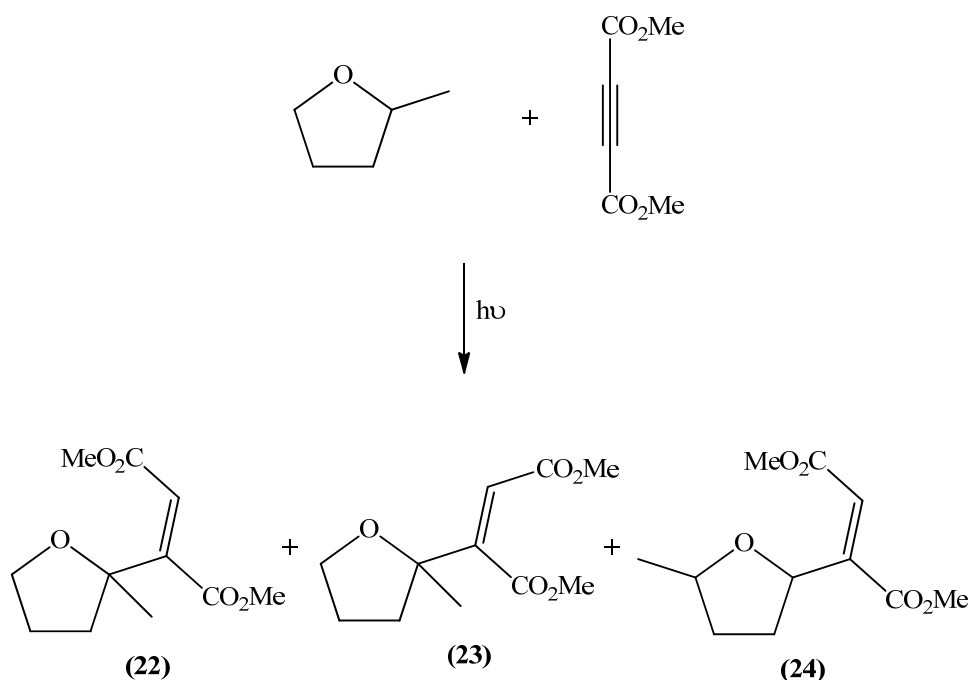
Scheme 29

Cyclic ethers have also been shown to add to DMAD⁵¹. Singh found that upon irradiating a solution of DMAD in THF for 20 h with a 250 W Hanovia lamp, 1:1 adducts, identified as the *trans* and *cis* isomers (**20**) and (**21**), were obtained in a 60% combined yield (**Scheme 30**).



Scheme 30

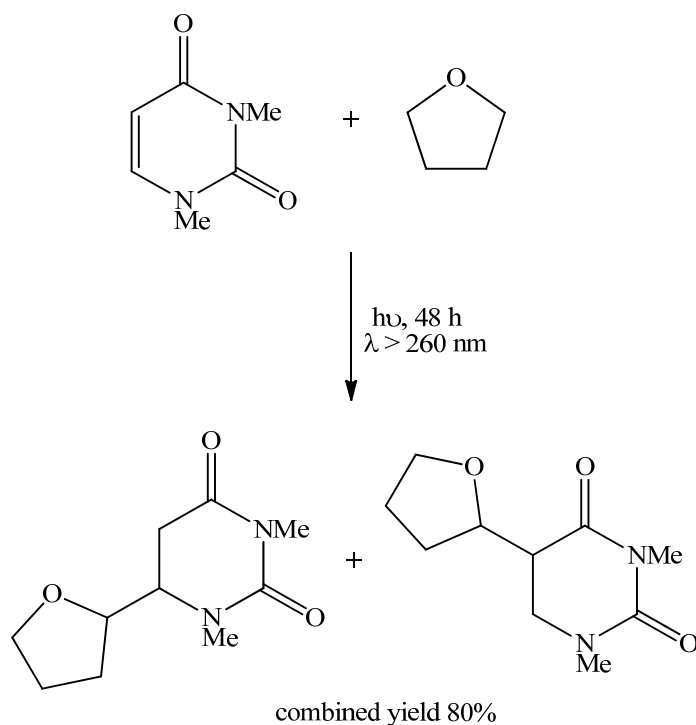
Similarly, irradiation of a solution of DMAD and 2-methyltetrahydrofuran led to the formation of three 1:1 adducts, namely the *cis* and *trans* isomers, (**22**) and (**23**), and a third minor product (**24**) (**Scheme 31**). A 2,5-dimethylated furan structure was suggested for this minor product; this is presumably a mistake. It is worth noting in this case that the regioselectivity of the reaction is determined by the greater stability of a 3° radical relative to a 2° radical.



Scheme 31

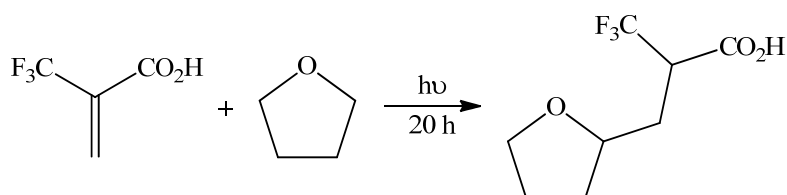
Neither reaction involved an added photomediator, and the possibility that an excited state DMAD was responsible for H-abstraction from an ether molecule was ruled out by Singh⁵¹ who showed that when tetrahydropyran (THP) was used, no addition to the unsaturated bond occurred unless acetone was present. He suggested that carbon radical generation involved impurities in the solvent and this was supported by the fact that use of THF dried over lithium aluminium hydride, led to a much slower reaction and a poor yield (10%).

Another early example involves the direct irradiation of 1,3-dimethyluracil in THF. It was suggested that the formation of a regioisomeric mixture was due to the competitive H-abstraction from the ether by the carbonyl group (β -addition) and the β -carbon of the enone (α -addition)⁵², followed by recombination of the radicals thus formed (**Scheme 32**).



Scheme 32

It has also been shown that cyclic ethers add to electron deficient fluorinated alkenes. Thus O'Hagan has reported the photomediated addition of THF (and alcohols) to 2-(trifluoromethyl)acrylic acid using benzophenone as the photomediator⁵³. Although the results were mostly positive, the difficulty experienced in removing benzophenone and its dimerisation product from the reaction mixture reduced the attractiveness of the method. This prompted work on the direct irradiation of these solutions (Scheme 33) and although the reaction times were longer (20 h as opposed to 5 h), this was compensated by the fact that the purification process was much simpler.



Scheme 33

In the direct reaction, the alkene, upon irradiation with UV light, is excited to a triplet state of diradical nature which abstracts a H-atom from a molecule of THF.

This forms a nucleophilic radical which adds to a ground state molecule of the alkene; abstraction of a hydrogen atom forms the desired product⁵⁴.

Chambers described the decrease in activity observed with increasing substitution of the alkene with fluoroalkyl groups in reactions with cyclic ethers⁵⁵. Very high conversions were obtained when the alkenes **(25)**, **(26)** and **(27)** (**Figure 10**) were used; no reaction however took place with alkene **(28)** (**Figure 10**) and this result has been attributed to steric effects⁵⁵.

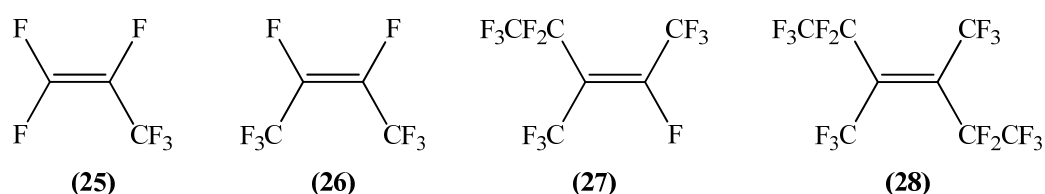


Figure 10

Both Chambers⁵⁵, and Malatesta and Scaiano⁵⁶, listed the order of reactivity for the reaction of α -alkoxyalkyl radicals derived from cyclic ethers with fluorinated alkenes (**Figure 11**). In keeping with the discussion above (**Section 1.5.3**) this order has been rationalised on the basis of the ability of the rings to adopt a conformation in which there is an almost eclipsing relationship between a lone pair on the oxygen atom and one of the CH bonds.

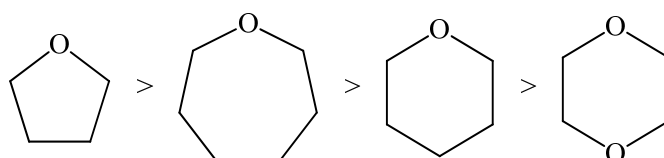
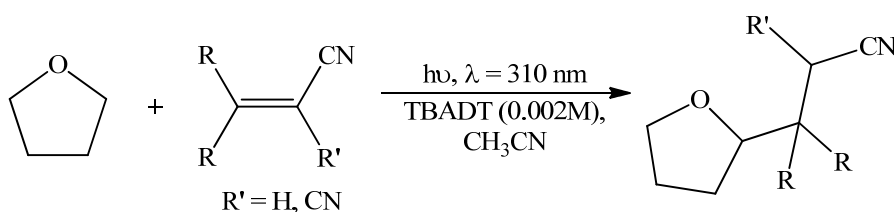


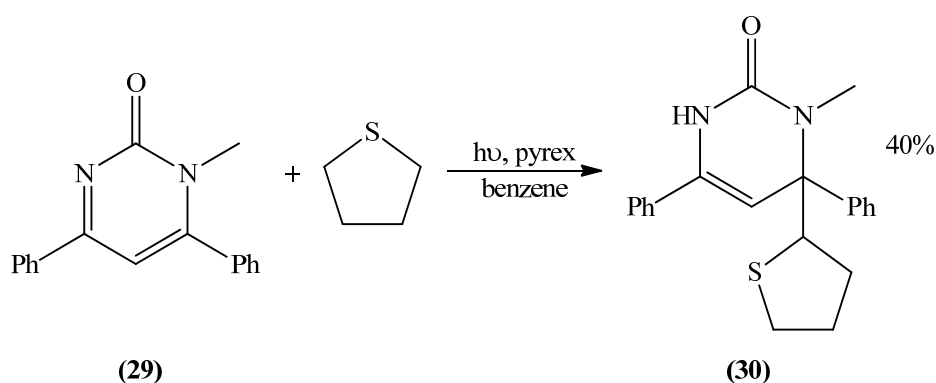
Figure 11

Work reported by Albini and Fagnoni⁴⁷ in 2006 demonstrated the use of TBADT as a photocatalyst in the reaction of THF with electron poor alkenes (**Scheme 34**).



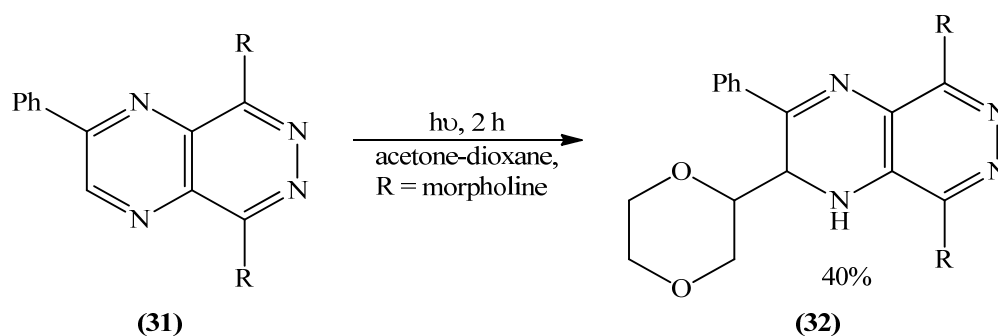
Scheme 34

The direct addition of an α -sulfanylalkyl radical, derived from a cyclic ether, to a C=N bond has also been described⁵⁷. Thus irradiation of the pyrimidin-2-one (**29**) in the presence of the cyclic ether tetrahydrothiophene, led to the formation of a 1:1 adduct, (**30**), generated *via* intermolecular hydrogen abstraction by the imino nitrogen of an excited pyrimidin-2-one (**Scheme 35**).



Scheme 35

Miyake has reported acetone promoted reactions involving cyclic ethers and C=N bond substrates⁵⁸. The photomediated reaction of 1,4-dioxane with (**31**) in acetone, for example, led to the formation of a single diastereomer, (**32**) (**Scheme 36**).

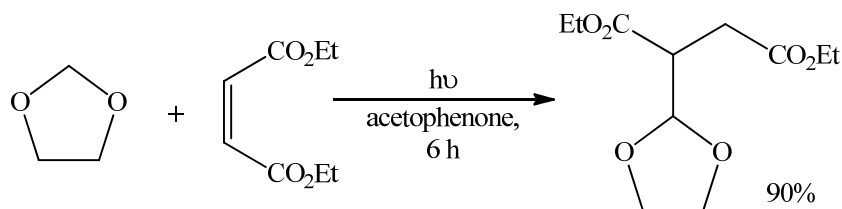


Scheme 36

1.8.3 The photochemical addition reactions of 1,3-dioxolanes

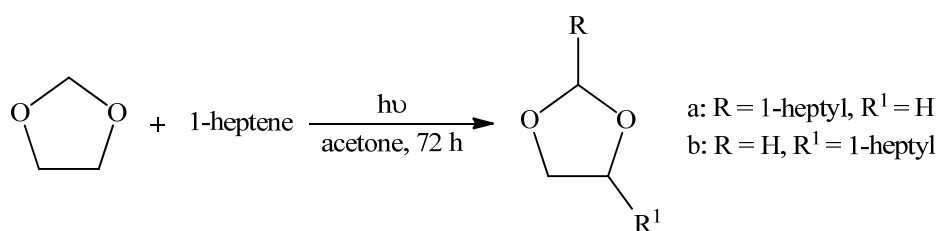
Photochemical hydrogen abstraction from a molecule of 1,3-dioxolane results in the formation of a 1,3-dioxolan-2-yl radical. This is facilitated by the stereoelectronic effect of at least one of the oxygen lone pairs of electrons. The 1,3-dioxolan-2-yl radical can then form a carbon-carbon bond through addition to an electron deficient unsaturated substrate, such as an alkene or an alkyne, with one or two EWGs.

In 1968, Rosenthal and Elad provided the first example of the photomediated alkylation of 1,3-dioxolane⁵⁹. The reactions involved acetone, acetophenone, or benzophenone, generated 1,3-dioxolan-2-yl radicals which in the presence of alkenes such as diethyl maleate, underwent addition to yield a 1:1 adduct (**Scheme 37**).



Scheme 37

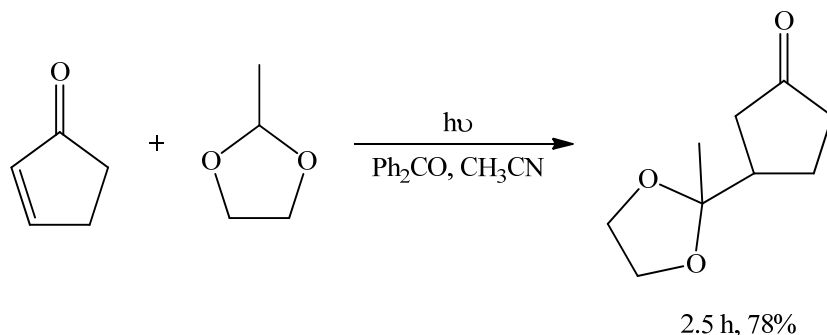
An ($n-\sigma^*$) transition results in the lowest energy excited state available for acetals, and light of less than 200 nm is required for the direct excitation of such molecules. The reactions were carried out by Rosenthal at 290 nm, a wavelength lower in energy than that required to excite the acetals and so it can be assumed that only the ketone is absorbing light. This results in the formation of the ($n-\pi^*$) state of the ketone which abstracts a hydrogen from the 2-position of the 1,3-dioxolane forming a dioxolan-2-yl radical that is subsequently trapped by an alkene. The formation of 2-propanol in acetone mediated reactions and benzpinacol in reactions involving benzophenone confirmed this was the case. In the reaction of 1-heptene and 1,3-dioxolane (**Scheme 38**), the regioselective addition of a nucleophilic radical to the 1-position of a terminal alkene is again observed suggesting that as in other cases (**Scheme 29**) steric factors are outweighing electronic effects.



Scheme 38

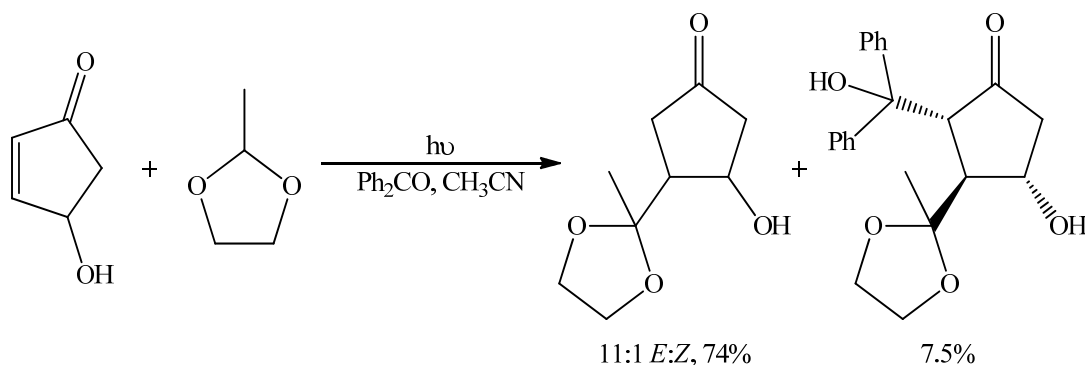
Fagnoni carried out a study of the reactions of 2-alkylated 1,3-dioxolanes with both acyclic and cyclic enones⁶⁰. The benzophenone mediated reaction of 3-buten-2-one and 2-methyl-1,3-dioxolane in acetonitrile required an irradiation time of 2.5 h but gave a poor yield (28%). A slightly higher yield (49%) was obtained when the

reaction was carried out in neat 2-methyl-1,3-dioxolane. In contrast, cyclic enones such as cyclopentenone performed better, even in acetonitrile, giving higher yields (78%) in short reaction times (2.5 h) (**Scheme 39**).



Scheme 39

The reactions were also extended to include 4-hydroxy-cyclopentenone which was reacted with 2-methyl-1,3-dioxolane (**Scheme 40**) under the same conditions used in the previous example.

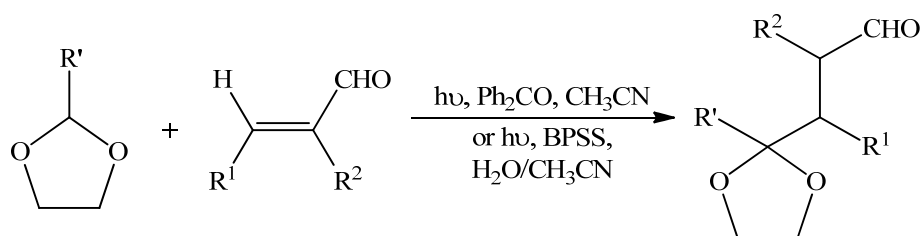


Scheme 40

A good overall yield (74%) was obtained and the *trans* isomer was the major product obtained (11:1, *trans:cis*). A small amount of a coupling product was also obtained. No reaction was observed when 2-phenyl-1,3-dioxolane was used and this can be attributed to the fact that hydrogen abstraction by the photomediator generates a tertiary benzylic radical which is highly stable and non-nucleophilic and thus will not undergo addition to the alkene. It is worth noting that little or no alkylated product was observed when the thermal initiators benzoyl peroxide (3%) or AIBN (0%) were used for the reaction of 3-buten-2-one and 2-methyl-1,3-dioxolane⁶⁰.

It was concluded that the yield of alkylation depends on the efficiency of the dioxolan-2-yl radical trapping and this in turn depends on the structure of the enone. The acyclic enones performed poorly giving low yields while five- and six-membered cyclic enones, gave high yields in short reaction times. It was thought that this was due to the rigidity of the ring structures, which allowed better interaction with the dioxolan-2-yl radical for both steric and electronic reasons⁶⁰.

Fagnoni carried out similar work involving the photochemical reactions of α,β -unsaturated aldehydes and either 1,3-dioxolane or 2-alkylated 1,3-dioxolanes yielding monoprotected 1,4-dialdehydes or monoprotected 4-ketoaldehydes, respectively⁶¹ (**Scheme 41**).



Scheme 41

The reactions were carried out in an organic medium (dioxolane/acetonitrile), but changing to an organic-aqueous medium (dioxolane/acetonitrile/H₂O or dioxolane/H₂O) did not affect the yield and also offered a simpler work-up. The solution reactions in the organic phase were mediated by benzophenone, while those in the aqueous media involved the water soluble photomediator, benzophenone disodium disulfonate (BPSS) (**Figure 12**).

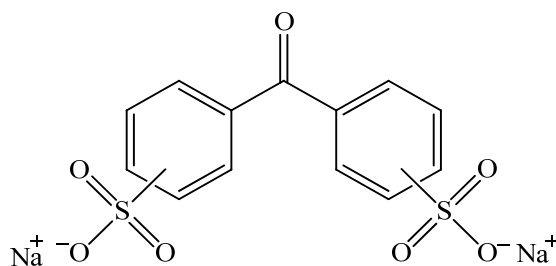
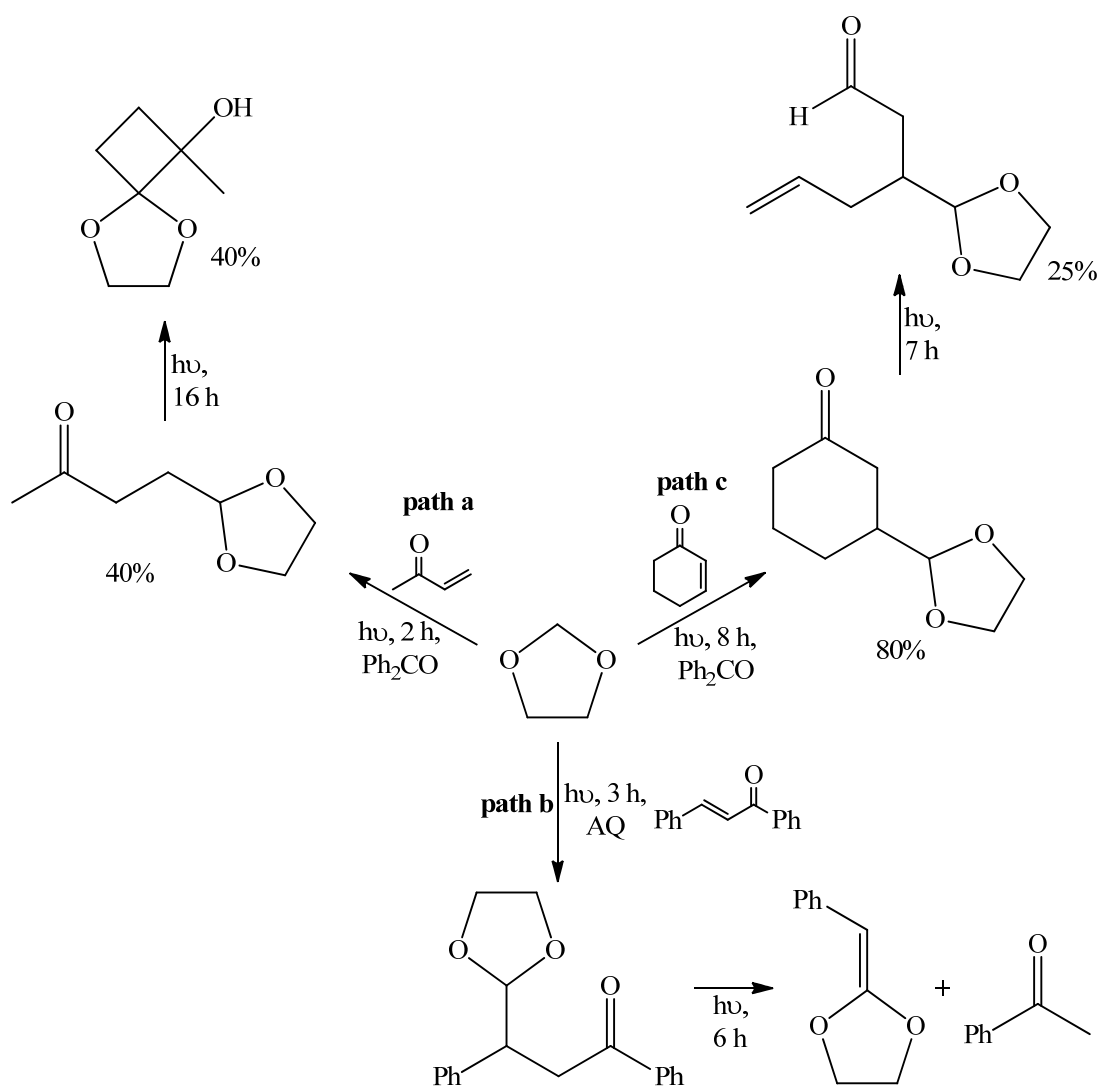


Figure 12

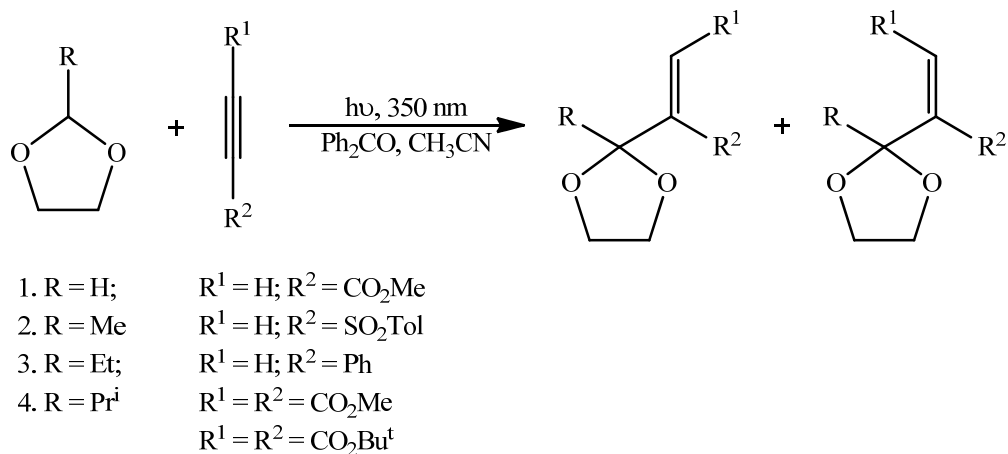
Albini and Fagnoni have also reported work relating to the photochemical synthesis of 4-oxobutanal acetals⁶². The photomediated (benzophenone/anthraquinone (AQ)) reaction of a variety of unsaturated acyclic and cyclic aliphatic ketones, and of aryl

substituted unsaturated ketones, in 1,3-dioxolane led to the formation of 4-oxobutanal acetals. These reactions were effected in mostly good yield. On further irradiation, 4-oxobutanal acetals underwent a variety of processes each typical of a ketone in the ($n-\pi^*$) state. Open chain aliphatic ketones underwent γ -hydrogen abstraction, and afforded hydroxycyclobutanols *via* a Yang cyclisation⁶³ (**path a**). Aryl derivatives underwent a Norrish Type 2 cleavage (**path b**), again involving γ -hydrogen abstraction, while cyclic ketones took part in a Norrish Type 1 cleavage (α -cleavage process) (**path c**) (**Scheme 42**).



Scheme 42

More recently, Geraghty presented work on the radical addition of 1,3-dioxolanes to both mono- and disubstituted alkynes (**Scheme 43**)³⁶. The reactions were carried out by irradiating a solution of a dioxolane (20 mmol), an alkyne (1 mmol) and a photomediator (0.4 mmol) in acetonitrile (20 ml) at 350 nm. The results were good with high yields and short reaction times.



Scheme 43

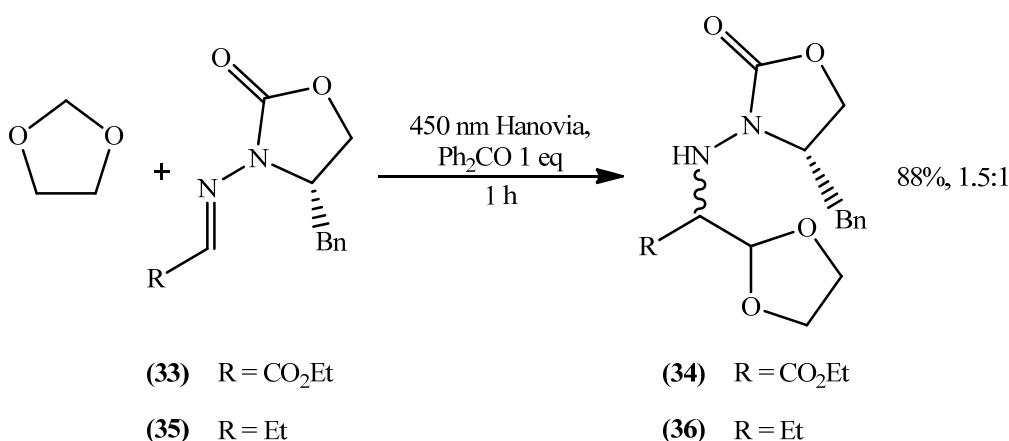
Alkyl group substitution at the 2-position was found to enhance the rate of reaction³⁶, with that between DMAD and 2-methyl-1,3-dioxolane, for example, being complete in just 15 min, affording *cis* and *trans* addition products in a combined yield of 89%.

Quantum yield studies indicated that the reaction of 2-methyl-1,3-dioxolane with DMAD and methyl propiolate occurred with quantum yields of 4.8 and 1.4, respectively. This suggests that these reactions proceed *via* a chain reaction, in which the alkenyl radical formed from the addition of the dioxolanyl radical to the alkyne, abstracts a H-atom from a molecule of dioxolane, rather than the ketyl radical formed from benzophenone. It is suggested that this occurs as a result of efficient H-abstraction from the 2-alkylated dioxolane as a result of a particularly favourable stereoelectronic effect involving the 2-H and the oxygen lone pairs of electrons.

In keeping with the reaction of 1-heptene (**Section 1.8.2, Scheme 38**), a small amount of C-4 alkenylated product is observed in reactions between 1,3-dioxolane and propiolate esters. However, no C-4 products were obtained when 2-alkylated dioxolanes were used and this is again attributed to the fact that the C-2 hydrogen

atom in these molecules enjoys a more favourable stereoelectronic interaction with the oxygen than is the case for 1,3-dioxolane itself³⁶.

1,3-Dioxolanyl radicals have been shown to undergo addition to C=N bonds and a synthetically useful application of this, due to Alonso, is the formation of amino acid derivatives⁶⁴. A solution of *N*-acyl hydrazone (**33**) and benzophenone in 1,3-dioxolane, for example, was irradiated for 1 h affording (**34**) as a mixture of diastereomers in a 1.5:1 ratio (**Scheme 44**).



Scheme 44

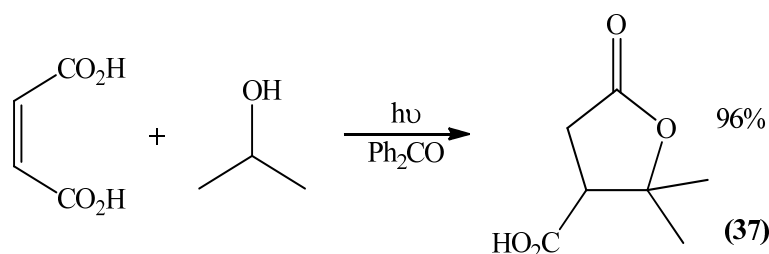
When the reaction was carried out at -78 °C, the diastereoselectivity increased to 4.1:1 but no further enhancement was achieved when the chelating agent InCl₃ was added. Alonso also found that the reaction of 1,3-dioxolane and the hydrazone (**35**)⁶⁴, which is unactivated as it bears an ethyl group rather than the electron withdrawing ethyl ester group in (**33**), proceeded well at room temperature (0.5 h), affording (**36**) in slightly higher diastereoselectivity than the activated hydrazone reaction (1.8:1). Interestingly however, the addition of InCl₃ in this case caused a significant effect, the diastereomeric ratio increasing to 10.1:1 and the reaction time being reduced. This result can be attributed to the dioxolanyl radical preferentially adding to the indium chelated *N*-acyl hydrazone on the opposite face to the benzyl group. It is worth noting that the photomediated addition of 1,3-dioxolanes has been a key step in the synthesis of a number of biologically active molecules^{65,66}.

1.8.4 The photochemical addition reactions of alcohols

The photomediated addition of α -hydroxyl radicals to unsaturated systems is another valuable method of forming carbon-carbon bonds. This again involves hydrogen abstraction from the α -position of an alcohol by a triplet state ketone and the trapping of the resulting nucleophilic radical with an electron deficient unsaturated substrate.

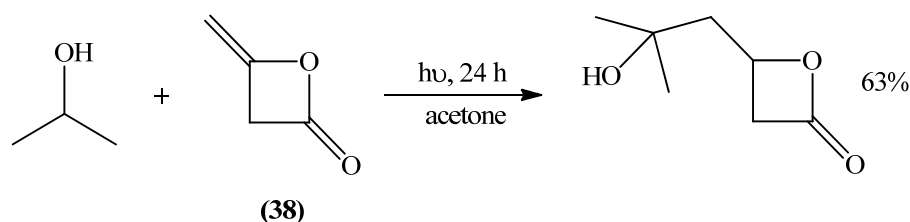
The first reported examples of the photomediated addition of alcohols to alkenes came in 1954⁶⁷. Urry demonstrated that in the presence of light, various primary and secondary alcohols could be added to unactivated alkenes under direct conditions to give addition products as well as telomeric products. He noticed that the benzyl radical failed to react with ethene providing yet another example of the resonance induced stability associated with this radical.

A synthetically useful application of the methodology was first reported in 1957 when Schenck demonstrated that terebic acid, (**37**), could be synthesised *via* the photomediated reaction of the disubstituted alkene maleic acid and 2-propanol⁶⁸ (**Scheme 45**).



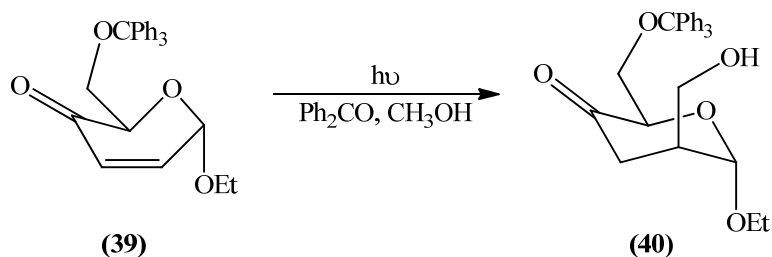
Scheme 45

The work carried out by Kato involves the addition of secondary alcohols to the exocyclic double bond of diketene⁶⁹ (**Scheme 46**). The reaction involved dissolving the diketene (**38**) in acetone containing a large excess of 2-propanol, followed by irradiation using a 400 W mercury lamp until complete reaction had occurred (24 h). The reaction is interesting as it involves radical addition to a formally electron rich alkene.



Scheme 46

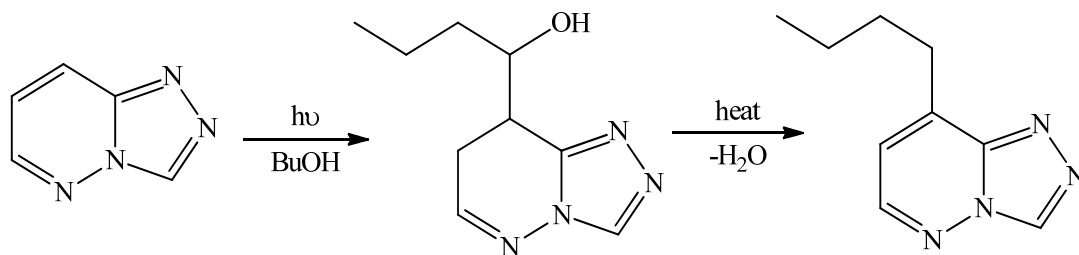
The central role photomediated hydrogen abstraction plays in the addition of methanol to enones has been described by Fraser-Reid⁷⁰. It was suggested that the reaction involved hydrogen abstraction from the α -CH bond in methanol by an excited state benzophenone affording, in the usual way, an α -hydroxyalkyl radical as well as a ketyl radical. The α -hydroxyalkyl radical then undergoes conjugate addition to, for example, the enone (39) at the β -position generating an alkyl radical; back hydrogen transfer from the ketyl radical or methanol affords the product (40) (Scheme 47).



Scheme 47

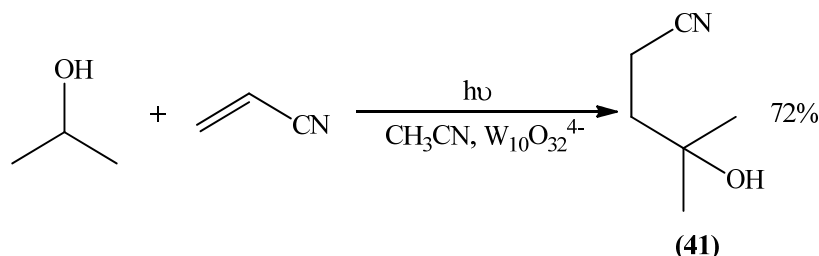
It was found that both stereoelectronic and steric effects were influential in product formation for these reactions; however, steric effects played a predominant role. The α -hydroxyalkyl radical approached the enone from the face *anti* to the axial ethoxy substituent, accounting for the observed stereochemistry of the product. Where no axial substitution was present at the γ -position, only a moderate preference for the axial product was evident.

Vernon described the addition of alcohols to maleimides⁷¹ while Bown described the addition of alcohols (present in a large excess, as is usual for reactions of this type), such as 1-butanol, to pyridazine; subsequent dehydration of the adduct rearomatises the product⁷² (Scheme 48).



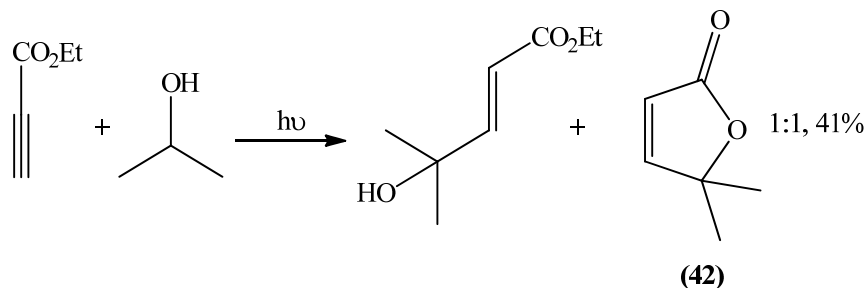
Scheme 48

The more recent work by Albini and Fagnoni demonstrating that TBADT can be used in catalytic amounts to mediate the reaction of 2-propanol and acrylonitrile in acetonitrile is of considerable synthetic importance. A single product, **(41)**, was formed in good yield (72%) (Scheme 49)⁴⁷.



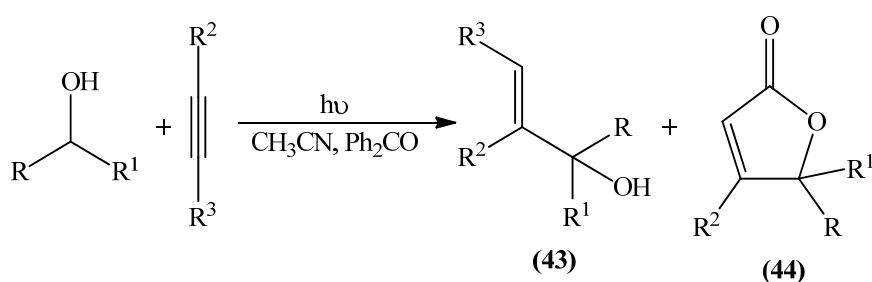
Scheme 49

In 1969, Buchi reported the first example of the photoaddition of an alcohol to an alkyne *via* direct irradiation⁴¹. Experimentally, the reaction involved a dilute solution of ethyl propiolate in 2-propanol which was irradiated, using a quartz jacketed mercury lamp emitting over a wide wavelength range, for up to two weeks, under a nitrogen atmosphere (Scheme 50). Irradiation was continued until the alkyne was completely consumed, either by conversion to products or polymerisation. The spontaneous cyclisation of the initially formed *trans* addition product generates the γ -butenolide lactone **(42)**.



Scheme 50

The long reaction times however meant that no further work was carried out in this area until relatively recently, when the use of a photomediator was shown to greatly enhance the rate and yield of reactions involving acetylenic esters¹². The scope of the reaction was extended to include primary and secondary alcohols (both acyclic and cyclic), and diols (**Scheme 51, Table 9**).



Scheme 51

	RCOHR^1	$\text{R}^2\text{C}\equiv\text{CR}^3$	Time (h)	Yield ^a (43), (44) %
a	R = Me R ¹ = Et	R ² = CO ₂ Me R ³ = H	1.75	24, 21
b	R, R ¹ = -(CH ₂) ₃ -	R ² = R ³ = CO ₂ Me	0.2	32, 29
c	R = H R ¹ = Et	R ² = R ³ = CO ₂ Me	3.25	34, -
d	R = H R ¹ = CH ₂ OH	R ² = R ³ = CO ₂ Bu ^t	0.58	67, -

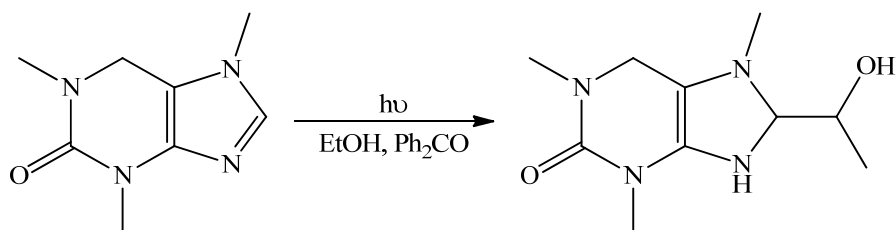
^a Isolated yields

Table 9: Benzophenone mediated reaction of acetylenic esters and various alcohols

It is also found possible to convert the *cis* addition product to the corresponding, and synthetically interesting⁷³, butenolide using *N*-bromosuccinimide (NBS). Although sub-stoichiometric amounts of the photomediator were used, the synthetic potential of this methodology was reduced by the requirement for column chromatography to

remove the photomediator. This problem led to preliminary work on the use of supported photomediators based on Merrifield resins and silica which indicated that the supported photomediators could be easily removed by filtration and that recycling was an option¹². Both of these developments enhanced the methodology from a synthetic view point. This thesis is concerned with a systematic evaluation of supported photomediators in terms of the generation of carbon radicals for synthetic purposes.

Alcohols, both primary and secondary, have also been added to C=N bonds in both a direct and photomediated manner^{58,74,75}. Under direct conditions, an electronically excited heterocyclic system abstracts a hydrogen atom from the α -CH bond of the alcohol, with subsequent recombination at the α -position forming the product. When a photomediator is employed, H-abstraction to yield an α -hydroxyalkyl radical occurs followed by addition to the heterocyclic system⁷⁶ (**Scheme 52**).



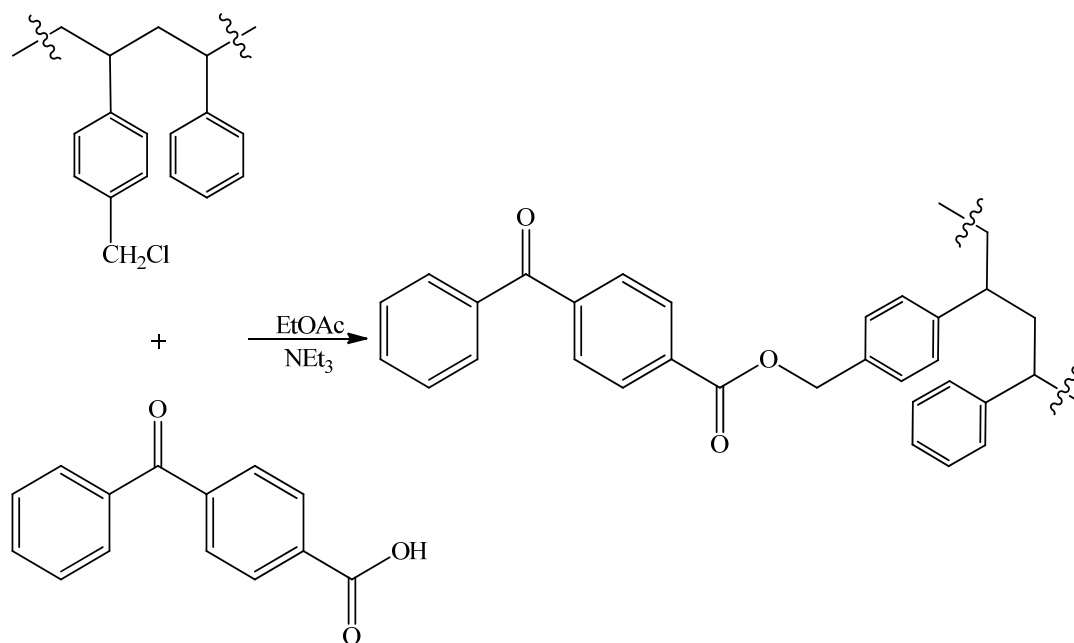
Scheme 52

1.9 Supported catalysts

The removal of benzophenone from photomediated reactions upon completion requires column chromatography which is a tedious and time consuming process that requires large amounts of solvents and often leads to the products being isolated in low yields. This has led to the use of supported photosensitisers and photomediators, in the form of silica and polymer bound benzophenone equivalents^{12,20}. Solid supports have been used for many years and have found application in many areas⁷⁷, their advantage being that the supports are easily separated from the reaction mixture by filtration, facilitating product purification, and that at least in principle they can be recycled. There are hundreds of reactions that have been mediated by solid supported reagents and substrates and these have been detailed by Fenniri⁷⁸.

Merrifield is known as the pioneer of solid phase peptide synthesis and developed what is now termed, Merrifield's resin, a chloromethylated polystyrene resin cross linked with 2% divinylbenzene⁷⁹. In 1963, it was demonstrated that an *N*-protected amino acid could be coupled *via* its carboxylic acid, resulting in an ester group which was to a great extent stable to deprotection and the conditions required for coupling reactions; it could however, be cleaved by hydrogen fluoride⁷⁹.

Early work on the use of solid supported photosensitisers by Blossey and Neckers in 1974⁸⁰ showed the remarkable advantages of supported photomediators over their soluble counterparts. It was found that conversion of coumarin to its dimers proceeded well giving purer products on simple filtration, when a benzoylated polystyrene-divinylbenzene photosensitiser (**Scheme 53**) was used instead of soluble benzophenone⁸⁰.



Scheme 53

The present work involves silica supported photomediators and so a discussion on the previous use of such supported systems is useful. In 1995, Soumillion's work described the use of some silica supported benzophenone derivatives in the *cis* to *trans* isomerisation of stillbene⁸¹. For comparative reasons, homogenous counterparts were also synthesised. The results clearly showed that the presence of an amino side chain reduced the lifetime of the triplet state of the supported sensitiser relative to benzophenone⁸¹, an effect that has been attributed to the quenching of the T₁ state *via* an intramolecular electron transfer. The amino group has been implicated in this as the reactivity is upgraded to that of benzophenone upon protonation of the amino group. In 1996, Soumillion prepared an aminopropyl silica bound photosensitiser (**45**) by reacting 2-hydroxynaphthoic acid (**46**) and 3-aminopropyl silica gel (**Figure 13**)⁸². Again, soluble equivalents were synthesised for comparison purposes. The photodechlorination of chlorinated aromatics was carried out and it was found that the grafted photomediator (**45**) was more efficient than the corresponding homogenous sensitiser (**47**) (**Figure 13**)⁸².

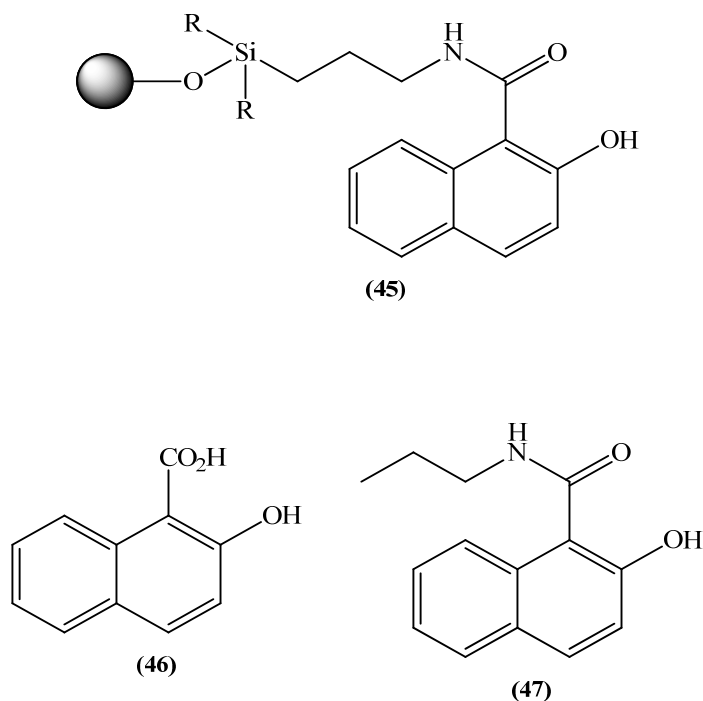


Figure 13

More recently, results have been reported that have paved the way for the work discussed in this thesis. Geraghty found that the reaction of methyl propiolate and cyclopentane could be promoted using supported photomediators. In keeping with the results obtained with benzophenone, it was found that the *E/Z* ratio was dependent on the supported photomediator used and on the length of the reaction²⁰. This was due to a secondary photosensitised *E/Z* isomerisation. No photoreactions took place when the Merrifield resin (**Figure 14**) was used on its own, proving that the reaction was due to the supported molecule. More recently supported photomediators were used to mediate the reactions of acyclic alcohols and alkynes¹². Overall, the reactions worked well, with the siloxane bonded supported photomediator (**Figure 15**) being the most efficient in terms of the reaction times. The Merrifield bound photomediator recycled poorly which, it was suggested, was possibly due to the resin adhering to the walls of the Pyrex glass. The overall conclusion was that the supported photomediators made the isolation of products easier and also facilitated the recovery and subsequent recycling of the photomediator. However, it was concluded that the silica bound photomediators were more efficient than the polymer bound photomediators, and also recycled better

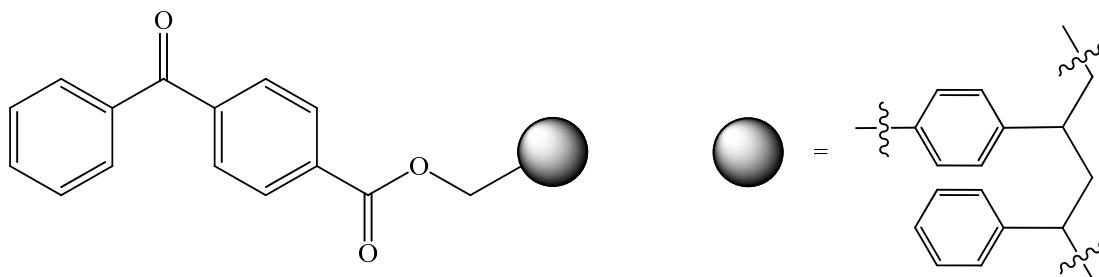


Figure 14

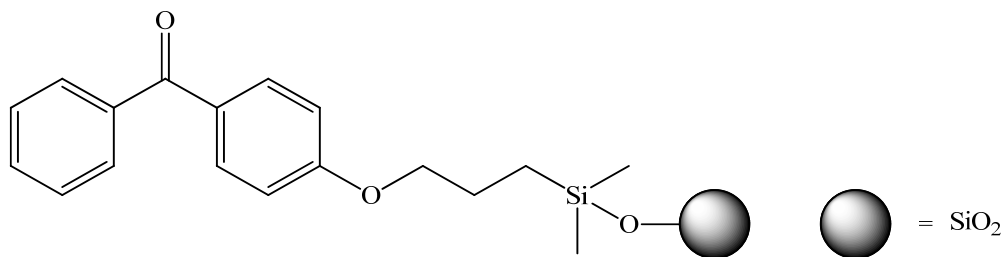


Figure 15

1.10 Molecular modelling

1.10.1 Introduction

Molecular modelling is a very useful tool for investigating, analysing and visualising chemical structures. It has been used to study the geometry, chemical properties and energy of chemical systems *in silico* and from this it is possible to predict the behaviour of molecules and outcome of reactions. In relation to this work, molecular modelling is used as an attempt to rationalise the observed reactivities of the supported photomediators synthesised. On an everyday basis, scientists use two-dimensional drawings on paper to describe reactions; however this gives little or no insight into the actual shape of molecules and makes the visualisation of what is actually happening in a molecule or a reaction, very difficult. Early work aimed at improving the visualisation of the shapes of molecules was carried out in the 1800s. In 1860, Pasteur introduced the theory of three-dimensional molecular structure and shortly after in 1865, Hoffmann is credited with being the first to use a physical model when he described methane. Interestingly, the colours he chose for the atoms are still in use today⁸³.

Further investigation into the theory of three dimensional molecular structure led Paterno in 1869, and van't Hoff and le Bell in 1874 to state that carbon compounds had a tetrahedral geometry. Almost one hundred years later, in 1959, Dreiding introduced models which represented the bonds as metal rods and the atoms as rod junctions. Another commonly used physical model is the Corey-Pauling-Koltun (CPK) model; atoms are represented by spheres whose radii are proportional to their Van der Waals radii. This is a space filling model and allows scientists to visualise the space molecules occupy. As useful as these models are, an important aspect is missing - the ability to determine the physical properties of a chemical system.

In light of this, computational models were developed to provide a visual representation as well as to allow the calculation of important physical properties. Today, many virtual models are available for calculating molecular structure and energetics, and can be classified as either molecular mechanics (MM) or quantum mechanics (QM) based models. MM was the model of choice for the work described in this thesis and so is described in detail in the following section (**Section 1.10.2**).

1.10.2 Molecular mechanics

MM describes molecules as balls and springs where the balls represent the desired atoms and the springs denote the bonds. Hooke's Law (**Equation 2**) can be used to represent this model and is used to quantify the energy associated with the spring stretching.

$$E = - kx$$

Equation 2

Here k is the force constant and this determines, for example, the strength of the bond that the spring represents. The displacement of a spring's end from its equilibrium position is represented by x .

The energy of the molecule varies with changes in structural features such as bond length, bond angle and torsion angle, non-bonded interactions such as van der Waals, and Coulombic effects (**Figure 16**).

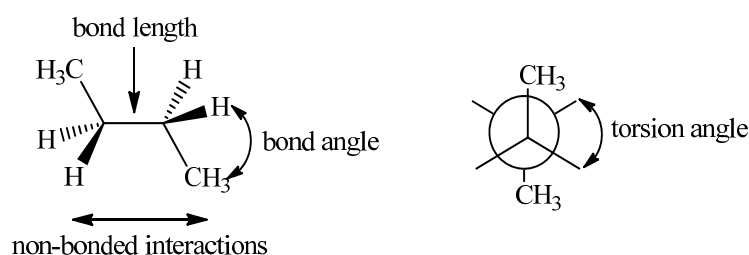


Figure 16

Overall, the forces involved in determining these features describe a forcefield (**Equation 3**)⁸⁴ which gives rise to an energy that is commonly referred to as strain energy as it defines the strain felt by real molecules relative to ideal molecules⁸⁵.

$$E = E_{\text{bonds}} + E_{\text{bond angles}} + E_{\text{torsion angles}} + E_{\text{vdw}} + E_{\text{coulombic}}$$

Equation 3

Bond energy (E_{bonds})

This energy is caused by the compression or stretching of bonds from their normal length and is calculated using Hooke's Law:

$$E_{\text{bonds}} = k_{\text{bonds}}(l - l_{\text{eq}})^2$$

Equation 4

The difference between the natural bond length (l_{eq}) and the actual bond length (l), and the force constant k which reflects the resistance of a bond to stretching, determines the bond energy.

Bond angle energy (E_{angles})

Upon distorting the bond angle of a molecule from its equilibrium or natural position, the strain energy increases. The equilibrium bond angle is given by θ_{eq} and the actual bond angle is represented by θ . The bond angle energy is again calculated using Hooke's Law (**Equation 5**):

$$E_{\text{angles}} = k_{\text{angles}}(\theta - \theta_{\text{eq}})^2$$

Equation 5

Torsion angle energy (E_{torsion})

The torsion angle (**Figure 16**) is the apparent angle between two adjacent C-X bonds when viewed along the connecting C-C bond. Rotating the substituents around this C-C bond results in a change in torsion energy (**Figure 17, X = H**).

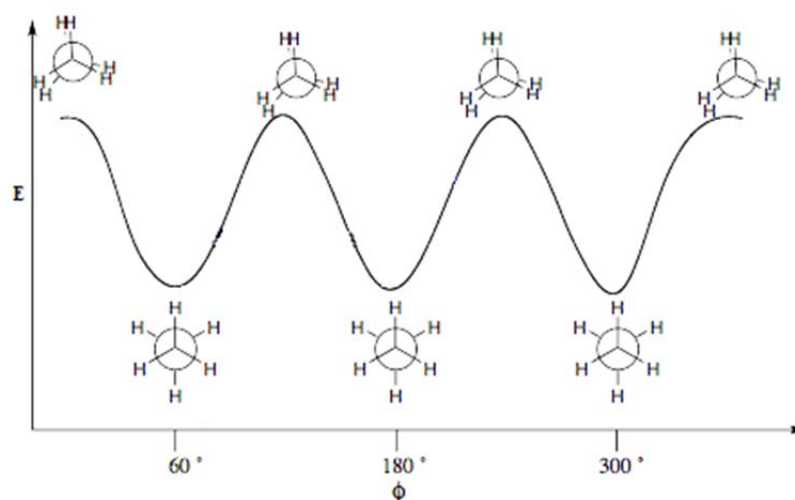


Figure 17

The torsion angle energy rises and falls as rotation occurs and so a mathematical description of this energy requires a periodic function. The variation in the torsion angle energy, also referred to as the dihedral angle energy, can thus be given by a trigonometric function (**Equation 6**). The parameters A and n relate to the size of the barrier to rotation and the periodicity, respectively. Although the energy of rotation is often low, it is this torsion strain that can lead to a molecule preferring a particular conformation⁸⁶.

$$E_{\text{torsion}} = A[1 + \cos(n\phi)]$$

Equation 6

van der Waals energy (E_{vdw})

The van der Waals energy is the sum of the repulsion and attraction between atoms that are not bonded directly to one another (**Equation 7**).

$$E_{\text{vdw}} = \frac{A}{r^{12}} - \frac{B}{r^6}$$

Equation 7

In the above equation (**Equation 7**), A and B are system dependent parameters while r is the distance between the interacting non-bonded atoms. A small attraction is observed for a large separation, while at short distances E_{vdw} becomes repulsive, the electrons repelling each other as the electron clouds of the atoms involved begin to

overlap. Weak attractive forces, also known as dipole-dipole interactions, occur for intermediate distances and the energy is at a minimum when the atoms are separated by a distance equal to the sum of their VDW radii^{84,86}.

Coulombic energy ($E_{\text{coulombic}}$)

The Coulombic energy takes into account the interaction of charges in a molecule⁸⁷. This energy can be calculated using Coulomb's Law (**Equation 8**), where q_1 and q_2 are the charges and r is the distance between them.

$$E_{\text{coulombic}} = \frac{1}{4\pi\epsilon} \frac{q_1 q_2}{r}$$

Equation 8

For a given system, the energy of different conformations, due to the factors discussed above, is calculated to determine the minimum energy conformation. This structure optimisation or energy minimisation procedure will eventually locate an energy minimum corresponding to a low energy conformation⁸⁴.

A central problem in this energy minimisation/structure optimisation procedure is how to distinguish a structure corresponding to a local minimum from that corresponding to the global minimum. This is discussed below (**Section 1.10.3**).

The number and nature of the terms considered, as well as the parametrisation incorporated (together termed the forcefield), differentiates the MM models available. Some forcefields such as SYBYL, which was developed in 1989, do not give quantitatively accurate results. The MMFF forcefield used in the molecular modelling studies reported in this thesis, which was developed by Merck Pharmaceuticals, is better able to provide a quantitative account of geometry and conformation on a molecular level⁸⁵.

1.10.3 Conformational searching

The main advantage of MM is the speed at which calculations can be performed. MM allows for the optimisation of molecules with thousands of atoms. It is thus of considerable importance in terms of the conformational analysis of such molecules. Conformational isomers are molecules with the same molecular formula and connectivity, but with different arrangements in space; unlike configurational

isomers they can be interconverted through rotation around one or more single bonds. Initially when a molecule is minimised in energy, one possible low energy conformer is obtained. A key question is whether this conformer represents a local or global energy minimum. Conformational searching is used to find all low energy conformers and to rank them in order of their energies. Since large molecules can have large numbers of conformations, a semi-random approach termed Monte Carlo searching is used. Monte Carlo searching works on the basis that low energy conformations have structural features in common and thus by selecting one of these low energy geometries and making small alterations, other low energy conformers should be obtained.

The molecule's structure is optimised in the usual way and the resulting structure is saved. A small change is made in the geometry and the resulting structure is used as the starting point for a new optimisation. The new optimised structure is compared to that obtained initially and if it is of lower energy, the first one is discarded. If it is of higher energy, it is discarded. Normally, all structures within a certain energy window, say 10 kJ mol^{-1} about the global minimum are saved⁸⁸.

Although MM works very well for the systems studied here, there are a few limitations. MM may not be very successful in describing structures of new molecules with unusual structures as suitable parameters may not be available. In addition, only equilibrium geometries and conformations are available as MM forcefields have not been parametrised to deal with non-equilibrium forms such as transition states. Finally, even though modelling of chemical reactivity and selectivity requires knowledge of the electron density, MM does not deal explicitly with electrons in orbitals⁸⁹. Despite this, the success of MM in modelling an enormous range of molecular systems is remarkable. This is very encouraging as when one is dealing with large molecules, from polysaccharides and proteins to the molecular systems considered in the work reported here, MM is the only viable computational method.

1.10.4 Quantum mechanics

1.10.4.1 Basic concepts

Quantum chemical models are based on the Schrödinger equation (**Equation 9**) which was first published in 1925, and explicably treats molecules as a combination of nuclei and electrons. As a result quantum chemical models are fundamentally different to MM models which completely ignore electrons. The geometry of a molecule is determined by the minimum energy arrangement of the nuclei; however, the Schrödinger equation is only useful for one electron systems, that is, a hydrogen atom. This led to the development of approximations which could take into account multiple electron systems and these various approximations give rise to a number of different quantum chemical models, all of which vary in terms of reliability, capability and cost.

$$E\Psi(X)=\Psi(X)\left[-\frac{1}{2}\nabla^2-\frac{Z}{r}\right]$$

Equation 9

In the Schrödinger equation, the kinetic and potential energy of an electron, at a distance r from a nucleus of charge Z , is given by the term in brackets, where ∇^2 represents a differential equation that takes into account the three dimensional nature of the atom, Ψ is a function of the electron coordinates, X is a wavefunction describing the motion of an electron as fully as possible, and E is the electronic energy in atomic units.

The major limitation of the Schrödinger equation is the fact that, as mentioned above, it is only useful for a hydrogen atom and so approximations are needed to give practical methods for solving the equation for multiple electron systems. The most commonly used approximations are described below.

Born-Oppenheimer Approximation

This approximation assumes that the nuclei are almost static with relation to the rapidly moving electrons and simplifies the Schrödinger equation, allowing systems of more than one electron to be studied. The energy of the molecule is then obtained by adding the solution of the Schrödinger equation to the internuclear repulsion.

Hartree-Fock Approximation

This approximation assumes that the electrons move independently of one another. In practice, electrons are thought to move in molecular orbitals which are determined using the Hartree-Fock Approximation which assumes that the electron is moving within an average field of all the other electrons.

Linear Combination of Atomic Orbitals Approximation

The Hartree-Fock Approximation yields a set of equations, each involving coordinates for a single electron. These one electron solutions of multiple electron systems are similar to single electron system and knowing that molecules are made up of atoms, it is reasonable to assume that molecular solutions can be made up of atomic solutions. The Linear Combination of Atomic Orbitals Approximation transforms the set of single electron equations obtained from Hartree-Fock Approximation into an algebraic form which describes the electronic structure of a molecule⁹⁰.

These approximations are the most widely used and provide a starting point for the majority of quantum models. The main models used are described briefly below (**Section 1.10.4.2**).

1.10.4.2 QM models

***Ab initio* methods**

The term, *ab initio*, is Latin for “from the beginning” and these methods are so called as they do not involve any empirical or even semi-empirical parameters in their equations but are derived directly from theory. In this case, the molecular structure is based on the values for the fundamental constants, the Schrödinger equation and the atomic numbers of the atoms present. However, as the equation cannot be solved completely, a method is chosen that gives rise to an approximate solution⁹⁰. This method is implemented by selecting a basis set which is a combination of simpler functions called basis functions. These basis functions can be used to generate an atomic orbital and through the process of linear combination, molecular orbitals are formed⁹¹. Many basis sets are used including, the minimal basis set STO-3G, the split valence basis sets 3-21G, 6-31G and 6-311G, the polarisation basis sets 6-31G*, 6-31G** and 6-311G** as well as the diffuse function basis sets 6-31+G* and 6-

31++G*. The simplest kind of *ab initio* calculation is the Hartree-Fock calculation and a solution to the Schrödinger equation is obtained by replacing actual electron-electron interactions with the interaction between a single electron and the average field created by all the other electrons.

Semi-empirical methods

Semi-empirical methods are simplified versions of Hartree-Fock models, which involve the use of both theory and experimental data. The calculations are restricted to the valence electrons and these are then represented by basis sets. Semi-empirical methods reduce the overall computation time by assuming that atomic orbitals of different atomic centres do not overlap. This therefore simplifies the evaluation of electron repulsion terms.

Correlated models

In the Hartree-Fock model the motions of individual electrons are treated as being independent of each other in an average field created by all the other electrons. As a result of this, an unrealistic image emerges of the electrons interacting to a greater extent than is actually the situation, and this leads to a higher energy than is in fact the case in reality⁹¹. Electron correlation accounts for coupling of electron motions and reduces the total energy. The correlation energy is given by the difference between the Hartree-Fock energy and the experimental energy. There are many correlation models available but the main models used are the Møller-Plesset model and density functional models.

Møller-Plesset models

This model enhances the Hartree-Fock model by mixing ground-state and excited-state wavefunctions but is more costly than the Hartree-Fock model. It uses electron correlation based on perturbation theory. The Møller-Plesset approach involves the calculation of more complex realistic systems by using an altered, perturbed, version of the ideal system which is not much different to the system being considered. MP2 is the simplest Møller-Plesset model, and involves making a slight perturbation to the energy calculated using the Hartree-Fock model. The energy is lowered as the electrons are promoted from occupied to unoccupied molecular orbitals and so can better avoid each other⁹¹. Higher order Møller-Plesset models such as MP3 and MP4 have been formulated but are better suited to very small molecular systems⁹⁰.

Density functional models

This particular model is used to determine the electronic structure of matter in terms of electron density rather than molecular wavefunctions. Electron density is an experimentally measurable quantity, unlike a wavefunction, and can be calculated by X-ray diffraction or electron diffraction. Electron density models are based on three variables, the spatial coordinates, x , y and z . Thus while the complexity of the wavefunction increases with the number of electrons, the electron density will have the same number of variables, independent of the size of the system⁸⁶.

Density Functional Theory (DFT) was introduced in two papers in the 1960s, the first in 1964 by Hohenburg and Kohn⁹² and the second in 1965 by Kohn and Sham⁹³. Hohenburg and Kohn developed and proved two theorems that are implemented using the Kohn-Sham equations. The first theorem states that all the properties of a molecule in a ground electronic state are determined by the ground state electronic density and the second theorem states that any electron density calculation must give an energy greater or equal to the true energy of the molecule.

The Kohn-Sham equations are used to express the ground state electronic energy as the sum of the electron's kinetic energy, the electron-nuclear interaction energy, the Coulombic interaction of the electrons and the exchange-correlation energy⁹⁰. All of these components depend on the electron density, except for the kinetic energy. Unfortunately the exchange-correlation energy is an unknown functional (effectively a rule that transforms a function into a number) and thus can only be approximated. Nonetheless, DFT calculations are one of the most successful quantum mechanical approaches available.

1.11 Aims of this project

As outlined above, the photomediated generation of carbon-carbon bonds *via* carbon radicals is very attractive. While this approach has proven to be very successful¹², there are some drawbacks. The main disadvantage of this method is the need to remove up to 1 eq. of the photomediator from the reaction product. This requires column chromatography which can be a tedious process requiring large volumes of solvent. Furthermore, it has been found that photochemical reactions involving aromatic ketones, the most commonly used photomediators, can involve the competitive formation of the ketyl radical dimers thus removing the photomediator from the reaction cycle.

It was in light of these drawbacks that silica supported photomediators were considered on the basis that it should be possible to easily remove them from the reaction product by simple filtration. This would not only allow the rapid isolation of products without the need for column chromatography, but would also allow the photomediator to be recovered and recycled. It was also envisioned that ketyl radical dimerisation would be less of a problem with supported photomediators as the recombination of surface bound radicals should be less efficient than that of radicals in solution.

It was planned to synthesise a range of silica bound photomediators and to assess their preference in the context of a range of representative hydrogen donors and electron deficient unsaturated systems. It was also planned to develop a molecular modelling approach which would allow the rationalisation of the reactivities of the supported photomediators.

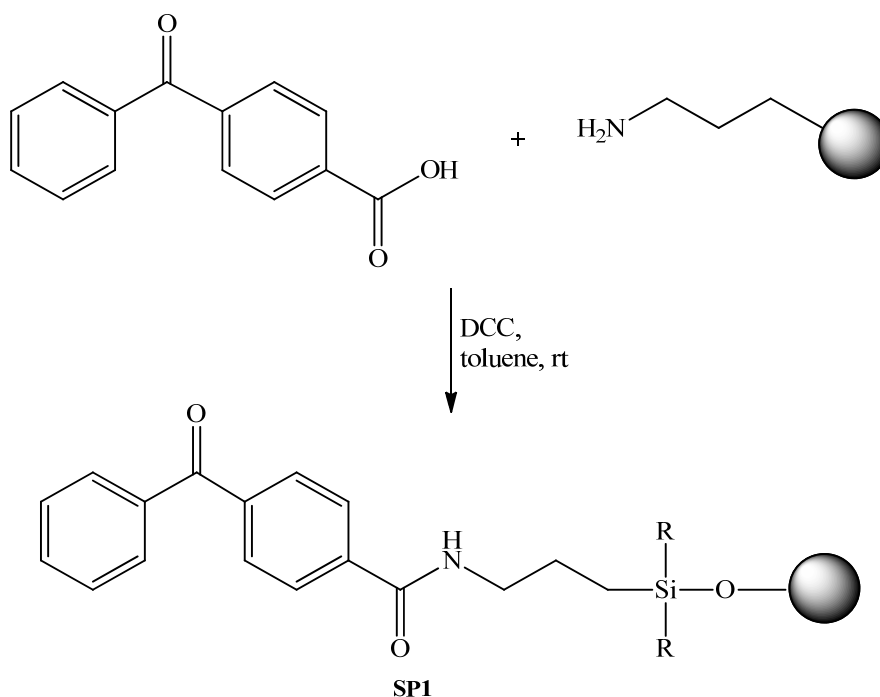
Chapter 2

Results and discussion

2.0 Results and discussion

2.1 Preparation of supported photomediators

2.1.1 Synthesis of 3-aminopropyl silica bound benzophenone⁸² SP1

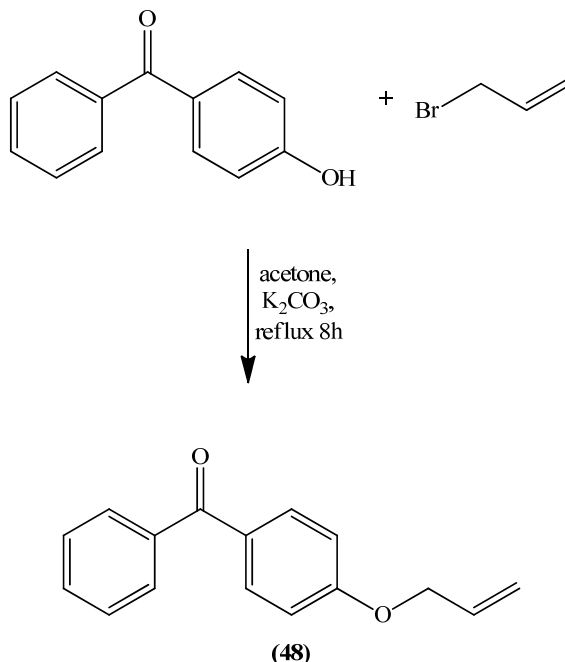


Scheme 54

The synthesis of the supported photomediator **SP1** was carried out following a previously reported procedure of Ayadim⁸¹ (**Scheme 54**). *p*-Benzoylbenzoic acid and *N,N'*-dicyclohexylcarbodiimide were dissolved in dry toluene and 3-aminopropyl silica, which was previously dried in a vacuum oven, was added. The mixture was left to stir, under nitrogen, at room temperature (rt) for two days and following this the solid was filtered off. The solid was placed in a soxhlet thimble and washed with a range of solvents: toluene, methanol, ethanol and diethyl ether. The resulting white solid, (**SP1**), was then dried in a vacuum oven and stored in a desiccator prior to use. The loading was determined gravimetrically on the basis of the masses of the silica used and of the supported photomediator. A loading of 1.60 mmol photomediator/g was obtained.

2.1.2 Synthesis of propyl linked 4-hydroxybenzophenone silica SP2

2.1.2.1 Synthesis of 4-(allyloxy)benzophenone (**48**)⁹⁴



Scheme 55

Following the procedure by Prucker⁹⁴, 4-hydroxybenzophenone and allyl bromide were dissolved in acetone and potassium carbonate was added. After heating the mixture at reflux for 8 h the product was isolated using standard work-up procedures, including extraction with sodium hydroxide solution. Purification by recrystallisation from ethyl acetate gave 4-(allyloxy)benzophenone (**48**) as a white solid in a yield of 86%. The physical and spectroscopic data obtained were in good agreement with the data in the literature^{94,95}. In the IR spectrum, the main absorption bands were due to the carbonyl group (1638 cm⁻¹), the olefinic double bond (1598 cm⁻¹) and the C-O bonds (1247 and 1172 cm⁻¹). The ¹H-NMR spectrum (**Figure 19**) had a double triplet at δ 4.62 ($J_{LR} = 1.6$ Hz, $J_{vic} = 5.2$ Hz) due to the OCH₂ protons, while a proton (H_A) of the olefinic CH₂ resonated as a double quartet at δ 5.33 due to *geminal* ($J_{gem} = 1.6$ Hz), long range ($J_{LR} = 1.6$ Hz) and *cis vicinal* coupling ($J_{cis} = 10.4$ Hz). Similarly, the other proton (H_B) of the terminal CH₂ resonated as a double quartet at δ 5.44 ($J_{gem} = J_{LR} = 1.6$ Hz, $J_{trans} = 17.2$ Hz) (**Figure 18**). The olefinic CH proton appeared as a multiplet at δ 6.07. The ¹³C-NMR spectrum was as expected, with a

signal at 195.7 ppm due to the carbonyl group and a signal at 162.3 ppm due to the aromatic carbon attached to the OCH₂ group. Seven signals were observed for the other aromatic carbons, the methine olefinic carbon resonated at 132.6 ppm and the signal for the terminal carbon of the alkene was observed at 118.3 ppm. The remaining signal at 69.0 ppm was due to the carbon of the OCH₂ group.

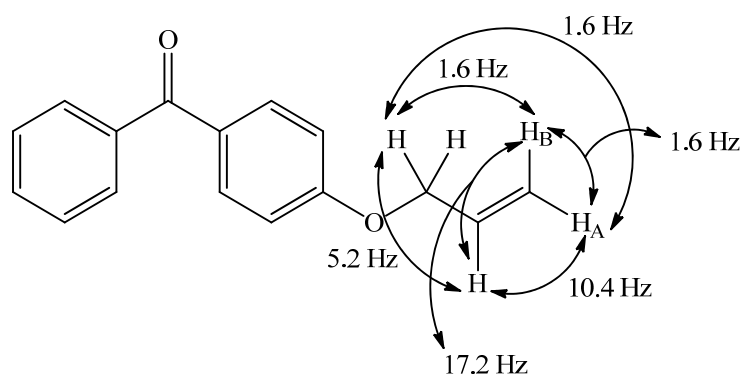


Figure 18: ¹H-NMR coupling constants for (48)

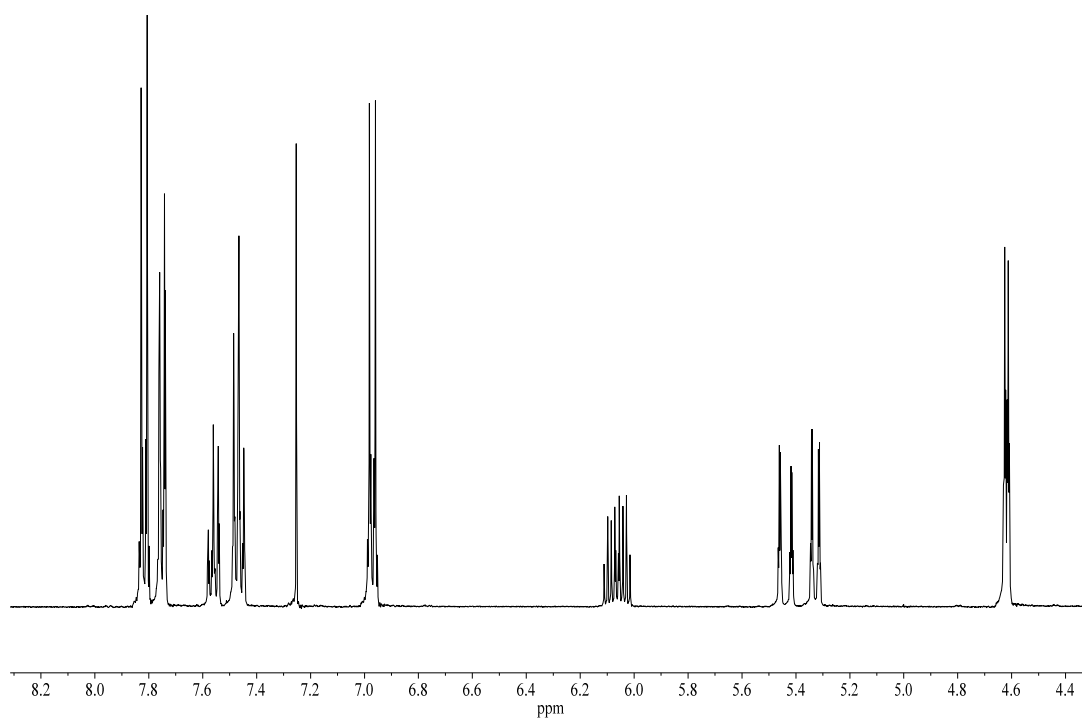
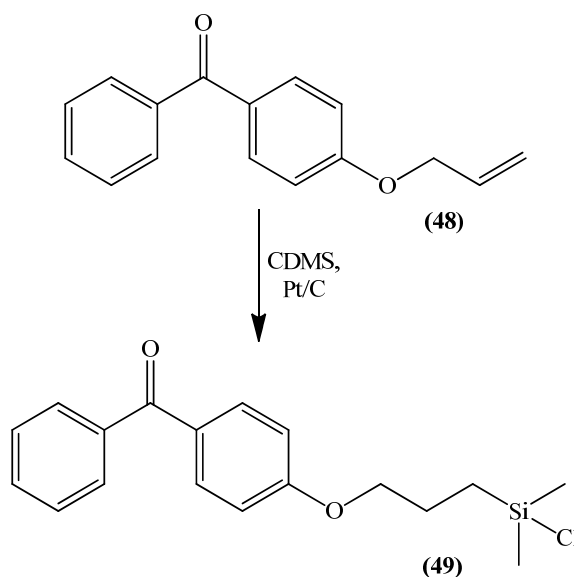


Figure 19: ¹H-NMR spectra of (48)

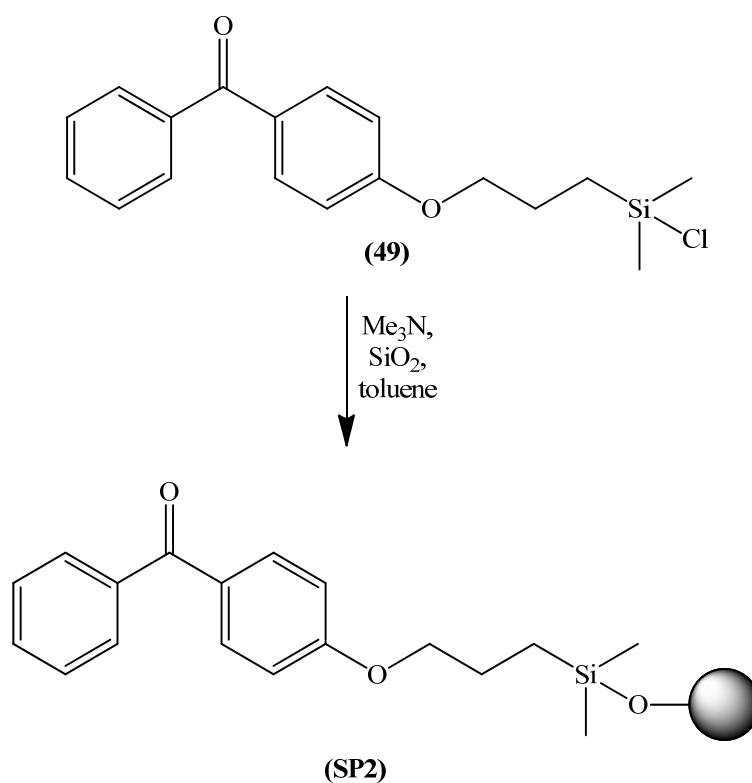
2.1.2.2 Synthesis of 4-[3-(chlorodimethylsilyl)propyloxy]benzophenone (**49**)⁹⁴

Scheme 56

Platinum on carbon was added to a solution of **(48)** in chlorodimethylsilane (CDMS) and the solution was heated at reflux. TLC confirmed that the reaction was complete after 6 h. The catalyst was filtered off and excess chlorodimethylsilane was removed by distillation leaving 4-[3-(chlorodimethylsilyl)propyloxy]benzophenone (**49**), as a colourless oil in a good yield (88%). The spectroscopic data correlated well with those published previously⁹⁴. The IR spectrum had absorption bands for the carbonyl group and the olefinic double bond at 1652 and 1598 cm^{-1} , respectively, and absorption bands for the C-O bonds appeared at 1247 and 1171 cm^{-1} . In the $^1\text{H-NMR}$ spectrum, a singlet at $\delta 0.45$ accounted for the two methyl group protons and the protons of the CH_2 group attached to the silicon group resonated as a multiplet at $\delta 0.96\text{-}1.00$. A multiplet for the central CH_2 group was observed at $\delta 1.90\text{-}1.97$, and a triplet at $\delta 4.02$ ($J_{\text{vic}} = 6.4$ Hz) accounted for the OCH_2 protons.

In the $^{13}\text{C-NMR}$ spectrum, signals for the carbonyl and aromatic carbons were as expected. The OCH_2 carbon resonated at 70.0 ppm, the central methylene carbon appeared at 23.0 ppm and the methylene carbon attached to the silicon resonated at 15.3 ppm. The remaining signal at 1.8 ppm was due to the two methyl carbons.

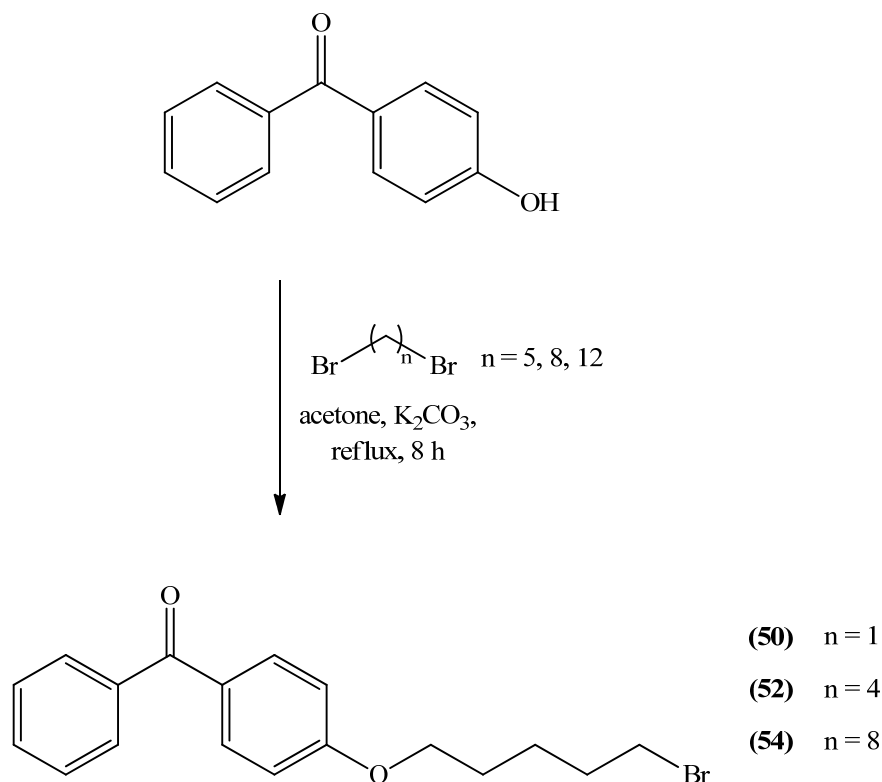
2.1.2.3 Attachment of 4-[3-(chlorodimethylsilyl)propoxy]benzophenone to silica



Scheme 57

The chloro silane (49) was dissolved in toluene containing trimethylamine. Silica, previously dried in a vacuum oven, was then added and the mixture was left to stand overnight. The solid, SP2, was filtered off and washed with chloroform before being dried in a vacuum oven. The loading for SP2 was calculated gravimetrically in a similar fashion to that used for SP1. This showed that SP2 contained 2.90 mmol photomediator/g.

2.1.3 Synthesis of the silica supported C-5 quaternary ammonium salt SP3

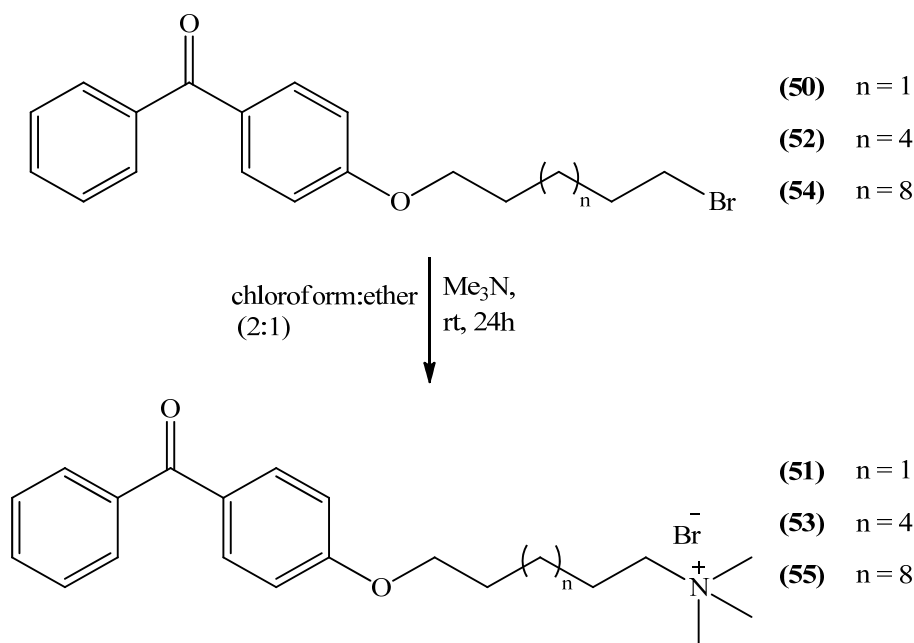
2.1.3.1 Preparation of 4-(5-bromopentyloxy)benzophenone⁹⁶ (**50**)

Scheme 58

A series of silica supported quaternary ammonium salts were synthesised, starting with one having a C-5 chain linking the benzophenone moiety to the silica surface. The bromoalkylated hydroxybenzophenone, (**50**), was synthesised following a previously published method⁹⁶. 4-Hydroxybenzophenone and 1,5-dibromopentane were dissolved in acetone and potassium carbonate was added. The solution was heated at reflux for 8 h. Standard work-up, removal of excess dibromopentane by kugelrohr distillation and column chromatography of the resulting yellow oil gave 4-(5-bromopentyloxy)benzophenone (**50**) as a colourless oil in excellent yield (90%). Analysis of the IR spectrum showed absorptions at 1639, 1601 and 744 cm^{-1} , corresponding to the carbonyl group, the aromatic carbon-carbon bonds and the C-Br bond, respectively. The $^1\text{H-NMR}$ contained a series of multiplets from $\delta 1.65$ - 1.97 due to the three central CH_2 groups while the protons of the $\text{CH}_2\text{-Br}$ group resonated as a triplet at $\delta 3.44$ ($J_{vic} = 6.7$ Hz). The OCH_2 protons also appeared as a triplet at

$\delta 4.04$ ($J_{vic} = 6.3$ Hz). The signals of the ^{13}C -NMR were in agreement with those observed previously⁹⁴.

2.1.3.2 Synthesis of *N,N,N,N*-5-(4-benzoylphenoxy)pentyltrimethyl ammonium bromide



Scheme 59

The bromo compound was dissolved in a 2:1 chloroform ether solution and trimethylamine was added, using the method reported by Hassoon⁹⁷. The solution was stirred at rt for 48 h which led to the formation of a white precipitate. The solid was filtered off and the solution was washed with diethyl ether to remove unreacted bromide, leaving *N,N,N,N*-5-(4-benzoylphenoxy)pentyltrimethyl ammonium bromide (**51**) as a white solid. The melting point obtained was 164.8-165.3 °C. The IR spectrum confirmed that no unreacted bromide was present as the C-Br absorption had disappeared. The ^1H -NMR spectrum (**Figure 20**) showed multiplets at $\delta 1.56$ -1.63 and $\delta 1.82$ -1.92 for the protons of the three central CH_2 groups while the CH_2N protons appeared as a multiplet at $\delta 3.65$ -3.70. A triplet at $\delta 4.05$ was observed for the OCH_2 protons. The protons of the three methyl groups attached to the nitrogen appeared as a singlet at $\delta 3.44$ ppm.

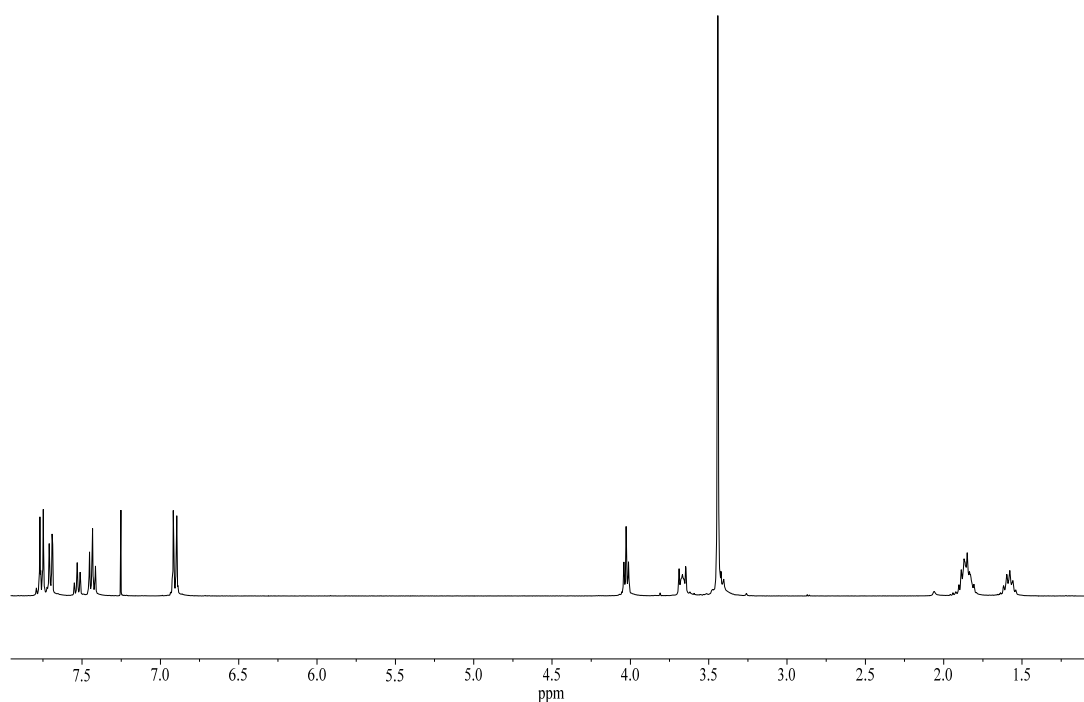


Figure 20: ^1H -NMR spectra of (51)

The ^{13}C -NMR showed signals characteristic of the carbonyl carbon and of the aromatic carbon attached to the oxygen atom at 195.7 and 162.5 ppm, respectively. The OCH_2 and NCH_2 carbons resonated at 67.6 and 66.8 ppm, respectively, while the remaining aromatic signals were observed between 138.2 and 114.2 ppm. The three methyl carbons appeared at 53.6 ppm while the central CH_2 appeared at 28.7 ppm. The remaining two CH_2 groups were evident as an unresolved signal at 23.0 ppm.

2.1.4 Synthesis of silica supported C-8 quaternary ammonium salt SP4

2.1.4.1 Preparation of 4-(8-bromooctyloxy)benzophenone (**52**)⁹⁸

The longer C-8 chain bromoalkylated hydroxybenzophenone (**52**) was synthesised in the same manner as (**50**) (Scheme 58), and was obtained in 89% yield. The IR and ¹H-NMR spectra (Figure 21) were similar to the corresponding spectra obtained for (**50**).

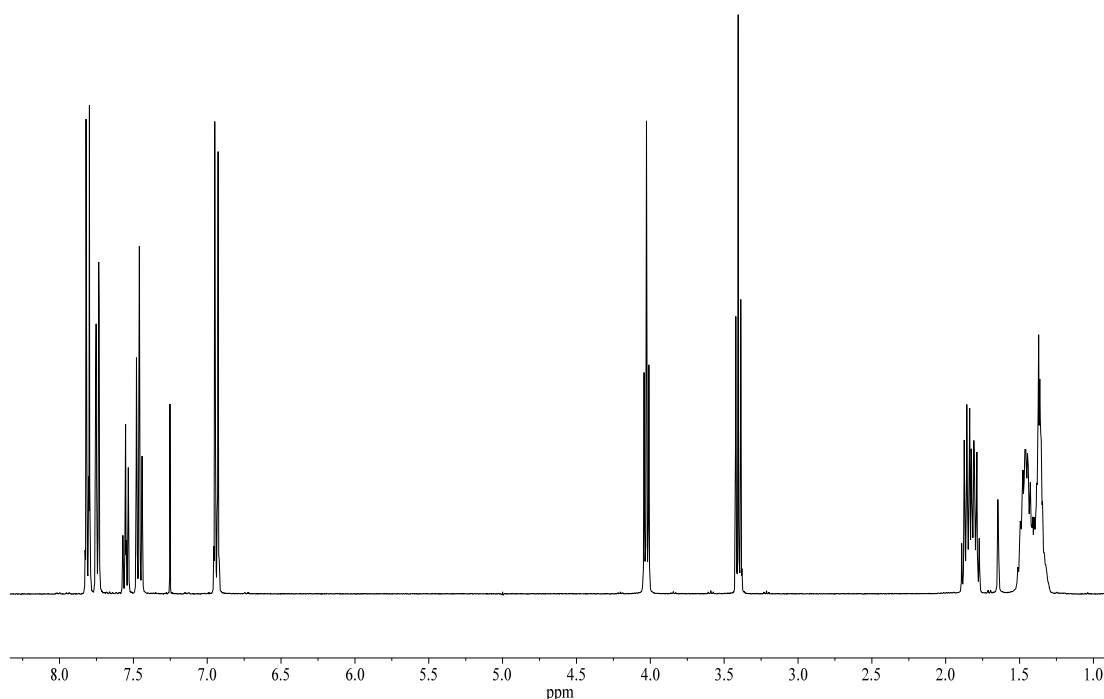


Figure 21: ¹H-NMR spectra of (**52**)

The ¹³C-NMR contained signals for the carbonyl group and the aromatic carbon attached to the oxygen atom at 195.6 and 162.9 ppm, respectively, as well as seven signals corresponding to the remaining aromatic carbons. The OCH₂ and CH₂Br carbons appeared at 68.3 and 34.1 ppm, respectively. The remaining signals, due to the other methylene carbon atoms, were as expected.

2.1.4.2 Synthesis of *N,N,N,N*-8-(4-benzoylphenoxyoctyl)trimethyl ammonium bromide (**53**)

The synthesis of the quaternary ammonium salt (**53**) was carried out as for the quaternary ammonium salt (**51**) (Scheme 59). *N,N,N,N*-8-(4-benzoylphenoxyoctyl)trimethyl ammonium bromide (**53**) was obtained as a white

solid in 65%, and had a melting point of 171.6-172.5 °C. The spectroscopic data were very similar to those obtained for **(51)** (Section 2.1.3.2).

The $^1\text{H-NMR}$ spectrum (**Figure 22**) contained multiplets at δ 1.37-1.48 due to the protons of four CH_2 groups and multiplets at δ 1.70-1.81 due to the protons of two other CH_2 groups. The protons of the three methyl groups attached to the nitrogen appeared as a singlet at δ 3.45 and a multiplet at δ 3.56-3.60 was observed for the protons of the CH_2 group attached to the nitrogen. The OCH_2 protons resonated as a triplet at δ 4.01 ($J_{vic} = 6.4$ Hz). As expected, the aromatic protons appeared as a series of multiplets at δ 6.92-7.78.

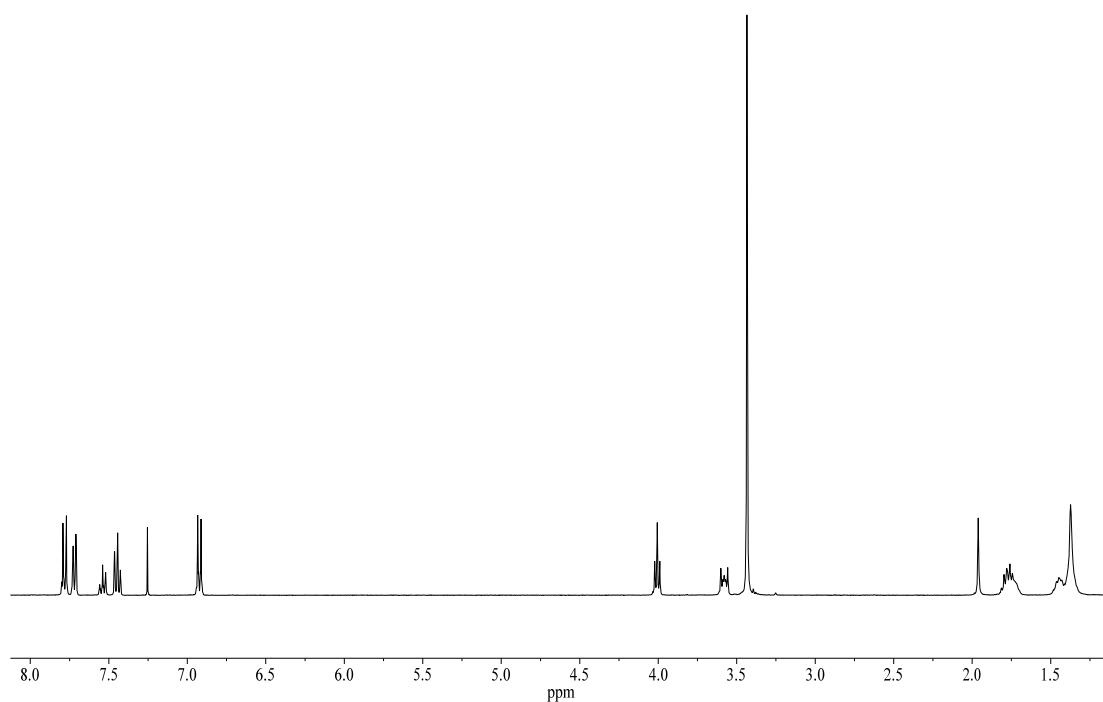


Figure 22: $^1\text{H-NMR}$ spectra of **(53)**

In the $^{13}\text{C-NMR}$, the signals for the carbonyl carbon and the aromatic carbon attached to the oxygen atom were as expected, while a series of signals was observed for the other aromatic carbons at 138.4-114.1 ppm. The OCH_2 and CH_2Br carbons resonated at 68.2 and 67.0 ppm, respectively, while the carbons of the methyl groups appeared at 53.5 ppm. A series of six peaks was observed for the CH_2 carbons of the alkyl chain (29.2-23.3 ppm).

2.1.4.3 Attachment of the quaternary ammonium salt (53) to silica

The quaternary ammonium salt, (53), was attached to the silica surface using **Method A (Section 2.1.3.3)** and this was dried in a vacuum oven prior to use. Gravimetrically (**Section 2.1.1**), this supported photomediator contained 0.30 mmol photomediator/g.

2.1.5 Synthesis of silica supported C-12 quaternary ammonium salt SP5

2.1.5.1 Preparation of 4-(12-bromododecyloxy)benzophenone (54)

The synthesis of 4-(12-bromododecyloxy)benzophenone (**54**) was carried out as for (**50**) and (**52**). The bromide was obtained as a white solid with a melting point of 69.2-70.4 °C (73-75 °C⁹⁹). The spectroscopic data agreed with those reported previously⁹⁹. The IR spectrum was almost identical to those obtained for the C-5 and C-8 bromides (**50**) and (**52**). The ¹H- and ¹³C-NMR spectral data for (**54**) were the same as those reported by Nakagaki in 1999⁹⁹. The ¹H-NMR spectrum contained multiplets at δ 1.35-1.78 for ten CH₂ protons and triplets at δ 3.34 ($J_{vic} = 6.8$ Hz) and δ 3.98 ($J_{vic} = 6.5$ Hz) due to the CH₂Br and OCH₂ protons, respectively. The aromatic protons appeared as a series of multiplets at δ 6.90-7.77. The ¹³C-NMR spectrum for (**54**) was very similar to that obtained for (**52**), with the main difference being the presence of two extra signals due to the extra CH₂ carbons.

2.1.5.2 Synthesis of *N,N,N,N*-12-(4-benzoylphenoxydodecyl)trimethyl ammonium bromide (55)

N,N,N,N-12-(4-Benzoylphenoxydodecyl)trimethyl ammonium bromide (**55**) was synthesised using the same method as before (**Section 2.1.3.2**). It was obtained as a white solid in 70% yield with a melting point of 178-179.0 °C. The salt was characterised using IR and NMR (**Figure 23**) spectral data, which were very similar to those obtained for (**51**) and (**53**) (**Sections 2.1.3.2** and **2.1.4.2**). The ¹³C-NMR spectrum differed only in the number of signals for the CH₂ groups.

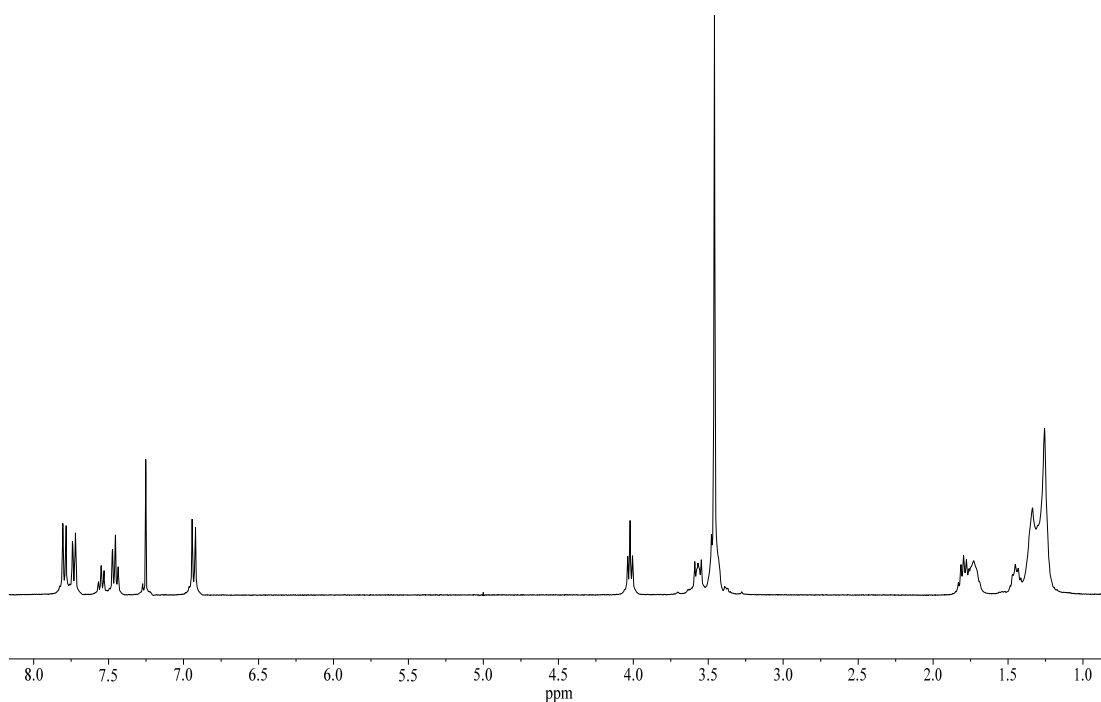


Figure 23: ¹H-NMR spectra of (55)

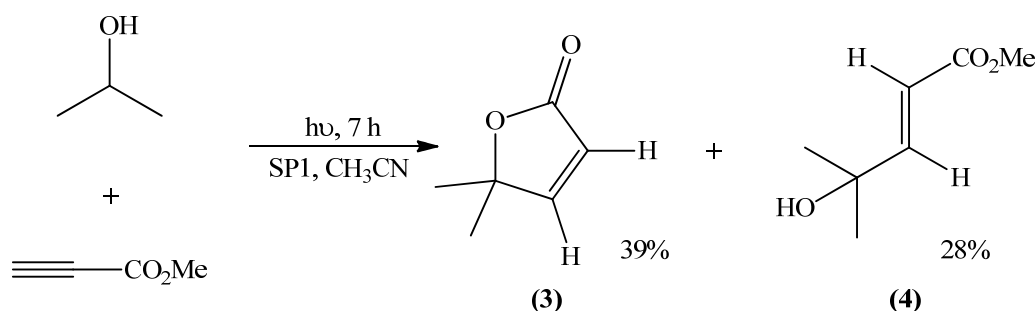
2.1.5.3 Attachment of the quaternary ammonium salt to silica

The quaternary ammonium salt (**55**) was attached to the silica surface using **Method B** (Section 2.1.3.3). This was then dried in a vacuum oven prior to use. Gravimetrically (Section 2.1.1), **SP5** contained 0.33 mmol photomediator/g.

2.2 Photochemical reactions using 3-aminopropyl silica bound benzophenone SP1

2.2.1 Reactions with the monosubstituted alkyne methyl propiolate using SP1

2.2.1.1 Photochemical reaction of methyl propiolate with 2-propanol



Scheme 61

A solution of methyl propiolate and 2-propanol in acetonitrile was degassed with nitrogen for 20 min and **SP1** was added. The solution was irradiated for 7 h, at which time no further reaction was occurring (GC). GC analysis indicated a 68% conversion of the methyl propiolate to three products in a 25:28:47 ratio. The supported photomediator was filtered off and the solvent was removed leaving the crude product as a yellow oil which contained only two components (GC). The product that disappeared is assumed to be the (*Z*)-isomer of (**4**) as its disappearance is associated with an increase in the amount of lactone (GC). The crude product is essentially analytically pure (**Figure 24**). The fact that there are only very small signals in the δ 7.00-7.50 region, which is where photomediator leached from the silica would appear, indicates that **SP1** is stable under the reaction conditions. The two products were isolated by column chromatography.

5,5-Dimethylfuran-2(5*H*)-one, (**3**), eluted first as yellow oil in 39% yield (57% taking unreacted methyl propiolate into account). The spectroscopic data for this product were identical to those reported in the literature¹⁰⁰. The IR spectrum contained a carbonyl band at 1750 cm⁻¹, characteristic of an α,β -unsaturated γ -lactone, and a C=C band at 1660 cm⁻¹. The lactone C-O bands appeared at 1277 and 1132 cm⁻¹, while a band at 699 cm⁻¹ was characteristic of the olefinic CH of a *cis*

alkene¹⁰¹. The ¹H-NMR spectrum contained three signals. A singlet at δ 1.45 represents the protons of two methyl groups while the alkene protons give doublets at δ 5.99 (α -CH) and 7.38 (β -CH). The coupling constant, 5.6 Hz, was consistent with *cis* alkene coupling. The ¹³C-NMR spectrum showed a signal at 172.0 ppm for the carbonyl carbon and the olefinic carbons appeared at 161.6 (β -carbon) and 120.0 ppm (α -carbon). The quaternary carbon appeared at 86.9 ppm and the remaining signal at 25.4 ppm accounts for the two methyl carbons. The formation of lactone (**3**) is of particular interest as such butenolides are of considerable synthetic importance.

Methyl (*2E*)-4-hydroxy-4-methylpent-2-enoate, (**4**), eluted next and was obtained in a slightly lower yield (28%, 41% taking unreacted methyl propiolate into account) as a yellow oil. The spectroscopic data were in agreement with those reported by Zwanenburg¹⁰². The IR spectrum had a broad peak at 3441 cm⁻¹ characteristic of an OH bond and the ester carbonyl group was observed at 1707 cm⁻¹; C-O absorptions appeared at 1287 and 1256 cm⁻¹. A band at 1660 cm⁻¹ was observed for the olefinic double bond and the *trans* alkene gave a CH absorption band at 981 cm⁻¹. A *trans* alkene CH band would normally show up between 970-960 cm⁻¹; conjugation, to an ester group in this case, shifts the band towards 990 cm⁻¹¹⁰¹. The ¹H-NMR spectrum (**Figure 24**) showed two singlets, one at δ 1.33 representing the protons of the two methyl groups, and one at δ 3.70 for the ester OCH₃ group. The *trans* alkene protons appear as two doublets, the α -proton at δ 5.96 and the β -proton at δ 6.98, with a *J* value of 15.7 Hz which is consistent with *trans* coupling. The ¹³C-NMR contained an ester carbonyl carbon signal at 167.6 ppm, and the α - and β -carbon signals at 117.6 and 155.3 ppm, respectively. The quaternary carbon at 70.9 ppm, the methoxy group carbon at 51.8 ppm and the two methyl carbons at 29.3 ppm, were also in agreement with the literature data¹⁰².

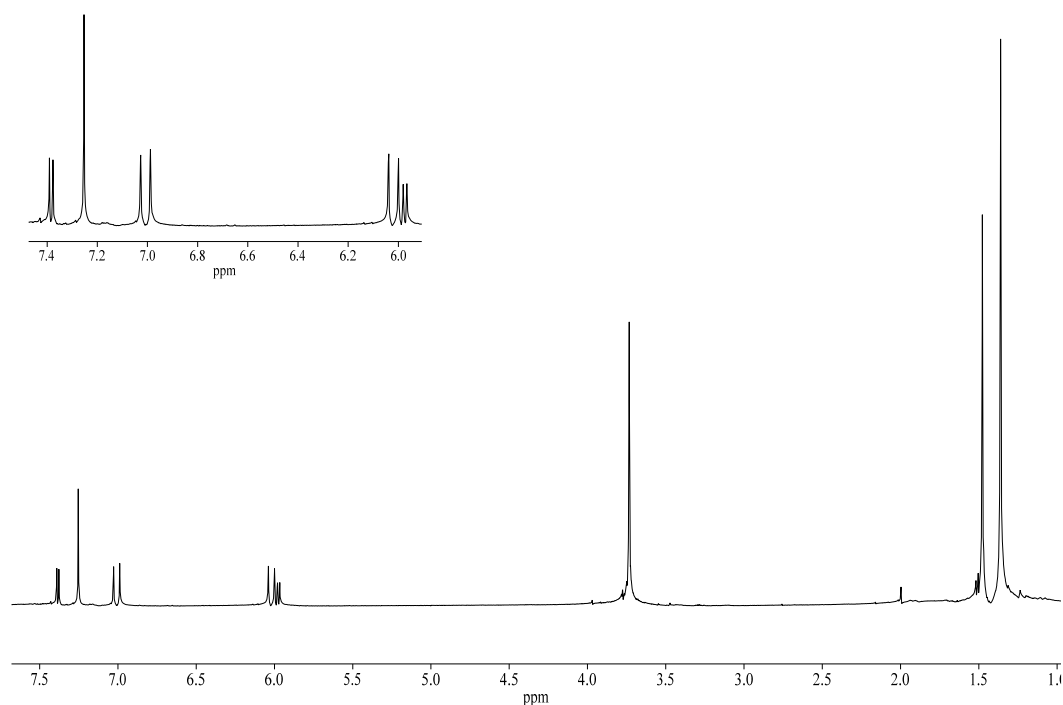
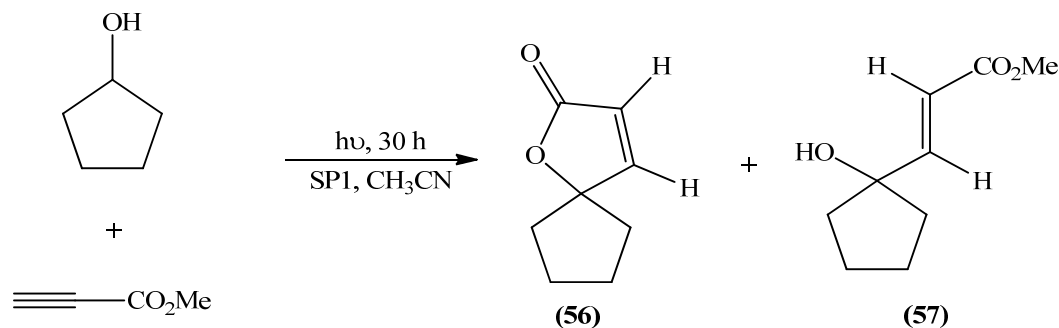


Figure 24: ^1H -NMR spectrum of the crude mixture of (3) and (4)

2.2.1.2 Photochemical reaction of methyl propiolate with cyclopentanol



Scheme 62

The reaction was carried out as before (Section 2.2.1.1) and irradiation was continued until no further reaction of the alkyne was occurring (30 h). GC analysis indicated that a 50% conversion to product had occurred (GC) and the presence of two products in a 45:55 ratio. Once the supported photomediator had been filtered off, the solvent was removed leaving a yellow oil from which excess cyclopentanol was removed by kugelrohr distillation. Analysis of the NMR spectra of the crude product allowed the two expected products, 1-oxaspiro[4.4]non-3-en-2-one (56) and methyl (2*E*)-3-(1-hydroxycyclopentyl)-2-propenoate (57), to be identified. Once

again there was no sign of significant leaching of the photomediator, even after 30 h irradiation.

The spectroscopic data for **(56)** were in agreement with the data reported by Albrecht in 2007¹⁰³. The IR data shows the carbonyl band at 1746 cm⁻¹ and an alkene band at 1600 cm⁻¹. It was also possible to identify the appropriate signals in the ¹H-NMR of the crude mixture, namely the two doublets for the α - and β -protons of the lactone, at δ 5.96 and 7.35, respectively. A coupling constant of 5.6 Hz confirmed the *cis* geometry of the alkene. The ¹³C-NMR had signals at 170.0, 159.3 and 120.3 ppm due to the carbonyl carbon, and the β - and α -carbons of the olefin, respectively. The C-O carbon appeared at 97.1 ppm and the CH₂ carbons of the ring showed up at 36.9 and 24.0 ppm.

The IR spectrum for methyl (*2E*)-3-(1-hydroxycyclopentyl)-2-propenoate **(57)** showed a broad band at 3441 cm⁻¹ for the OH group, a band at 1704 cm⁻¹ for the ester carbonyl group, and an absorption at 1654 cm⁻¹ which was due to the alkene bond. The ¹H-NMR spectrum (**Figure 25**) had a singlet at δ 3.72 for the methoxy protons. Two doublets at δ 6.09 and 7.04, with $J = 15.6$ Hz, confirmed the presence of the alkene protons in a *trans* geometry. An analysis of the ¹³C-NMR spectrum indicated signals at 167.5, 154.6, 117.3 and 81.7 ppm due to the carbonyl carbon, the β - and α -alkene carbons, and the quaternary carbon, respectively. A signal at 51.6 ppm represented the methoxy carbon while the two remaining signals are due to the CH₂ carbons of the ring. These data are consistent with those reported previously¹².

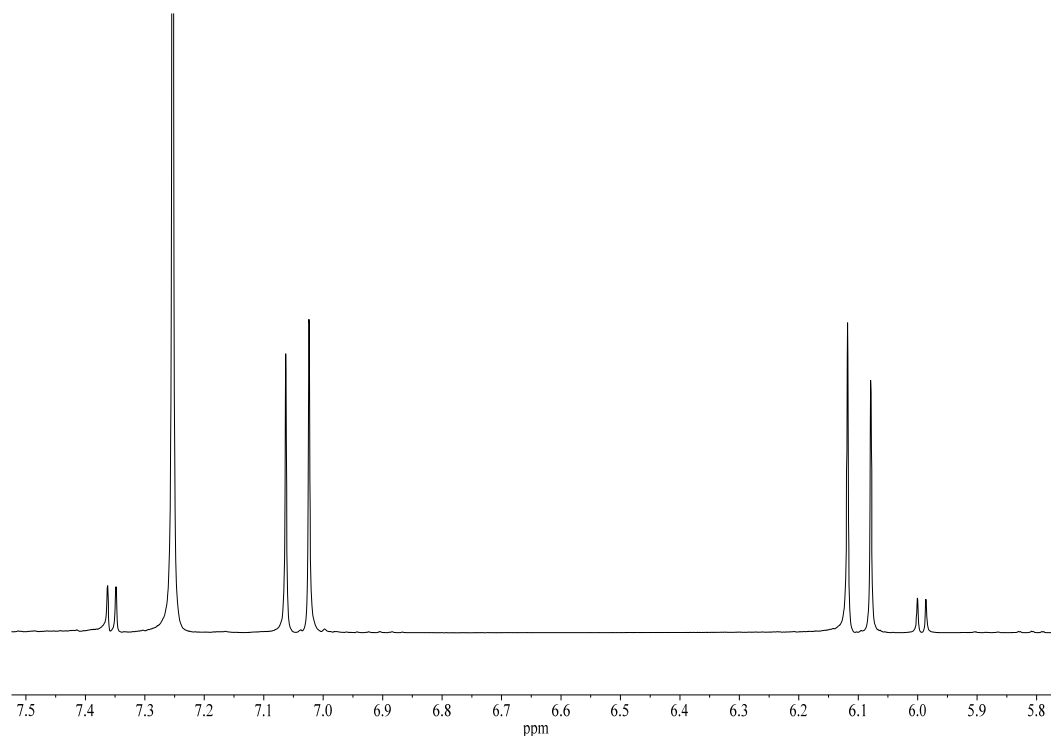
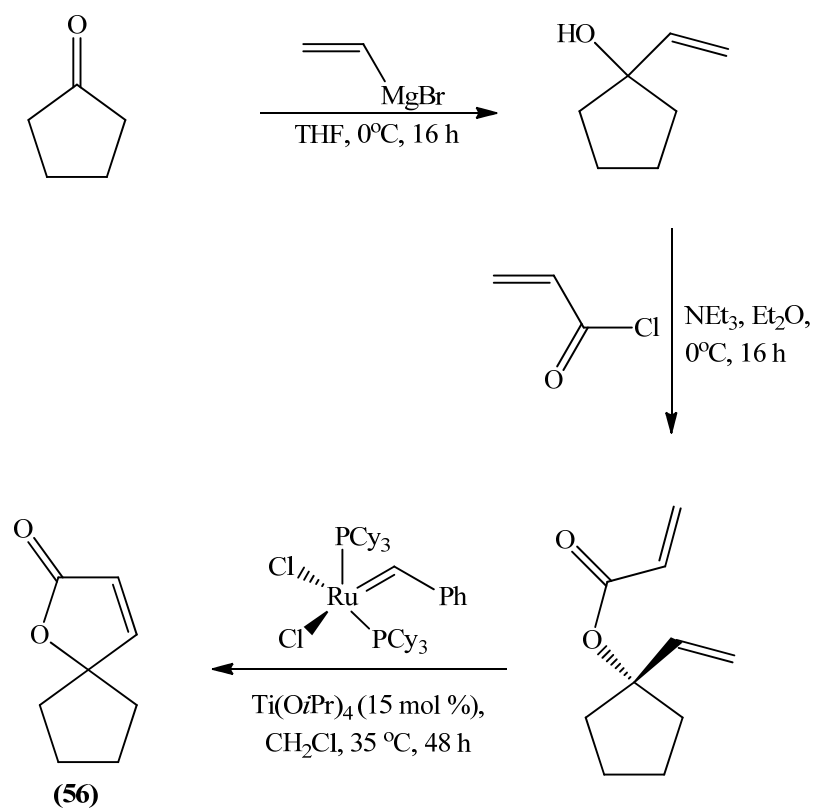


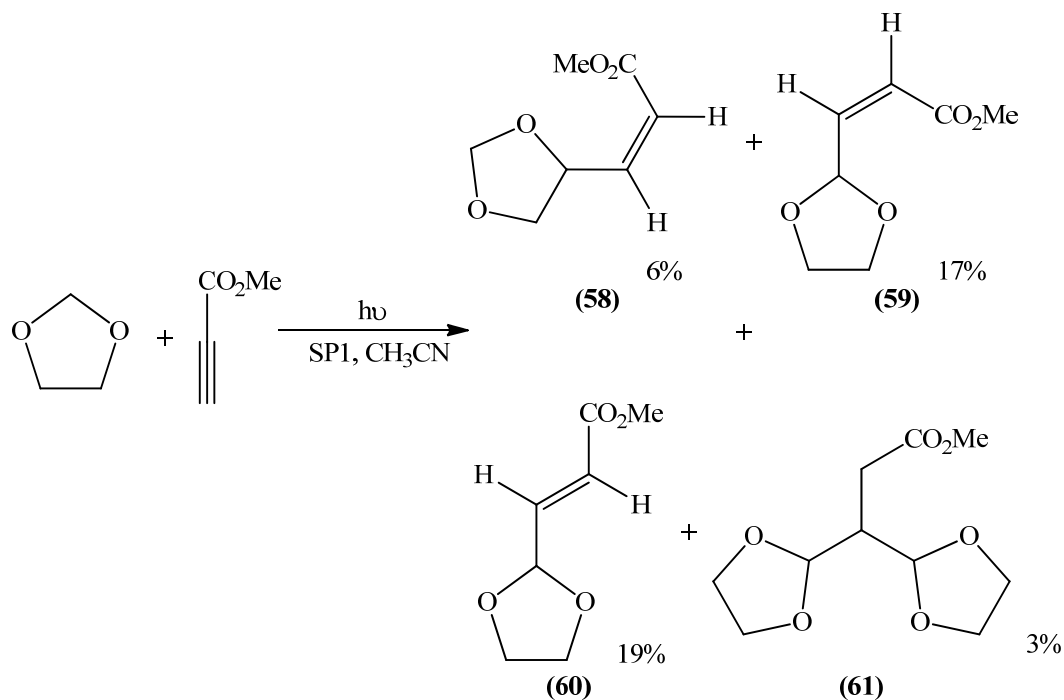
Figure 25: ^1H -NMR spectrum of the crude mixture of **(56)** and **(57)**

The lactone **(56)** was synthesised previously by Albrecht and Langer¹⁰³ (**Scheme 63**). Cyclopentanone was reacted with vinylmagnesium bromide to yield the corresponding alcohol that was transformed into an ester using acryloyl chloride. Finally, a ring closing metathesis using Grubbs first generation catalyst gave the lactone **(56)**. This is a multistep system involving expensive reagents. The photochemical approach¹², is simpler and more direct, even if the conversion of the *trans* product, **(57)**, to **(56)** has to be carried out in a secondary reaction⁷³.



Scheme 63

2.2.1.3 Photochemical reaction of methyl propiolate with 1,3-dioxolane



Scheme 64

The reaction of methyl propiolate with 1,3-dioxolane was carried out as before (Section 2.2.1.1). Irradiation was continued for 17 h, at which point no further reaction of the alkyne was occurring (GC). GC analysis indicated a 60% conversion to product and the presence of four products, three short retention time products and one long retention time product, in a 6:39:49:6 ratio. The supported photomediator was filtered off and the solvent was removed leaving a yellow oil. The products were isolated using column chromatography, eluting in the following order: methyl (2*Z*)-3-(1,3-dioxan-4-yl)-2-propenoate (**58**) (6%), methyl (2*Z*)-3-(1,3-dioxan-2-yl)-2-propenoate (**59**) (17%), methyl (2*E*)-3-(1,3-dioxan-2-yl)-2-propenoate (**60**) (19%) and methyl 3,3-di(1,3-dioxolan-2-yl)propanoate (**61**) (3%). The spectroscopic data obtained for each product were in agreement with the data previously obtained¹⁰⁴.

Methyl (2*Z*)-3-(1,3-dioxan-4-yl)-2-propenoate (**58**) was the first product to elute and was obtained as a yellow oil in just 6% yield. The IR spectrum clearly showed the carbonyl band at 1715 cm⁻¹ and the olefin band at 1645 cm⁻¹ as expected. Three C-O bands were observed at 1207, 1186 and 1085 cm⁻¹. The ¹H-NMR spectrum showed a double doublet at δ3.53 (OCH(**H**)CH) with a *geminal* coupling constant value of 8.2

Hz and a *vicinal* coupling constant of 6.4 Hz. The triplet at $\delta 4.27$ (OCH(H)CH) had $J_{gem} = J_{vic} = 8.2$ Hz. The methine ring proton appeared as a multiplet at $\delta 5.35$ due to coupling to four different protons. Two double doublets at $\delta 5.85$ and $\delta 6.36$ accounted for the α - and β -olefinic protons, respectively, a coupling constant ($J_{cis} = 11.6$ Hz) confirming the *cis* geometry of the alkene; in addition the α -proton is involved in long range coupling to the CH of the ring, and the β -proton is coupled vicinally to the same CH (**Figure 26**).

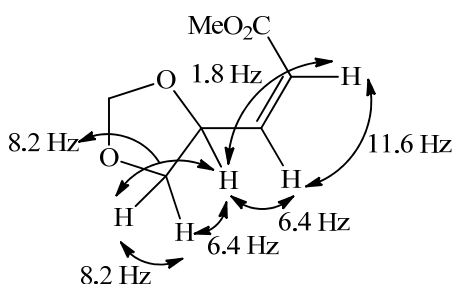


Figure 26: $^1\text{H-NMR}$ coupling constants for (**58**)

The $^{13}\text{C-NMR}$ contained the characteristic signals which confirmed the structure of (**58**). Signals at 166.2, 149.1 and 120.6 ppm were due to the carbonyl carbon, and the β - and α -olefinic carbons, respectively. The formation of (**58**) in such a small proportion is evidence of the preference for the 2-substituted product over the 4-substituted product, attributed to a stereoelectronic effect (**Section 1.5.3**).

Methyl (2*Z*)-3-(1,3-dioxan-2-yl)-2-propenoate (**59**) eluted next and was obtained as a yellow oil in 17% yield. As for (**58**), the IR spectrum had the characteristic bands that confirmed the structure of (**59**). The $^1\text{H-NMR}$ spectrum also confirmed the structure of the 2-substituted dioxolane. The methoxy protons resonated as a singlet at $\delta 3.71$, while multiplets were observed for the protons of the two CH_2 groups. The α -CH of the unsaturated ester showed up as a doublet ($\delta 5.98$), with a coupling constant of 11.6 Hz, confirming the *cis* geometry of the alkene. The β -CH of the alkene, coupled to both the α -CH (*cis* coupling) and the methine proton of the ring (*vicinal* coupling), appears as a double doublet at $\delta 6.06$. The remaining signal, a doublet at $\delta 6.23$, is due to the methine proton of the ring. The $^{13}\text{C-NMR}$ spectrum contained signals at 165.6, 143.2, 124.3 and 97.8 ppm, corresponding to the carbonyl carbon, the β - and α -olefinic carbons and the methine carbon of the ring,

respectively. The carbons of the CH₂ groups resonated at 65.9 and 65.3 ppm, while the methoxy carbon signal appeared at 51.7 ppm.

The next product isolated was methyl (2*E*)-3-(1,3-dioxan-2-yl)-2-propenoate (**60**). Absorption bands for the carbonyl and the alkene bonds were present in the IR spectrum at 1725 and 1664 cm⁻¹, respectively; C-O absorption bands appeared at 1265, 1173 and 1030 cm⁻¹. Analysis of the ¹H-NMR spectrum (**Figure 27**) showed a singlet at δ3.70 for the methoxy protons and multiplets at δ3.89-3.95 for the two CH₂ groups. The ring CH appeared as a double doublet at δ5.39 with *vicinal* coupling (4.6 Hz) to the β-olefinic proton and long range coupling (1.0 Hz) to the α-olefinic proton. The *trans* geometry of the alkene was evident from an analysis of the signals generated by the olefinic protons. A double doublet was observed at δ6.09 for the proton α to the ester group and had a coupling constant of 15.8 Hz, consistent with *trans* coupling, as well as a coupling constant of 1.0 Hz, due to long range coupling to the ring methine proton. The β-proton of the alkene appeared at δ6.72 also as a double doublet ($J_{trans} = 11.8$ Hz, $J_{vic} = 4.6$ Hz). The ¹³C-NMR spectrum contained signals for the carbon of the carbonyl group, and the β- and α-alkene carbons at 166.3, 142.3 and 123.9 ppm, respectively. The methine ring carbon signal appeared at 101.2 ppm, the ring CH₂ carbons at 65.1 ppm and the methoxy carbon signal at 51.9 ppm.

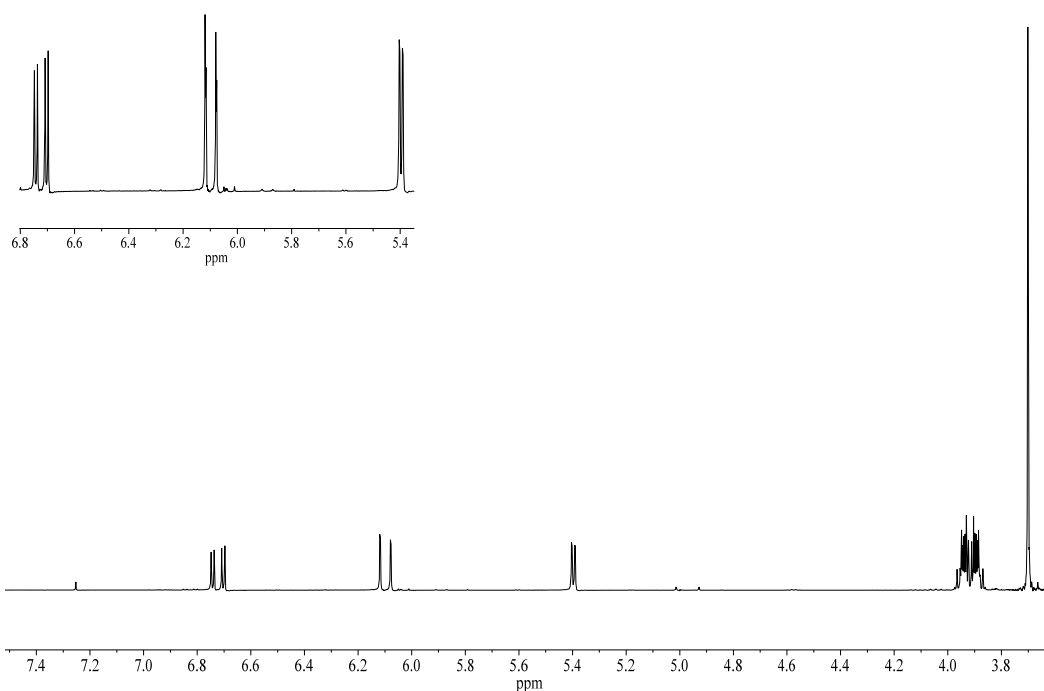
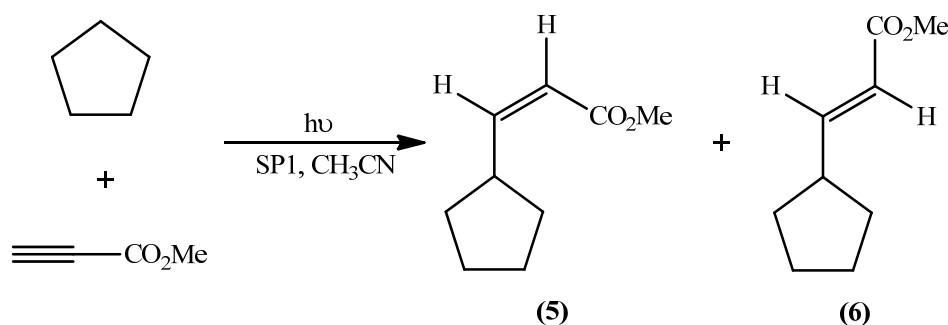


Figure 27: ^1H -NMR spectrum of (60)

Methyl 3,3-di(1,3-dioxolan-2-yl)propanoate (**61**) was the final product isolated, again as a yellow oil. This product is formed as a result of the addition of a 1,3-dioxolan-2-yl radical to one of the initially formed alkene products, (**59**) or (**60**), followed by back hydrogen transfer. The lack of a C=C absorption band in the IR spectrum proved that the molecule was saturated. In the IR spectrum, the ester carbonyl group appeared at 1735 cm^{-1} and the C-O bands at 1260 , 1130 and 1031 cm^{-1} which is consistent with the data reported previously. Further evidence of the nature of the product is available from the ^1H -NMR spectrum¹⁰⁴. A doublet at $\delta 2.45$ ($J_{vic} = 6.5\text{ Hz}$) is due to the CH_2 α to the ester group and a multiplet at $\delta 2.60$ accounts for the proton β to the ester group. The methoxy protons resonate as a singlet at $\delta 3.60$ while the CH_2 protons appear as multiplets at $\delta 3.79$ - 3.97 . The remaining signal in the spectrum is due to the two ring CH group protons, appearing as a doublet at $\delta 5.00$ ($J_{vic} = 4.2\text{ Hz}$). The ^{13}C -NMR assignments were also in agreement with those reported previously. The ring CH carbons appeared as a signal at 103.2 ppm , while the CH_2 carbons resonated at 65.1 and 64.9 ppm . The methoxy carbons resonated at 51.6 ppm while the carbon β to the ester group had a signal at 43.3 ppm and the signal at 28.5 ppm was due to the CH_2 carbon α to the ester group.

2.2.1.4 Photochemical reaction of methyl propiolate with cyclopentane



Scheme 65

The reaction was carried out as before (Section 2.2.1.1) and irradiation was continued until no further reaction of the alkyne was occurring (30 h, 71% conversion). GC analysis indicated the presence of two products in a 66:34 ratio. The supported photomediator was filtered off and the solvent was removed leaving a yellow oil, a mixture of the two products, methyl (2Z)-3-cyclopentyl-2-propenoate (5) and methyl (2E)-3-cyclopentyl-2-propenoate (6). The products were not isolated by column chromatography as identification was possible by comparing the IR and NMR (Figure 28) spectra of the crude mixture with published data^{21,105}.

Methyl (2Z)-3-cyclopentyl-2-propenoate (5) had an olefinic CH stretch at 823 cm⁻¹ in the IR spectrum, a value slightly higher than that generally observed for *cis* disubstituted alkenes¹⁰⁶. The geometry was also confirmed by the ¹H-NMR spectrum (Figure 28). A double doublet at δ5.67 accounted for the α-CH, the signal resulting from *cis* coupling ($J_{cis} = 11.6$ Hz) to the other alkene proton, and long range coupling to the ring CH ($J_{LR} = 1.2$ Hz). The β-proton also resonated as a double doublet at δ6.11 ($J_{cis} = 11.4$ Hz, $J_{vic} = 10.0$ Hz). The ¹³C-NMR spectrum showed signals at 167.6, 155.8 and 117.6 ppm due to the carbonyl carbon, and the β- and α-olefinic carbons, respectively. A signal due to the methoxy carbon appeared at 51.0 ppm while the ring methine carbon resonated at 39.2 ppm. The data observed for this product were in agreement with those previously published²¹.

It was also possible to identify methyl (2E)-3-cyclopentyl-2-propenoate (6) based on the data available from the IR and NMR spectra of the crude mixture, and those in the literature¹⁰⁵. The IR spectrum showed an olefinic CH absorption band at 956 cm⁻¹

which confirmed *trans* geometry of **(6)**¹⁰⁶. Two double doublets in the ¹H-NMR spectrum were due to the olefinic protons. The first, a double doublet at δ 5.78 for the α -proton of the alkene, had one coupling constant consistent with *trans* coupling ($J_{trans} = 15.6$ Hz) and another with long range coupling to the methine proton of the ring. The second double doublet (δ 6.94) also had *trans* coupling (15.6 Hz) and a *vicinal* coupling constant of 8.0 Hz. The ¹³C-NMR spectrum had signals which were in agreement with those observed by Stiller¹⁰⁵, including signals at 154.0 and 118.9 ppm due to the β - and α -olefinic carbons and a signal at 42.9 ppm due to the methine ring carbon.

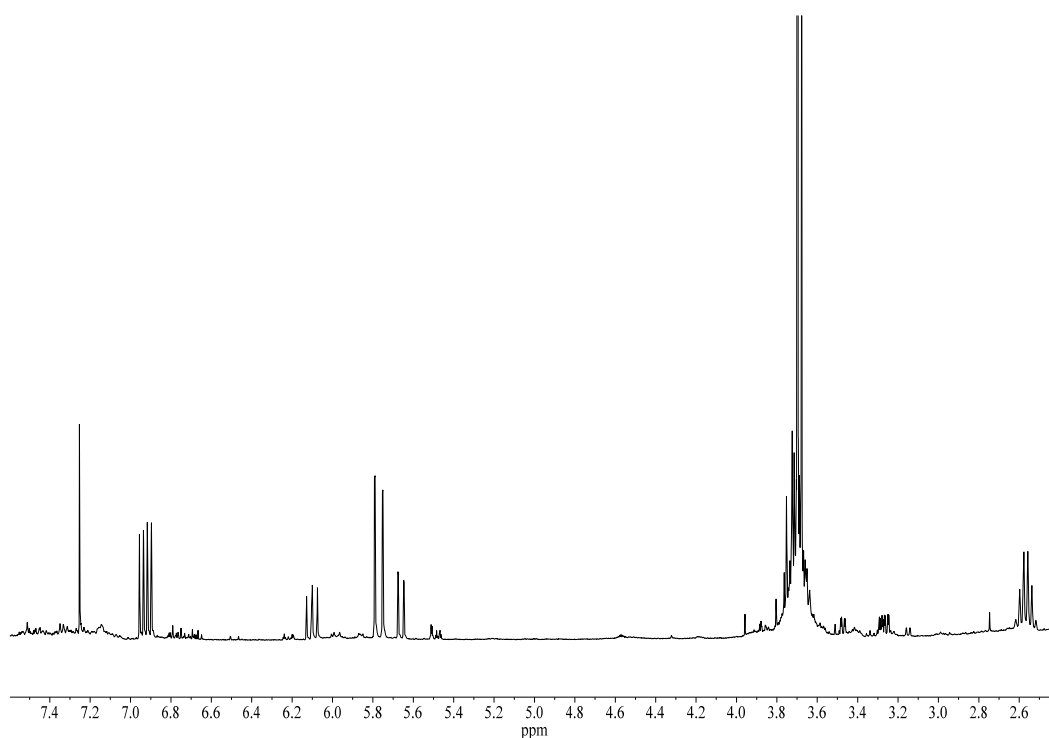
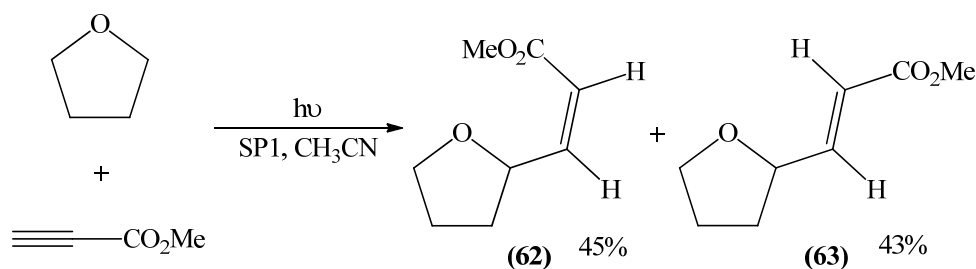


Figure 28: ¹H-NMR spectrum of the crude mixture of **(5)** and **(6)**

2.2.1.5 Photochemical reaction of methyl propiolate with THF



Scheme 66

A solution of methyl propiolate and THF was prepared as before (**Section 2.2.1.1**) and irradiated until complete reaction of the alkyne had occurred (GC, 1.5 h). Two products were present (GC) in a 43:57 ratio, and these were shown to be methyl (2Z)-3-(tetrahydrofuran-2-yl)-2-propenoate (**62**) and methyl (2E)-3-(tetrahydrofuran-2-yl)-2-propenoate (**63**). The supported photomediator was filtered off and the solvent was removed leaving a mixture of the products as a yellow oil. The products were isolated by column chromatography using a diethyl ether/petroleum ether gradient.

Methyl (2Z)-3-(tetrahydrofuran-2-yl)-2-propenoate (**62**) eluted first and was obtained as a yellow oil in 45% yield. The spectroscopic data obtained for (**62**) were in excellent agreement with those reported by Pak in 1993¹⁰⁷. IR analysis showed an absorption band at 1718 cm^{-1} for the carbonyl group, as well as bands at 1178 and 1054 cm^{-1} for the C-O bonds. An absorption band at 670 cm^{-1} was characteristic of a CH in a *cis* alkene¹⁰⁶. The $^1\text{H-NMR}$ spectrum showed multiplets at $\delta 3.78$ - 3.94 for the OCH_2 protons of the tetrahydrofuran ring and multiplets at $\delta 1.48$ - 2.35 for the other methylene protons. The methoxy protons resonated as a singlet at $\delta 3.69$. The ring methine proton resonated as a multiplet at $\delta 5.25$ while the olefinic protons appeared as double doublets at $\delta 5.74$ (α) and $\delta 6.28$ (β) with a *vicinal* coupling constant of 11.7 Hz which confirmed the *cis* geometry of the alkene (**Figure 29**).

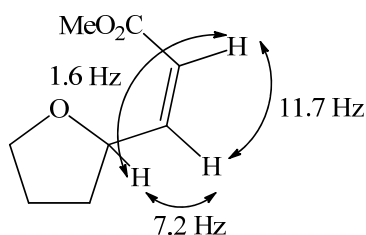


Figure 29: $^1\text{H-NMR}$ coupling constants for **(62)**

The $^{13}\text{C-NMR}$ spectrum contained signals for the ester carbonyl carbon, the β - and α -olefinic carbons, and the ring methine carbon at 166.3, 151.7, 118.8 and 76.0 ppm, respectively.

Methyl (*2E*)-3-(tetrahydrofuran-2-yl)-2-propenoate (**63**) eluted second and, upon removal of solvent, was obtained as a yellow oil in 43% yield. Analysis of the IR spectrum showed absorption bands at 1720, 1161 and 1035 cm^{-1} due to the ester carbonyl group and the C-O bonds, respectively. A band at 980 cm^{-1} was due to the olefinic CH and is typical of a *trans* alkene. This geometry was again evident from an analysis of the $^1\text{H-NMR}$ spectrum (**Figure 30**). A double doublet at $\delta 5.98$ accounted for the proton α to the ester group and had *trans* and long range coupling constants (15.6 Hz and 1.6 Hz) that were in very good agreement with those reported by Pak¹⁰⁷. The ring methine CH resonated as a multiplet at $\delta 4.48$, a value further upfield than the corresponding methine CH in the *cis* isomer (**62**) as has been observed previously by Larson¹⁰⁸. This has been attributed to the deshielding effect of the ester group on the ring methine proton in the case of the *cis* isomer.

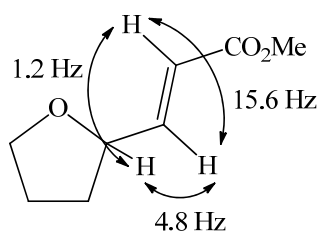
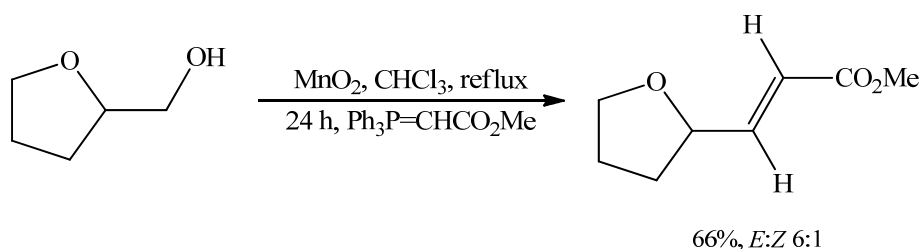


Figure 30: $^1\text{H-NMR}$ coupling constants for **(63)**

In the ^{13}C -NMR, the expected signals were again present, including therefore the carbonyl carbon, the olefinic carbons, and the ring methine carbon at 167.9, 149.6, 120.3 and 77.3 Hz, respectively.

Both **(62)** and **(63)** have previously been synthesised by Blackburn in 1999¹⁰⁹ (**Scheme 67**). A ‘semi-activated’ alcohol underwent a tandem manganese dioxide oxidation-Wittig procedure whereby the alcohol is treated with manganese dioxide in the presence of a Wittig reagent, a process based on a method developed by Taylor in 1998¹¹⁰. The resulting aldehyde is trapped to produce an α,β -unsaturated ester. A mixture of the *cis* and *trans* isomers (*E:Z* 6:1) was obtained in a yield of 66% after 24 h at reflux.



Scheme 67

2.2.2 Reaction with a larger quantity of methyl propiolate using SP1

2.2.2.1 Photochemical reaction of methyl propiolate with 1,3-dioxolane

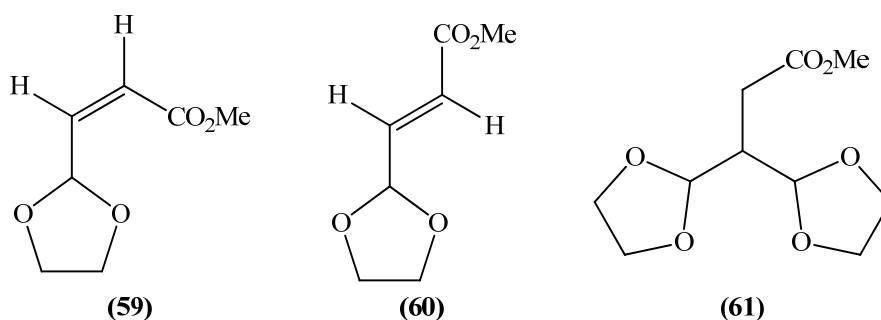


Figure 31

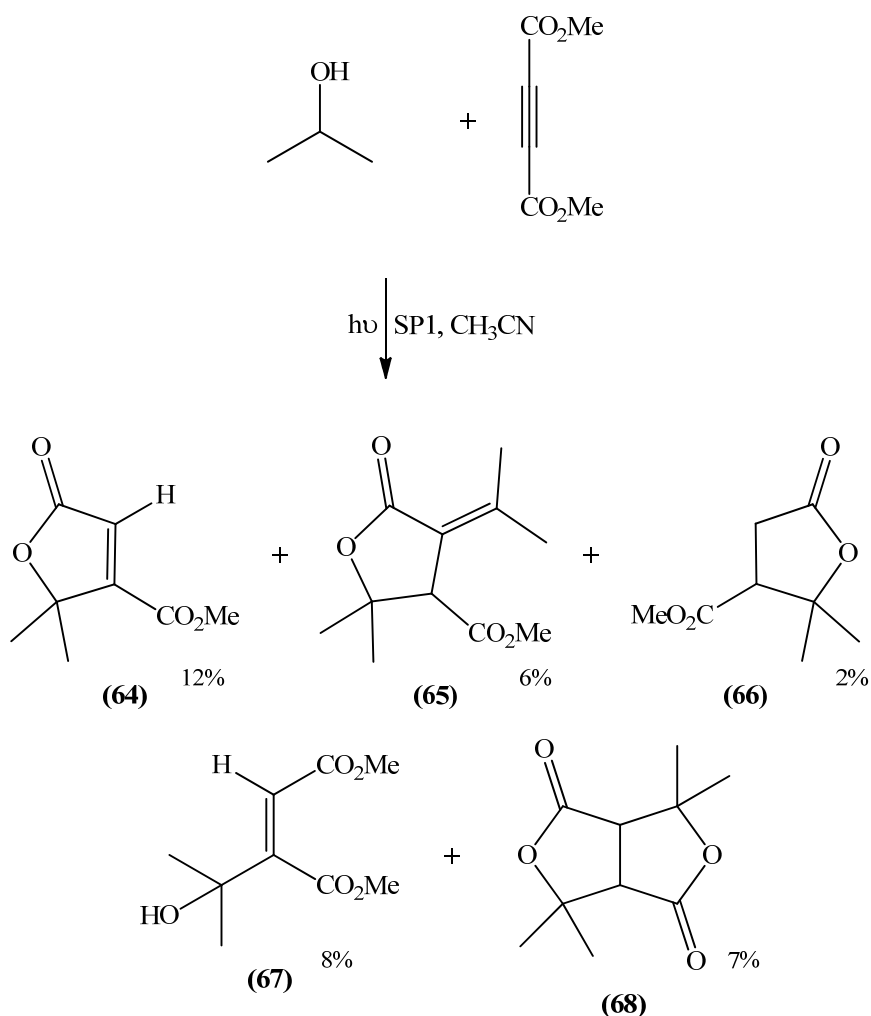
The reaction was carried out as before (**Section 2.2.1.1**), using double the amount of methyl propiolate. The reaction was irradiated for 17 h at which point GC analysis showed that the alkyne had been completely consumed. Three products were present (GC), **(59)**, **(60)** and **(61)**, in a 29:49:22 ratio. As before, the supported

photomediator was filtered off and the solvent was removed, leaving a yellow oil. The spectroscopic data for the crude mixture confirmed the presence of **(59)**, **(60)** and **(61)**, but in contrast to the reaction involving relatively less methyl propiolate (**Section 2.3.1.3**), **(58)**, is not formed.

Interestingly this reaction, with double the amount of alkyne as before (**Section 2.2.1.3**), takes the same length of time to reach completion as the previous reaction (**Section 2.2.1.3**) took to reach 60% conversion.

2.2.3 Reactions with the disubstituted alkyne DMAD using SP1

2.2.3.1 Photochemical reaction of DMAD with 2-propanol



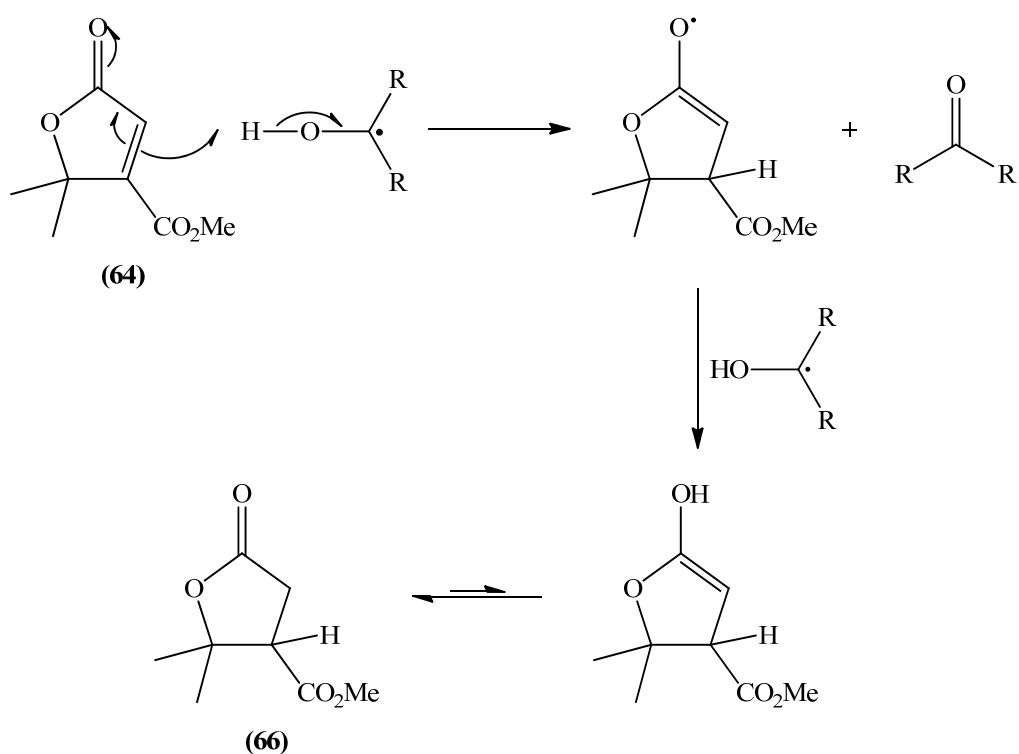
Scheme 68

The reaction of DMAD and 2-propanol was carried out as described before (**Section 2.2.1.1**). The solution was irradiated for 4.5 h at which point GC analysis indicated that the alkyne had been completely consumed giving five products in a 42:13:2:25:18 ratio. The supported photomediator was removed by filtration and the solvent evaporated, leaving a yellow oil. The crude mixture was adsorbed onto silica and the products eluted using a diethyl ether/petroleum ether gradient.

Methyl 2,2-dimethyl-5-oxo-2,5-dihydrofuran-3-carboxylate (**64**) was eluted first as a yellow oil in a yield of 12%. The spectroscopic data for this product are in excellent agreement with those obtained by Patel¹¹¹. Analysis of the IR spectrum showed two carbonyl bands at 1763 and 1730 cm^{-1} , due to the lactone and ester carbonyls, respectively. This is in keeping with the fact that saturated γ -lactones absorb at shorter wavelengths than esters. The $^1\text{H-NMR}$ spectrum contained three singlets due to the protons of the two methyl groups (δ 1.60), the methoxy protons (δ 3.86) and the olefinic proton (δ 6.56). The $^{13}\text{C-NMR}$ also confirmed the structure of the product isolated. Two ester carbonyl carbons were evident (169.8 and 161.2 ppm) as was a quaternary carbon (87.2 ppm) and two methyl groups (25.2 ppm).

Second to elute, methyl 2,2-dimethyl-4-(1-methylethylidene)-5-oxotetrahydrofuran-3-carboxylate (**65**), was obtained in 6% yield, also as a yellow oil. IR analysis indicated the presence of only one carbonyl band in this case (1737 cm^{-1}). A band at 1664 cm^{-1} was also observed, characteristic of an alkene. The $^1\text{H-NMR}$ spectrum had two singlets at δ 1.37 and 1.40 due to four methyl groups, but lacked olefinic protons which suggested that an initially formed unsaturated product had undergone further addition. A singlet at δ 3.60 accounted for the ring methine proton. Two carbonyl carbons were present in the $^{13}\text{C-NMR}$ spectrum (170.9 and 168.3 ppm) due to the saturated ester and unsaturated lactone, respectively, confirming that the structure contained a lactone moiety. In addition, the signal at 154.1 ppm due to a quaternary carbon (DEPT spectrum), accounted for the dimethyl substituted olefinic carbon. Four signals at 34.5, 30.2, 23.9 and 20.4 ppm were due to the four methyl carbons. This lactone is presumably derived from a molecule of lactone (**64**) that underwent addition of a second propan-2-yl radical to the α -carbon of the lactone bond, followed by dehydration.

The next product eluted was methyl 2,2-dimethyl-5-oxotetrahydrofuran-3-carboxylate¹¹² (**66**). This minor product, which was obtained in a low yield (2%) as a yellow oil, has not been obtained before as a product in reactions of this type. It is reasonable to assume that this product is formed *via* reduction of the olefinic bond in lactone (**64**) (**Scheme 69**).



Scheme 69

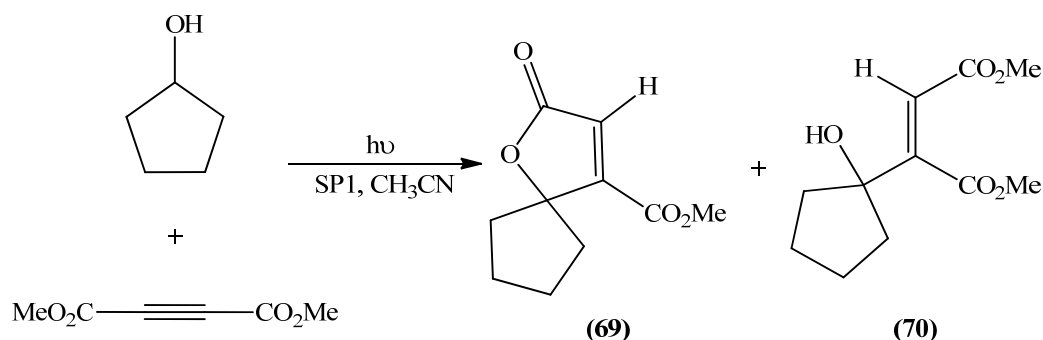
The IR spectrum contained two carbonyl absorption bands at 1776 and 1730 cm^{-1} . As expected the ester carbonyl group absorbs at a longer wavelength than the lactone carbonyl bond. However, the lactone carbonyl bond absorption is at a higher frequency (1776 cm^{-1}) than that of the unsaturated lactone (**64**) (1763 cm^{-1}), due to the lack of conjugation as a result of the olefin undergoing reduction. The $^1\text{H-NMR}$ spectrum contained singlets for the methyl protons (δ 1.30 and 1.60) and the methoxy protons at δ 3.76. The saturated nature of the lactone was again evident due to the presence of two double doublets, at δ 2.70 ($J_{gem} = 17.7$ Hz, $J_{vic} = 8.6$ Hz) and at δ 3.08 ($J_{gem} = 17.7$ Hz, $J_{vic} = 9.7$ Hz), which were due to the diastereomeric methylene protons.

The ring methine proton resonated as a double doublet at $\delta 3.19$ ($J_{vic} = 8.8$ Hz, $J_{vic} = 9.6$ Hz). The ^{13}C -NMR contained signals for both lactone and ester carbonyl carbons (173.9 and 170.4 ppm, respectively) in addition to signals for the methine and methylene carbons (52.5 and 31.9 ppm, respectively). This spectroscopic data correlated well with previous data¹¹².

Dimethyl (2*Z*)-2-(1-hydroxy-1-methylethyl)but-2-enedioate¹¹³ (**67**), the product of a formal *cis* addition, was isolated next and was obtained in 8% yield, also as a yellow oil. The IR spectrum contained a broad O-H band at 3478 cm^{-1} as well as a carbonyl absorption band at 1722 cm^{-1} . The ^1H -NMR spectrum was consistent with published data¹¹³, showing four signals, all of which were singlets, accounting for the methyl protons ($\delta 1.41$), the methoxy protons ($\delta 3.68$ and 3.80), and lastly the olefinic proton ($\delta 6.06$). In the ^{13}C -NMR spectrum, the two ester carbonyl carbons and the two olefinic carbons resonated at 168.5 and 165.6 ppm, and at 157.9 and 117.0 ppm, respectively.

Lastly, dimethyl (2*E*)-2,3-bis(1-hydroxy-1-methylethyl)but-2-enedioate¹¹⁴ (**68**) was isolated as a white solid in 7% yield. This bicyclic structure gave rise to one carbonyl absorption in the IR spectrum due to the lactone (1757 cm^{-1}). The four methyl groups were accounted for in the ^1H -NMR spectrum by the presence of two singlets ($\delta 1.51$ and 1.57). The protons at the bridgehead resonated as a singlet at $\delta 3.37$. The ^{13}C -NMR had a carbonyl carbon signal at 172.2 ppm and the quaternary carbons resonated at 83.8 ppm. The bridgehead carbons appeared as one signal at 52.1 ppm, while the four methyl groups resonated at 31.2 and 24.7 ppm. This product presumably arises in the same way as (**65**), through the addition of a second molecule of 2-propanol to the lactone (**64**). Subsequent lactonisation would yield (**68**), whereas dehydration gives (**65**).

2.2.3.2 Photochemical reaction of DMAD with cyclopentanol



Scheme 70

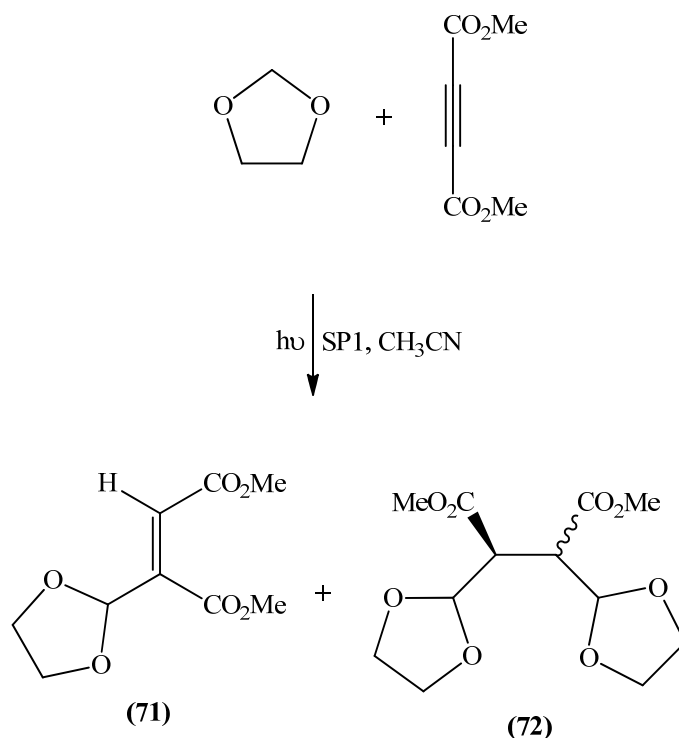
A solution of DMAD and cyclopentanol was prepared as before (Section 2.2.1.1) and irradiated for 5 h at which point only 25% conversion of the alkyne to two products (54:46) had been achieved (GC). The reaction was stopped, the supported photomediator was filtered off and the solvent was removed. Kugelrohr distillation was used to remove excess cyclopentanol from the mixture and this left the crude product as a yellow oil. Analysis of the spectroscopic data confirmed the products to be methyl 2-oxo-1-oxaspiro[4.4]non-3-ene-4-carboxylate¹¹¹ (**69**), the minor product, and dimethyl (2Z)-2-(1-hydroxycyclopentyl)but-2-enedioate¹¹⁵ (**70**).

The presence of (**69**) was initially confirmed by the carbonyl band at 1763 cm^{-1} which corresponds to that of an unsaturated lactone. From the $^1\text{H-NMR}$, it was possible to identify signals which correlated well with those in spectroscopic data previously reported¹¹¹. The methoxy protons resonated as a singlet at $\delta 3.86$, and most characteristically, a singlet $\delta 6.62$ was due to the olefinic proton of the lactone. In the $^{13}\text{C-NMR}$ spectrum, the α -carbon resonated at 126.9 ppm .

Dimethyl (2Z)-2-(1-hydroxycyclopentyl)but-2-enedioate¹¹⁵ (**70**) was in part identified by the presence of an O-H band in the IR spectrum (3323 cm^{-1}) and a carbonyl band at 1727 cm^{-1} . Unlike in the case of the lactone product (**69**), the $^1\text{H-NMR}$ spectrum of (**70**) had two singlets at $\delta 3.74$ and 3.85 due to two methoxy groups. The olefinic proton resonated at $\delta 6.17$, while in the $^{13}\text{C-NMR}$ the associated olefinic carbon resonated at 117.5 ppm , further upfield than the corresponding carbon in (**69**). There was also a signal for the carbon attached to the hydroxyl group

at 82.2 ppm. All of the above data confirmed the structures of the products of this reaction.

2.2.3.3 Photochemical reaction of DMAD with 1,3-dioxolane



Scheme 71

A solution of DMAD and 1,3-dioxolane was prepared as before (Section 2.2.1.1) and the solution was then irradiated for 16 h, at which time complete reaction of the alkyne had occurred (GC). GC analysis confirmed the formation of three products (19:25:56), one of short retention time and two of longer, but similar, retention times. Further purification was not carried out, identification of the products being possible on the basis of a comparison of the spectroscopic data obtained for the crude mixture with those found for each individual product previously¹⁰⁴.

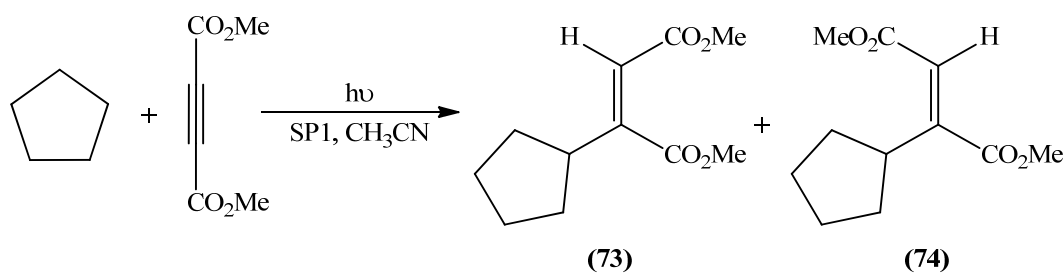
Confirming the formation of dimethyl (2Z)-2-(1,3-dioxany-2-yl)but-2-enedioate¹⁰⁴ (71), the IR spectrum of the mixture had a band at 1660 cm^{-1} for the olefinic double bond. The $^1\text{H-NMR}$ spectrum had singlets at $\delta 5.67$ and 6.24 corresponding to the ring methine proton and the olefinic proton, respectively. Two carbonyl carbons and two olefinic carbons were evident in the $^{13}\text{C-NMR}$ spectrum at 166.1 and 165.2 , and

144.6 and 122.7 ppm, respectively. There was no trace of the corresponding *trans* isomer in the product mixture.

The formation of the two diastereomers of dimethyl 2,3-di(1,3-dioxolan-2-yl)butanedioate¹⁰⁴ (**72**), presumably formed by the addition of a 1,3-dioxolan-2-yl radical to (**71**), or its *trans* isomer, was also confirmed by the spectroscopic data. The ¹H-NMR spectrum of the crude mixture had a double doublet at δ 5.22 with *vicinal* and long range coupling constants of 4.0 and 1.9 Hz, respectively, due to the two ring methine protons of one diastereomer. The corresponding signal in the ¹H-NMR of the other diastereomer appears as a multiplet at δ 5.36-5.38. The protons α to the ester groups for the two diastereomers resonated as multiplets at δ 3.15-3.17. The ¹³C-NMR spectrum for the mixture also contained the expected signals for the diastereomers: carbonyl carbons at 170.6 and 170.8 ppm, ring methine carbons at 103.1 and 102.3 ppm, and carbons α to the ester at 48.9 and 48.1 ppm.

It is worth noting that in the reactions involving monosubstituted alkynes, the coupling constants of the alkenes formed can be used to determine the stereochemistry. However, this is not possible for the reactions of disubstituted alkynes and so the stereochemistry is defined by using the chemical shifts of the olefinic and methine ring protons. In the case where the ester group is *cis* to the methine ring proton, the latter experiences a downfield shift, relative to when it is *trans* to the ester group. A similar effect is observed for the olefinic proton.

2.2.3.4 Photochemical reaction of DMAD and cyclopentane



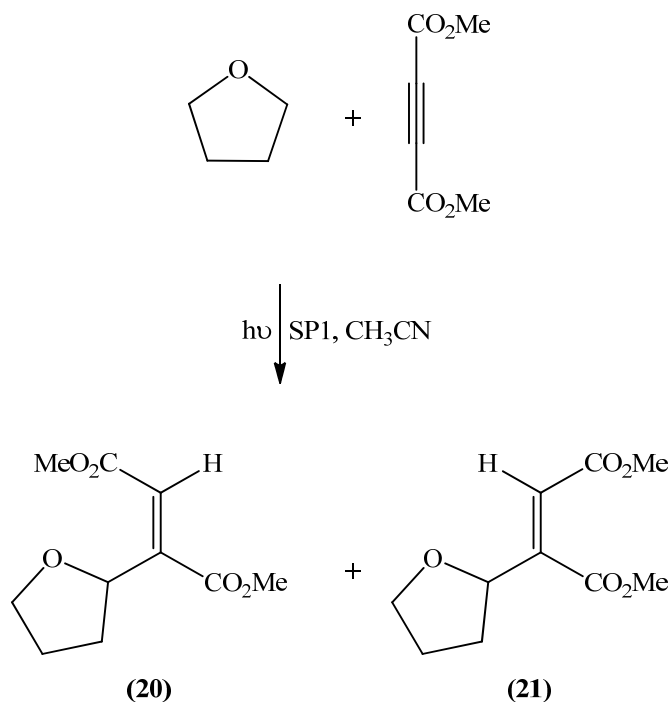
Scheme 72

This reaction was carried out in the same manner as before (**Section 2.2.1.1**). After irradiating for 52 h, only a 62% conversion of DMAD had been achieved with GC analysis indicating the presence of one major and one minor product. Dimethyl (2*Z*)-2-cyclopentylbut-2-enedioate²¹ (**73**) and dimethyl (2*E*)-2-cyclopentylbut-2-enedioate^{18,19,21} (**74**) were identified as the two products; they were present in a ratio of 93:7 (GC). Column chromatography was not necessary as identification of the products was possible from analysis of the spectroscopic data for the crude mixture, which, as in previous cases, was very clean.

The spectroscopic data obtained for the major product, dimethyl (2*Z*)-2-cyclopentylbut-2-enedioate²¹ (**73**), was in excellent agreement with those published by Geraghty²¹. The IR spectrum showed a carbonyl absorption at 1724 cm⁻¹ and an olefin absorption band at 1646 cm⁻¹. The expected C-O absorptions were seen at 1266 and 1172 cm⁻¹. The ¹H-NMR spectrum had two singlets due to the methoxy protons at δ3.68 and 3.80, as well as a singlet further downfield at δ5.79 corresponding to the olefinic proton. The ¹³C-NMR confirmed the presence of two ester carbonyl groups, with signals at 169.0 and 165.7 ppm; the α- and β-olefinic carbons appeared at 116.9 and 155.0 ppm, respectively.

The *trans* isomer dimethyl (2*E*)-2-cyclopentylbut-2-enedioate²¹ (**74**), was unfortunately present in such a small proportion that complete spectroscopic data could not be obtained. However, in the ¹H-NMR spectrum of the crude mixture, two singlets due to the methoxy protons were observed at δ3.70 and 3.81. The olefinic proton appeared at δ6.25, thus confirming the *trans* structure (**74**) as the signal for the olefinic proton is further downfield than that for the *cis* isomer (**73**), again due to the deshielding effect of the ester group.

2.2.3.5 Photochemical reaction of DMAD and THF



Scheme 73

The photochemical reaction of DMAD and THF was carried out as usual (**Section 2.2.1.1**) and after 3 h irradiation, GC analysis indicated the formation of two products, **(20)** and **(21)**, in a 55:45 ratio. Once the supported photomediator had been filtered off, the solvent was removed leaving a mixture of the two products as a yellow oil. Column chromatography was not carried out as the NMR spectra (**Figure 32**) of the crude product were of sufficient quality to allow identification of the products. For dimethyl (*E*)-2-(tetrahydrofuran-2-yl)but-2-enedioate⁵¹ (**(20)**), as expected, the two methyl groups resonated as singlets at δ 3.75 and 3.77, while the ring methine proton appeared as a multiplet at δ 5.20. The olefinic proton resonated as a doublet (δ 6.54) due to long range coupling to the ring methine proton ($J_{LR} = 1.0$ Hz). Three signals in the ¹³C-NMR spectrum, at 166.4, 125.7 and 146.4 ppm, were due to the ester carbonyl group, and the α - and β -carbons of the olefin, respectively. A signal at 76.2 ppm was due to the methine ring carbon. The remaining signals were also in agreement with Singh's data⁵¹.

The ¹H-NMR data for dimethyl (*Z*)-2-(tetrahydrofuran-2-yl)but-2-enedioate⁵¹ (**(21)**) were similar to those for **(20)** but there were some notable differences. The main

differences were the shifts associated with the olefinic proton and the methine ring proton. Both the methine ring proton and the olefinic proton appeared at higher field, at δ 4.66 and 6.11, respectively, than the corresponding signals of the *trans* isomer. The ^{13}C -NMR data for **(21)** were also as expected, including a carbonyl carbon at 165.7 ppm, and the α - and β -carbons of the olefin at 118.4 and 150.9 ppm, respectively. The remaining signals were also consistent with the literature⁵¹.

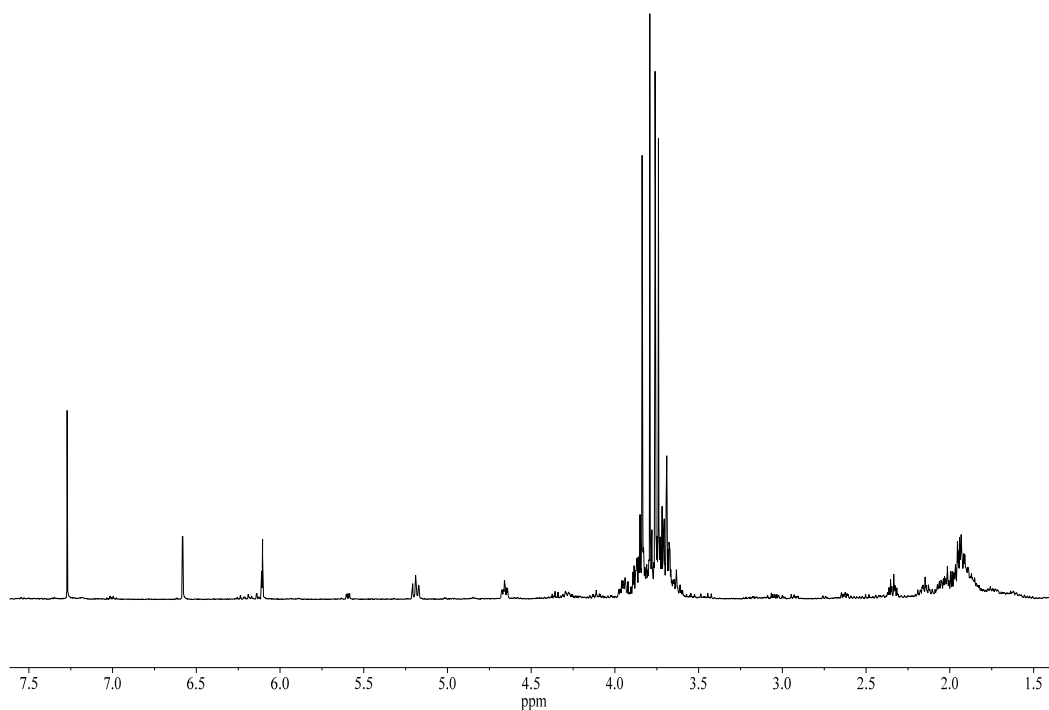


Figure 32: ^1H -NMR spectrum of the crude mixture of **(20)** and **(21)**

2.3 Photochemical reactions using propyl linked 4-hydroxybenzophenone silica SP2

2.3.1 Reactions with the monosubstituted alkyne methyl propiolate using SP2

2.3.1.1 Photochemical reaction of methyl propiolate with 2-propanol

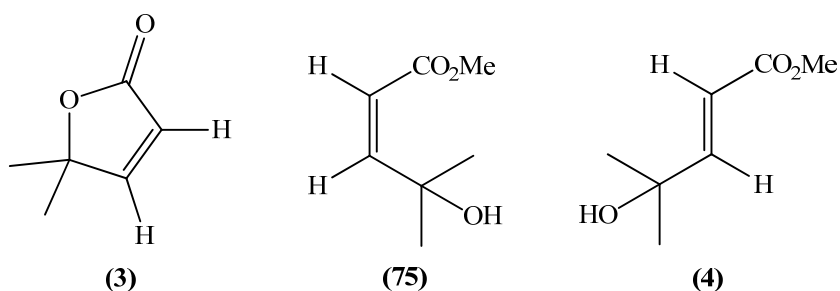


Figure 33

The reaction mixture was prepared as before (Section 2.2.1.1) using the propyl linked 4-hydroxybenzophenone silica photomediator, SP2. It was irradiated for 36 h, at which point the alkyne had completely reacted. GC analysis at this point indicated the formation of two products, (3) and (4) (Figure 33), in a 42:58 ratio. As before, the supported photomediator was filtered off and the solvent was removed which gave a mixture of the two products as a yellow oil. It was clear from both the GC retention times and the spectroscopic data that the two products were, as expected, (3) and (4).

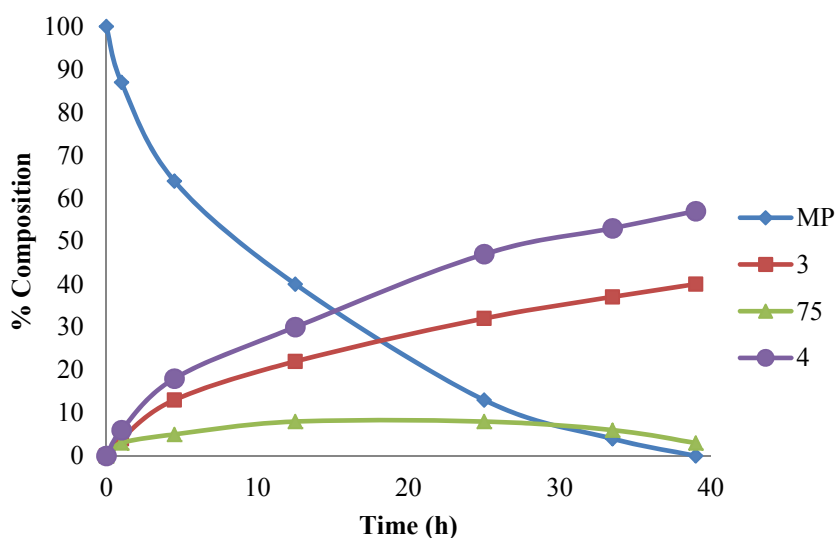


Figure 34

It is worth noting that GC monitoring of the reaction (**Figure 34**) showed that initially three products were formed, as is the case for the reaction using **SP1** (**Section 2.2.1.1**). However the third product, which is presumably the *cis* isomer (**75**), was over time converted to the lactone (**3**). The lack of any aromatic signals in the NMR spectra, indicated that the photomediator remained bound to the silica surface.

2.3.1.2 Photochemical reaction of methyl propiolate with cyclopentanol

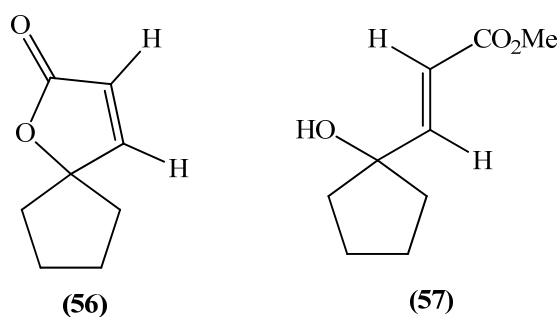


Figure 35

The reaction of methyl propiolate and cyclopentanol was carried out as before (**Section 2.2.1.1**) using **SP2**, with irradiation being continued until no further product formation was occurring. After 53 h irradiation, 88% conversion of the alkyne to two products, (**56**) and (**57**), had occurred. The supported photomediator was filtered off

and the solvent was evaporated. Excess cyclopentanol was removed using kugelrohr distillation leaving a mixture of the two products as a yellow oil. The spectroscopic data for the crude mixture were used to confirm the presence of the expected products with particular attention being paid to the series of doublets of the $^1\text{H-NMR}$ spectrum, the J -values of which confirm the *cis/trans* geometry of the olefinic bonds in the two products.

The $^1\text{H-NMR}$ spectrum of the crude product (**Figure 36**) clearly confirms the presence of the expected products, but also the fact that the reaction was mediated by photomediator bound to the silica surface as there are no aromatic signals corresponding to benzophenone type molecules present in the spectrum.

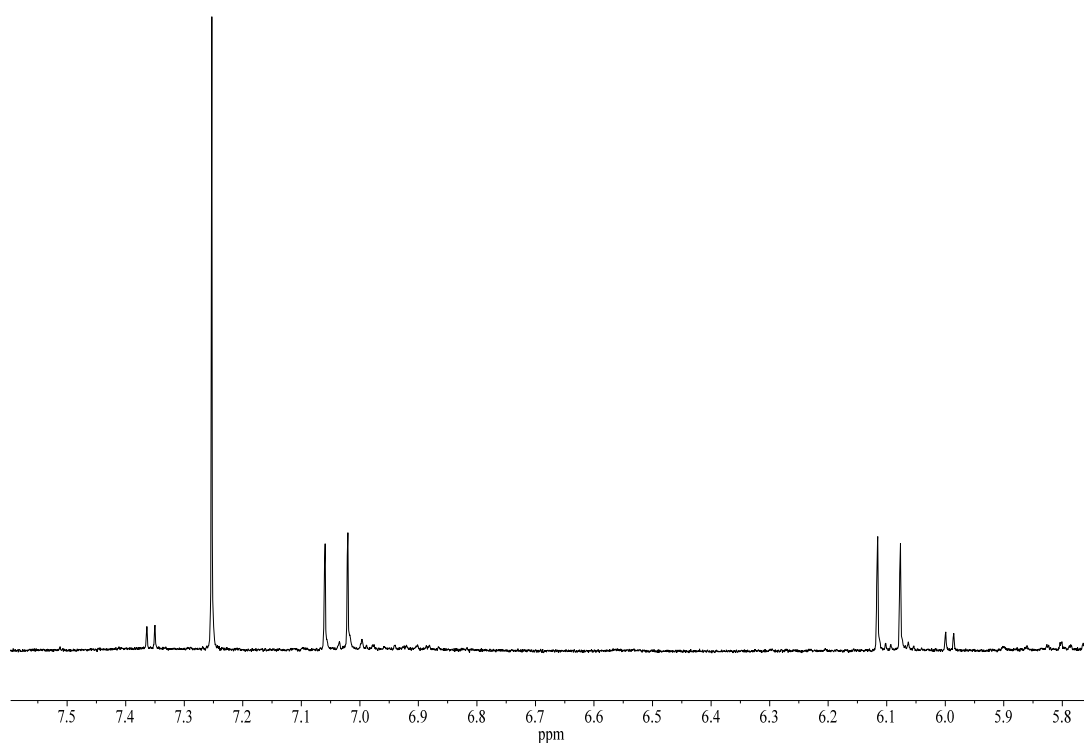


Figure 36: $^1\text{H-NMR}$ spectrum of the crude mixture of (56) and (57)

2.3.1.3 Photochemical reaction of methyl propiolate with 1,3-dioxolane

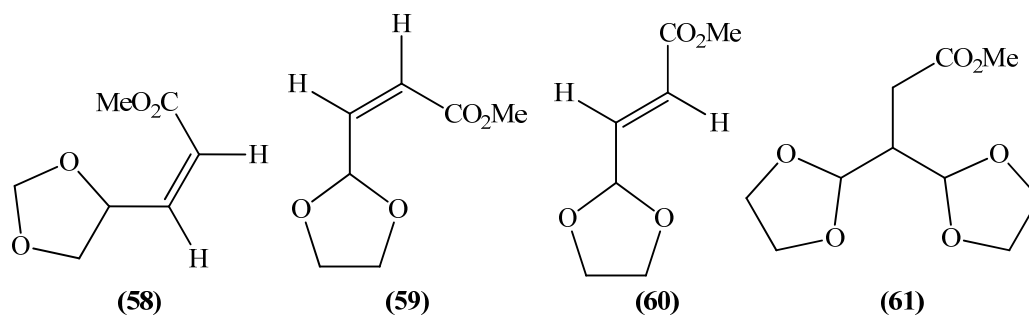


Figure 37

This reaction was carried out as before using **SP2** as the photomediator. A long irradiation time of 50 h was required to reach a conversion of 80% (GC). Analysis of the GC showed that four products were formed and from a comparison with the chromatogram of the reaction mediated by **SP1** (Section 2.2.1.3), it was clear that the products formed were (58), (59), (60) and (61) in a 7:34:49:10 ratio. It can be seen from the time course plot (Figure 38) obtained from the GC data that the reaction is initially very rapid but becomes very slow after about 2 h and that after 50 h irradiation no further reaction of the methyl propiolate is occurring.

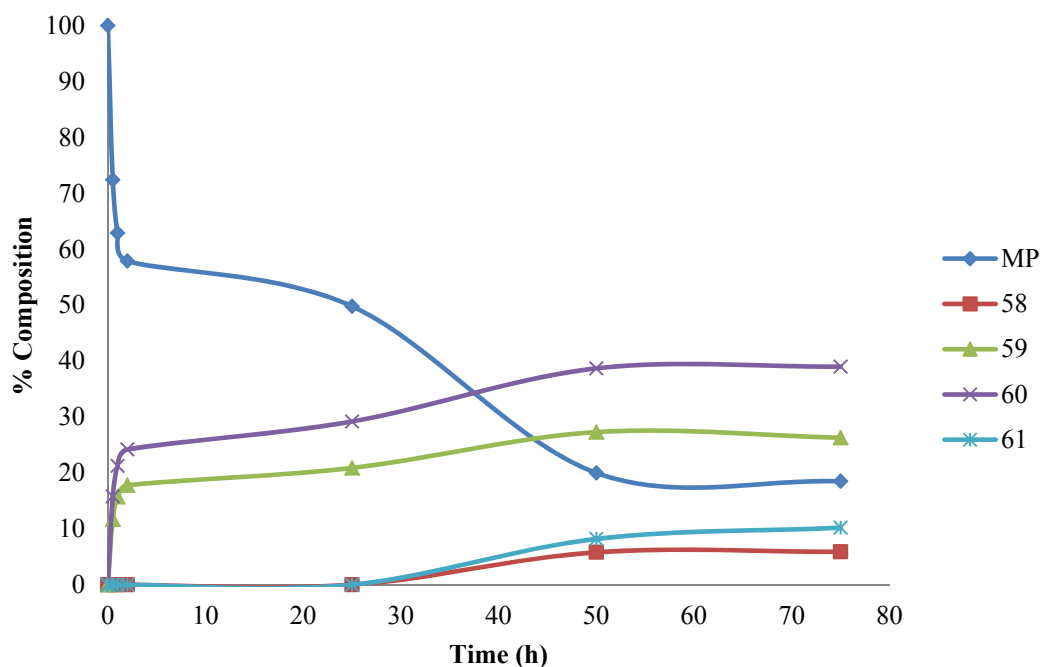


Figure 38

The spectroscopic data for the crude product mixture further confirmed the formation of **(58)**-**(61)** and were in agreement with those described earlier (**Section 2.2.1.3**).

2.3.1.4 Photochemical reaction of methyl propiolate with cyclopentane

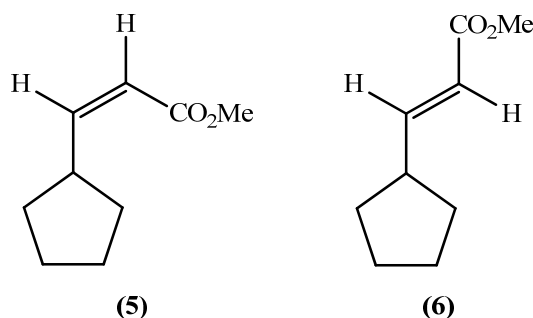


Figure 39

A solution of methyl propiolate and cyclopentane in acetonitrile was prepared as before (**Section 2.2.1.4**) with **SP2** as the photomediator. The solution was irradiated for 120 h at which point complete reaction of the alkyne had occurred. GC analysis showed two products in a 35:65 ratio, which were shown to be **(5)** and **(6)** by comparing their GC retention times with those observed for the products of the reaction mediated by **SP1** (**Section 2.2.1.4**). The spectroscopic data for the product mixture confirmed the formation of **(5)** and **(6)**. The reaction was disappointing in that the length of time required to reach completion was extremely long, the general pattern for the reactions mediated by the propyl linked 4-hydroxybenzophenone silica photomediator, **SP2**. However, even though a very long irradiation time is required, the ¹H-NMR spectrum of the crude product (**Figure 40**) showed that it is free of benzophenone type signals. This suggests that although this supported photomediator is not the most efficient, the photomediator remains tightly bound to the silica surface.

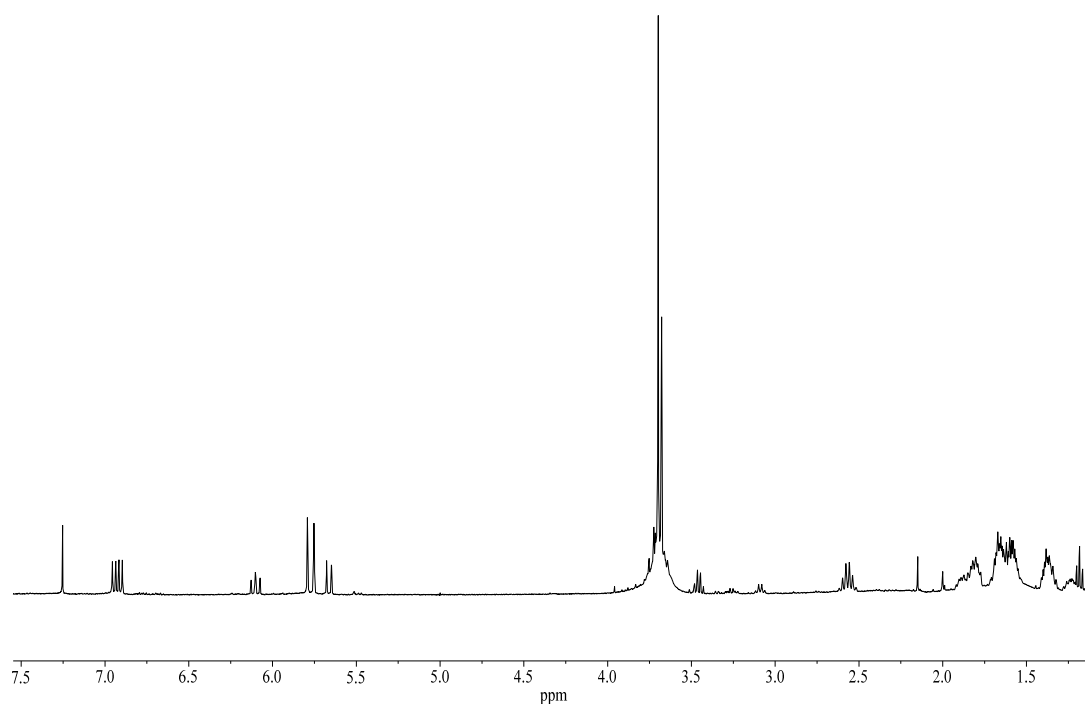


Figure 40: ^1H -NMR spectrum of the crude mixture of (5) and (6)

2.3.1.5 Photochemical reaction of methyl propiolate with THF

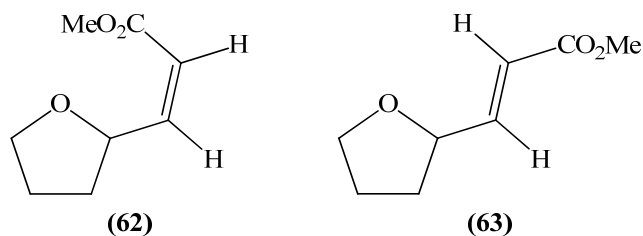


Figure 41

The reaction of methyl propiolate and THF was carried out in the standard way (Section 2.2.1.1) using the supported photomediator **SP2**. An irradiation time of 2.5 h was required to give complete conversion of the alkyne to the two expected products, (62) and (63), in a 43:57 ratio (GC). In the usual manner, the supported photomediator was filtered off and the solvent was removed leaving the crude mixture as a yellow oil. Again, it was possible to confirm the nature of the products using the spectra obtained for the crude mixture, which were exceptionally clean, considering no purification had been carried out (Figure 42). Noteworthy here again

is the absence of any aromatic signals, confirming the photostability of the photomediator.

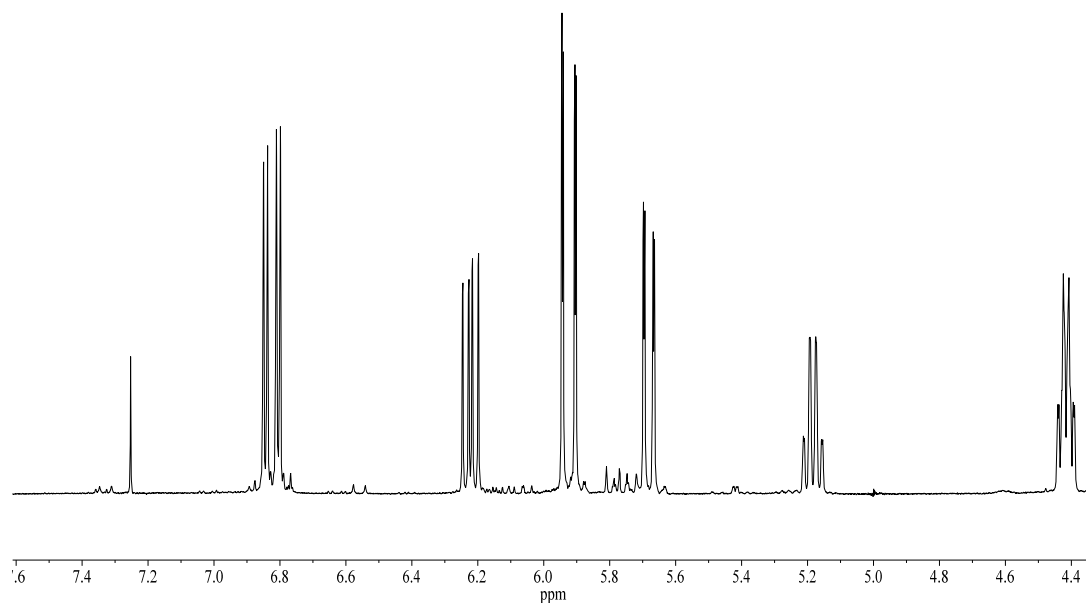


Figure 42: ^1H -NMR spectrum of the crude mixture of (62) and (63)

2.3.2 Reactions with the disubstituted alkyne DMAD using SP2

2.3.2.1 Photochemical reaction of DMAD with 2-propanol

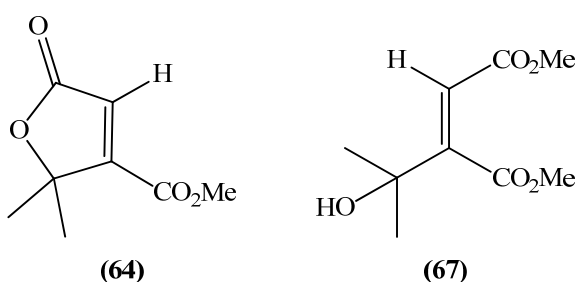


Figure 43

The reaction of DMAD and 2-propanol was carried out as described above (Section 2.2.1.1), the solution being irradiated for 8.5 h at which time GC analysis showed that all the DMAD had completely reacted. Two major products were present in a ratio of 47:53 (Figure 44) and had retention times identical to those obtained for (64)

and (67) in the reaction mediated by **SP1** (Section 2.2.3.1). After the usual work-up, the product was obtained as a yellow oil, and the spectroscopic data obtained correlated well with the spectroscopic data obtained for (64) and (67) previously (Section 2.2.3.1). In contrast to the reaction with **SP1**, the bicyclic product (68) was not detected by GC or NMR. The spectroscopic data again confirmed that no photomediator was present in solution at the end of the reaction. The reaction time in this case was similar to the **SP1** reaction which took 4.5 h (Section 2.2.3.1).

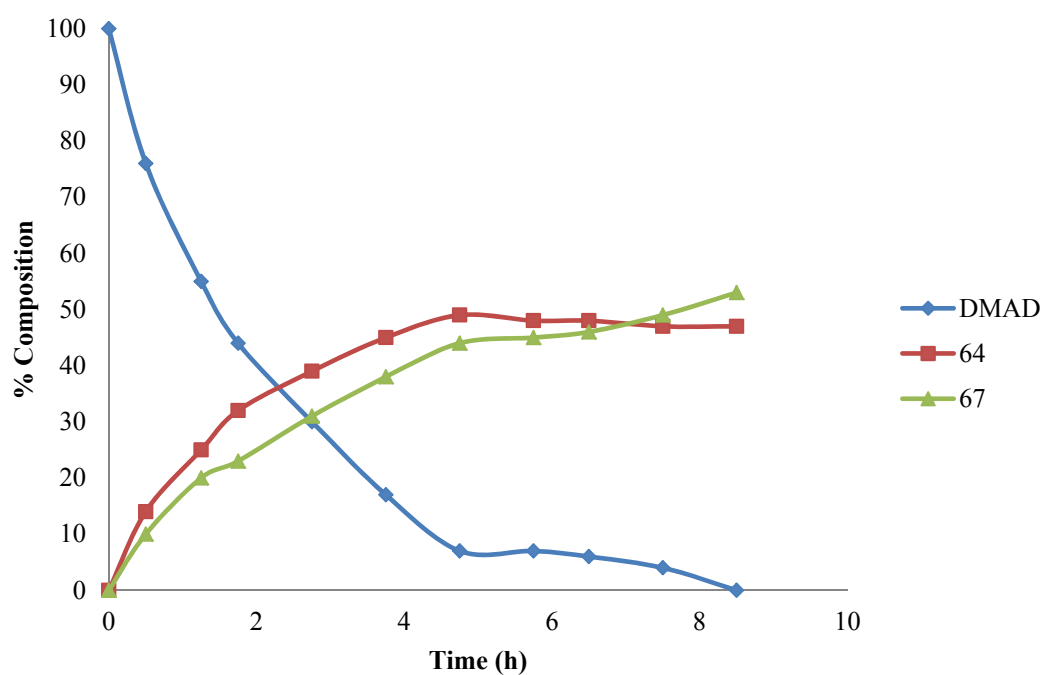


Figure 44

2.3.2.2 Photochemical reaction of DMAD with cyclopentanol

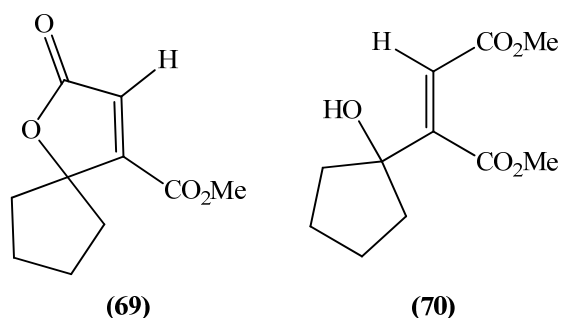


Figure 45

A solution of DMAD and cyclopentanol was prepared as normal (Section 2.2.1.1) and irradiated. The reaction was monitored by GC and after 21 h the reaction was discontinued as no reaction had taken place. The supported photomediator was removed by filtration and the solvent was removed. The NMR data for the crude product showed no sign of product formation. This result is not unlike that observed for the reaction mediated by **SP1** where product formation ceased after just 25% conversion of the alkyne (GC, 5 h).

2.3.2.3 Photochemical reaction of DMAD with 1,3-dioxolane

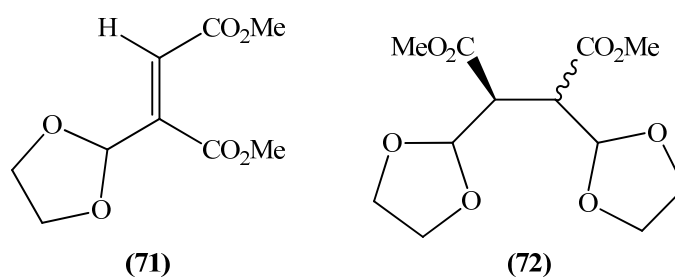


Figure 46

The reaction of DMAD and 1,3-dioxolane was carried out in the usual way (Section 2.2.1.1). The solution was irradiated for 22 h, when complete conversion of the alkyne had occurred. GC analysis showed the formation of one major product, the *cis* unsaturated ester (71), while in contrast to the **SP1** mediated reaction (Section 2.2.3.3), it showed there were only trace amounts of (72). The spectroscopic data confirmed the presence of (71) as the major component in the crude product.

2.3.2.4 Photochemical reaction of DMAD and cyclopentane

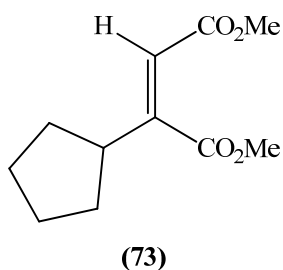


Figure 47

A solution of DMAD and cyclopentane containing **SP2**, prepared as above (**Section 2.2.1.1**), was irradiated and the reaction was monitored by GC. After 27 h irradiation, only 8% conversion of the alkyne had been achieved. The GC retention time of the only product formed was the same as that for **(73)** (**Section 2.2.3.4**). In the usual, manner, the supported photomediator was filtered off and the solvent evaporated leaving a yellow oil. The $^1\text{H-NMR}$ spectrum identified the product formed as the *cis* unsaturated diester **(73)**.

2.3.2.5 Photochemical reaction of DMAD and THF

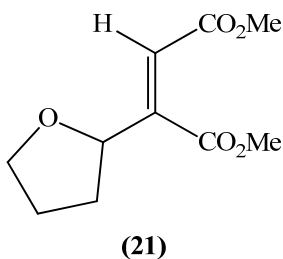


Figure 48

The reaction of DMAD and THF was carried out as described previously (**Section 2.2.1.1**). The solution was irradiated for 4.5 h, at which point GC analysis indicated that all the alkyne had been consumed forming a single product. The supported photomediator was removed and the solvent was evaporated leaving a yellow oil. The spectroscopic data correlated well with the data obtained for the (*Z*)-isomer **(21)** formed in the reaction carried out using **SP1** (**Section 2.2.3.5**).

2.4 Photochemical reactions using silica supported C-5 quaternary ammonium salt SP3

2.4.1 Reactions with the monosubstituted alkyne methyl propiolate using SP3

2.4.1.1 Photochemical reaction of methyl propiolate with 2-propanol

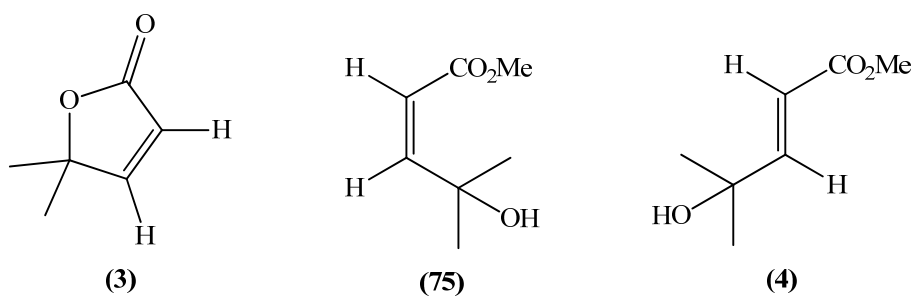


Figure 33

A solution of methyl propiolate and 2-propanol containing **SP3** was prepared in the same manner as that described above (**Section 2.2.1.1**). The solution was irradiated for just 2.75 h, at which point the alkyne had completely reacted to give three products (GC) (**Figure 49**). The products were present in a 22:21:57 ratio and corresponded to (3), the presumed *cis* isomer (75), and (4) (**Figure 33**). The supported photomediator was filtered off and the solvent was removed leaving a yellow oil. Surprisingly, in view of the experience of the reactions involving **SP1** and **SP2** (**Sections 2.2.1.1** and **2.3.1.1**), three products were still observed in the GC chromatogram of the crude product. The spectroscopic data also had signs of a third product. As expected, (3) and (4) were identified on the basis of the NMR data, which corresponded with the values obtained previously for these compounds (**Sections 2.2.1.1** and **2.3.1.1**). Methyl (*Z*)-4-hydroxy-4-methylpent-2-enoate (75) was identified as the third product based on the signals observed in the NMR data. Two doublets were observed at δ 5.75 and 6.40, due to the olefinic protons, with both coupling constants corresponding to olefinic protons in a *cis* geometry ($J_{cis} = 12.0$ Hz).

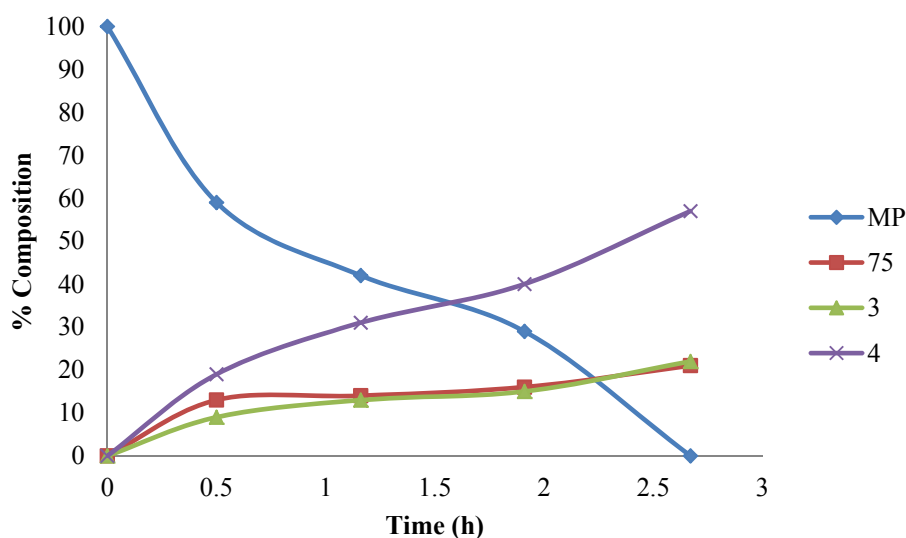


Figure 49

The identification of the (*Z*)-isomer (**75**) in this reaction is in contrast to the experience of methyl propiolate/2-propanol reactions that were mediated by **SP1** (Section 2.2.1.1) and **SP2** (Section 2.3.1.1), and indeed by benzophenone¹², whereby this isomer was only observed in a GC chromatogram, being converted to the lactone (**3**) in the course of solvent removal. This conversion is assumed to be due to the presence of some trace acid in the reaction mixture which would induce ring closure. It is not clear why lactonisation occurs less readily in this case.

This reaction, mediated by the C-5 quaternary ammonium salt supported photomediator, **SP3**, is complete in a much shorter time than the reaction mediated by **SP1** or **SP2**, and the spectroscopic data for the product is free of the aromatic signals which would indicate loss of photomediator from the surface.

2.4.1.2 Photochemical reaction of methyl propiolate with cyclopentanol

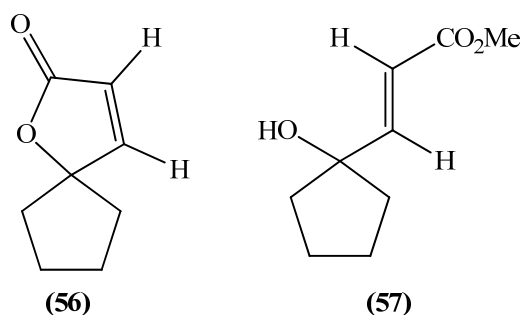


Figure 35

The reaction of methyl propiolate and cyclopentanol was carried out as detailed before (Section 2.2.1.1). The photoreaction was continued for 9 h when GC analysis confirmed that complete conversion of the alkyne to the two expected products, (56) and (57), in a 34:66 ratio, had occurred. Analysis of the spectroscopic data obtained for the mixture on removal of solvent and the photomediator confirmed the products present were (56) and (57), and that no photomediator had been washed from the silica surface.

Although the nature of the products and the ratios in which they are formed are relatively consistent when this particular reaction is mediated by **SP1**, **SP2** or **SP3**, the conversion achieved depends on the supported photomediator used. The use of **SP1** or **SP2** failed to achieve complete conversion and the irradiation time was very lengthy in both cases (30 and 53 h, respectively). In contrast, the supported photomediator **SP3** achieved 100% conversion in just 9 h.

2.4.1.3 Photochemical reaction of methyl propiolate with 1,3-dioxolane

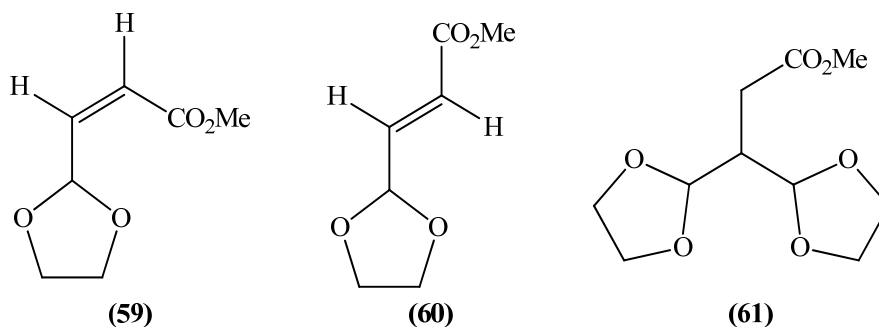


Figure 50

The reaction of methyl propiolate and 1,3-dioxolane using **SP3** was carried out as before (**Section 2.2.1.1**) with irradiation being continued for 7.75 h. GC analysis (**Figure 51**) showed that no further reaction of the alkyne was occurring at this point and that 80% conversion had been achieved. Three products, (**59**), (**60**) and (**61**) (**Section 2.2.1.3**) were observed in a 23:39:38 ratio (GC). The supported photomediator was filtered off and the solvent was evaporated. Both the ^1H - and ^{13}C -NMR spectra confirmed the formation of the *cis* and *trans* 2-substituted dioxolanes (**59**) and (**60**), and the saturated product (**61**). The product from the **SP3** reaction again shows no evidence for the leaching of the photomediator from the surface.

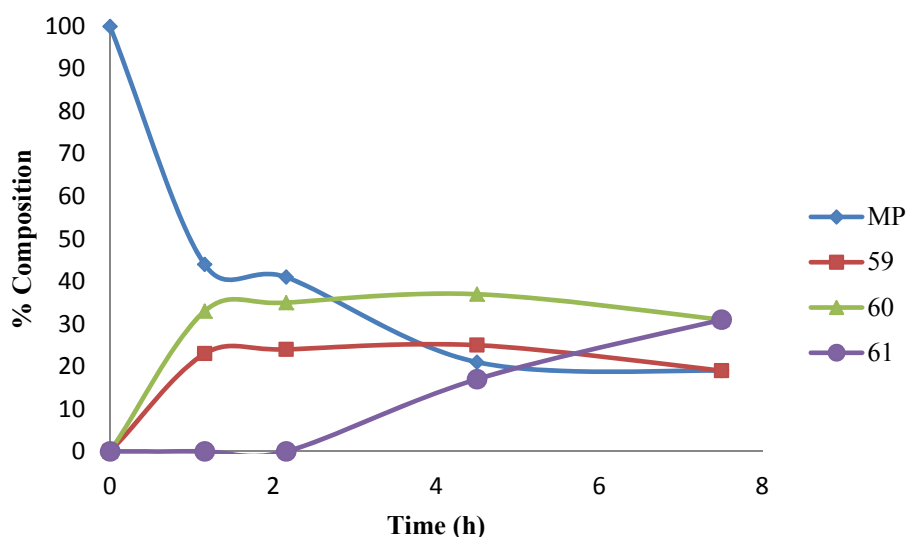


Figure 51

This result is a great improvement on the previous methyl propiolate/1,3-dioxolane reactions mediated by **SP1** (**Section 2.2.1.3**), which took 17 h to reach 60% conversion, and **SP2** (**Section 2.3.1.3**) which took 50 h to reach the same conversion (80%).

2.4.1.4 Photochemical reaction of methyl propiolate with cyclopentane

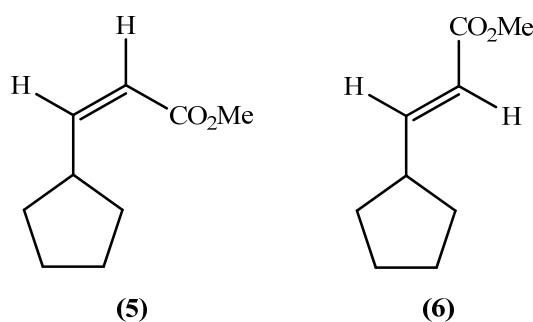


Figure 39

A solution of methyl propiolate and cyclopentane, with **SP3** as the supported photomediator, was prepared and irradiated in the usual manner (**Section 2.2.1.1**). The reaction was monitored by GC which showed that no further reaction was occurring after 11 h. A 92% conversion of the alkyne to the two expected products, the *cis* and *trans* isomers (5) and (6), had been achieved at this point. The ratio of the products was 30:70, which was similar to that observed for the previous **SP1** and **SP2** mediated methyl propiolate/cyclopentane reactions (**Sections 2.2.1.4** and **2.3.1.4**). Once the supported photomediator and the solvent had been removed, the NMR data for the crude product confirmed that (5) and (6) were formed in the reaction (**Figure 52**).

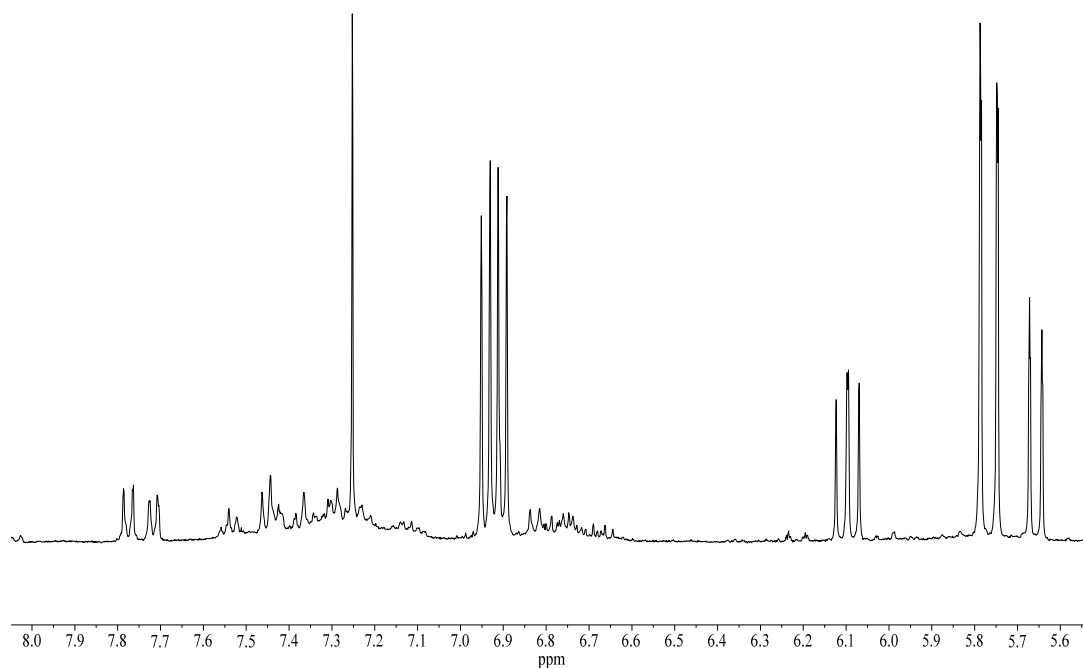


Figure 52: ^1H -NMR spectrum of the crude mixture of (5) and (6)

Although the ^1H -NMR spectrum of the product was clean in respect of product formation, small signals were present in the region normally associated with aromatic compounds. This suggested that some of the photomediator had been washed from the silica surface, opening up the possibility that the reaction was in part mediated by photomediator in solution rather than that which was bound to the silica surface. This would have implications for product purification and also photomediator recycling.

2.4.1.5 Photochemical reaction of methyl propiolate with THF

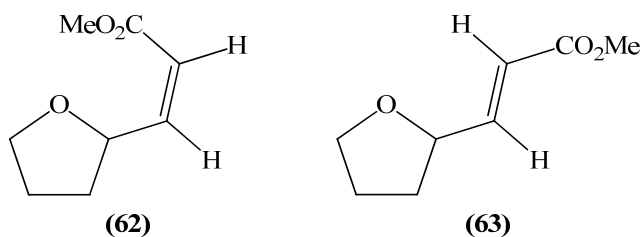


Figure 41

As before (Section 2.2.1.1), the reaction of methyl propiolate and THF was carried out using **SP3** and irradiation was continued until complete reaction of the alkyne had occurred (1.5 h). GC analysis indicated that two products were formed in a 43:57 ratio. This was consistent with the result observed for the other methyl propiolate/THF reactions (Sections 2.2.1.5 and 2.3.1.5). In the usual fashion, the supported photomediator and solvent were removed affording a yellow oil. It was clear from the spectroscopic data for the crude material that two products, (62) and (63), were present as expected, the data agreeing with those obtained previously (Section 2.2.1.5). The NMR spectrum of the crude product (Figure 53) was exceptionally clean allowing for the easy identification of the two products. It was also evident that there was no aromatic material present in the crude product. The time required to reach completion is also worth noting; the use of **SP3** appears to result in faster reactions than is the case for supported photomediators **SP1** and **SP2**.

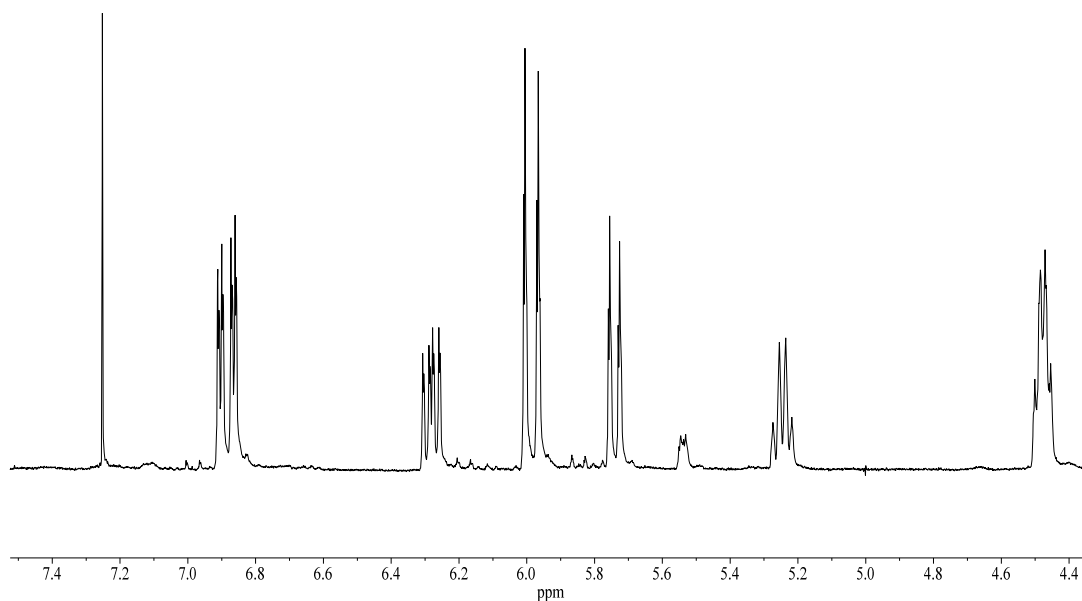


Figure 53: $^1\text{H-NMR}$ spectrum of the crude mixture of (62) and (63)

2.4.2 Reactions carried out using larger quantities of SP3

2.4.2.1 Photochemical reaction of methyl propiolate with 2-propanol

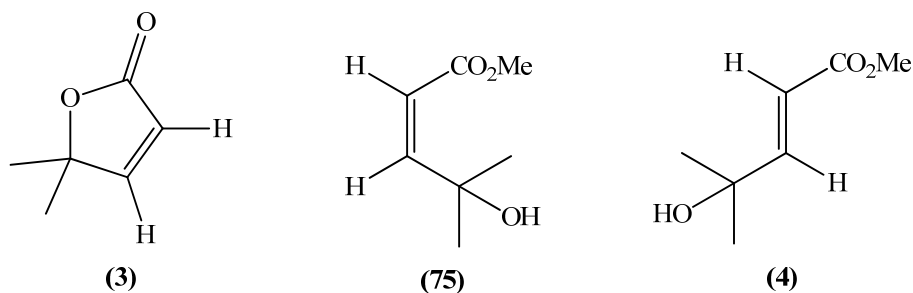


Figure 33

The reaction of methyl propiolate and 2-propanol was carried out as before (**Section 2.2.1.1**), using a larger amount of **SP3** (2.00 g instead of 1.20 g). GC analysis indicated that the reaction had reached completion after 2.5 h and that as before, three products (**Figure 33**) were present in a 14:21:65 ratio. The spectroscopic data obtained from the crude mixture confirmed the presence of **(3)**, **(75)** and **(4)**, and were in excellent agreement with the literature data^{100,102}. Overall, increasing the

amount of supported photomediator did not affect the length of the reaction or the product outcome.

2.4.2.2 Photochemical reaction of methyl propiolate with 1,3-dioxolane

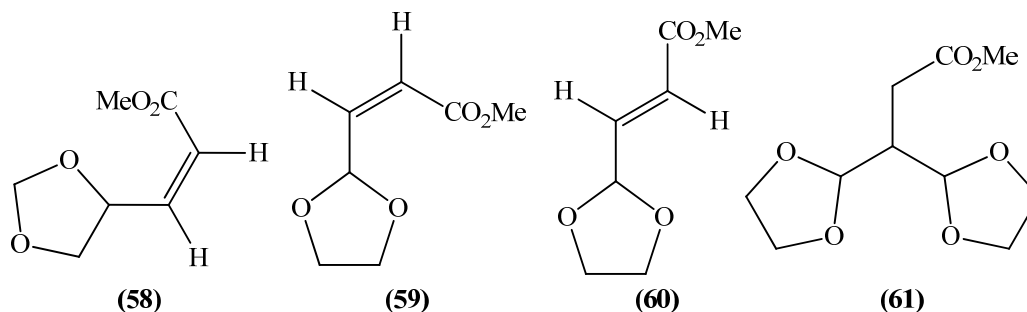


Figure 37

A solution of methyl propiolate and 1,3-dioxolane was prepared as detailed before (Section 2.2.1.1), using a larger amount of SP3 (2.00 g). Using standard irradiation, the reaction took just 4.3 h to achieve complete conversion of methyl propiolate to four products in a 16:29:9:49 ratio. The supported photomediator was filtered off and the solvent was removed leaving a yellow oil. The NMR spectra of the crude material identified (58), (59), (60) and (61) (Figure 37) as the four products, the data concurring with those obtained previously¹⁰⁴. This time, increasing the amount of supported photomediator led to complete reaction of the alkyne in just over half the time, a dramatic decrease given that increasing the amount of photomediator had no effect on the SP3 mediated reaction of methyl propiolate and 2-propanol (Section 2.4.2.1).

2.4.2.3 Photochemical reaction of methyl propiolate with THF

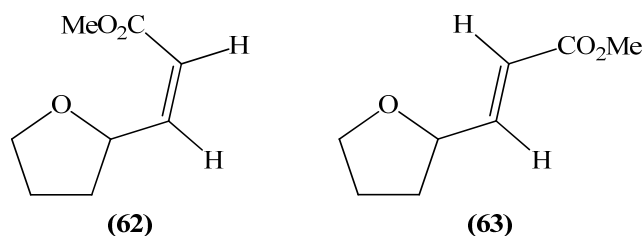


Figure 41

The photoreaction of methyl propiolate and THF using an increased amount of SP3 (2.00 g), was complete in just 1 h and, as before, two products were observed in a

43:57 ratio. The supported photomediator was removed by filtration and the filtrate concentrated *in vacuo*. The spectroscopic data for the crude mixture were in good agreement with the data previously published^{107,109,110} and confirmed that the products present were **(62)** and **(63)** (**Figure 41**). As in the case of the methyl propiolate/2-propanol reaction (**Section 2.4.2.1**), the extra photomediator had little effect.

2.4.3 Reaction carried out using a smaller quantity of SP3

2.4.3.1 Photochemical reaction of methyl propiolate with 2-propanol

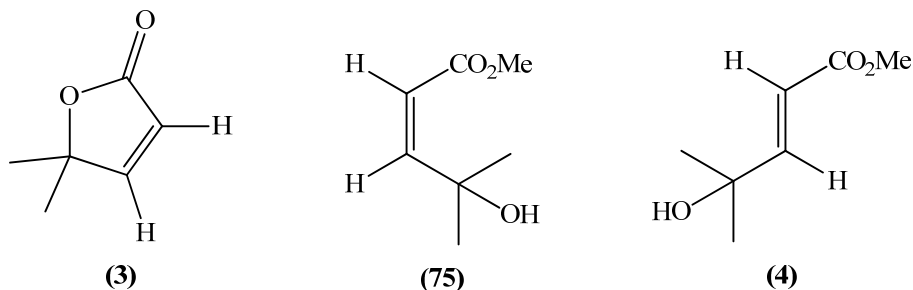


Figure 33

A solution of methyl propiolate with 2-propanol containing **SP3** (0.155 g, 0.05 mmol of photomediator) was prepared as before (**Section 2.2.1.1**) and irradiated for 5 h. The reaction was stopped at this point (80% conversion, GC) as no further reaction was occurring. GC analysis indicated the formation of three products, **(3)**, **(75)** and **(4)**, in a 23:25:52 ratio. The NMR data of the material isolated, containing **(3)**, **(75)** and **(4)**, were identical to those obtained previously (**Section 2.2.1.1**) and with those in the literature^{100,102}. Although the reaction did not go to completion, it is worth noting that as little as 1.67 mol% of the supported photomediator (with respect to the alkyne) is sufficient to achieve 80% conversion of the alkyne to products.

2.4.4 Reactions with the disubstituted alkyne DMAD using SP3

2.4.4.1 Photochemical reaction of DMAD with 2-propanol

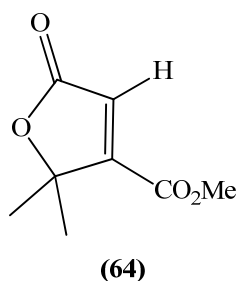


Figure 54

In a similar fashion to before (**Section 2.2.1.1**), a solution of DMAD and 2-propanol, containing **SP3**, was prepared. After irradiating, for 3.75 h, GC analysis indicated that the reaction had reached completion and that a mixture of products had formed, corresponding to that obtained for the reaction mediated by **SP1** (**Section 2.2.3.1**). One major product was identified in the mixture and after removing the supported photomediator and solvent in the usual way, the spectroscopic data confirmed that this major product was the lactone (**64**). This reaction was only slightly faster than that mediated by **SP1** but was more than twice as fast as that mediated by **SP2** (**Section 2.3.2.1**).

2.4.4.2 Photochemical reaction of DMAD with cyclopentanol

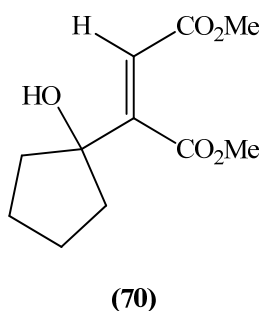


Figure 55

A solution of DMAD and cyclopentanol, containing **SP3**, was prepared as described earlier (**Section 2.2.1.1**). The photoreaction was complete after 5 h when complete conversion of the alkyne to a single product was observed by GC. The retention time of the product peak was identical to that of the *cis* isomer (**70**) formed in previous

reactions (Sections 2.2.3.2 and 2.3.2.2). The spectroscopic data obtained from the crude product were in excellent agreement with those obtained earlier for (70), and also with the data reported by Oka¹¹⁵. In contrast to the reactions of DMAD and cyclopentanol mediated by SP1 (5 h, 25% conversion) and SP2 (21 h, 0% conversion), this reaction went to completion in just 5 h again demonstrating the efficiency of SP3.

2.4.4.3 Photochemical reaction of DMAD with 1,3-dioxolane

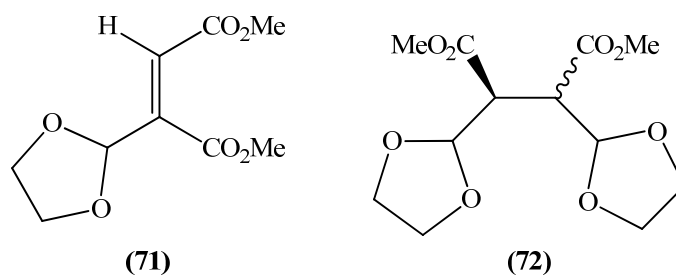


Figure 46

The reaction of DMAD and 1,3-dioxolane was carried out as detailed before (Section 2.2.1.1) using SP3, with irradiation, being continued for 10 h. GC analysis at this point, indicated all the alkyne had reacted and that three products were present in a 27:39:34 ratio, with retention times identical to those observed previously in the SP1 mediated reaction (Section 2.2.3.3). The spectroscopic data obtained for this crude product were the same as those obtained earlier for the reaction mediated by SP1 (Section 2.2.3.3), confirming the presence of (71), and (72) as a mixture of diastereomers. In agreement with the general trend being observed for this series of reactions, this SP3 mediated reaction is complete in a shorter time than those mediated by SP1 or SP2.

2.4.4.4 Photochemical reaction of DMAD with cyclopentane

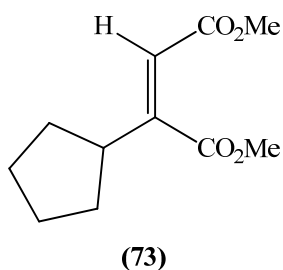


Figure 47

A solution of DMAD and cyclopentane containing **SP3** was prepared as before (Section 2.2.1.1). The solution was irradiated for 26 h, however only a 28% conversion to a single product was achieved (GC). The reaction was stopped and the supported photomediator was filtered off. The solvent was evaporated affording a yellow oil which gave spectroscopic data consistent with those obtained previously for the *cis* isomer (73) (Section 2.2.3.4). This reaction appears to perform poorly with each of the supported photomediators, with **SP2** being the most inefficient (Section 2.3.2.4). This is in contrast to previous work using benzophenone, that found the reaction reached completion in just 2.5 h, affording the two expected products (73) and (74) in a 12:1 ratio²⁰.

2.4.4.5 Photochemical reaction of DMAD with THF

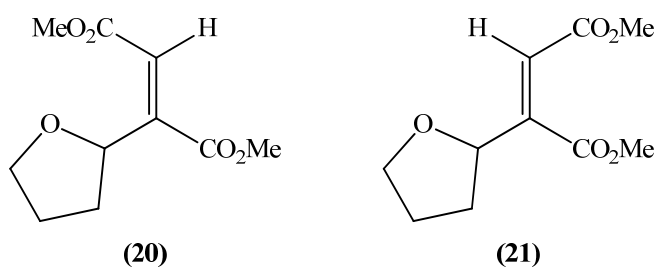


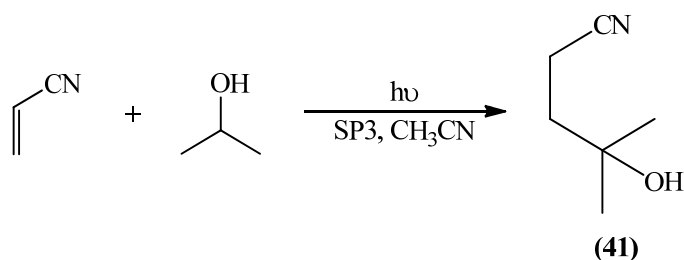
Figure 56

This reaction was carried out as before (Section 2.2.1.1), this time using **SP3** as the supported photomediator. The solution was irradiated and the reaction was monitored by GC. After 2.5 h irradiation, the reaction was complete. Two products, in a 40:60 ratio, were observed using GC. As before, the supported photomediator and the solvent were removed affording a yellow oil. The spectroscopic data

identified **(20)** and **(21)** as the two products; this finding was in agreement with what was observed for the other DMAD/THF reactions (Sections 2.2.3.5 and 2.3.2.5).

2.4.5 Reactions with monosubstituted alkenes using SP3

2.4.5.1 Photochemical reaction of acrylonitrile with 2-propanol



Scheme 74

A solution of acrylonitrile and 2-propanol was prepared in the standard way (Section 2.2.1.1) using SP3 as photomediator (Scheme 74). After 14 h irradiation, the alkene had completely reacted to give a mixture of products (GC). In the usual manner, the supported photomediator was filtered off and the solvent was removed leaving an orange oil. The spectroscopic data for the crude product identified 4-hydroxy-4-methylpentanenitrile **(41)** as the major component (Figure 57). The crude product was then adsorbed onto silica and eluted with an ethyl acetate/petroleum ether gradient, however, no identifiable products were isolated. Albini and Fagnoni have reported that the TBADT (2 mol%, relative to the alkene) mediated reaction of 2-propanol and acrylonitrile in acetonitrile gave **(41)** in a 72% isolated yield⁴⁷.

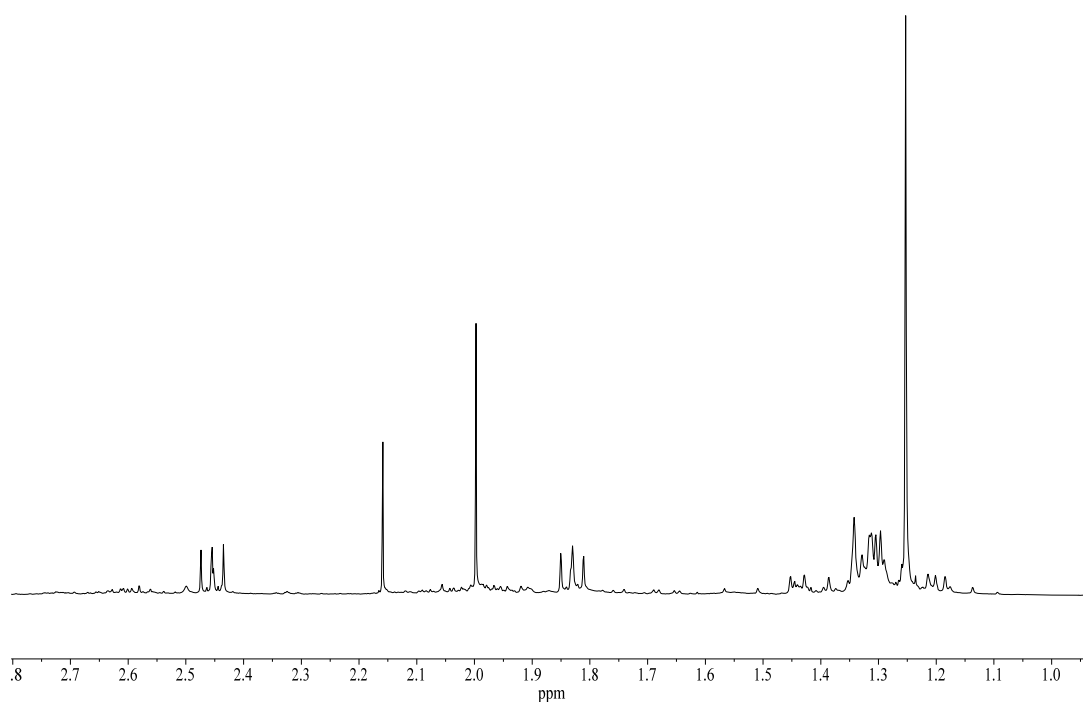
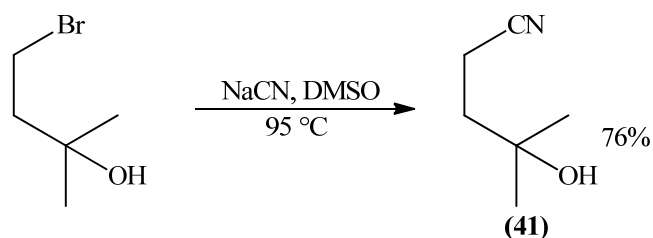


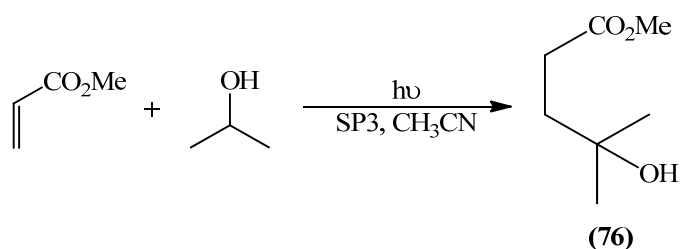
Figure 57: ^1H -NMR spectrum of the crude product (41)

The IR spectrum of the crude product had absorption bands at 3379 and 2252 cm^{-1} due to the OH and the nitrile bonds, respectively. The ^1H -NMR spectrum had a singlet at $\delta 1.25$ for the two methyl protons as well as two triplets at $\delta 2.46$ and 1.83 ($J_{vic} = 7.6\text{ Hz}$) for the CH_2 groups α and β to the nitrile group, respectively. In the ^{13}C -NMR spectrum, a signal at 120.6 ppm was due to the nitrile carbon and a signal at 69.8 ppm was due to the COH carbon. The carbon β to the nitrile group appeared at 38.7 ppm and the methyl carbons at 29.2 ppm , while a signal at 12.2 ppm was due to the carbon α to the nitrile group. The spectroscopic data reported here are in good agreement with those reported by Torneiro in 1997¹¹⁶, who obtained (41) in 76% yield by reacting 4-bromo-2-methylbutan-2-ol with sodium cyanide in dimethyl sulfoxide (DMSO), at $96\text{ }^\circ\text{C}$ (Scheme 75).



Scheme 75

2.4.5.2 Photochemical reaction of methyl acrylate with 2-propanol

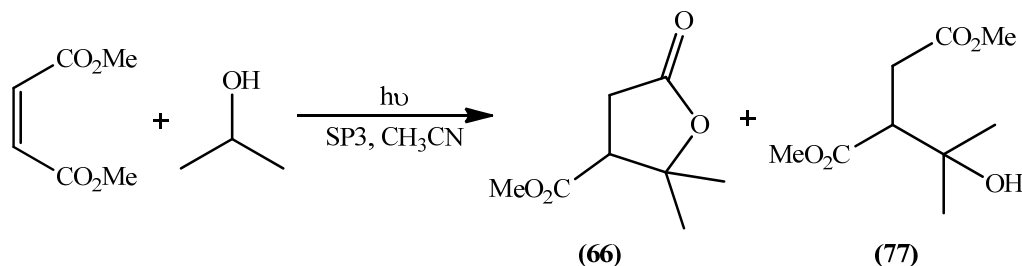


Scheme 76

The reaction was carried out as outlined above (**Section 2.2.1.1**) using methyl acrylate, 2-propanol and **SP3** (2.00 g) as photomediator. A short irradiation time of 4 h was required for complete conversion of the alkene to two products in a 69:31 ratio (GC). As before, the supported photomediator and the solvent were removed affording an orange oil which was adsorbed onto silica for purification. However, the sample appeared to break down during column chromatography as no identifiable products were isolated. As in the reaction above, the spectroscopic data for the crude product was used to deduce the nature of the products present. These showed that the product did not contain any lactone and that the major product was methyl 4-hydroxy-4-methylpentanoate (**76**), whose data were consistent with those published previously¹¹⁷. The IR spectrum contained a saturated ester carbonyl absorption band at 1730 cm⁻¹ and C-O absorption bands at 1264 and 1162 cm⁻¹. The ¹H-NMR spectrum contained two triplets at δ 1.81 and 2.44 ($J_{vic} = 7.4$ Hz) due to the methylene protons β and α to the ester group, respectively.

2.4.6 Reactions with disubstituted alkenes using SP3

2.4.6.1 Photochemical reaction of dimethyl maleate with 2-propanol



Scheme 77

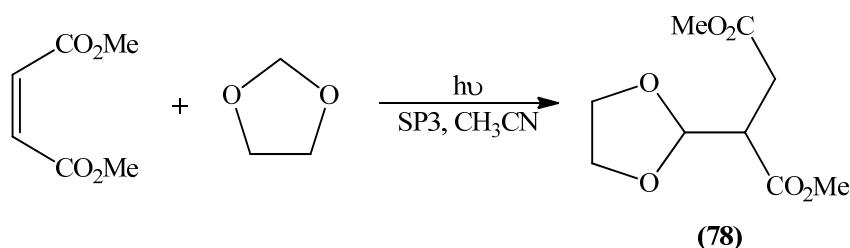
A solution of the disubstituted alkene dimethyl maleate and 2-propanol was prepared as before (Section 2.2.1.1) containing SP3 as photomediator (Scheme 77). The reaction was monitored by GC and after 36 h irradiation, no further reaction was occurring (GC, 90% conversion). Two products were observed in a 17:83 ratio, with the minor product having an identical retention time to that observed for the saturated lactone (66) formed in the DMAD/2-propanol reaction (Section 2.2.3.1). When the supported photomediator was filtered off and the solvent was evaporated, a yellow oil was obtained. Column chromatography was not carried out as identification of the products was possible using the spectroscopic data for the crude product. The lactone (66) was identified on the basis of the IR data which contained a band at 1776 cm^{-1} , together with other bands identical to those observed previously (Section 2.2.3.1). The major product present was (77), resulting from the addition of the α -hydroxyalkyl radical to the double bond of dimethyl maleate. The IR spectrum had a broad band at 3463 cm^{-1} for the OH group, as well as an absorption band at 1735 cm^{-1} for the ester carbonyl group. In the $^1\text{H-NMR}$ spectrum, a series of overlapping multiplets ($\delta 2.64\text{--}2.91$), was observed for the CH-CH₂ group, as well as two singlets for the protons of the two methoxy groups at $\delta 3.67$ and 3.74 . In the $^{13}\text{C-NMR}$ spectrum, two signals were observed for the carbonyl carbons at 174.8 and 172.9 ppm. The rest of the signals were as expected and in good agreement with published data¹¹⁸.

The reaction described above was carried out using an alkene/SP3 ratio of 30:1. In a second reaction, the amount of SP3 was doubled (0.61 g) to determine the effect this

would have on the reaction time, product ratios, etc. GC analysis indicated that after 28.5 h, the reaction had reached completion, an improvement on the previous reaction that stopped after 36 h and resulted in only 90% conversion. The ratio of the products observed (GC) did not however change significantly (15:85). As before, the spectroscopic data for the crude product confirmed that **(77)** was the major product and that only smaller amounts of **(66)** were present.

Upon increasing the amount of **SP3** used further (2.00 g), the reaction was complete in 30 h, a slightly longer reaction time than that of the previous reaction. As before, the ratio of products was 15:85 and **(77)** was again the major product.

2.4.6.2 Photochemical reaction of dimethyl maleate with 1,3-dioxolane



Scheme 78

A solution of dimethyl maleate and 1,3-dioxolane was prepared as before (**Section 2.2.1.1**) using the supported photomediator **SP3**. The solution was irradiated for 7 h, at which point complete conversion of the alkene to a single product was indicated by GC. It was possible to identify this as dimethyl 2-(1,3-dioxolan-2-yl)succinate (**78**) from the spectroscopic data obtained for the crude product which was sufficiently clean without purification. The IR spectrum had carbonyl and C-O absorption bands at 1733 cm^{-1} , and at 1266 and 1166 cm^{-1} , respectively. Two doublets in the $^1\text{H-NMR}$ spectrum (**Figure 58**) at $\delta 2.62$ ($J_{vic} = 4.8\text{ Hz}$, $J_{gem} = 16.9\text{ Hz}$) and 2.79 ($J_{vic} = 9.3\text{ Hz}$, $J_{gem} = 16.9\text{ Hz}$) were due to the CH_2 group α to the ester functionality. A multiplet at $\delta 3.24$ was due to the CH α to the ester group. The $^{13}\text{C-NMR}$ signals were as expected and were in excellent agreement with the literature values¹¹⁹.

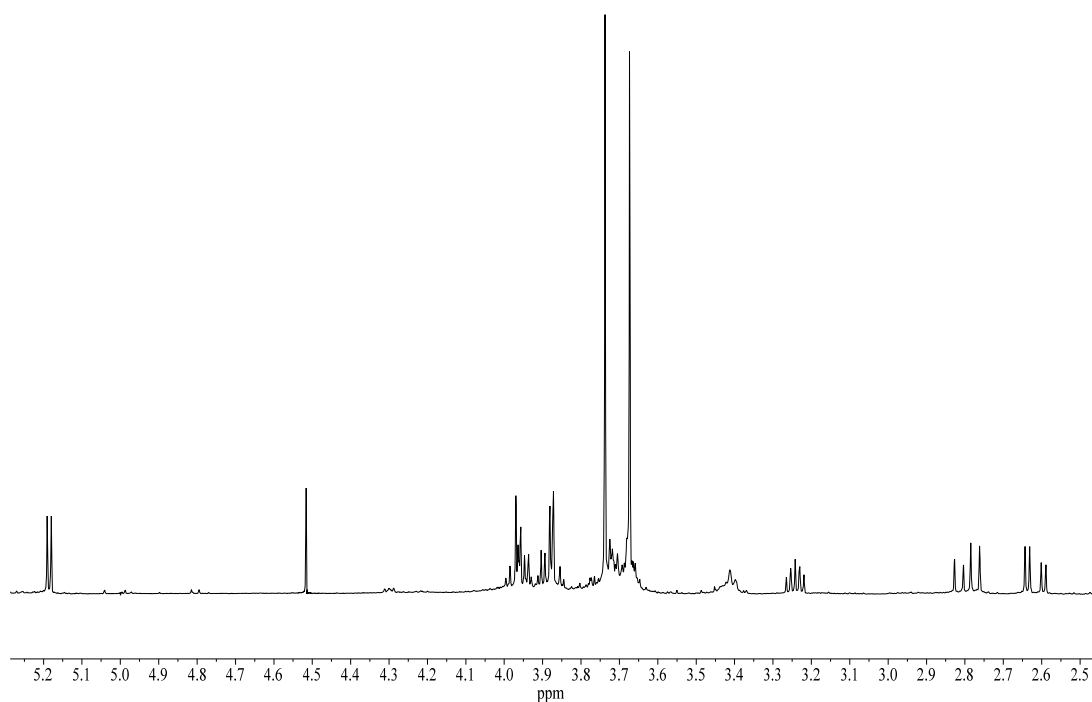
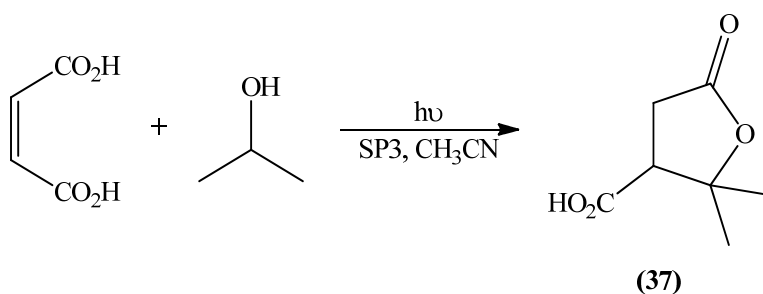


Figure 58: $^1\text{H-NMR}$ spectrum of the crude product (78)

2.4.6.3 Synthesis of terebic acid



Scheme 79

Terebic acid is a γ -lactone and derivatives of this small molecule have been found to possess a range of biological activities, including antitumor activity¹²⁰. It has been synthesised using the benzophenone mediated reaction of maleic acid in 2-propanol¹²¹ and so this reaction is a useful reference standard for evaluating photomediators. More recently, Albini, Fagnoni and Dondi reported the synthesis of terebic acid using the water soluble photomediator, benzophenone disodium disulfonate¹²². The synthesis of terebic acid was carried out by preparing a solution of maleic acid and 2-propanol (**Section 2.2.1.1**) with **SP3** as the supported

photomediator (**Scheme 79**). After just 6 h, GC analysis showed that the alkene had been completely consumed and that a single product had formed. The supported photomediator was removed by filtration and the solvent was removed by evaporation affording a white solid. The spectroscopic data identified terebic acid (**37**) as the only product and indicated that the crude product was very pure. The melting point obtained was 170.0-171.5 °C and was in good agreement with the literature value of 172-174 °C obtained by Kawazu¹²³. The IR data contained a broad band due to the OH group at 3118 cm⁻¹ as well as two distinct absorptions at 1775 and 1728 cm⁻¹ due to the lactone carbonyl group and the carbonyl group of the carboxylic acid, respectively.

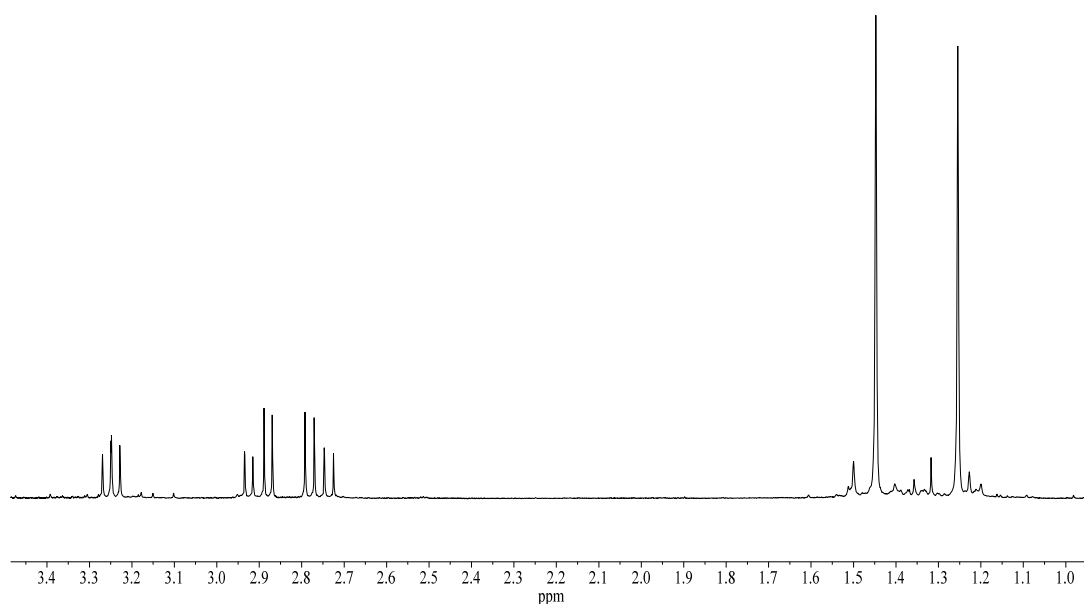


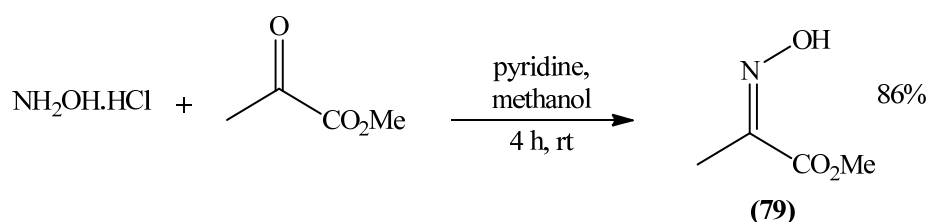
Figure 59: ¹H-NMR spectrum of the crude product (**37**)

The ¹H-NMR spectrum (**Figure 59**) of the crude product was very clean and contained all the appropriate signals. Two singlets at δ 1.23 and 1.43 were due to the methyl protons while the double doublets at δ 2.76 ($J_{vic} = 8.6$ Hz, $J_{gem} = 18.2$ Hz) and 2.90 ($J_{vic} = 7.8$ Hz, $J_{gem} = 18.2$ Hz) represented the CH₂ protons. The CH proton resonated as a double doublet at δ 3.23 ($J_{vic} = 8.6$ Hz, $J_{vic} = 7.8$ Hz). The ¹³C-NMR spectrum was as expected. Two carbonyl carbons resonated at 178.8 and 174.4 ppm while the quaternary carbon resonated at 87.1 ppm. The CH carbon signal at 50.1

ppm and the CH₂ carbon signal at 32.2 ppm were as expected, as were the signals for the CH₃ carbons at 27.2 and 22.5 ppm. All the data concurred with those reported by Kawazu¹²³.

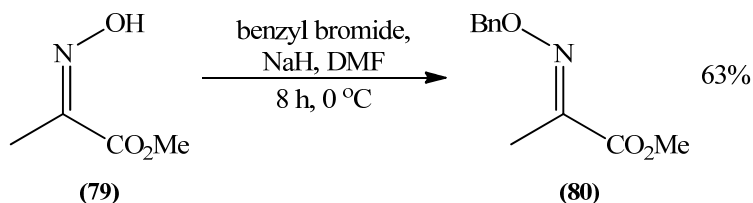
2.5 Synthesis of methyl (2*E*)-2-[(benzyloxy)imino]propanoate

2.5.1 Synthesis of methyl (2*Z*)-2-(hydroxyimino)propanoate



Scheme 80

A solution of hydroxylamine hydrochloride in pyridine was added to a solution of methyl pyruvate in methanol (**Scheme 80**). After stirring at rt for 4 h, standard work-up gave the product as a yellow oil. This was then purified by column chromatography using an ethyl acetate/petroleum ether gradient. Methyl (2*Z*)-2-(hydroxyimino)propanoate (**79**) was obtained as a white solid in 86% yield. Confirmation of the structure of the product was based on the spectroscopic data obtained. The IR spectrum had a broad absorption band at 3235 cm⁻¹ due to the OH group and a band at 1721 cm⁻¹ for the ester carbonyl. In the ¹H-NMR spectrum, two singlets at δ2.11 and 3.85 corresponded to the methyl and methoxy protons, respectively. The OH group resonated as a broad singlet at δ9.47. The ¹³C-NMR spectrum was as expected: the carbonyl carbon resonating at 164.2 ppm, the C=N carbon at 149.5 ppm, the methoxy carbon at 52.8 ppm, and the remaining signal at 10.3 ppm due to the methyl carbon, were all in agreement with the data published by Mirjafari in 2011¹²⁴.

2.5.2 Synthesis of methyl (2*E*)-2-[(benzyloxy)imino]propanoate

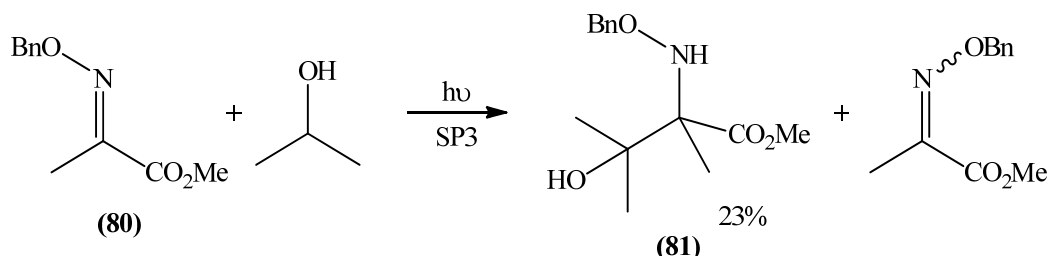
Scheme 81

Solutions of benzyl bromide and (79) in DMF were added to a solution of sodium hydride in DMF at 0 °C, and the mixture was stirred at this temperature for 8 h (Scheme 81). Standard work-up procedures gave a yellow oil which was purified by column chromatography using a diethyl ether/petroleum ether gradient. Methyl (2*E*)-2-[(benzyloxy)imino]propanoate (80) was isolated as a colourless oil in 63% yield. Although the starting material, (79), had *cis* geometry, the benzylated oxime formed is *trans*, the stereochemistry in both cases being assigned on the basis of a comparison of the ¹H-NMR data obtained and those in the literature. The *cis* product was not evident in either the GC or spectroscopic data.

The IR spectrum showed an absorption band at 1725 cm⁻¹ due to the carbonyl and bands at 1255 and 1071 cm⁻¹ due to the C-O bonds. The expected signals were also seen in the ¹H-NMR spectrum: a singlet at δ2.09 due to the methyl protons and a singlet at δ3.85 for the methoxy protons, in addition to a singlet at δ5.31 representing the OCH₂ protons. The remaining aromatic signals were as expected¹²⁵. In the ¹³C-NMR spectrum, the carbonyl carbon resonated at 164.2 ppm while the C=N carbon carbon appeared at 149.5 ppm. The substituted carbon of the phenyl ring resonated at 136.5 ppm, the remaining aromatic signals showing at 128.4 and 128.2 ppm. The remaining signals were in agreement with the data published previously¹²⁵.

2.6 Photochemical reactions of methyl (2*E*)-2-[(benzyloxy)imino]propanoate using SP3

2.6.1 Photochemical reaction of benzylated oxime with 2-propanol

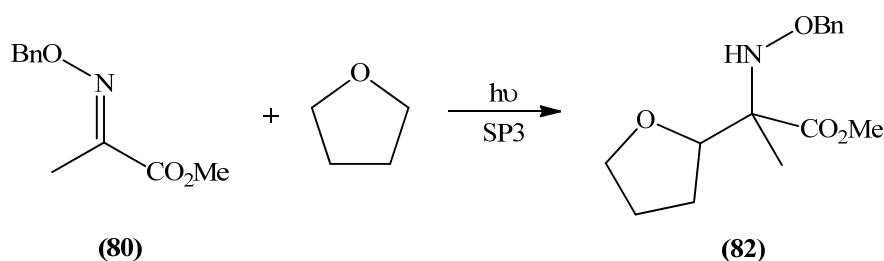


Scheme 82

A solution of methyl (2*E*)-2-[(benzyloxy)imino]propanoate (**80**) in 2-propanol containing SP3 was prepared as described earlier (Section 2.2.1.1). The solution was irradiated for 5.5 h until GC analysis indicated that no further reaction of (**80**) was occurring (70% conversion). From analysis of the GC chromatogram, only one main product had formed, however a peak with a very similar retention time to that of (**80**) had also appeared. The supported photomediator was filtered off and the solvent was removed affording a yellow oil. The product of the addition of an α -hydroxyalkyl radical to (**80**), methyl *N*-(benzyloxy)-3-hydroxy-3-methylisovalinate (**81**), was identified as the major product on the basis of the NMR spectra of the crude product. In addition to the *trans* isomer of the starting material (**80**), the corresponding *cis* isomer was also observed. Column chromatography was carried out using an ethyl acetate/petroleum ether gradient and (**81**) was isolated as a yellow oil in 23% yield (33% taking into account the 70% conversion). The IR spectrum had an absorption band at 3442 cm^{-1} due to the OH and NH bonds, and a band at 1733 cm^{-1} for the ester carbonyl bond. In the $^1\text{H-NMR}$ spectrum, three singlets were observed due to the protons of the three methyl groups (δ 1.15, 1.24 and 1.38). A double doublet was observed for the OCH_2 protons, the corresponding signal in (**80**) appearing as a singlet. In the $^{13}\text{C-NMR}$ spectrum, the carbonyl carbon resonated at 175.0 ppm and the substituted aromatic carbon resonated at 137.7 ppm. In addition, the quaternary carbon α to the ester group resonated at 71.4 ppm and the carbon of the OCH_2 group appeared at 73.8 ppm. The remaining signals were in agreement with published

data¹²⁵. The *cis* isomer of **(80)** could also be identified from the NMR spectra. In the ¹H-NMR spectrum, three singlets at δ 2.03, 3.82 and 5.11 were due to the methyl protons, the methoxy protons and the OCH₂ protons, respectively. In the ¹³C-NMR spectrum, the signal at 76.3 ppm was due to the OCH₂ carbon and the methyl carbon resonated as a signal at 16.8 ppm.

2.6.2 Photochemical reaction of benzylated oxime with THF



Scheme 83

A solution of methyl (2E)-2-[(benzyloxy)imino]propanoate **(80)** in THF containing **SP3** was prepared as detailed before (Section 2.2.1.1). After irradiating for 22 h it was apparent (GC) that no further reaction was occurring (80% conversion). Two products had formed in a 57:43 ratio, which were subsequently shown to be diastereomers of the addition product, methyl 3,6-anhydro-2-[(benzyloxy)amino]-2,4,5-trideoxy-2-methylhexonate **(82)**. After removing the solvent and supported photomediator in the usual way, the crude product was adsorbed onto silica and eluted with an ethyl acetate/petroleum ether gradient. The benzylated oxime **(80)** eluted first followed by one diastereomer of **(82)** in 18% yield (23% taking the 80% conversion into account). A mixture of both diastereomers eluted last in 45% yield. The structure of the pure diastereomer **(82)** was confirmed using the spectroscopic data obtained.

In the IR spectrum, an absorption band at 1730 cm⁻¹ accounted for the carbonyl group of the ester. In the ¹H-NMR spectrum, the methyl protons resonated as a singlet at δ 1.33, while the β CH₂ protons of the THF rings resonated as multiplets at δ 1.74-1.95 and the methoxy protons were seen as a singlet at δ 3.72. The THF ring methine proton resonated as a multiplet at δ 3.74 and a multiplet at δ 3.93-3.99 was

due to the CH₂ α to the ring oxygen. The benzyl CH₂ resonated as a double doublet at δ 4.60-4.69 and the aromatic signals appeared as multiplets at δ 7.25-7.35.

In the ¹³C-NMR spectrum (**Figure 60**), signals for the carbonyl carbon and the substituted aromatic carbon appeared at 173.9 and 137.9 ppm, respectively. The remaining aromatic carbons appeared at 128.5, 128.4 and 127.8 ppm, the methine ring carbon at 81.4 ppm and the benzyl CH₂ carbon at 77.2 ppm. The methylene carbon adjacent to the oxygen of the THF ring resonated at 69.0 ppm and the quaternary carbon attached to the ester group appeared at 68.7 ppm. The methoxy carbon resonated at 52.4 ppm and the two remaining THF methylene carbons appeared at 26.9 and 16.9 ppm. The final signal was due to the methyl carbon, and appeared at 25.8 ppm.

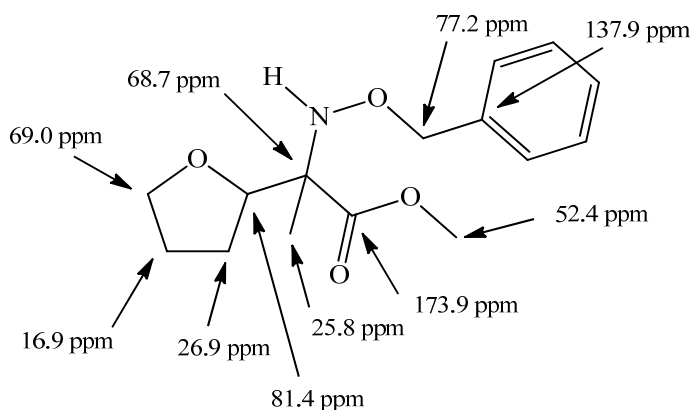
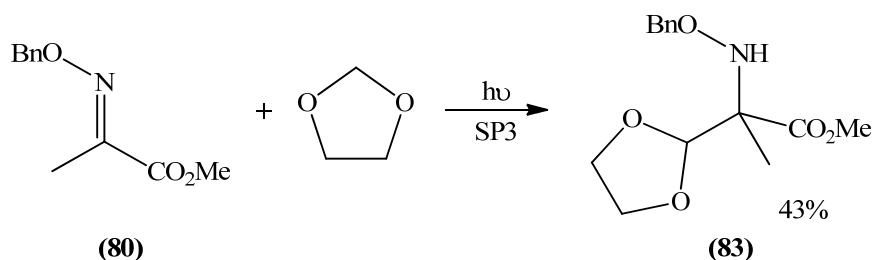


Figure 60: ¹³C-NMR chemical shifts for (82)

2.6.3 Photochemical reaction of benzylated oxime with 1,3-dioxolane



Scheme 84

A solution of methyl (2*E*)-2-[(benzyloxy)imino]propanoate (**80**) in 1,3-dioxolane containing **SP3** was prepared as described before (Section 2.2.1.1). The solution was irradiated for 4 h, at which point GC analysis indicated that complete reaction of the benzylated oxime (**80**) to a single product had occurred. After removing the supported photomediator by filtration and evaporating the solvent, a yellow oil was obtained. This crude product was adsorbed onto silica and eluted with an ethyl acetate/petroleum ether gradient. Methyl 2-[(benzyloxy)amino]-2-(1,3-dioxolan-2-yl)propanoate (**83**) was isolated as a yellow oil (43%), its spectroscopic data being in agreement with the data published previously¹²⁵.

The IR spectrum showed a broad band at 3510 and 1724 cm^{-1} due to the NH and the carbonyl groups, respectively. In the $^1\text{H-NMR}$ spectrum, the methyl protons and the methoxy protons were observed as singlets at δ 1.38 and 3.75, respectively. The methine ring proton appeared as a singlet at δ 5.05. In the $^{13}\text{C-NMR}$ spectrum a signal at 172.6 ppm confirmed the presence of a carbonyl carbon, while the methine ring carbon resonated at 104.1 ppm and the carbon attached to the ester group appeared at 68.6 ppm. This product has been synthesised previously using benzophenone as the photomediator¹²⁵. A solution of the benzylated oxime in excess 1,3-dioxolane was prepared and benzophenone (1 eq.) was added. The solution was irradiated with a 450 W Hanovia medium-pressure mercury lamp for 2 h. TLC confirmed that the benzylated oxime had been fully consumed. The crude product was purified by column chromatography affording (**83**) in 73% yield.

2.7 Photochemical reactions using silica supported C-8 quaternary ammonium salt SP4

2.7.1 Reactions with the monosubstituted alkyne methyl propiolate using SP4

2.7.1.1 Photochemical reaction of methyl propiolate with 2-propanol

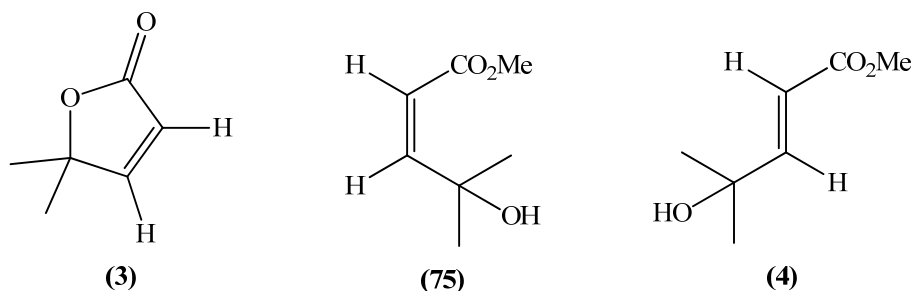


Figure 33

A solution of methyl propiolate and 2-propanol containing **SP4** was prepared as normal (Section 2.2.1.1). The solution was irradiated for 2.5 h until the alkyne was completely consumed. GC analysis indicated the formation of the three expected products, (3), (75) and (4), in a 17:15:68 ratio. After removing the supported photomediator by filtration and the solvent by evaporation, the spectroscopic data of the crude mixture confirmed the presence of the above products.

2.7.1.2 Photochemical reaction of methyl propiolate with THF

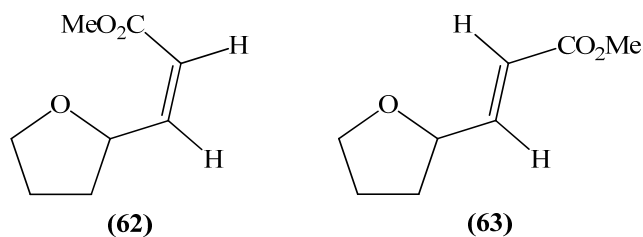


Figure 41

As before, a solution of methyl propiolate and THF, this time containing **SP4**, was prepared according to the general procedure (Section 2.2.1.1). After 1 h of irradiation, the alkyne had been completely consumed affording two 1:1 adducts, (62) and (63), in a 43:57 ratio (GC). The spectroscopic data of the crude product

indicated the presence of (62) and (63) (Figure 41). In addition to confirming the products, the NMR data also indicated that no aromatic material was present in the solution (Figure 61), demonstrating the photostability of the supported photomediator.

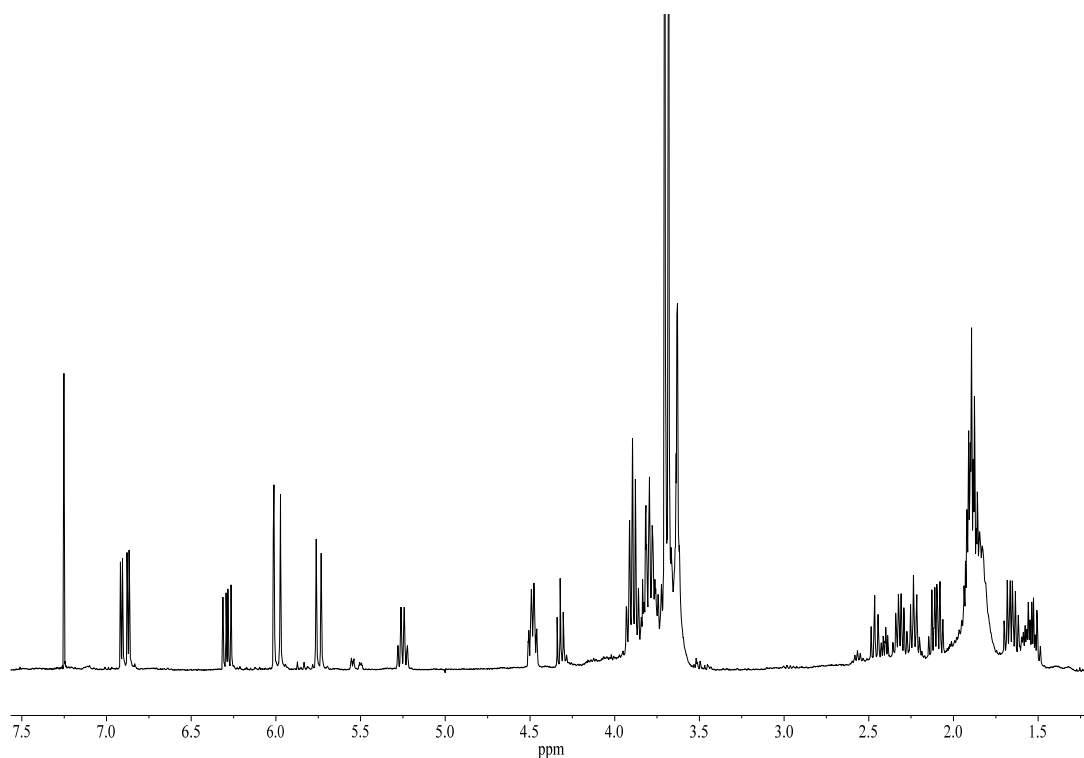


Figure 61: ^1H -NMR spectrum of the crude mixture of (62) and (63)

2.7.1.3 Photochemical reaction of methyl propiolate with cyclopentane

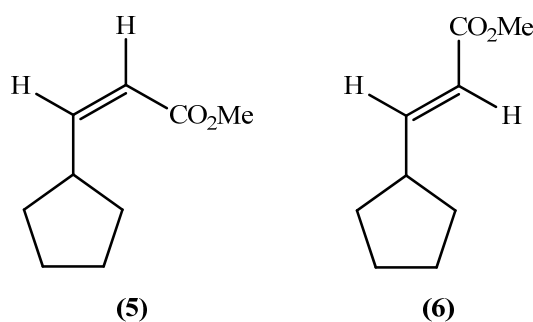


Figure 39

After preparing a solution of methyl propiolate and cyclopentane, containing SP4, as normal (Section 2.2.1.1), it was irradiated for 10.5 h. GC analysis indicated at this point that complete conversion of the alkyne to two products had occurred and that

they were present in a 32:68 ratio. The spectroscopic data obtained for the crude product, confirmed that the products formed were **(5)** and **(6)** (**Figure 39**), being in agreement with the data previously published^{21,105}.

2.7.2 Reaction with the disubstituted alkyne DMAD using SP4

2.7.2.1 Photochemical reaction of DMAD with 2-propanol

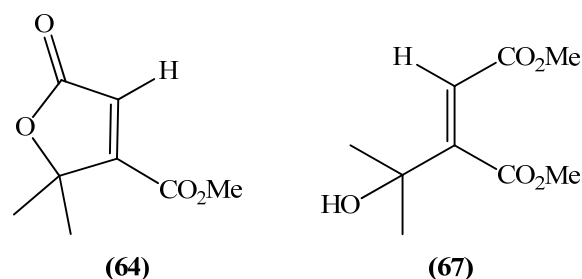


Figure 43

A solution of DMAD and 2-propanol containing **SP4**, was prepared as before, (**Section 2.2.1.1**) and irradiated. Complete reaction of the alkyne had occurred after just 2 h (GC) and two products, **(64)** and **(67)** were formed in a 28:72 ratio. After the supported photomediator was filtered off and the solvent was removed, a yellow oil was obtained. The spectroscopic data for this product were identical to those obtained previously (**Section 2.2.3.1**) confirming the formation of **(64)** and **(67)**. The NMR data also agreed with those elsewhere in the literature^{111,113}.

2.8 Photochemical reactions using silica supported C-12 quaternary ammonium salt SP5

2.8.1 Reactions with monosubstituted alkyne methyl propiolate using SP5

2.8.1.1 Photochemical reaction of methyl propiolate with 2-propanol

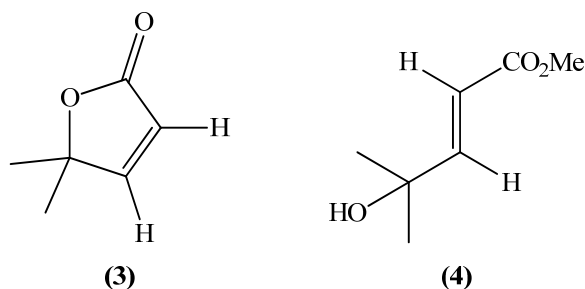


Figure 62

A solution of methyl propiolate and 2-propanol, containing **SP5** and dodecane as internal standard (IS), was prepared as described before (**Section 2.2.1.1**). After just 2.25 h irradiation, the GC analysis indicated that the alkyne had been completely consumed. Two products, **(3)** and **(4)**, were formed in a 32:68 ratio and obtained in a combined GC yield of 79%. Here again the spectroscopic data were as expected and in full agreement with published data^{100,102}.

2.8.1.2 Photochemical reaction of methyl propiolate with THF

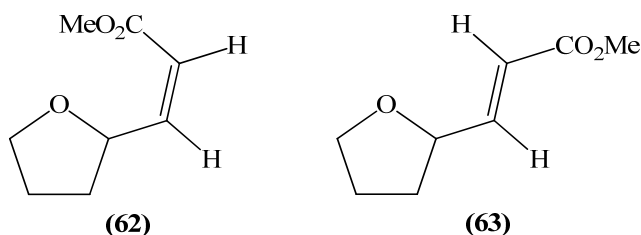


Figure 41

In the usual way (**Section 2.2.1.1**), a solution of methyl propiolate and THF, containing **SP5**, was prepared. Dodecane was added as the IS and the solution was irradiated for just 1 h when the reaction was complete (GC). Two products, **(62)** and **(63)**, were present in a 42:58 ratio and a combined GC yield of 99%. The

spectroscopic data of the crude product were consistent with those previously reported for (62) and (63) (Section 2.2.1.5).

2.8.1.3 Photochemical reaction of methyl propiolate with 1,3-dioxolane

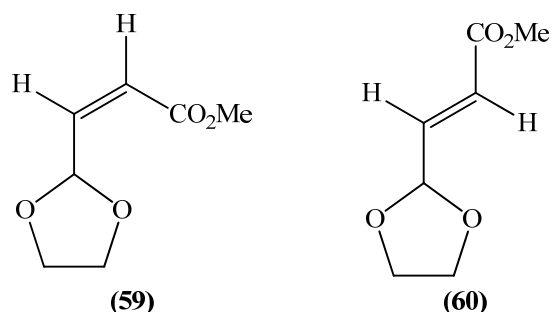


Figure 63

A solution of methyl propiolate and 1,3-dioxolane was prepared as before using SP5. After 1 h irradiation, the reaction was stopped as no further reaction of the alkyne was occurring (75% conversion, GC). The two products, (59) and (60), were observed in a 22:78 ratio. The usual work-up gave a yellow oil, the spectroscopic data for which were consistent with those obtained previously for (59) and (60) (Section 2.2.1.3).

2.8.2 Reaction with the disubstituted alkene maleic acid using SP5

2.8.2.1 Synthesis of (±)-terebic acid

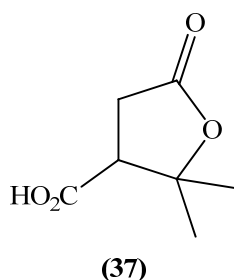


Figure 64

The synthesis of terebic acid was carried out as before (Section 2.4.6.3), this time using SP5. The solution was irradiated for 6 h when GC analysis indicated that the alkene had completely reacted to form a single product, terebic acid (37). The spectroscopic data of the product were consistent with the data obtained previously

(Section 2.4.6.3). As before, the crude product was extremely pure (IR, NMR). The reaction time was the same as that observed for the reaction using **SP3** (Section 2.4.6.3).

2.8.3 Reaction with methyl (2*E*)-2-[(benzyloxy)imino]propanoate using **SP5**

2.8.3.1 Photochemical reaction of benzylated oxime with 2-propanol

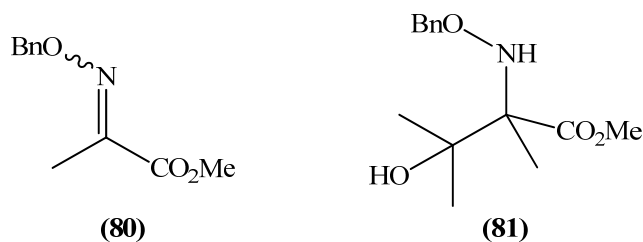


Figure 65

A solution of methyl (2*E*)-2-[(benzyloxy)imino]propanoate (**80**) in 2-propanol containing **SP5** was prepared as detailed before (Section 2.6.1). The solution was irradiated for 22 h. GC analysis indicated that no further reaction was occurring and that only a 13% conversion of the benzylated oxime to (**81**) had occurred. The supported photomediator was filtered off and the solvent was removed giving a mixture of (**81**) and both (*E*)- and (*Z*)- isomers of (**80**) (1:1.5) as a yellow oil. The spectroscopic data obtained for the crude product were in agreement with those obtained previously (Section 2.6.1) and with the results of the GC analysis.

2.9 Recycling of supported photomediators

2.9.1 Photochemical reaction of methyl propiolate and 2-propanol using SP1

The reaction of methyl propiolate and 2-propanol was carried out as before (**Section 2.2.1.1**) using dodecane (IS) and **SP1**. The solution was irradiated and stirred for 2.5 h until complete conversion of the alkyne to **(3)** and **(4)** in a 40:60 ratio had occurred. The supported photomediator was filtered off and the solvent was removed to give **(3)** and **(4)** in a combined GC yield of 86% (**Table 10, Run 1**). The spectroscopic data for the mixture were identical to those obtained previously (**Section 2.2.1.1**) and also showed no sign of any aromatic material. The supported photomediator was washed with acetonitrile on a sintered glass filter and then dried in a vacuum oven at 70 °C for 12 h. The reaction was then repeated a number of times using the recovered supported photomediator and the same mole ratio of reactants, taking into account any mechanical loss of **SP1** that may have occurred. The supported photomediator was reused until less than 100% conversion of the alkyne to product was observed when the reaction stopped (GC) (**Table 10**).

Run	Time (h)	Conversion (GC, %)	(3):(4)	Yield (GC, %)
1	7	100	40:60	86
2	22	100	32:68	84
3	28	100	37:63	85
4	48	86	36:65	61

Table 10: Recycling of supported photomediator SP1

The initial reaction, **Run 1**, takes 7 h to give 100% conversion of the alkyne to products, however **Run 2**, using the recovered photomediator, requires a longer reaction time of 22 h to give complete reaction of the alkyne. **Run 3** was complete in a slightly longer time, a reaction time of 28 h giving 100% conversion of the alkyne and a GC yield of 85%. **Run 4** using the recovered photomediator did not reach completion. After irradiating for 48 h, no further reaction was occurring; a 61% yield

was achieved. The NMR spectra (**Figure 66**) obtained for the crude product from each reaction showed no signs of aromatic material.

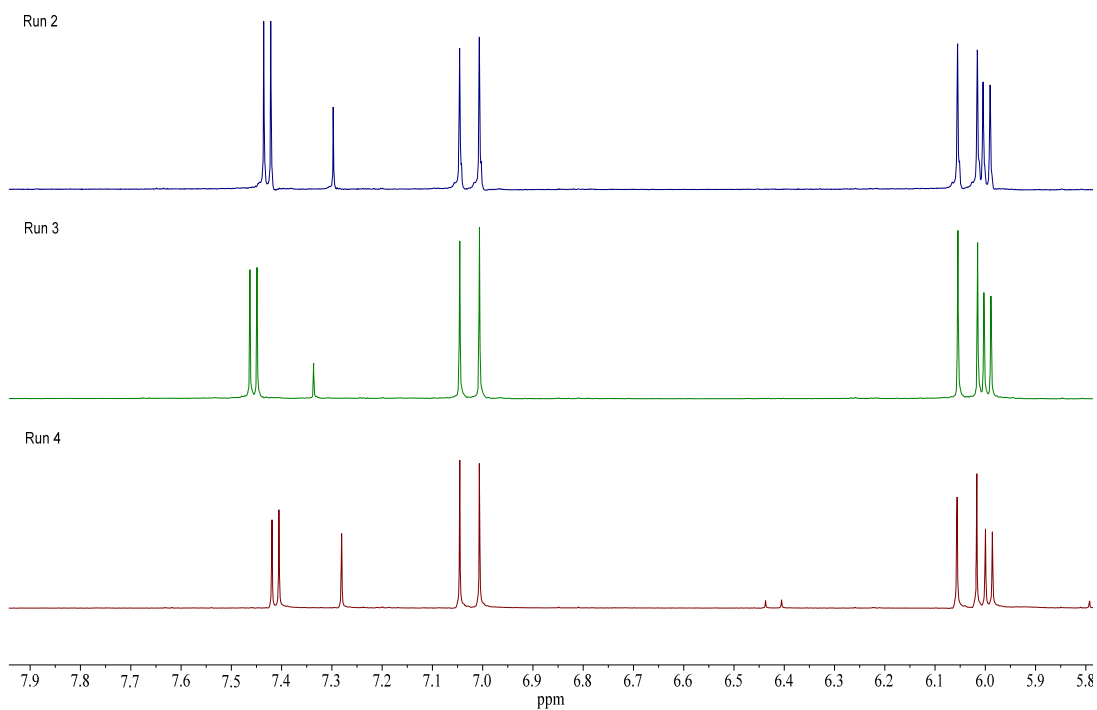


Figure 66: ¹H-NMR spectra of the crude product obtained for the methyl propiolate/2-propanol reaction obtained using recycled SP1

2.9.2 Photochemical reaction of methyl propiolate and 2-propanol using SP3

The reaction of methyl propiolate and 2-propanol, using **SP3**, was carried out as before (**Section 2.2.1.1**). The reaction mixture was irradiated and stirred until complete reaction of the alkyne had occurred (2.5 h). GC analysis showed three products, **(3)**, **(75)** and **(4)**, had formed in a 14:21:65 ratio. As before, the supported photomediator was filtered off and the solvent was removed. The spectroscopic data of the crude mixture was identical to those obtained previously. After washing the supported photomediator with acetonitrile, it was dried in a vacuum oven at 70 °C for 12 h. The resulting **SP3** was reused until the reaction no longer reached completion (**Table 11**).

Run	Time (h)	Conversion (GC, %)	(3):(75):(4)	Mass of product (g)
1	2.5	100	14:21:65	0.35
2	22	100	25:9:66	0.32
3	29	100	29:15:56	0.32
4	32	100	25:17:58	0.29
5	44	100	39:7:54	0.28
6	57	71	51:0:49	0.26

Table 11: Recycling of the supported photomediator SP3

As for **SP1**, a longer reaction time was observed for **Run 2** compared to **Run 1**, although complete conversion was observed. It was only on **Run 6** that the reaction did not reach completion. Nonetheless, a conversion of 71% was still achieved. None of the (*Z*)- isomer **(75)** remained at the end of the reaction (GC) presumably due to the long reaction time.

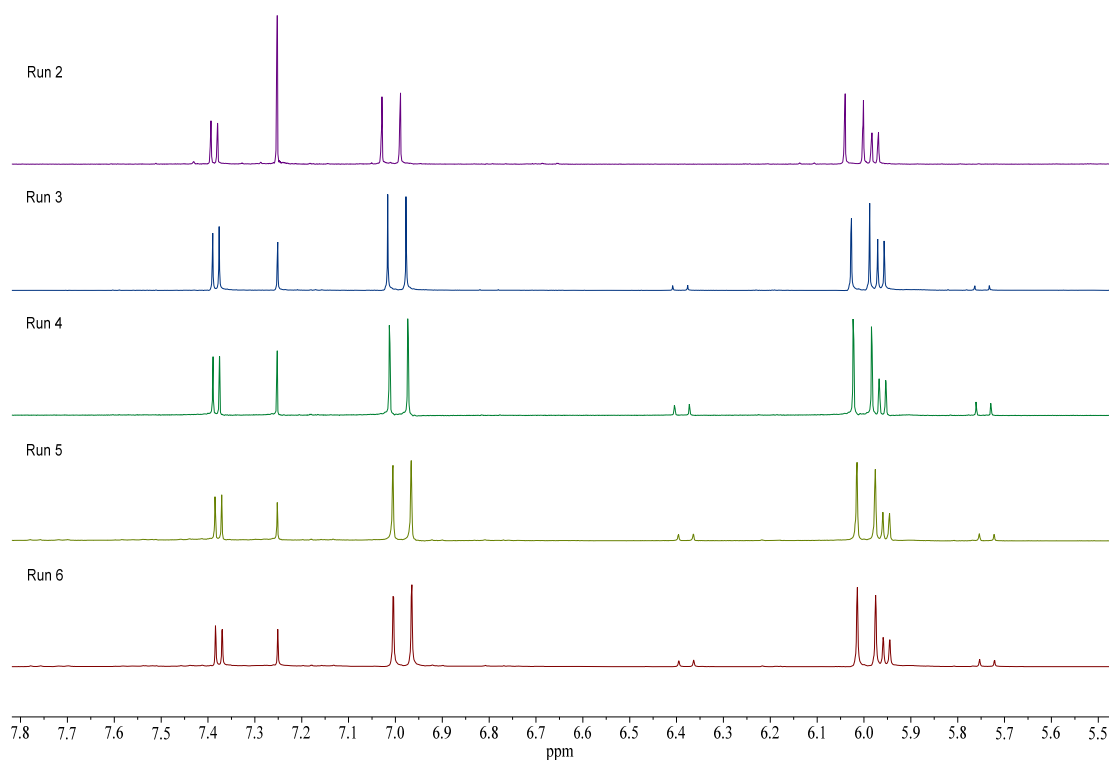


Figure 67: ^1H -NMR spectra of the crude product obtained for the methyl propiolate/2-propanol reaction obtained using recycled SP3

The ^1H -NMR spectra (**Figure 67**) of the crude products from each of the recycled runs show no aromatic signals suggesting that the photomediator is tightly bound to the silica surface.

2.9.3 Photochemical reaction of methyl propiolate and 2-propanol using SP5

The reaction of methyl propiolate and 2-propanol was carried out as before using dodecane (IS) and SP5. The recycling reactions were carried out as detailed above for both SP1 (Section 2.9.1) and SP3 (Section 2.9.2). The results clearly show that SP5 recycles very well in terms of consistently low reaction times and complete conversion of the alkyne (Table 12). It is only on Run 5 that the reactivity of the supported photomediator decreases, and less than 100% conversion is obtained (Table 12).

Run	Time (h)	Conversion (GC, %)	(3):(4)	Yield (GC, %)
1	2	100	34:66	84
2	2.25	100	41:59	85
3	3.25	100	40:60	84
4	4	100	38:62	76
5	8	40	37:63	24

Table 12: Recycling of the supported photomediator SP5

Although the reaction times remained short and the conversions were high, it was apparent from the NMR spectrum (Figure 68) that there was some leaching of the photomediator from the silica surface. Signals appeared around the region of the NMR associated with aromatic signals. Although the reaction time increases in the case of SP1 and SP3, the reaction times for SP5 are consistently low until Run 5.

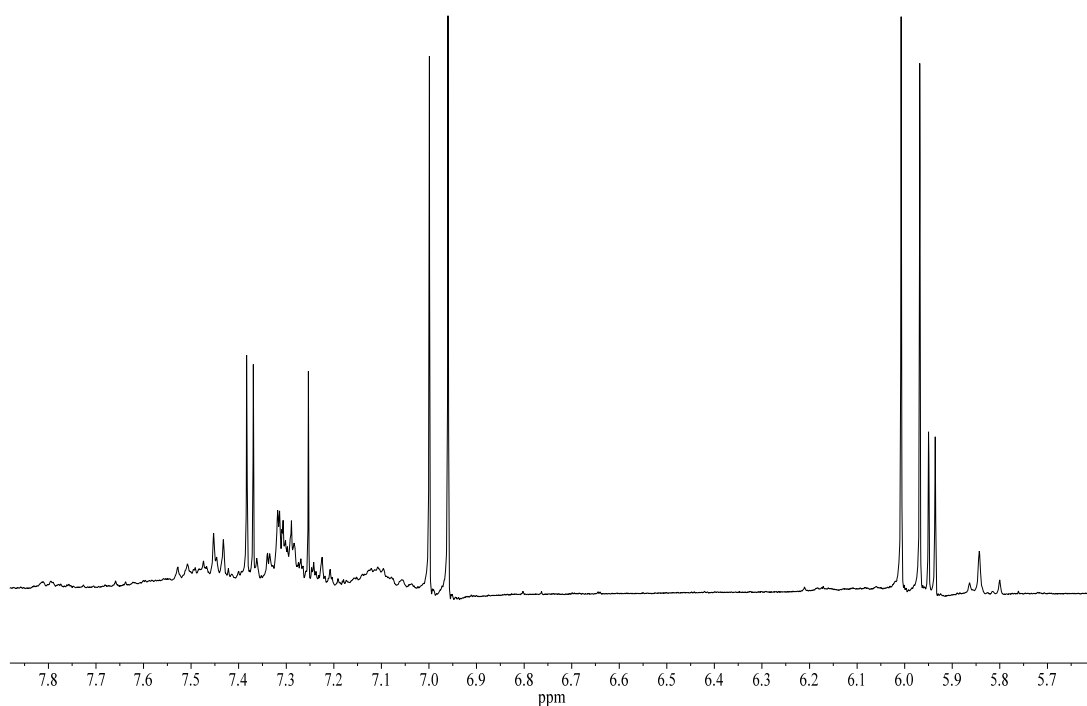


Figure 68: ^1H -NMR spectrum of the crude mixture of (3) and (4)

Overall, the results of the recycling studies clearly show the potential for the supported photomediators to be reused a number of times before a drop in conversion is observed.

2.10 Optimisation of the methyl propiolate/2-propanol reaction using SP3

A series of methyl propiolate/2-propanol reactions were carried out using **SP3** in order to optimise the reaction conditions. This particular reaction was complete in a relatively short time with each of the supported photomediators and so was ideal for optimisation experiments. The components of the reaction are the photomediator, the solvent, the unsaturated substrate and the H-donor. The ideal conditions would involve a catalytic quantity of the supported photomediator and the smallest volume of solvent possible. In addition, increasing the amount of the unsaturated substrate relative to the amount of the H-donor would be attractive. A further enhancement of the reaction conditions would be a reduction in the amount of H-donor, usually present in a large excess.

2.10.1 Effect of varying the quantity of photomediator

A solution of methyl propiolate and 2-propanol, containing **SP3** (2.00 g) was prepared as usual (**Section 2.2.1.1**) using dodecane as IS. After 2.5 h irradiation, the reaction was complete (GC) (**Rxn a, Table 13**). The products (**3**) and (**4**) were present in a 36:64 ratio and a yield of 89% was obtained (GC). When the amount of **SP3** was reduced by half (1.00 g), the reaction time increased only slightly from 2.5 to 3 h (**Rxn b, Table 13**). In addition, the product ratio (37:63) and the yield (91%) remained almost constant. Upon further reduction of the supported photomediator to just 0.50 g, the alkyne was completely consumed in 9 h (**Rxn c, Table 13**). Although this is a large increase on the previous reaction time, the reaction still goes to completion, in contrast to the reaction under standard conditions with **SP1** (**Section 2.2.1.1**), which only achieves 68% conversion when it comes to a stop after 7 h, and that with **SP2** (**Section 2.3.1.1**) which takes 36 h to go to completion. For subsequent reaction optimisation, 1.00 g of **SP3** (**Rxn b, Table 13**) was used.

Rxn	MP ^a	2-PrOH ^a	SP3 ^b	CH ₃ CN ^c	Time ^d (h)	(3):(4) ^e	Yield ^f (%)
a	3	60	2.00/0.68	60	2.5	36:64	89
b*	3	60	1.00/0.34	60	3	37:63	91
c	3	60	0.50/0.17	60	9.5	28:72	91

^a mmol, ^b mass (g) and mmol of photomediator, ^c mL of solvent, ^d reaction went to completion (GC) unless otherwise stated, ^e GC, ^f combined yield of (3) and (4) (GC), * reaction involving the optimum quantity of photomediator

Table 13: Effect of varying the quantity of supported photomediator

2.10.2 Effect of varying the quantity of solvent

A solution of methyl propiolate and 2-propanol containing **SP3** and dodecane (IS) was prepared using the smaller quantity of **SP3** which had been determined as optimum (**Rxn b**, **Table 13**). The quantity of solvent used was reduced by half to determine the effect on reaction time, product ratio and yield. After just 3.5 h irradiation, the reaction was complete and the ratio of products was unchanged (36:64); the yield, however, decreased from 91% to 75% (**Rxn d**, **Table 14**). As this decrease in yield was unexpected, the reaction was repeated. This time the reaction took 4.5 h to reach completion and a yield of 71% was obtained (**Rxn e**, **Table 14**). A further reduction in the amount of solvent led to no change in reaction time or product ratio, but surprisingly, the yield increased to 90% (**Rxn f**, **Table 14**). In view of this result, these reaction conditions were taken as standard for the next set of optimisation reactions (**Section 2.10.3**).

Rxn	MP ^a	2-PrOH ^a	SP3 ^b	CH ₃ CN ^c	Time (h) ^d	(3):(4) ^e	Yield ^f (%)
b	3	60	1.00/0.34	60	3	37:63	91
d	3	60	1.00/0.34	30	3.5	36:64	75
e	3	60	1.00/0.34	30	4.5	36:64	71
f*	3	60	1.00/0.34	15	4.5	36:64	90

^a mmol, ^b mass (g) and mmol of photomediator, ^c mL of solvent, ^d reaction went to completion (GC) unless otherwise stated, ^e GC, ^f combined yield of (3) and (4) (GC), * reaction involving the optimum quantity of solvent

Table 14: Effect of varying the quantity of solvent

2.10.3 Effect of varying the quantity of alkyne

In order to increase the amount of product accessible from each reaction, the amount of alkyne was varied. Using the quantities of photomediator and solvent that had been determined as optimum previously (**Rxn f, Table 14**), the amount of alkyne was doubled. The reaction time increased from 4.5 to 25 h, although the product yield decreased only slightly (**Rxn g, Table 15**). In an attempt to reduce this reaction time, the amount of solvent was increased (30 ml), with the result that the reaction time was reduced to just 11 h (**Rxn h, Table 15**). Although an increase in the quantity of product accessible from each reaction is desirable, the reaction using the lesser amount of solvent is more attractive from a clean/green chemistry perspective, and therefore **Rxn f, Table 15** was used as the starting point for the next series of optimisation reactions.

Rxn	MP ^a	2-PrOH ^a	SP3 ^b	CH ₃ CN ^c	Time (h) ^d	(3):(4) ^e	Yield ^f (%)
f*	3	60	1.00/0.34	15	4.5	36:64	90
g	6	60	1.00/0.34	15	25	37:63	80
h	6	60	1.00/0.34	30	11	38:62	95

^a mmol, ^b mass (g) and mmol of photomediator, ^c mL of solvent, ^d reaction went to completion (GC) unless otherwise stated, ^e GC, ^f combined yield of (3) and (4) (GC), * reaction involving the optimum quantity of alkyne

Table 15: Effect of varying the quantity of alkyne

2.10.4 Effect of varying the quantity of H-donor

The reaction solution was prepared as in **Rxn f, Table 15**, this time using a reduced quantity (30 ml) of the hydrogen donor, 2-propanol. Unfortunately this led to a substantial increase in the length of the reaction (30 h) (**Rxn i, Table 16**).

Rxn	MP ^a	2-PrOH ^a	SP3 ^b	CH ₃ CN ^c	Time (h) ^d	(3):(4) ^e	Yield ^f (%)
f*	3	60	1.00/0.34	15	4.5	36:64	90
i	3	30	1.00/0.34	15	30	38:62	80

^a mmol, ^b mass (g) and mmol of photomediator, ^c mL of solvent, ^d reaction went to completion (GC) unless otherwise stated, ^e GC, ^f combined yield of (3) and (4) (GC), * reaction involving the optimum quantity of hydrogen donor

Table 16: Effect of varying the quantity of H-donor

Thus, it appeared that **Rxn f, Table 14** represented the best conditions for the methyl propiolate/2-propanol reaction using **SP3**. Overall, relative to the conditions used in general, it was possible to reduce the amount of the supported photomediator by half and the amount of solvent by 75% without greatly affecting the reaction outcome.

2.11 Optimisation of the methyl propiolate/THF reaction using SP3

In the same way as above (Section 2.10), a series of reactions were carried out to optimise the methyl propiolate/THF reaction.

2.11.1 Effect of varying the quantity of photomediator

A solution of methyl propiolate and THF in acetonitrile containing dodecane (IS) and SP3 was prepared as described earlier (Section 2.2.1.1). Using the standard amount of SP3 (2.00 g), (Rxn a, Table 17) the reaction took just 1.5 h to reach completion and a high yield was obtained (81%). When the amount of SP3 used was reduced to just 1.00 g, the reaction time remained the same, as did the product ratio (44:56), while the yield of the reaction did not vary considerably (77%) (Rxn b, Table 17). A further reduction in the amount of SP3 (0.50 g) led to the reaction taking 7 h to achieve complete consumption of the alkyne, but also to a significant drop in the yield (Rxn c, Table 17). In light of this, Rxn b, Table 17 was considered to involve the optimum amount of the supported photomediator.

Rxn	MP ^a	THF ^a	SP3 ^b	CH ₃ CN ^c	Time (h) ^d	(62):(63) ^e	Yield ^f (%)
a	3	60	2.00/0.68	60	1.5	44:56	81
b*	3	60	1.00/0.34	60	1.5	44:56	77
c	3	60	0.50/0.17	60	7	46:54	58

^a mmol, ^b mass (g) and mmol of photomediator, ^c mL of solvent, ^d reaction went to completion (GC) unless otherwise stated, ^e GC, ^f combined yield of (62) and (63) (GC), * reaction involving the optimum quantity of photomediator

Table 17: Effect of varying the quantity of photomediator

2.11.2 Effect of varying the quantity of solvent

A solution of methyl propiolate using the optimum amount of **SP3** (**Rxn b**, **Table 17**) but with a reduced amount of the solvent acetonitrile (30 ml) was prepared as before. This led to a slightly longer reaction time but, disappointingly, to a substantial drop in the yield which decreased from 75% to just 45% (**Rxn d**, **Table 18**). An additional reduction in the amount of solvent led to a further increase in the reaction time, but no change in the yield (**Rxn e**, **Table 18**).

Rxn	MP^a	THF^a	SP3^b	CH₃CN^c	Time (h)^d	(62):(63)^e	Yield^f (%)
b*	3	60	1.00/0.34	60	1.5	44:56	77
d	3	60	1.00/0.34	30	3.8	47:53	45
e	3	60	1.00/0.34	15	4.25	47:53	44

^a mmol, ^b mass (g) and mmol of photomediator, ^c mL of solvent, ^d reaction went to completion (GC) unless otherwise stated, ^e GC, ^f combined yield of **(62)** and **(63)** (GC), * reaction involving the optimum quantity of solvent

Table 18: Effect of varying the quantity of solvent

2.11.3 Effect of varying the quantity of photomediator using a very large excess of THF

As a reduction in the amount of solvent had a very negative effect on the reaction, the effect of reducing the amount of photomediator in reactions involving a large volume of solvent was explored. It was found that using the standard amount of **SP3** (2.00 g), and a large excess of THF led to a fast reaction (**Rxn f**, **Table 19**). Disappointingly however, the yield was lower than the previous reaction using the standard amount of THF (**Rxn a**, **Table 17**). When a smaller amount of **SP3** (1.00 g) was used, the length of the reaction did not vary a lot, but the yield of the reaction actually increased to 70% (**Rxn g**, **Table 19**). A further reduction in the amount of **SP3** (0.50 g) resulted in a reaction that reached completion in just over 1.5 h and to a further increase in the yield (81%) (**Rxn h**, **Table 19**). Finally, the amount of the photomediator was reduced to just 3 mol% (0.25 g) (**Rxn i**, **Table 19**) with respect to

the alkyne. As before, the reaction time was short, with complete consumption of the alkyne occurring in 2.5 h. The yield was slightly lower than the previous reaction, but still remained high (71%).

Rxn	MP ^a	THF ^a	SP3 ^b	CH ₃ CN ^c	Time (h) ^d	(62):(63) ^e	Yield ^f (%)
f	3	247	2.00/0.68	60	1.66	44:56	60
g	3	247	1.00/0.34	60	1.83	45:55	70
h	3	247	0.50/0.17	60	1.66	46:54	81
i*	3	247	0.25/0.09	60	2.5	47:53	71

^a mmol, ^b mass (g) and mmol of photomediator, ^c mL of solvent, ^d reaction went to completion (GC) unless otherwise stated, ^e GC, ^f combined yield of (62) and (63) (GC), * reaction involving the optimum quantity of photomediator

Table 19: Effect of varying the quantity of photomediator using a very large excess of THF

In summary, the reaction of methyl propiolate with THF was most efficient when a large excess of THF was used. The reaction reached completion in just 2.5 h when 3 mol% SP3 was used.

Overall these optimisation studies show that although improvements can be achieved by changing the relative amounts of the various components, choosing the optimum conditions requires compromise in terms of the possible variables.

2.12 Molecular modelling

2.12.1 Introduction

The supported photomediators synthesised were modelled using the MMFF molecular mechanics forcefield implemented in Spartan '08 or Spartan '10. The surface of silica has been modelled in a variety of ways. Ugliengo, for example, produced a model of a hydroxylated silica surface¹²⁶ based on a 2-D slab cut from the surface of edingtonite, a crystalline silicate, in which both faces were hydroxylated to maximise symmetry. This model was subsequently used in a study of the adsorption of glycine¹²⁷. In 2008, Tielens reported a model for the hydroxylated surface of amorphous silica¹²⁸ that was based on a SiO₂ glass model reported previously¹²⁹. Tielens' model consisted of interconnected irregular sized rings with a total of twenty-six SiO₂ units. All of the free sites were terminated with hydroxyl groups and the molecular formula of the silica model was H₂₇O₆₅Si₂₆. In 2011¹³⁰, this silica model was used in DFT calculations to determine the energetically favourable conformations of a liposome, dipalmitoylphosphatidylcholine, adsorbed onto the silica surface.

The silica structure used in the molecular modelling study described in this thesis was developed using the latter approach. A relatively flat silica surface was built using a 2-D array of fused 12-14 atom siloxane rings and both faces were terminated with hydroxyl groups (**Figure 69**). The molecular formula of this model is H₅₀O₉₃Si₃₅. Reflecting what are believed to be features of the surface of silica, this model included *geminal* and *vicinal* silanol groups. It is also worth noting that it is possible to incorporate water molecules onto the silica surface mimicking its often solvated nature (**Figure 70**). The possible involvement of physisorbed water was not however considered in the present work.

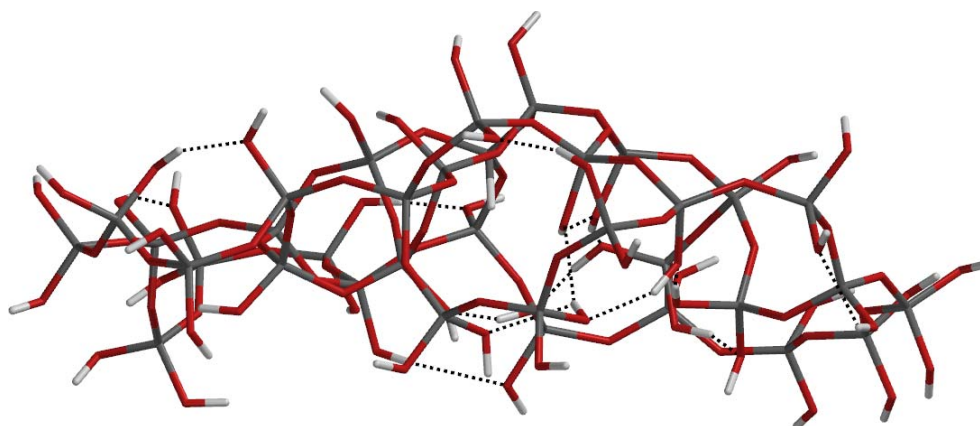


Figure 69: Silica surface used in conformational searching showing hydrogen bonding

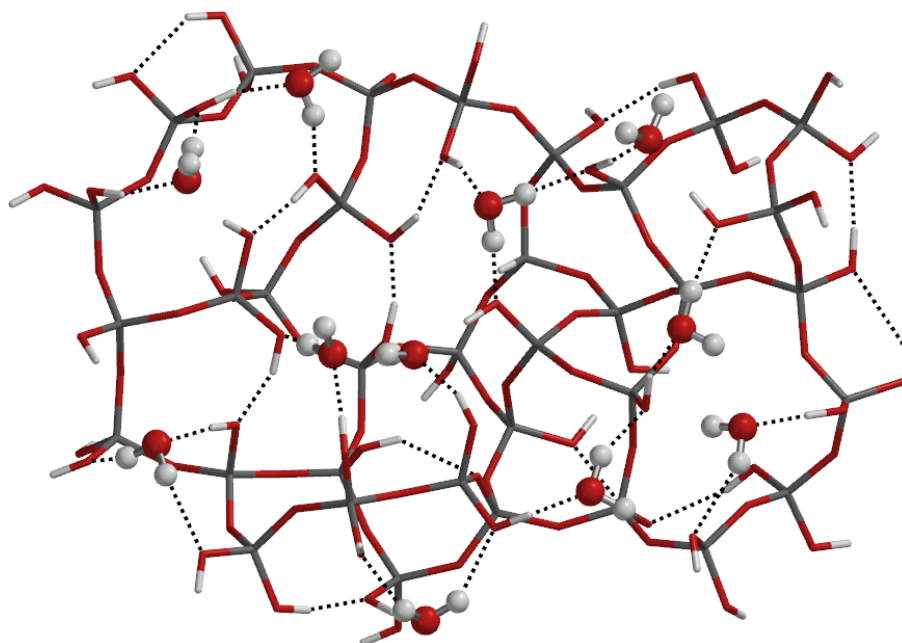


Figure 70: Water solvated silica surface showing hydrogen bonding

In each case the starting point for a Monte Carlo based conformational search procedure involved the photomediator and its linking chain in an approximately vertical relationship with the surface. It was considered that this starting geometry was most likely to lead to a representative set of conformers, including those in which the linking chain is vertical or parallel to the silica surface. In reality, the silica surface is part of a rigid 3-D network structure and would not undergo conformational changes. To reflect this, the heavy atoms in the silica model - the oxygen and the silicon atoms - were frozen in terms of the conformational search

calculations, and conformational flexibility was considered to involve only the photomediator, its linking chain, and the hydrogen atoms of the surface silanol groups.

2.12.2 Conformational search results

2.12.2.1 Conformational search results for SP1

The first supported photomediator studied was 3-aminopropyl silica bound benzophenone, **SP1**. 3-Aminopropyl silica is prepared by reacting (3-aminopropyl)triethoxysilane with silica. This can lead to a surface linkage involving one, two or three of the ethoxy groups. A consideration of the distribution of the silanol groups would suggest that a linkage involving all three ethoxy groups would be improbable. For this reason a linkage involving two ethoxy groups was employed; it was assumed that the third ethoxy group was converted to a silanol group during the preparation of the 3-aminopropyl silica. The Si-O-Si groups connecting the linking chain to the surface were constrained to have a standard Si-O bond length (1.60 Å)¹³¹ and Si-O-Si bond angle (150 °)¹³¹. A molecular mechanics optimised 4-benzoyl-*N*-propylbenzamide group was attached to the silica model in an approximately vertical arrangement and in keeping with the above considerations (**Figure 71**); this was used as the starting geometry for a conformational search procedure.

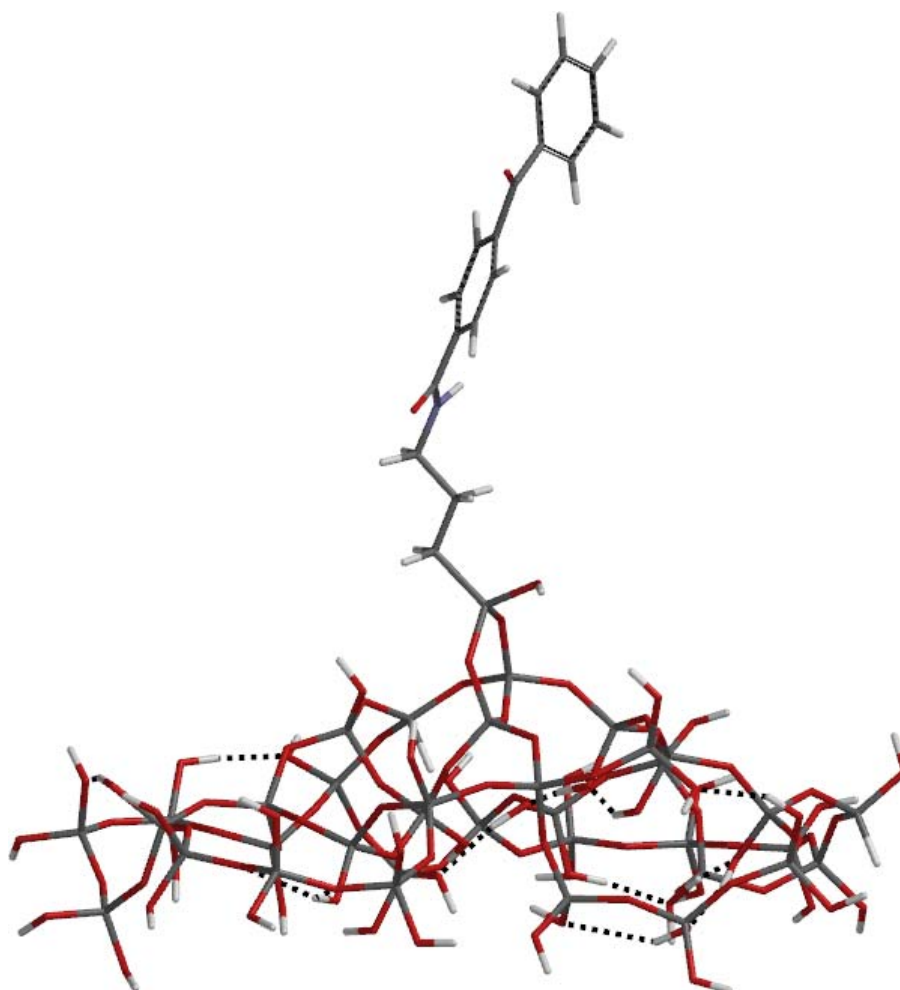


Figure 71: Initial conformation of SP1 showing hydrogen bonding

Molecular mechanics and Monte Carlo based conformational searching produced a set of low energy conformers (**Table 20**) in an energy window of 400 kJ mol^{-1} above the lowest energy form.

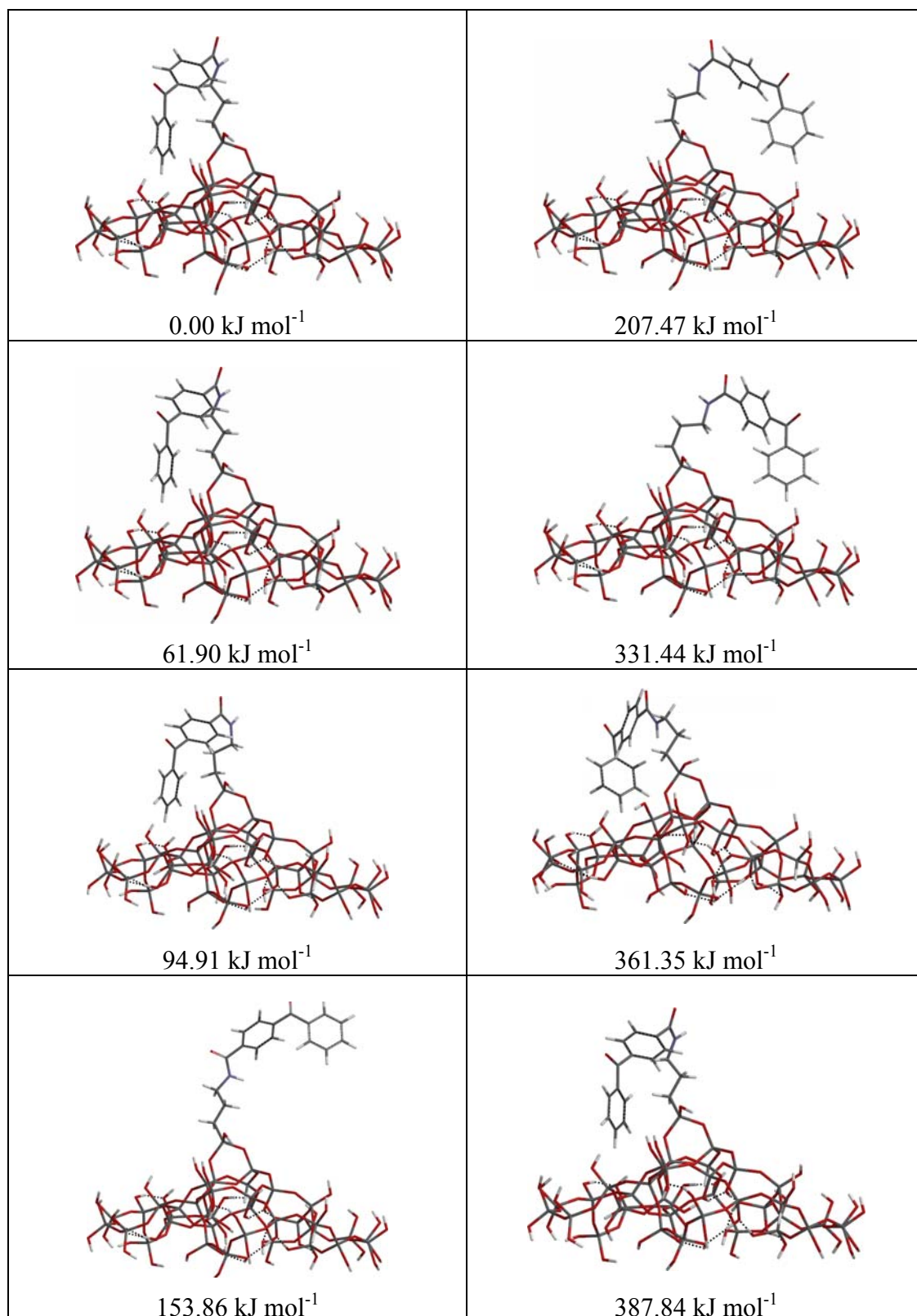


Table 20: Representative conformations of SP1 within 400 kJ mol⁻¹ of the lowest energy conformation

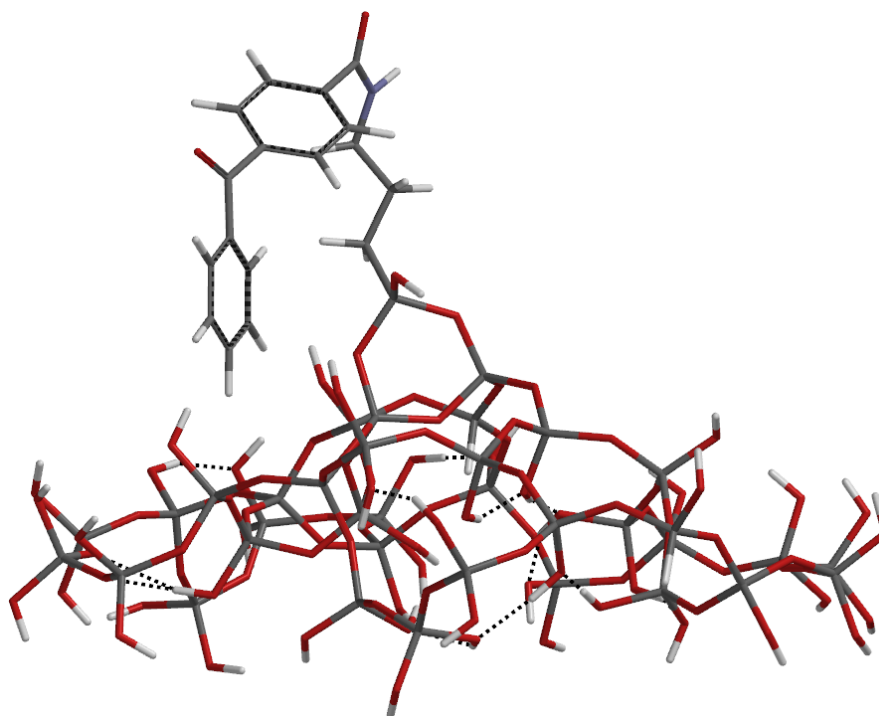


Figure 72: Lowest energy conformation of SP1 showing hydrogen bonding

In the lowest energy conformer (M0001) (**Figure 72**), the photomediator is no longer in an approximately vertical position relative to the surface but has folded over towards the silica surface even though it is apparent there is no hydrogen bonding between the photomediator and the surface silanol groups. The results of the conformational search indicated in fact that hydrogen bonding between the photomediator and the silica surface was absent in all the conformers obtained from the conformational search. The search indicated that the lowest energy vertical structure had a relative energy of $153.86 \text{ kJ mol}^{-1}$ (**Figure 73**).

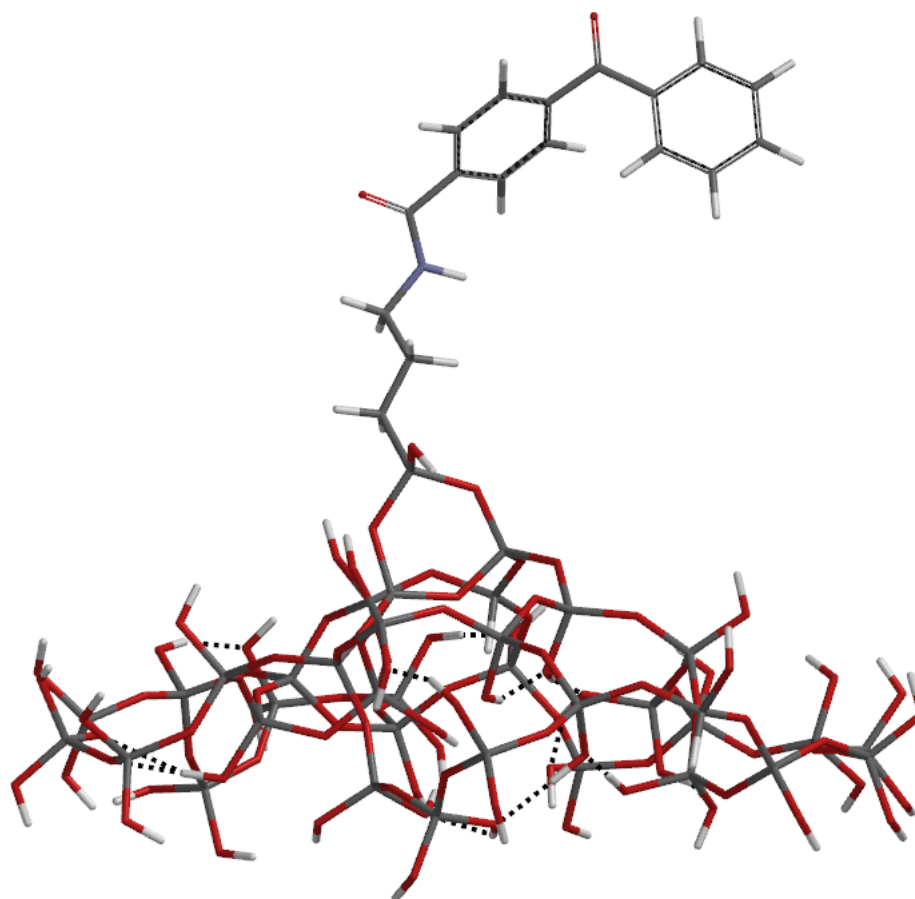


Figure 73: Lowest energy vertical conformation of SP1 showing hydrogen bonding

2.12.2.2 Conformational search results for SP2

The second supported photomediator studied was the siloxane bonded photomediator **SP2**. This photomediator was built in the usual fashion and the molecular mechanics optimised structure was then covalently attached to the silica model *via* a single siloxane linkage in an approximately vertical arrangement (**Figure 74**).

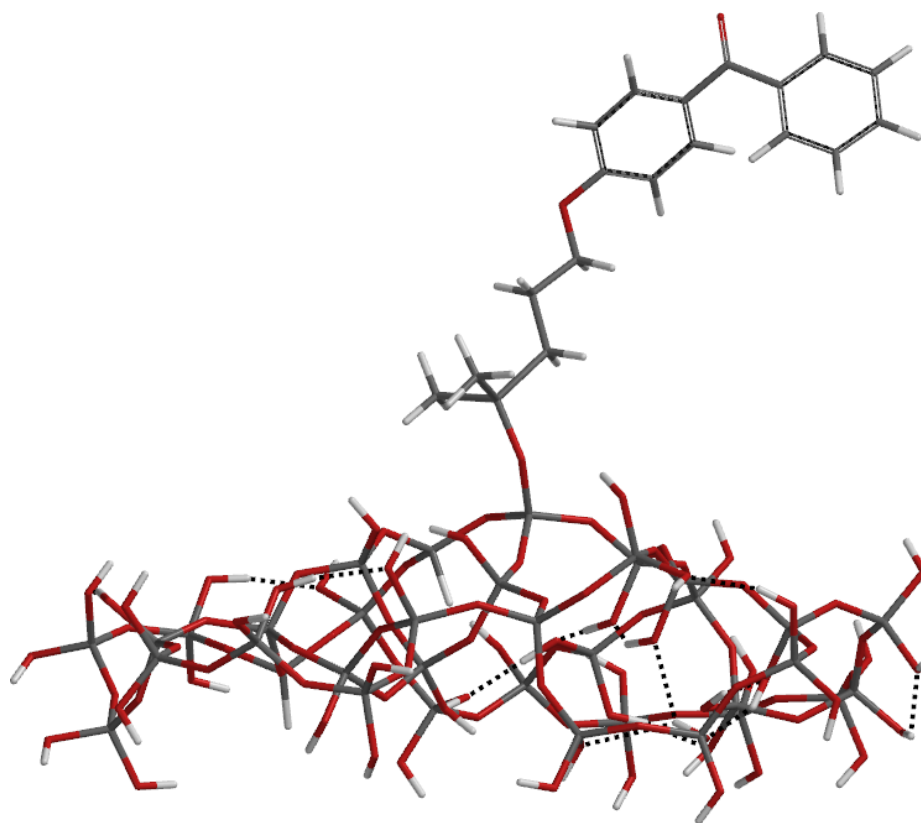


Figure 74: Initial conformation of SP2 showing hydrogen bonding

The results of a conformational search with the usual 400 kJ mol^{-1} window (**Table 21**) identified the lowest energy conformer as one involving the photomediator collapsed onto the silica surface (**Figure 75**). Hydrogen bonding between the benzophenone carbonyl oxygen and a silanol hydrogen atom is evident in this conformer and in many of the other low energy conformers identified, most of which are very similar in structure. There is no indication of any hydrogen bonding between the ether oxygen of the linking chain and a surface silanol groups.

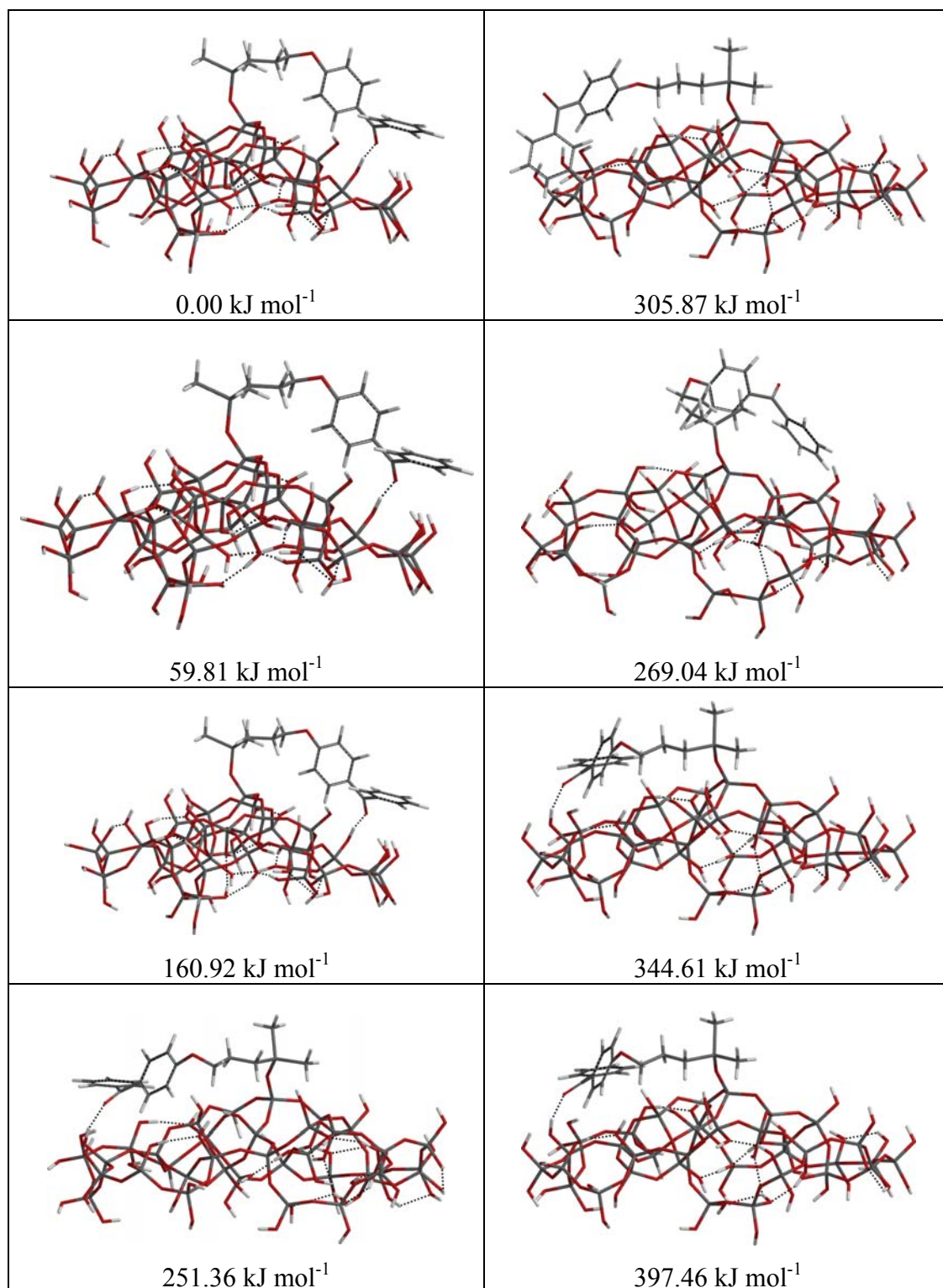


Table 21: Representative conformations of SP2 within 400 kJ mol⁻¹ of the lowest energy conformation

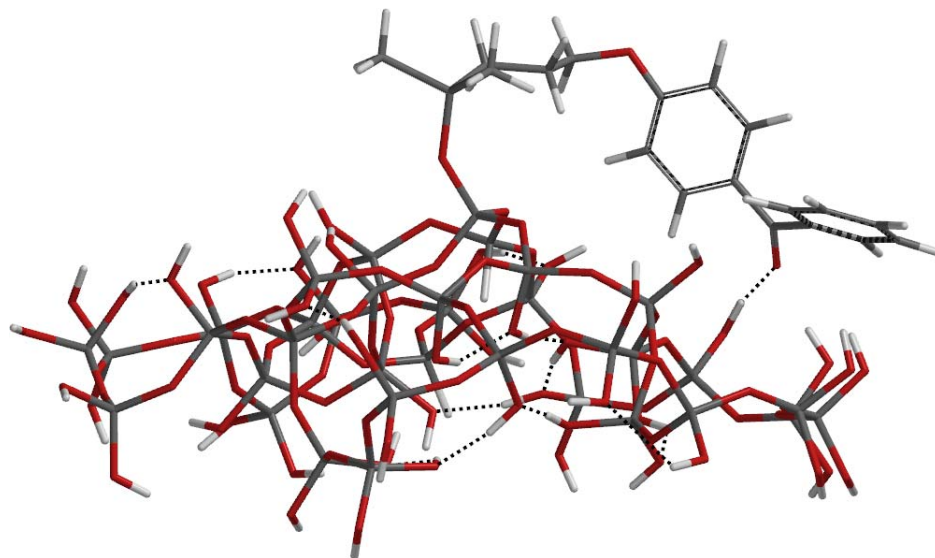


Figure 75: Lowest energy conformation of SP2 showing hydrogen bonding

None of the low energy conformations identified involve the photomediator in an approximately vertical position relative to the surface; even with an energy window of 400 kJ mol^{-1} no vertical conformation was identified. The flexibility afforded by the longer linking chain and the single siloxane linkage may account for the greater interaction between the benzophenone group and the surface observed in **SP2** relative to **SP1**.

2.12.2.3 Conformational search results for SP3

The photomediator (**51**), involving a five carbon methylene chain between the aromatic system and the quaternary ammonium centre, was built and optimised in the usual way. Unlike the previous supported photomediators, this photomediator is electrostatically bound to the silica surface and to represent this, a constraint was placed on the distance between the quaternary nitrogen atom of the photomediator and a surface silanol oxygen atom. A distance of 3.50 \AA was used to represent the combined VDW radii of the $\text{N}(\text{CH}_3)_3$ and OH groups; this was arrived at using space filling Dreiding molecular models. The initial conformation for the standard conformational search procedure again involved the photomediator in an approximately vertical position with respect to the silica surface (**Figure 76**).

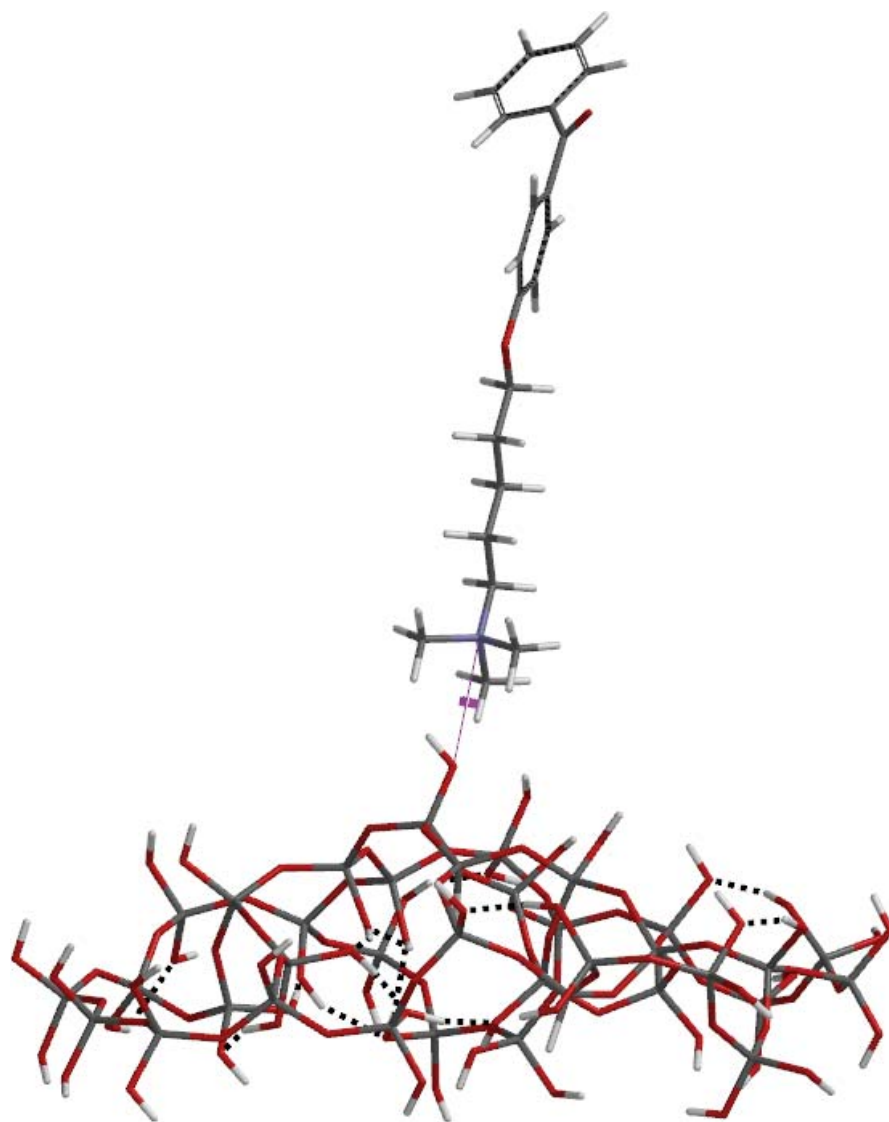


Figure 76: Initial conformation of SP3 showing hydrogen bonding

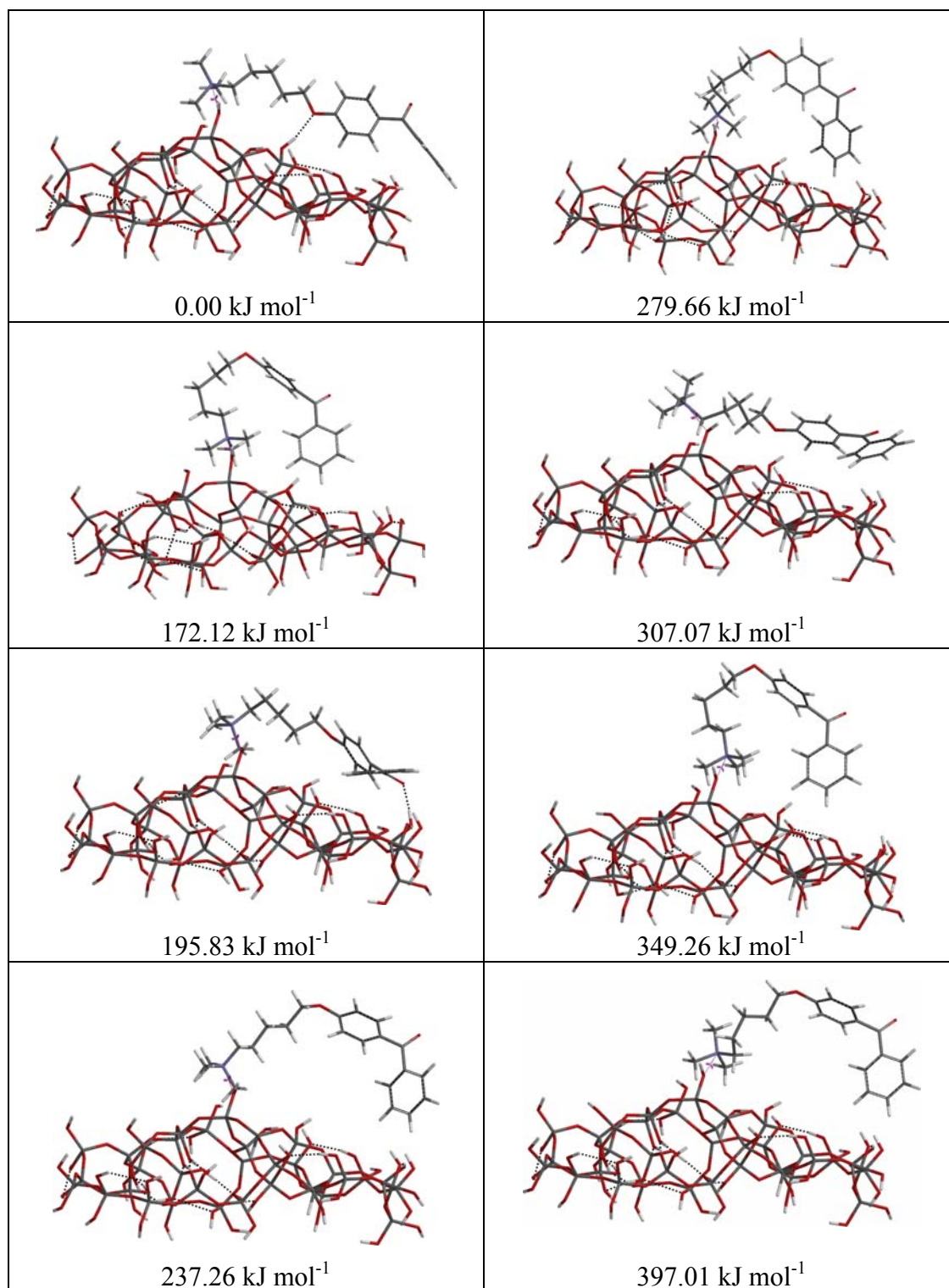


Table 22: Representative conformations of SP3 within 400 kJ mol⁻¹ of the lowest energy conformation

The lowest energy conformer identified by this analysis (**Table 22**) involved the photomediator lying relatively flat on the silica surface (**Figure 77**). The other low energy conformers were of two types, one in which the photomediator is effectively parallel to the surface and the other in which it rises away from the surface then folds over towards it. However even using an energy window of 400 kJ mol^{-1} no conformer involved the photomediator orientated perpendicular to the silica surface. Notably, unlike the lowest energy conformer of **SP2** (**Figure 75**), the benzophenone carbonyl group in the lowest energy form of **SP3** (**Figure 77**) points away from the silica surface and does not engage in hydrogen bonding to a surface silanol group. On the other hand, the ether oxygen atom of the linking chain hydrogen bonds to a surface silanol group.

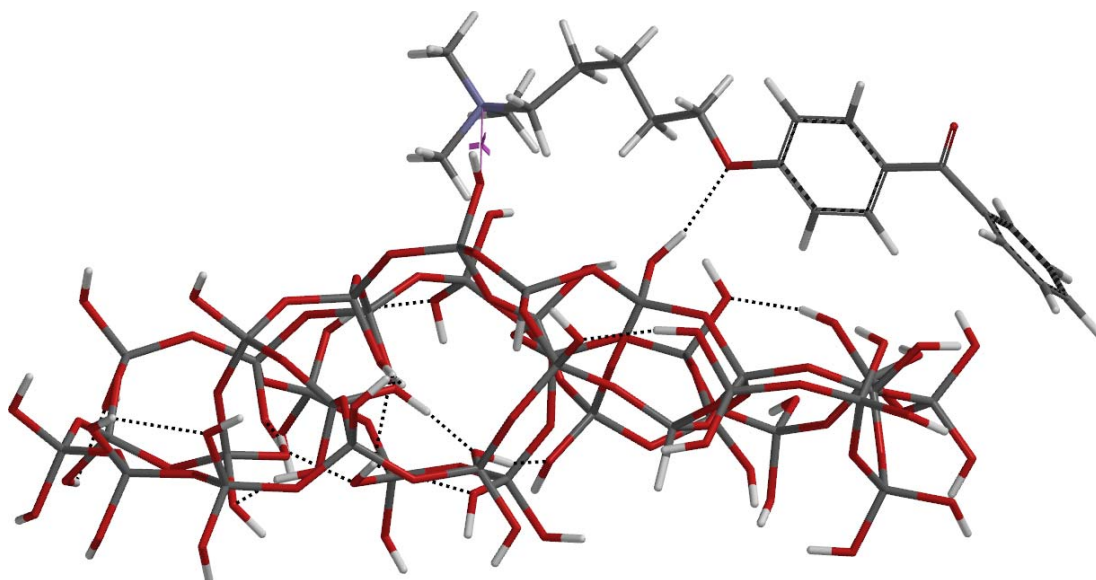


Figure 77: Lowest energy conformation of SP3 showing hydrogen bonding

2.12.2.4 Conformational search results for SP4

The quaternary ammonium salt (**53**) was built and attached to the silica surface as before (**Section 2.12.2.3**). The initial geometry used for the conformational search analysis again involved the photomediator in an approximately orthogonal relationship with the surface (**Figure 78**).

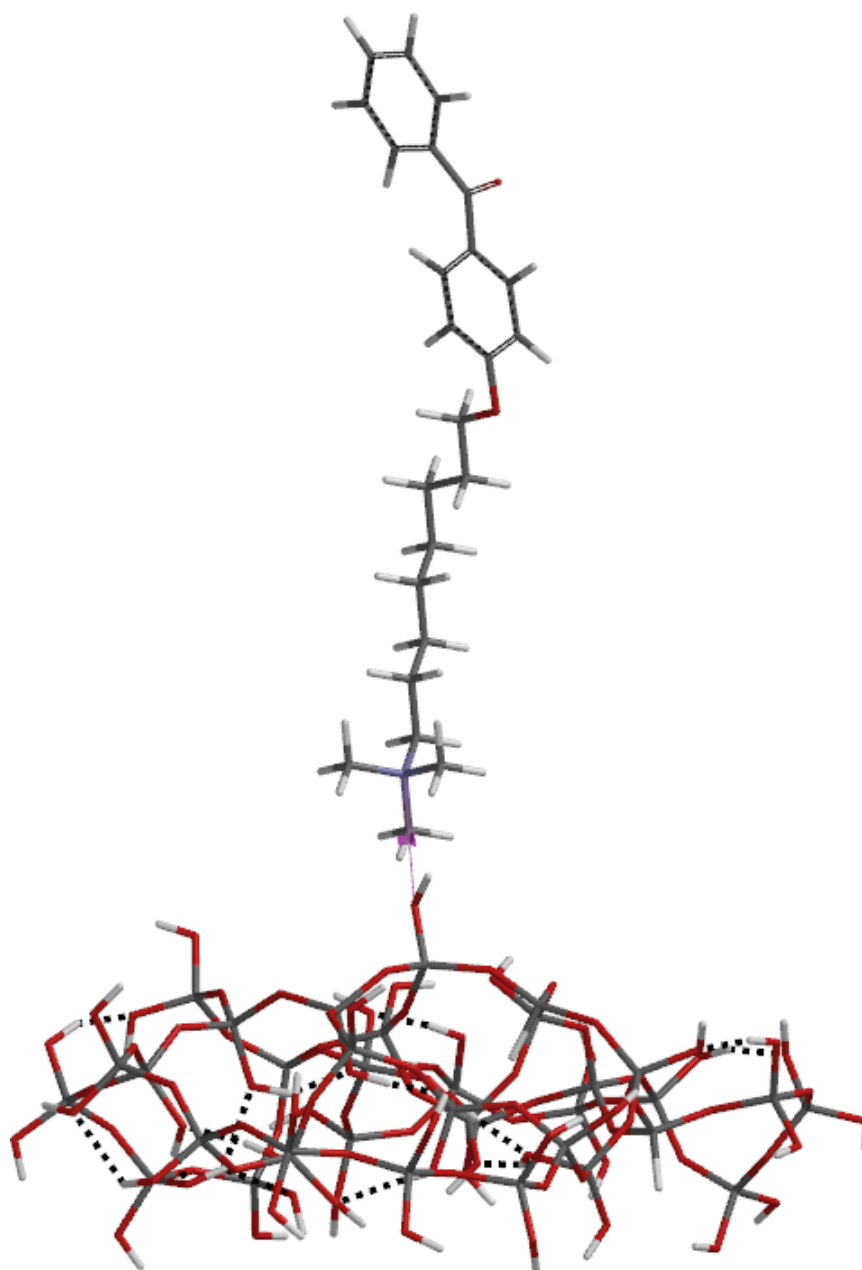


Figure 78: Initial conformation of SP4 showing hydrogen bonding

The results of the conformational search (**Table 23**) clearly show that the lowest energy conformer involves the photomediator folded onto the silica surface (**Figure 79**).

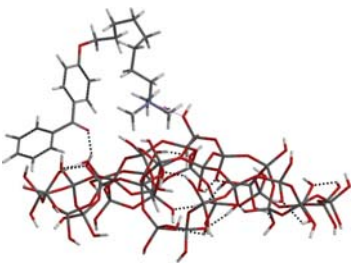
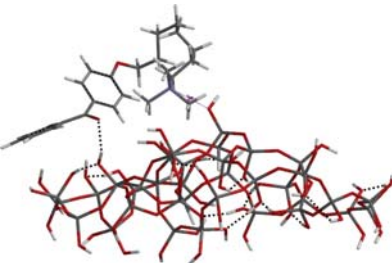
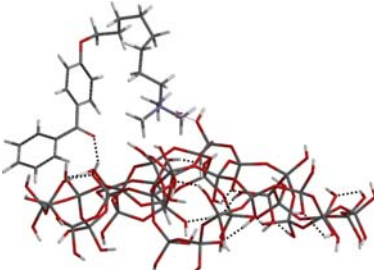
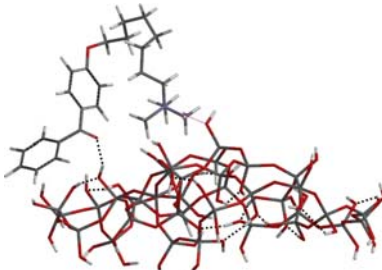
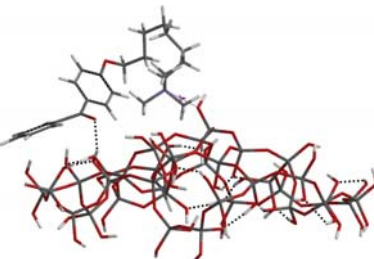
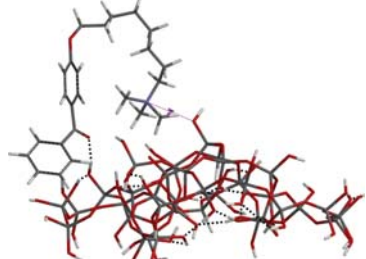
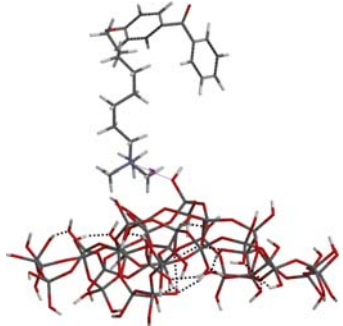
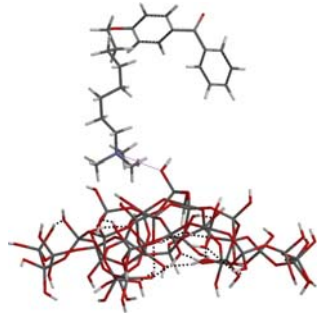
 0.00 kJ mol ⁻¹	 269.94 kJ mol ⁻¹
 158.28 kJ mol ⁻¹	 314.90 kJ mol ⁻¹
 183.30 kJ mol ⁻¹	 341.31 kJ mol ⁻¹
 251.09 kJ mol ⁻¹	 395.12 kJ mol ⁻¹

Table 23: Representative conformations of SP4 within 400 kJ mol⁻¹ of the lowest energy conformation

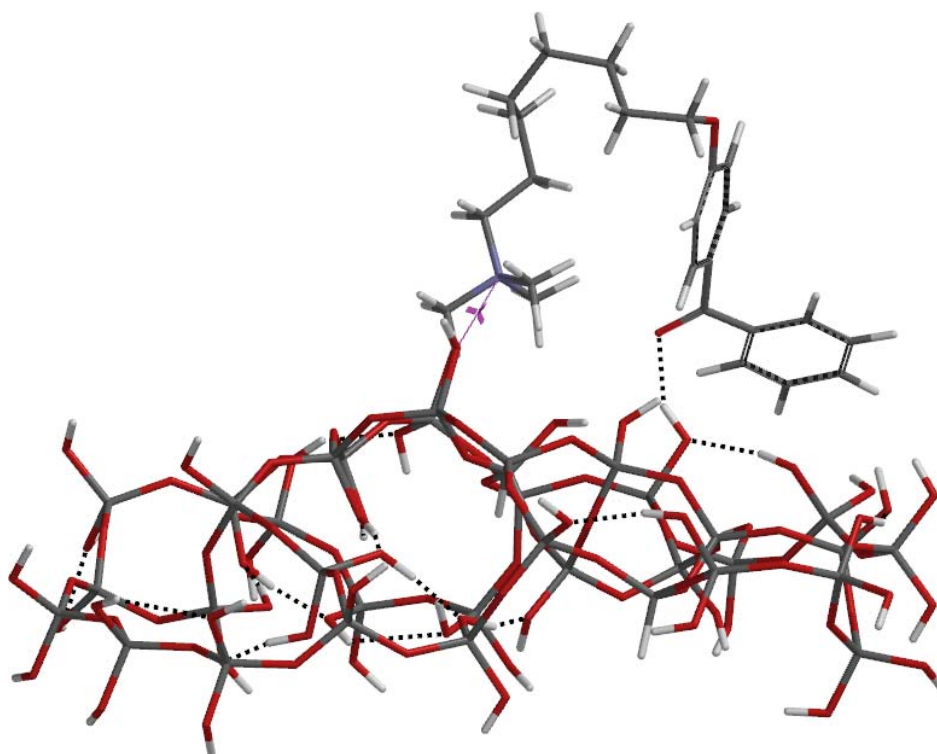


Figure 79: Lowest energy conformation of SP4 showing hydrogen bonding

As in the case of SP2 (**Figure 75**), hydrogen bonding between the photomediator carbonyl oxygen atom and the silanol hydrogen atom on the silica surface is evident and in fact is present in most of the energy forms located (**Figure 79**). The conformational search shows that in a number of cases, the photomediator is orientated vertically to the silica surface (**Figure 80**), one of which has an energy of $251.09 \text{ kJ mol}^{-1}$ above the minimum energy conformer (**Figure 79**).

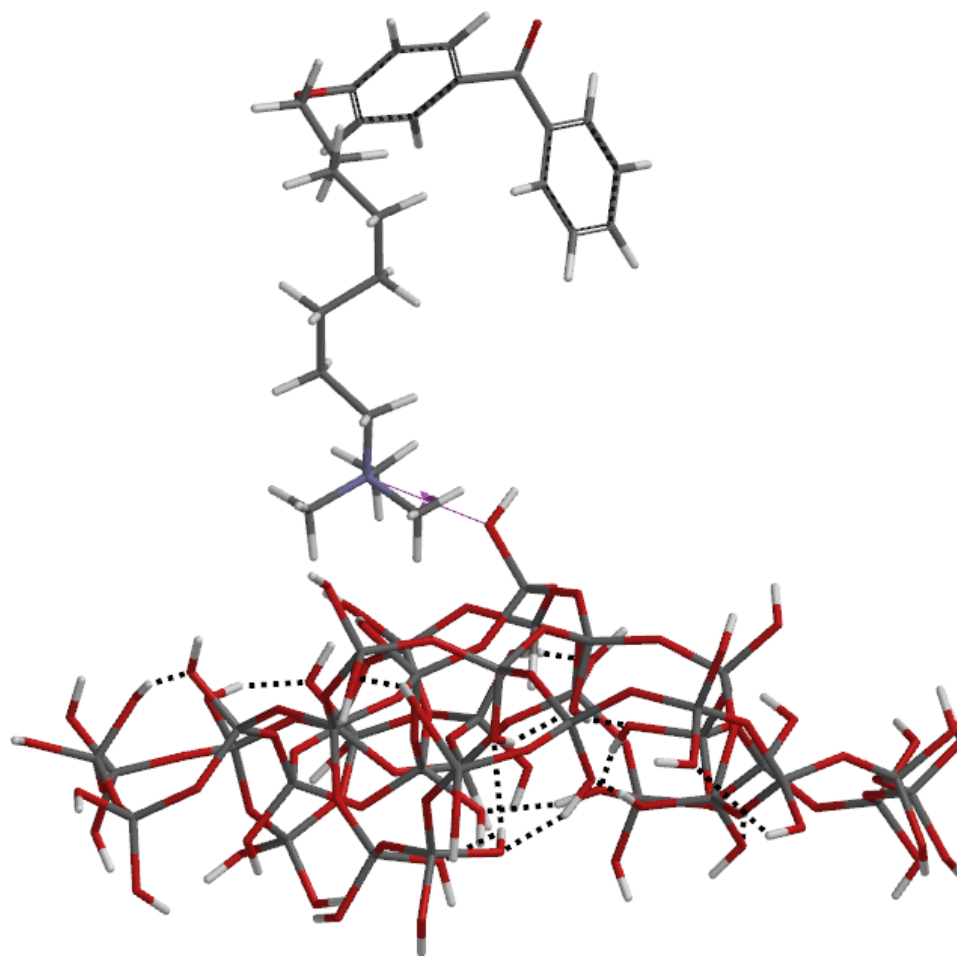


Figure 80: Lowest energy vertical conformation of SP4 showing hydrogen bonding

2.12.2.5 Conformational search results for SP5

The C12 quaternary ammonium salt was attached to the silica surface (**Section 2.12.2.3**) and a vertical orientation was used as before as the initial geometry in the conformational search procedure (**Figure 81**).

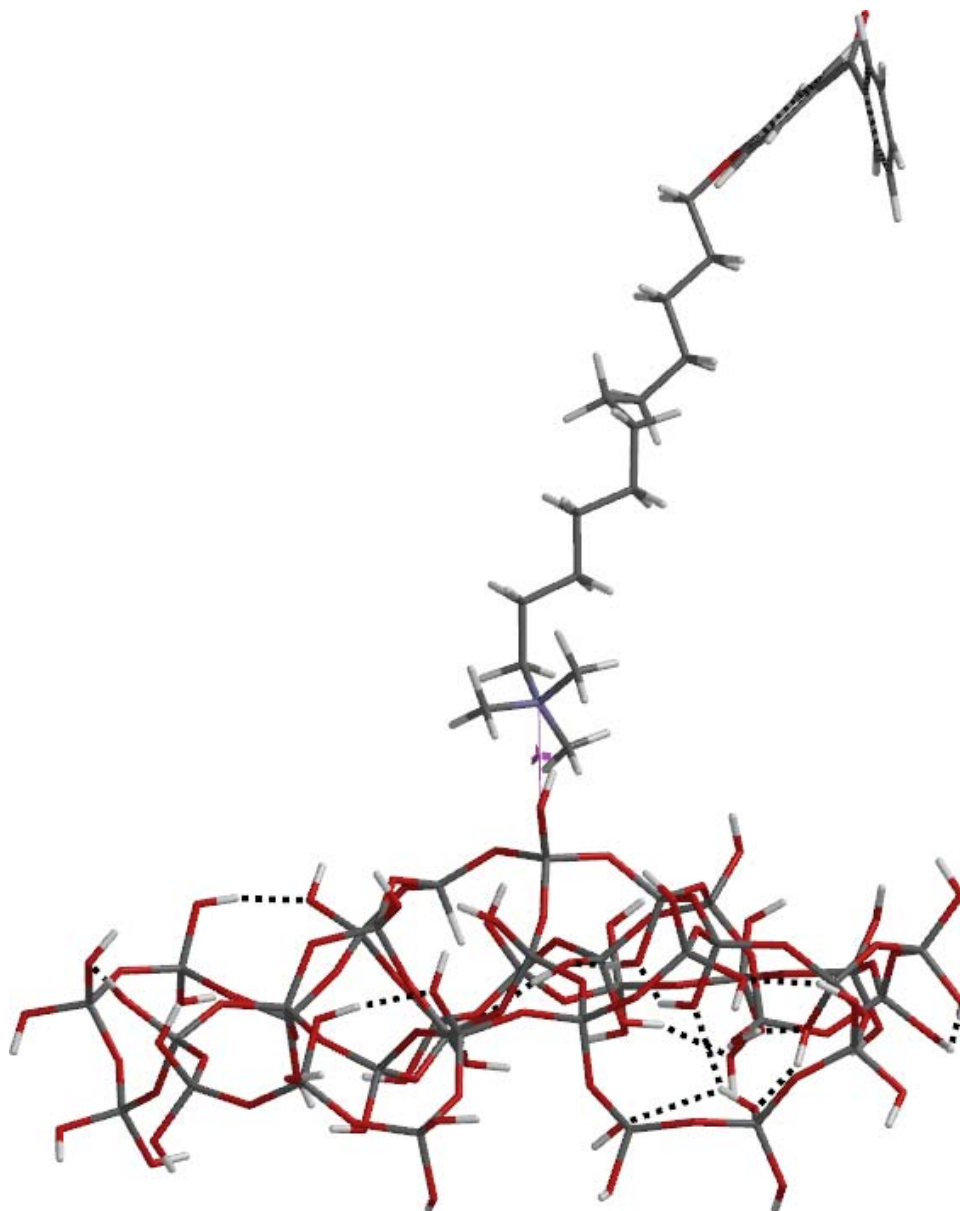


Figure 81: Initial conformation of SP5 showing hydrogen bonding

The results of the conformational search (**Table 24**) indicated that the lowest energy conformer involved the photomediator folded over towards the silica surface (**Figure 82**). Again, as for SP2 (**Figure 75**) and SP4 (**Figure 79**), hydrogen bonding between the photomediator carbonyl oxygen atom and the silanol hydrogen atom on the silica

surface was evident in the lowest energy conformation (**Figure 82**) and in a number of low energy forms.

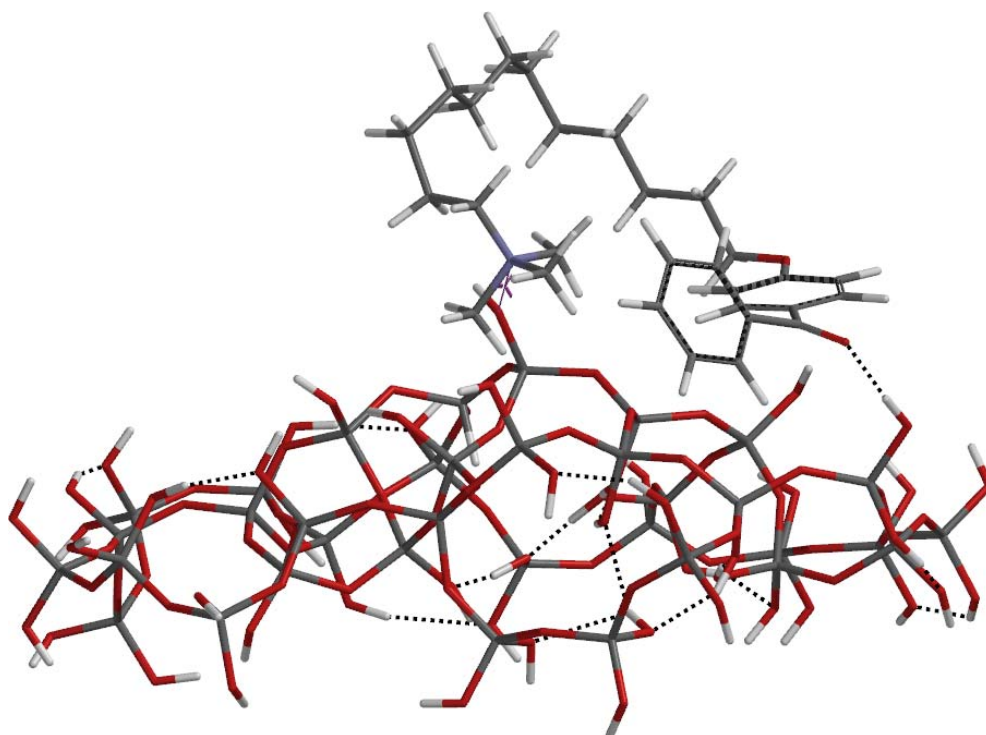


Figure 82: Lowest energy conformation of SP5 showing hydrogen bonding

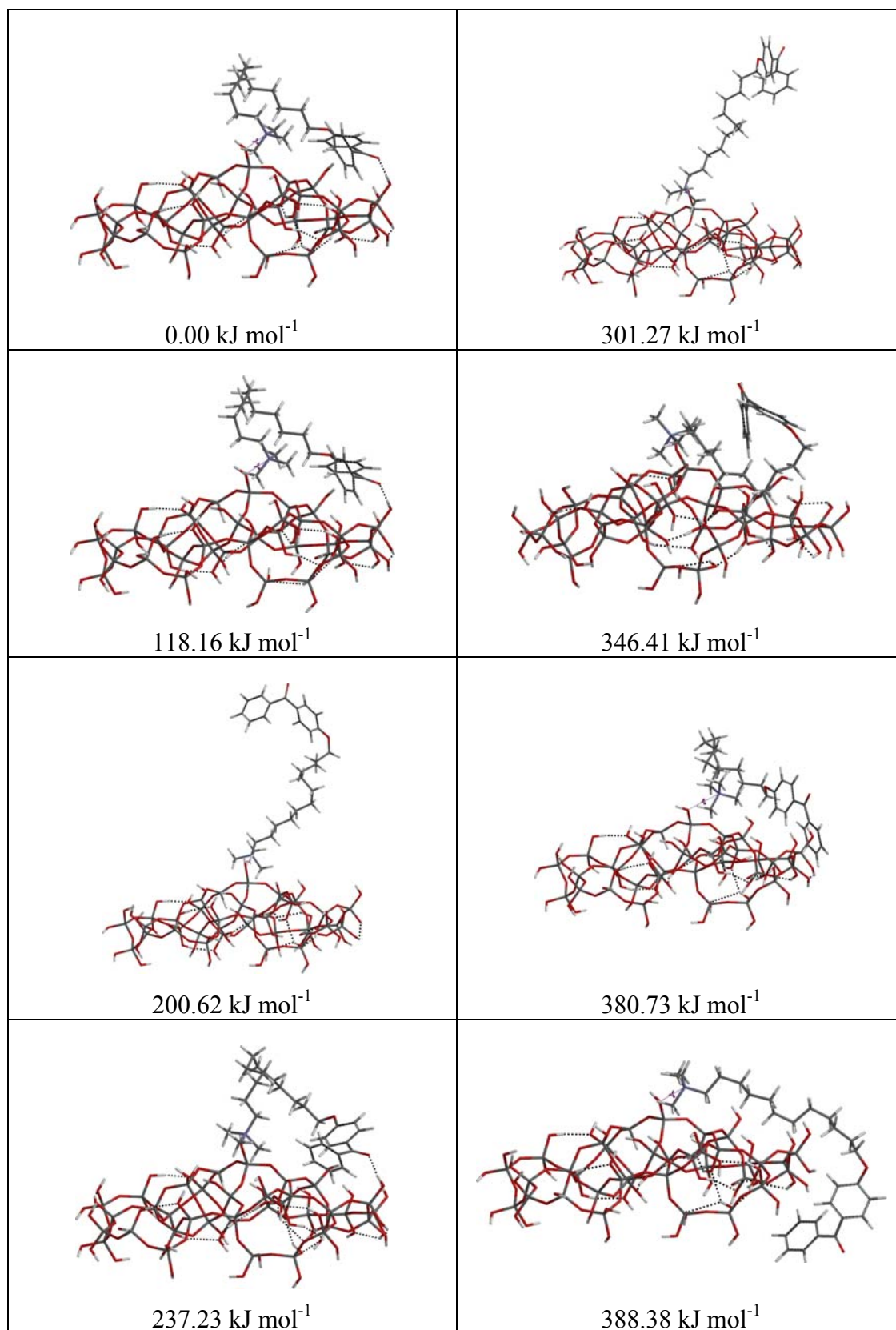


Table 24: Representative conformations of SP5 within 400 kJ mol⁻¹ of the lowest energy conformation

The lowest energy conformation involving the photomediator vertical to the silica surface had an energy 200 kJ mol^{-1} greater than the lowest energy conformation (**Figure 83**).

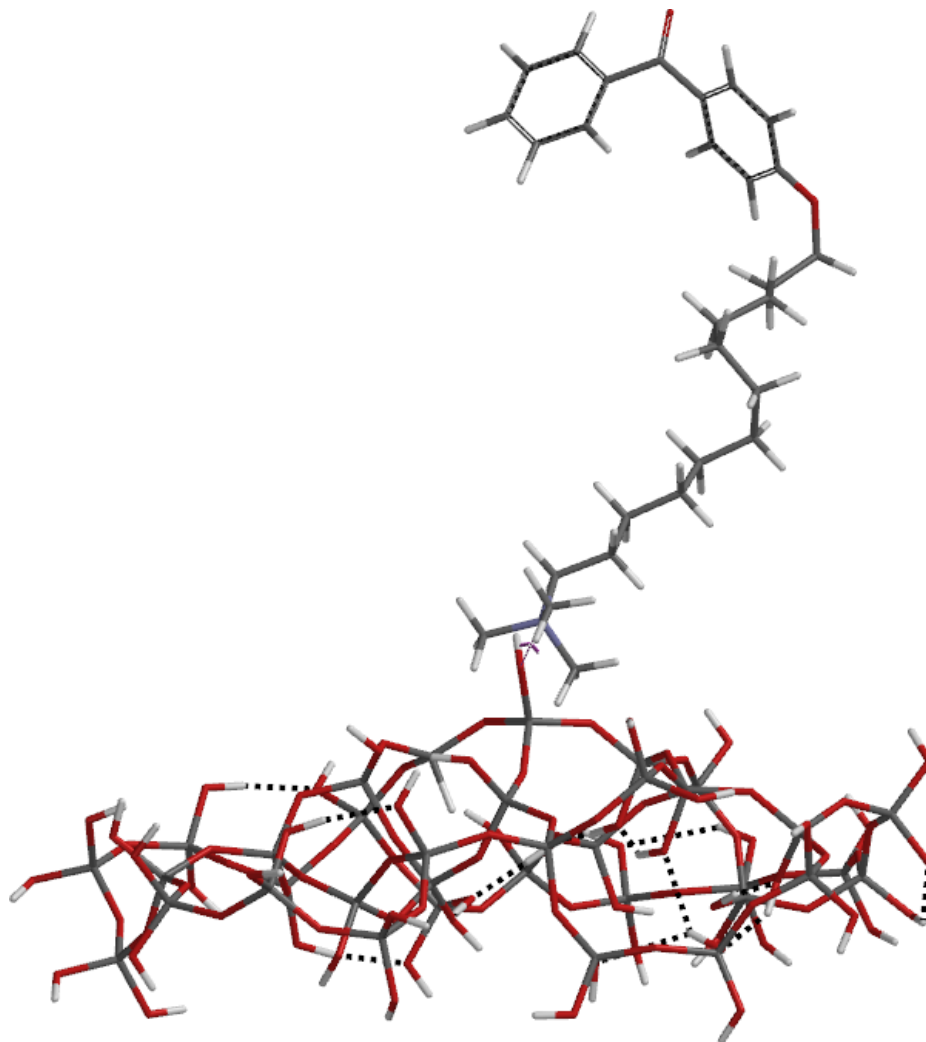


Figure 83: Lowest energy vertical conformation of SP5 showing hydrogen bonding

2.13 Discussion

In order to draw conclusions from the work presented in this thesis, a number of topics need to be discussed: reactivity of hydrogen donors, reactivity and robustness of the supported photomediators, synthetic potential of the process and reaction optimisation.

2.13.1 Reactivity of hydrogen donors

The results presented relate to 2-propanol, cyclopentanol, 1,3-dioxolane, cyclopentane and THF. It is clear that the structure of the hydrogen donor plays an important role in determining the efficiency of the photochemical reaction. The general order of reactivity is THF > 2-propanol > 1,3-dioxolane > cyclopentane > cyclopentanol. This order of reactivity is reflected in the **SP1** promoted reactions of methyl propiolate (**Table 25**) and the **SP2** mediated reactions of DMAD (**Table 26**). Although in these reactions cyclopentane is more reactive than cyclopentanol, this is not generally the case. The cyclic ether, THF, is the most reactive hydrogen donor as the reactions with both methyl propiolate and DMAD have the shortest reaction times and complete conversion to products is achieved in each case.

H-donor	Time (h) ^a	Conversion (% GC)
THF	1.5	100
2-PrOH	7	68
1,3-Dioxolane	17	60
Cyclopentane	30	71
Cyclopentanol	30	50

^a Time for complete reaction of the alkyne or the time at which the reaction ceased

Table 25: Photochemical reactions of methyl propiolate mediated by SP1 showing the order of reactivity of the H-donors

H-donor	Time (h) ^a	Conversion (% GC)
THF	4.5	100
2-PrOH	8.5	100
1,3-Dioxolane	22	100
Cyclopentane	27	80
Cyclopentanol	No reaction	

^a Time for complete reaction of the alkyne or the time at which the reaction ceased

Table 26: Photochemical reactions of DMAD mediated by SP2 showing the order of reactivity of the H-donors

The second most reactive hydrogen donor is the secondary alcohol, 2-propanol which is surprising as in previous work using benzophenone as the photomediator, cyclopentanol was found to be more reactive than 2-propanol¹³². Geraghty carried out DFT calculations and found that both cyclopentanol and 2-propanol had low energy conformers that facilitated stereoelectronic interaction between the non-bonding pair of electrons on the oxygen atom and the CH bond undergoing cleavage. Thus, in terms of stereoelectronic effects, both alcohols should be equally reactive¹³². The BDEs of the α -CH bonds in these alcohols, also suggest that cyclopentanol should be the more reactive hydrogen donor, in keeping with results obtained with benzophenone. The photochemical reactions of 2-propanol with methyl propiolate and DMAD, irrespective of the supported photomediator used, are more efficient than the corresponding reactions of cyclopentanol. The difference in reactivity is most clearly highlighted in the SP2 mediated reactions of DMAD (Table 26) with 2-propanol (Section 2.3.2.1) and cyclopentanol (Section 2.3.2.2): the reaction with 2-propanol is complete in 8.5 h while the cyclic alcohol fails to react at all.

The reactions involving 1,3-dioxolane generally involve relatively long reaction times and complete conversion to product is not achieved in every case. Based on a consideration of the BDEs of the α -CH bonds, one would assume that reactions involving 1,3-dioxolane would be more efficient than those involving THF, yet the former is considerably less reactive. However, it was found that the benzophenone

mediated photochemical reaction of methyl propiolate with THF (using 0.22 eq. of benzophenone with respect to methyl propiolate) (**Section 3.12.2**) required 1 h to reach completion while the corresponding 1,3-dioxolane reaction, albeit with less benzophenone, (0.13 eq.) required 1.5 h. These results are in agreement with those presented here.

It would appear that in general, cyclopentane has the lowest reactivity with both methyl propiolate and DMAD. The photochemical reactions of cyclopentane usually require an irradiation time of 30 h and almost always fail to reach completion. This lack of reactivity can again be explained using BDE values: the BDEs of the α -CH bonds¹³³ in 2-propanol and THF are 396 and 385 kJ mol⁻¹, respectively, whereas that of cyclopentane is 400 kJ mol⁻¹. It should be pointed out that the benzophenone mediated reaction of methyl propiolate with cyclopentane was complete in just 3 h²¹. It is clear that the functionalisation of this cycloalkane using supported photomediators is not an attractive proposition.

The use of an internally consistent set of BDEs (**Table 27**) to rationalise the relative reactivities of the H-donors considered in this study is however, in general, less than successful, and would lead to the conclusion that dioxolane should be the most reactive and that 2-propanol should be more reactive than THF. The low reactivity of cyclopentane can be rationalised on the basis of its high BDE.

Hydrogen donor	BDE ^a	Polarity index ^b
THF	385	0.21
2-Propanol	396	0.55
1,3-Dioxolane	381	0.38
Cyclohexanol ^c	388	0.51
Cyclopentane ^d	400	0.01 ^d

^a Values taken from Luo¹³³; all values were obtained using a correlation approach, ^b values taken from Reichardt¹³⁴, ^c the values for cyclopentanol were not available, ^d value for cyclohexane as that of cyclopentane was not available

Table 27: BDE values and polarity indices for hydrogen donors

Interestingly a list of polarity indices¹³⁴ correlates better with the observed reactivities (**Table 27**). The values for cyclopentanol and cyclopentane are unavailable and so the values for cyclohexane and cyclopentane are given instead. This would place three of the five hydrogen donors considered in the correct order, 2-propanol > cyclopentanol > cyclopentane.

This correlation could be interpreted in terms of a need for the hydrogen donor to adsorb efficiently to the polar silica surface prior to hydrogen abstraction by the photomediator. The molecular modelling study indicates that many of the low energy conformations of the photomediator involve it lying flat on the silica surface, or with the benzophenone unit folded over towards the surface. This would suggest that adsorption on the silica surface would be a prerequisite to accessing the photomediator in such conformations, thus accounting for the correlation between reactivity and polarity.

The reactions of these hydrogen donors with benzylated oximes do not follow the above trend. 1,3-Dioxolane is the most reactive, giving 100% conversion to product in 4 h, whereas the THF reaction stopped after 22 h, reaching 80% conversion. The corresponding reactions mediated by benzophenone¹²⁵ both went to completion in just 2 h.

2.13.2 Reactivity of the unsaturated substrates

The results gathered suggest that the reactions of photochemically generated radicals with alkynes proceed slightly faster than those with alkenes. This is not surprising as examples of a second addition to the alkenes initially formed from alkynes are rare, indicating that it is not competitive with the initial addition to the alkyne. In terms of the reactivity of the alkynes, it is difficult to identify a clear trend. The reactions involving the disubstituted alkyne DMAD are usually more efficient than the corresponding methyl propiolate reactions when **SP1** and **SP2** are used. On the other hand, the reactions of methyl propiolate mediated by **SP3** are more efficient than the corresponding DMAD reactions.

2.13.3 Reactivity of the supported photomediators

From the results obtained, it appears that the reactions mediated by **SP3**, the C5 quaternary ammonium salt photomediator, are faster than those mediated by **SP1** or **SP2** in which the photomediator is covalently bonded to the surface. The C8 quaternary ammonium salt photomediator, **SP4**, mediates reactions in similar times to **SP3**; the reactivity of the C12 quaternary ammonium salt photomediator **SP5** is also comparable to that of **SP3**, with the synthesis of terebic acid taking the same length of time with both photomediators. This order of reactivity is reflected, for example, in the reactions of methyl propiolate with 2-propanol (**Table 28**) and DMAD with 1,3-dioxolane (**Table 29**). However, the reaction of the benzylated oxime (**80**) with 2-propanol performs poorly with **SP5** (**Section 2.8.3.1**), compared to **SP3** (**Section 2.6.1**). The reactivity of the supported photomediators in terms of the molecular modelling study undertaken is discussed below.

Supported photomediator	Mole ratio (MP:2-PrOH:SP)	Time (h) ^a	Conversion (GC)
Ph ₂ CO	3:60:0.68	1.25	100%
SP1	3:60:0.68	7	68%
SP2	3:60:0.68	36	100%
SP3	3:60:0.68	2.75	100%
SP4	3:60:0.68	2.5	100%
SP5	3:60:0.68	2.25	100%

^a Time for complete reaction of the alkyne or the time at which the reaction ceased

Table 28: Reactivity of the supported photomediators in the reaction of methyl propiolate with 2-propanol

Supported photomediator	Mole ratio (MP:1,3-dioxolane:SP)	Time (h) ^a	Conversion (GC)
Ph ₂ CO	3:60:1.20	0.5	100%
SP1	3:60:0.68	16	100%
SP2	3:60:0.68	22	100%
SP3	3:60:0.68	10	100%

^a Time for complete reaction of the alkyne or the time at which the reaction ceased

Table 29: Reactivity of the supported photomediators in the reaction of DMAD with 1,3-dioxolane

2.13.4 Stability of the supported photomediators

As one of the main aims of this project was to develop a series of supported photomediators that would eliminate the need for tedious removal of soluble photomediators from the reaction products and were potentially recyclable, it was important to detect the presence, if any, of unbound photomediator in the crude products of the reactions. No overall trend emerges from the results but it is fair to say that in the majority of the reactions, the photomediator remains bound to the silica surface (**Table 31**). The supported photomediators are discussed individually below.

SP1/SP2

The crude products obtained from the reactions mediated by **SP1** did not contain any photomediator ($^1\text{H-NMR}$, $^{13}\text{C-NMR}$).

SP3

This supported photomediator was initially synthesised using a rapid adsorption method, **Method A (Section 2.1.3.3)**. However, the NMR spectra obtained from the crude products of some of these reactions (**Sections 2.4.1.4, 2.4.4.1, 2.4.4.3 and 2.4.4.4**) showed that trace amounts of aromatic material were present. A slower adsorption method, **Method B (Section 2.1.3.3)**, was subsequently used to attach the quaternary ammonium salt (**51**) to the silica; the results were positive. With the exception of the reaction of acrylonitrile and 2-propanol (**Section 2.4.5.1**), the crude products of the reactions were free of aromatic material (NMR). Apart from this there was no difference in the performance of the photomediator prepared using the two methods.

SP4

This supported photomediator, was synthesised using **Method A (Section 2.1.4.3)**, and the results were not very encouraging. The product mixtures obtained from reactions mediated by **SP4**, with the exception of the methyl propiolate/THF reaction (**Section 2.7.1.2**), all showed some signs of aromatic products ($^1\text{H-NMR}$). However, the reaction times are very similar to those obtained by **SP3** and so it is unlikely that the trace amounts of aromatic material involved, presumed to be a benzophenone derivative, had any effect on the efficiency of the reaction. Nevertheless, the

presence of such aromatic products hampers the usefulness of the supported photomediator in terms of the ease of product isolation and the recyclability of the supported photomediator.

SP5

The photomediator was bound to the silica surface using **Method B (Section 2.1.5.3)** and again the results were generally positive, with no aromatic material being detected in the crude products obtained using it. However, the NMR spectra of the crude product obtained from the methyl propiolate/2-propanol reaction (**Section 2.8.1.1**) contained signals in the region associated with aromatic compounds. The recycling studies carried out with this photomediator were complicated by this problem. It is unclear why the photomediator has leached from the silica surface in this particular reaction and not in any of the other **SP5** mediated reactions. One possibility is that the quaternary ammonium salt is more soluble in 2-propanol than the other hydrogen donors. Nevertheless, it is again reasonable to suggest that the presence of this aromatic material, present in such a small quantity, is not enhancing the reactions, particularly as in some cases, the reactions do not give high conversions (**Section 2.8.3.1**).

Alkyne	H-Donor	SP1	SP2	SP3 ^{a,b}	SP4 ^a	SP5 ^b
MP	2-Propanol	x	x	X ^a , X ^b	✓ ^a	✓ ^b
	Cyclopentanol	x	x	X ^a , -	-	-
	1,3-dioxolane	x	x	X ^a , X ^b	-	X ^b
	Cyclopentane	x	x	✓ ^a , -	✓ ^a	-
	THF	x	x	X ^a , X ^b	X ^a	X ^b
DMAD	2-Propanol	x	x	✓ ^a , -	✓ ^a	-
	Cyclopentanol	x	x	-	-	-
	1,3-dioxolane	x	x	✓ ^a , X ^b	-	-
	Cyclopentane	x	x	✓ ^a , -	-	-
	THF	x	x	X ^a , -	-	-
Methyl acrylate	2-Propanol	-	-	X ^b	-	-
	1,3-dioxolane	-	-	X ^b	-	-
	THF	-	-	-	-	-
Acrylonitrile	2-Propanol	-	-	✓ ^b	-	-
Maleic acid	2-Propanol	-	-	-	-	X ^b
Dimethyl maleate	2-Propanol	-	-	X ^b	-	-
	1,3-dioxolane			X ^b	-	-

x = no aromatic signals present in the ¹H-NMR, ✓ = aromatic signals present in the ¹H-NMR, ^a Method A was used to prepare the supported photomediator, ^b Method B was used to prepare the supported photomediator

Table 30: Presence of aromatic signals in ¹H-NMR spectra

2.13.5 Summary of the reactivity of the supported photomediators

The overall picture emerging seems to be that, **SP1** and **SP2** mediated reactions are slow with the level of conversion achieved varying considerably; the photomediator however, remains tightly bound to the silica surface in both cases. The electrostatically bound photomediators, **SP3**, **SP4** and **SP5**, work very well in comparison, with short reaction times and high to complete conversion being observed in the majority of reactions. In addition, although the rapid adsorption of the photomediator onto the silica surface led to a very small quantity of photomediator leaching from the silica surface, this problem was overcome by the use of a slow adsorption technique. Thus, the photomediators are stable under the reaction conditions discussed in this thesis.

Increasing the length of the linking chain from the benzophenone moiety to the silica surface in the electrostatically bound photomediators appears to have a small overall effect on the reaction outcome, with a slight decrease in reaction time being observed as the chain length is increased from five carbons (**SP3**) to twelve carbons (**SP5**).

2.13.6 Rationalising the order of reactivity of the supported photomediators using molecular modelling

A number of important factors emerged from the molecular modelling study that help to rationalise the general order of reactivity of the supported photomediators observed over the course of this work: **SP2 < SP1 < SP3 ≈ SP4 ≈ SP5**

It is also worth noting, that the reactivity profile of the hydrogen donors with the supported photomediators is different to that observed in homogenous reactions using benzophenone, the greater reactivity observed for cyclopentanol relative to 2-propanol under the latter conditions¹², for example, being reversed when supported photomediators are used. It is attractive to seek an explanation for these patterns in terms of the conformations adopted by the photomediator when it is attached to the surface, and this was the aim of the molecular modelling study, the results of which are presented above (**Section 2.12.2**).

A number of structural motifs can be identified if the conformations resulting from the molecular modelling study are considered in their entirety.

- (a) Orthogonal structures in which the linking chain is approximately at a right angle to the surface.
- (b) Folded structures in which the connecting chain is initially orthogonal to the surface, but then folds back towards the surface.
- (c) Flat structures in which the chain and the benzophenone unit lie approximately parallel to the surface.

Hydrogen bonding between the surface silanols and the carbonyl group of the benzophenone unit is a common structural feature for all the supported photomediators except **SP1**; much less common is hydrogen bonding between the silanols and the ether oxygen atom which is part of the linking chain in **SP2**, **SP3**, **SP4** and **SP5**.

In terms of identifying the relative importance of the three types of conformations, it is worth noting that the set of lowest energy conformations for the five photomediators considered (**Table 31**), includes two flat and three folded conformations. It is important however to appreciate the limitations of the computational model being used: it does not, for example take interactions with solvent into account. As a result the energies of conformations in which the photomediator is off the surface, in particular the orthogonal forms, are likely to be over-estimated as no allowance is made for solvent stabilisation.

In seeking an explanation for the reactivities of the photomediators in terms of their conformation, one is assuming that the conformation does not change following hydrogen abstraction from the hydrogen donor. Such a change is quite possible both because the presence of an OH group in the ketyl radical formed by the hydrogen abstraction opens up new possibilities in terms of hydrogen bonding, and because the lifetime of the ketyl radical is long enough to allow a change to occur. This might impact on the reverse hydrogen transfer which is a key step in the reaction.

Accepting this, it might be intuitively expected that access to a low energy orthogonal form would be a positive feature in terms of reactivity, whereas a majority of flat conformations would be a negative feature. Such an analysis is supported by the fact that all of the low energy conformations of the least reactive

photomediator, **SP2**, can be categorised as flat (**Table 21**), whereas the more reactive photomediators **SP3**, **SP4** and **SP5** have access to orthogonal forms of relatively low energy (**Table 22-Table 24**). The relationship between structure and reactivity is however more complex as **SP1**, which is less reactive than **SP4** or **SP5**, also has access to low energy orthogonal forms (**Table 20**), whereas the majority of the low energy conformations of **SP3**, which is equally reactive, are either flat or folded. The issue is further complicated by the reactivity order of the hydrogen donors and its correlation with a polarity index, which suggests that interaction with the polar surface is a key step in the reaction pathway, thus suggesting that flat conformations are not as relatively unreactive as might intuitively appear to be the case.

Overall it has to be concluded that the molecular modelling study fails to identify a unique structural feature which might be responsible for the reactivity of the photomediators. There are however many aspects of the computational model developed which would encourage the belief that it has the capacity to deliver further insight into these systems. The incorporation of a solvent model would however be an essential addition in the further development of the model.

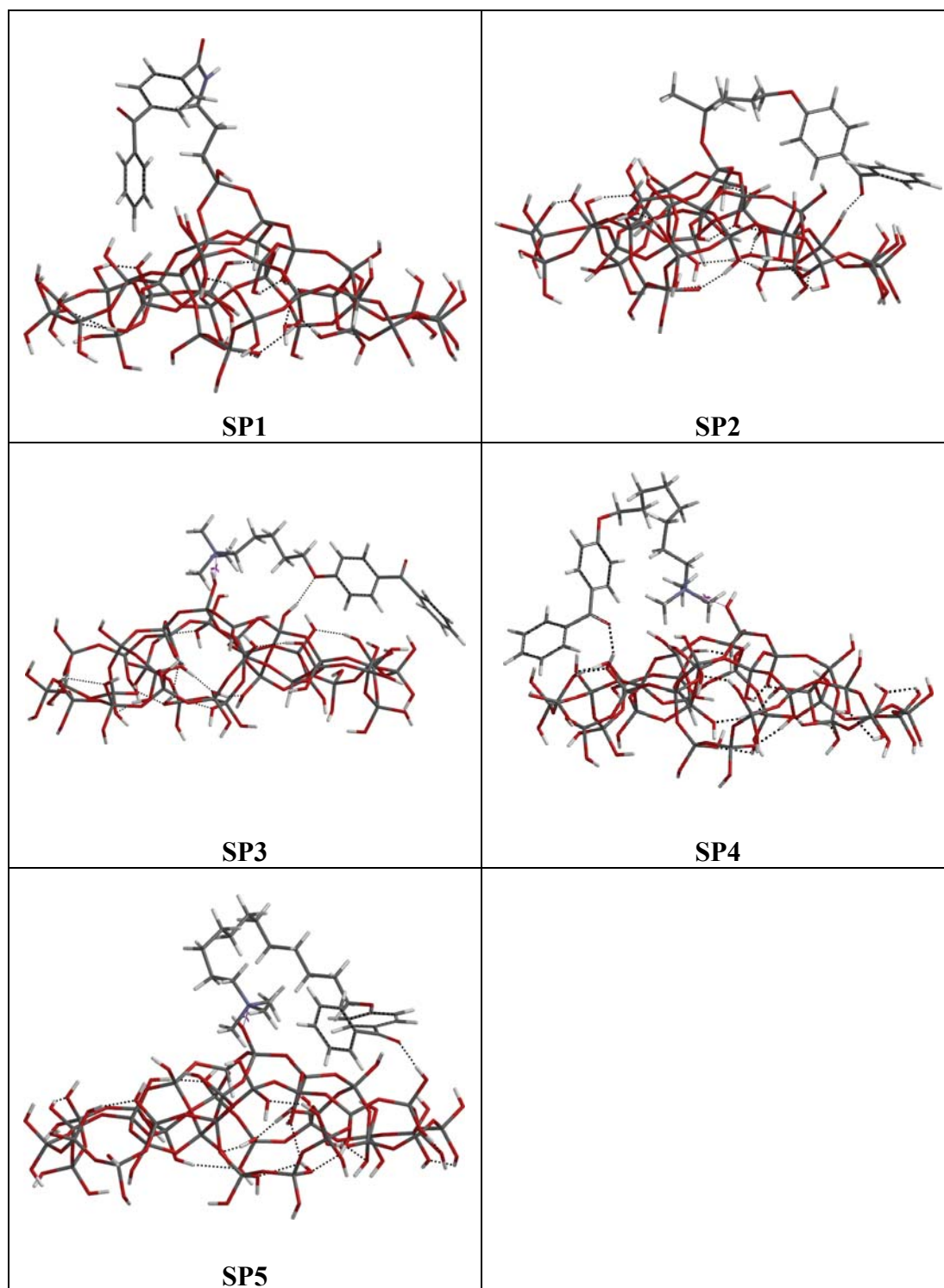


Table 31: Lowest energy conformation of each supported photomediator

2.13.7 Synthetic potential of the supported photomediators

From a synthetic point of view, product isolation is an important process and the easier this is, the more efficient is the overall process in terms of time and cost. The results presented in this thesis clearly show that the products can be isolated from the reaction mixture by simply filtering off the supported photomediator and evaporating the solvent. This affords the product in an often remarkably pure form (**Section 2.3.1.5, Figure 42**) and allows the supported photomediator to be recovered and reused. The results show that the supported photomediators are stable to the conditions used in the reactions considered and can be recycled numerous times before a drop in reactivity is observed.

Previous work using benzophenone as the photomediator found that dimerisation of the ketyl radical was a problem when back hydrogen transfer was slow¹². It was envisioned that this would be less of a problem when supported photomediators were employed. This expectation was based on the assumption that the benzophenone units would be bound to the surface making dimerization more difficult. The present work does not provide any evidence relating to the operation of such an effect. The fact that some reactions fail to go to completion could be taken as evidence that ketyl radical dimerization on the surface of silica does occur. However, it is difficult to see why this should occur in some reactions and not in others which involve a similar reaction time.

2.13.8 Reaction optimisation

Two reactions were chosen for the optimisation studies, the methyl propiolate/2-propanol reaction and the methyl propiolate/THF reaction.

The results of the methyl propiolate/2-propanol reaction optimisation (**Section 2.10**) showed that as little as 6 mol% of the supported photomediator **SP3** (relative to the alkyne) was effective. Similarly for the methyl propiolate/THF reaction (**Section 2.11**), it was found that as little as 3 mol% of the supported photomediator (relative to the alkyne) was effective (**Table 19**). This is of particular importance for reactions of this type which often require stoichiometric amounts of photomediator.

Unfortunately however, attempts to reduce the hydrogen donor/unsaturated reactant ratio significantly were not particularly successful and in common with most reactions of this type a large excess of the hydrogen donor relative to the unsaturated substrate (60:3) was found to be necessary.

2.14 Future work

The results presented here are encouraging and justify further work. The finding that a benzophenone chromophore can be attached to a silica surface *via* a methylene chain and a quaternary ammonium salt is particularly interesting as such benzophenone derivatives are easily synthesised. Although the resulting photomediator is generally stable to the reaction conditions leaching has been observed in some cases. One possible approach to increase the stability of the photomediator would be to use tertiary ammonium ions (R_3NH^+) as the linking group as these may bind more tightly to a silica surface.

The work reported is based on a single type of silica. An obvious extension of the work would be to investigate the effect of changing the type of silica used, to a macroporous silica, for example, particularly in relation to surface area. Lastly, adding a solvent model to the computational approach used in this current work would be of great value.

Chapter 3

Experimental

General experimental conditions

The photochemical reactions were carried out in a Rayonet Photochemical Reactor (RPR-200), consisting of sixteen 350 nm mercury lamps and a magnetic stir plate and using cylindrical pyrex tubes. Infra-red spectra were obtained using a Perkin-Elmer Spectrum One FT-IR spectrophotometer, where liquid samples were measured as thin films and solids were measured directly. $^1\text{H-NMR}$ and $^{13}\text{C-NMR}$ spectra were measured using a Jeol ECX400 spectrometer at probe temperatures ($\sim 20\text{ }^\circ\text{C}$) using deuterated chloroform (CDCl_3) as solvent unless otherwise stated and tetramethylsilane as an internal standard. Silica and supported photomediators were dried in a Heraeus VT 6025 Vacutherm vacuum oven. All gas chromatography (GC) analysis was carried out on a Varian 3900 chromatograph with a Restek RTX-1 column. Mass spectrometry was carried out using a Walters LCT Premier XE spectrometer. Melting points were determined using a Stuart Scientific SMP3 or SMP11 apparatus. Column chromatography was carried out using Merck silica gel 60, 230-400 mesh, and gradient elution with diethyl ether/petroleum ether ($40\text{-}60\text{ }^\circ\text{C}$) unless otherwise stated. All solvents were dried and distilled according to literature procedures¹³⁵, or obtained directly from an Innovative Technology Pure Sol PS-MD-5 Purification system. All chemicals were purchased from Aldrich Chemical Company, Fischer Scientific or Acros Organics.

3.0 Experimental

3.1 Preparation of supported photomediators

3.1.1 Synthesis of 3-aminopropyl silica bound benzophenone⁸² SP1

3-Aminopropyl silica (8.00 g, 1.00 meq/g) was dried at 100 °C under vacuum (1 mmHg) for 24 h and then suspended in a solution of *p*-benzoylbenzoic acid (5.43 g, 24.0 mmol) and *N,N'*-dicyclohexylcarbodiimide (4.95 g, 24.0 mmol) in anhydrous toluene (120 mL). The resulting mixture was stirred under nitrogen for two days. The solid was filtered off and washed consecutively in a soxhlet thimble with toluene (100 mL), methanol (100 mL), ethanol (100 mL) and diethyl ether (100 mL). It was dried under vacuum at 100 °C for 24 h affording the supported photomediator **SP1** (Figure 1) as a white powder (11.91 g) which was stored in a desiccator prior to use. Gravimetrically, **SP1** contained 1.60 mmol photomediator/g.

Supported photomediator SP1

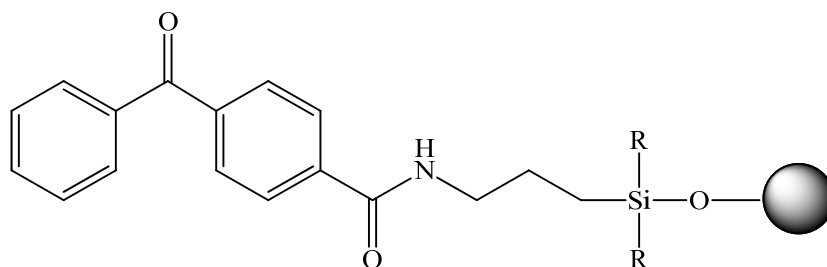


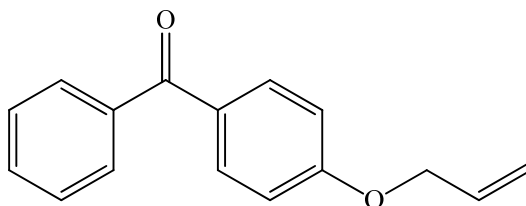
Figure 84

3.1.2 Synthesis of propyl linked 4-hydroxybenzophenone silica SP2

3.1.2.1 Synthesis of 4-(allyloxy)benzophenone⁹⁴ (48)

4-Hydroxybenzophenone (39.60 g, 0.20 mol) and allyl bromide (26.60 g, 0.22 mol) were dissolved in acetone (120 mL), and potassium carbonate (28.00 g, 0.20 mol) was added. The mixture was heated at reflux for 8 h and then cooled to rt. Water (60 mL) was added and the resulting solution was extracted twice with diethyl ether (100 mL). The combined organic layers were washed twice with aqueous sodium hydroxide (10%) and dried over sodium sulphate. Removal of the solvent under vacuum gave a yellow solid which was recrystallised from ethyl acetate to give 4-(allyloxy)benzophenone (**48**) as a white solid (18.55 g, 86%). mp 81.5-82.5 °C, lit⁹⁵. 77-78 °C.

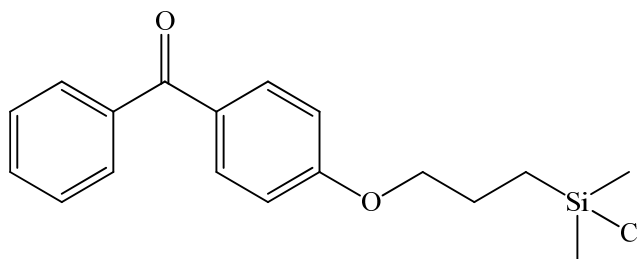
4-(allyloxy)benzophenone⁹⁴ (48)



IR (cm^{-1}): 1638 (C=O), 1598 (C=C), 1247, 1172 (C-O). **¹H-NMR** (δ): 4.62 (dt, 2H, OCH₂, $J_{LR} = 1.6$ Hz, $J_{vic} = 5.2$ Hz), 5.33 (dq, 1H, CH(H)=CH, $J_{gem} = J_{LR} = 1.6$ Hz, $J_{cis} = 10.4$ Hz), 5.44 (dq, 1H, CH(H)=CH, $J_{gem} = J_{LR} = 1.6$ Hz, $J_{trans} = 17.2$ Hz), 6.07 (m, 1H, CH₂=CHCH₂), 6.98-7.81 (ms, 9H, 9xCH_{Ar}). **¹³C-NMR** (ppm): 195.7 (C=O), 162.3 (CO), 138.4, 132.6, 132.0, 130.3, 129.3, 128.3, 114.4 (C_{Ar}), 132.6 (CH=CH₂), 118.3 (CH=CH₂), 69.0 (OCH₂).

3.1.2.2 Synthesis of 4-[3-(chlorodimethylsilyl)propyloxy]benzophenone (49)⁹⁴

4-(Allyloxy)benzophenone (**48**) (2.00 g, 8.00 mmol) was suspended in freshly distilled chlorodimethylsilane (20 mL, 17.04 g, 0.18 mol), and platinum on carbon (10 mg, 10% Pt) was added. The reaction was complete after refluxing for 6 h (TLC). After cooling to rt, the platinum catalyst was removed by filtration and the excess chlorodimethylsilane was removed under reduced pressure to yield 4-[3-(chlorodimethylsilyl)propyloxy]benzophenone (**49**) as a colourless oil (2.35 g, 88%).

4-[3-(chlorodimethylsilyl)propyloxy]benzophenone⁹⁴ (**49**)

IR (cm⁻¹): 1652 (C=O), 1598 (C=C), 1247, 1171 (C-O). **¹H-NMR (δ):** 0.45 (s, 6H, 2xCH₃), 0.96-1.00 (m, 2H, CH₂Si), 1.90-1.97 (m, 2H, OCH₂CH₂), 4.02 (t, 2H, OCH₂, *J*_{vic} = 6.4 Hz), 6.93-7.82 (ms, 9H, 9xCH_{Ar}). **¹³C-NMR (ppm):** 195.6 (C=O), 162.8 (CO), 138.4, 132.9, 132.0, 130.1, 130.0, 128.3, 114.1 (C_{Ar}), 70.0 (OCH₂), 23.0 (OCH₂CH₂), 15.3 (CH₂Si), 1.8 (SiCH₃).

3.1.2.3 Attachment of 4-[3-(chlorodimethylsilyl)propyloxy]benzophenone (**49**) to silica

Silica (8.00 g), previously dried in a vacuum oven at 100 °C for 24 h, was suspended in a solution of 4-[3-(chlorodimethylsilyl)propyloxy]benzophenone (**49**) (1.20 g, 3.65 mmol) in toluene (120 mL). Triethylamine (0.50 g, 4.90 mmol) was added and the solution was left to stand overnight. Following this, the supported photomediator was filtered off, washed with chloroform (100 mL) and dried under vacuum at 70 °C for 24 h giving the silica supported photomediator, **SP2 (Figure 2)**, as a white solid (8.72 g) which was stored in a desiccator prior to use. Gravimetrically, **SP2** contained 2.90 mmol photomediator/g.

Supported photomediator 2 SP2

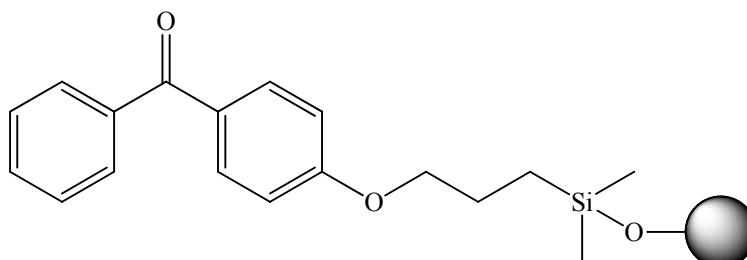


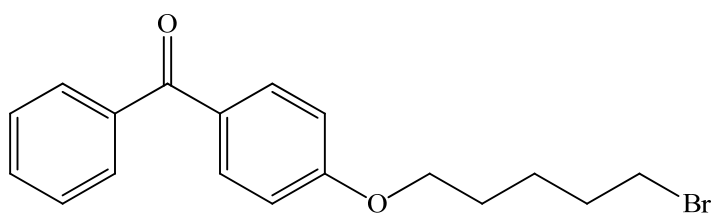
Figure 85

3.1.3 Synthesis of the silica supported C-5 quaternary ammonium salt SP3

3.1.3.1 Preparation of 4-(5-bromopentyloxy)benzophenone⁹⁶ (**50**)

4-Hydroxybenzophenone (5.98 g, 0.03 mol) and 1,5-dibromopentane (69.39 g, 0.30 mol) were dissolved in acetone (40 mL) and potassium carbonate (4.25 g, 0.03 mol) was then added. The mixture was heated at reflux for 8 h and then allowed to cool to rt. Water (50 mL) was added and the solution was extracted with dichloromethane (DCM) (2 x 60 mL). The organic layer was washed with 10% aq. sodium hydroxide (2 x 50 mL) and dried over sodium sulphate. The solvent was evaporated *in vacuo* and the excess 1,5-dibromopentane was removed by kugelrohr distillation, leaving a light yellow oil (9.83 g). This was adsorbed onto silica (60 g) and eluted with a DCM (10-40%)/petroleum ether gradient. 1,5-Dibromopentane was eluted first followed by the desired product, 4-(5-bromopentyloxy)benzophenone (**50**), as a colourless oil (9.48 g, 90%).

4-(5-bromopentyloxy)benzophenone⁹⁶ (**50**)



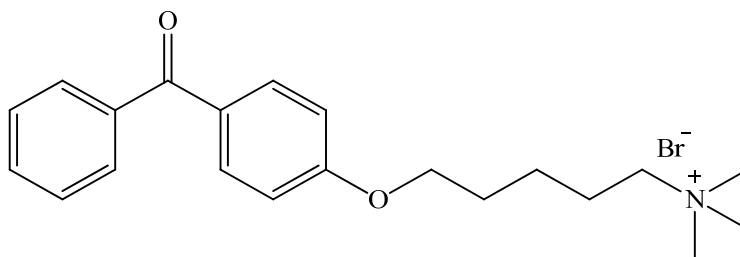
IR (cm^{-1}): 1639 (C=O), 1601 (C=C), 1257, 1173 (C-O), 744 (C-Br). **¹H-NMR** (δ): 1.60-1.67 (m, 2H, OCH₂CH₂CH₂), 1.80-1.97 (ms, 4H, OCH₂CH₂CH₂CH₂), 3.44 (t, 2H, CH₂Br, $J_{\text{vic}} = 6.7$ Hz), 4.04 (t, 2H, OCH₂, $J_{\text{vic}} = 6.3$ Hz), 6.94-7.79 (ms, 9H, 9xCH_{Ar}). **¹³C-NMR** (ppm): 195.7 (C=O), 162.7 (CO), 138.4, 132.7, 132.0, 130.1, 129.8, 128.3, 114.1 (C_{Ar}), 67.9 (OCH₂), 33.6 (CH₂Br), 32.5, 28.4, 24.9 (CH₂).

3.1.3.2 Synthesis of *N,N,N,N*-5-(4-benzoylphenoxy)pentyl)trimethyl ammonium bromide (**51**)⁹⁷

4-(5-Bromopentyloxy)benzophenone (**50**) (2.00 g, 5.76 mmol) and trimethylamine (1.78 mL, 7.49 mmol) were dissolved in a 2:1 chloroform/ether solution (30 mL) and the solution was stirred at rt for 48 h. A white precipitate formed which was filtered off and washed with diethyl ether giving the quaternary ammonium salt *N,N,N,N*-5-

(4-benzoylphenoxy)pentyltrimethyl ammonium bromide (**51**) as a white solid (1.33 g, 67%), mp 164.8-165.3 °C.

N,N,N,N-5-(4-benzoylphenoxy)pentyltrimethyl ammonium bromide (**51**)



IR (cm^{-1}): 1651 (C=O), 1600 (C=C), 1255, 1173 (C-O). **$^1\text{H-NMR}$** (δ): 1.56-1.63 (m, 2H, CH_2), 1.82-1.92 (m, 4H, $2\times\text{CH}_2$), 3.44 (s, 9H, $\text{N}(\text{CH}_3)_3$), 3.65-3.70 (m, 2H, CH_2N), 4.05 (t, 2H, OCH_2 , $J_{\text{vic}} = 6.0$ Hz), 6.93-7.79 (ms, 9H, $9\times\text{CH}_{\text{Ar}}$). **$^{13}\text{C-NMR}$** (**ppm**): 195.7 (C=O), 162.5 (CO), 138.2, 132.6, 132.1, 130.2, 129.8, 128.3, 114.2 (C_{Ar}), 67.6 (CH_2O), 66.8 (CH_2N), 53.6 (CH_3), 28.7 (OCH_2CH_2), 23.0 (CH_2). **HRMS** (**CI**): $\text{M}+\text{H}^+$, $\text{C}_{21}\text{H}_{28}\text{NO}_2$; Calculated: 326.2109; Found: 326.2120.

3.1.3.3 Attachment of the quaternary ammonium salt (51) to silica

Method A

The quaternary ammonium salt (**51**) (1.60 g, 4 mmol) was dissolved in ethanol (20 mL) and silica (10.00 g), previously dried in a vacuum oven at 70 °C overnight, was added. The solvent was removed under reduced pressure (15 min, 35 °C) and following this the supported photomediator was dried in a vacuum oven at 70 °C for 24 h, giving a white powder (11.56 g) which was stored in a desiccator prior to use. Gravimetrically **SP3** contained 0.34 mmol photomediator/g.

Method B

The quaternary ammonium salt (**51**) was attached to the silica surface by slow adsorption from methanol (30 mL). The salt (**51**) (1.60 g, 4 mmol) was dissolved in methanol (30 mL), and silica (10.00 g), previously dried in a vacuum oven at 70 °C overnight, was added. The solvent was removed under atmospheric pressure (45 min, 80 °C) leaving a white powder (11.58 g) which was dried in a vacuum oven at 70 °C for 24 h and then stored in a desiccator prior to use. Gravimetrically, **SP3** (**Figure 86**) contained 0.34 mmol photomediator/g.

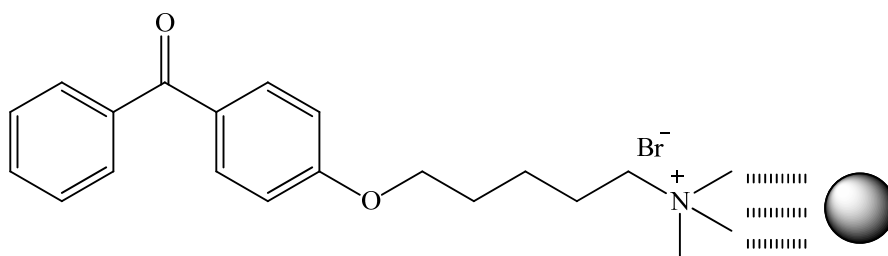


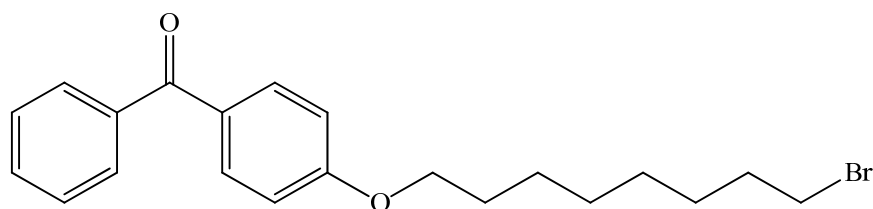
Figure 86

3.1.4 Synthesis of silica supported C-8 quaternary ammonium salt SP4

3.1.4.1 Preparation of 4-(8-bromooctyloxy)benzophenone (**52**)⁹⁸

4-Hydroxybenzophenone (5.98 g, 30.1 mmol) and 1,8-dibromooctane (82.14 g, 0.30 mol), previously distilled under vacuum, were dissolved in acetone (40 mL) and potassium carbonate (4.25 g, 30.8 mmol) was then added. The mixture was heated at reflux for 8 h and then allowed to cool to rt. Water (50 mL) was added and the solution was extracted with DCM (2x60 mL). The organic layer was washed with 10% aq. sodium hydroxide (2x50 mL) and dried over sodium sulphate. The solvent was evaporated *in vacuo* and excess 1,8-dibromooctane was removed by kugelrohr distillation, leaving a yellow oil (12.60 g). Column chromatography (DCM (5-40%)/petroleum ether) gave 1,8-dibromooctane followed by the desired product, 4-(8-bromooctyloxy)benzophenone (**52**), as a light yellow oil (10.40 g, 89%).

4-(8-bromooctyloxy)benzophenone (**52**)



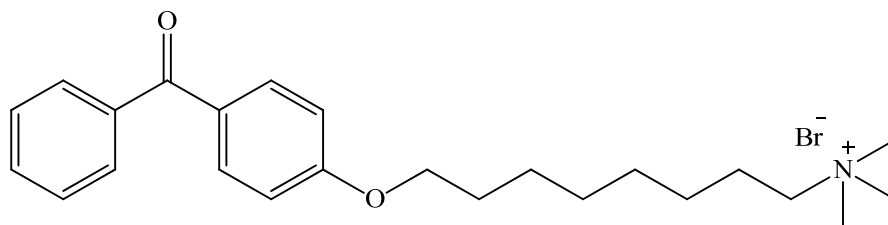
IR (cm^{-1}): 1651 (C=O), 1599 (C=C), 1252, 1172 (C-O), 726 (C-Br). **¹H-NMR** (δ): 1.32-1.52 (ms, 8H, 4xCH₂), 1.77-1.89 (m, 4H, 2xCH₂), 3.43 (t, 2H, CH₂Br, J_{vic} = 6.8 Hz), 4.03 (t, 2H, OCH₂, J_{vic} = 6.8 Hz) 6.92-7.79 (ms, 9H, 9xCH_{Ar}). **¹³C-NMR** (ppm): 195.6 (C=O), 162.9 (CO), 138.4, 132.7, 131.9, 130.0, 129.8, 128.3, 114.1 (C_{Ar}), 68.3 (OCH₂), 34.1 (CH₂Br), 32.9, 29.24, 29.16, 28.8, 28.2, 26.0 (CH₂).

3.1.4.2 Synthesis of *N,N,N,N*-8-(4-benzoylphenoxyoctyl)trimethyl ammonium bromide (**53**)

4-(8-Bromooctyloxy)benzophenone (**52**) (2.56 g, 5.76 mmol) and trimethylamine (1.78 mL, 7.49 mmol) were dissolved in a 2:1 chloroform/ether solution (30 mL) and the solution was stirred at rt for 48 h. The solvent was removed by reduced pressure distillation leaving a white solid which was then washed with diethyl ether to remove starting material. The desired product, *N,N,N,N*-8-(4-benzoylphenoxyoctyl)trimethyl

ammonium bromide (**53**), was obtained as a white solid (1.67 g, 65%), mp 171.6-172.5 °C.

***N,N,N,N*-8-(4-benzoyloxyoctyl)trimethyl ammonium bromide (**53**)**



IR (cm^{-1}): 1646 (C=O), 1600 (C=C), 1251, 1174 (C-O). **$^1\text{H-NMR}$** (δ): 1.37-1.48 (ms, 8H, 4xCH₂), 1.70-1.81 (m, 4H, 2xCH₂), 3.45 (s, 9H, N(CH₃)₃), 3.56-3.60 (m, 2H, CH₂N), 4.01 (t, 2H, OCH₂, $J_{vic} = 6.4$ Hz), 6.92-7.78 (ms, 9H, 9xCH_{Ar}). **$^{13}\text{C-NMR}$** (ppm): 195.7 (C=O), 162.9 (CO), 138.4, 132.6, 132.0, 130.0, 129.8, 128.3, 114.1 (C_{Ar}), 68.2 (CH₂O), 67.0 (CH₂N), 53.5 (CH₃), 29.2, 29.11, 29.06, 26.2, 25.9, 23.3 (CH₂). **HRMS (CI)**: M+H⁺, C₂₄H₃₄NO₂Br; Calculated: 368.2590; Found: 326.2598.

3.1.4.3 Attachment of the quaternary ammonium salt (53**) to silica**

The quaternary ammonium salt (**53**) (1.80 g, 4.00 mmol) was dissolved in ethanol (20 mL) and silica (11.78 g) was added. The solvent was evaporated under reduced pressure (35 °C, 15 min) and following this the silica was dried in a vacuum oven at 70 °C for 24 h giving a white powder (13.56 g) which was stored in a desiccator prior to use. Gravimetrically, **SP4 (Figure 87)** contained 0.30 mmol photomediator/g.

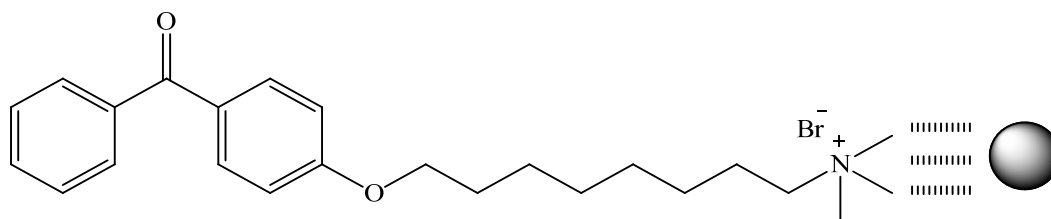


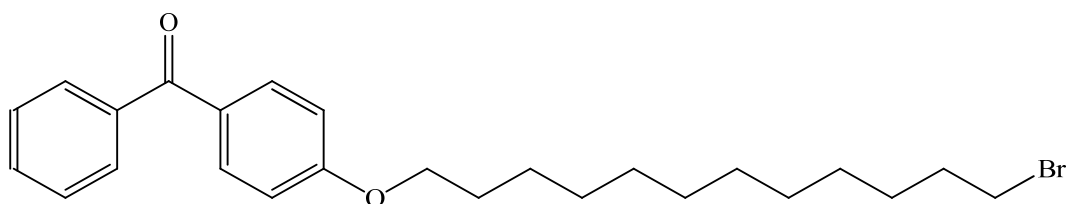
Figure 87

3.1.5 Synthesis of silica supported C-12 quaternary ammonium salt SP5

3.1.5.1 Preparation of 4-(12-bromododecyloxy)benzophenone (**54**)

4-Hydroxybenzophenone (3.00 g, 15.2 mmol) and 1,12-dibromododecane (50.10 g, 0.15 mol) were dissolved in acetone (70 mL) and potassium carbonate (2.24 g, 16.2 mmol) was then added. The mixture was heated at reflux for 8 h and then allowed to cool to rt. Water (50 mL) was added and the solution was extracted with DCM (2x60 mL). The organic layer was washed with 10% aq. sodium hydroxide (2x50 mL) and dried over sodium sulphate. The solvent was evaporated *in vacuo* giving a solid from which excess 1,12-dibromododecane was removed by washing with acetonitrile, leaving 4-(12-bromododecyloxy)benzophenone (**54**) as a white solid (6.36 g, 94%). mp 69.2-70.4 °C, lit⁹⁹. 73-75 °C.

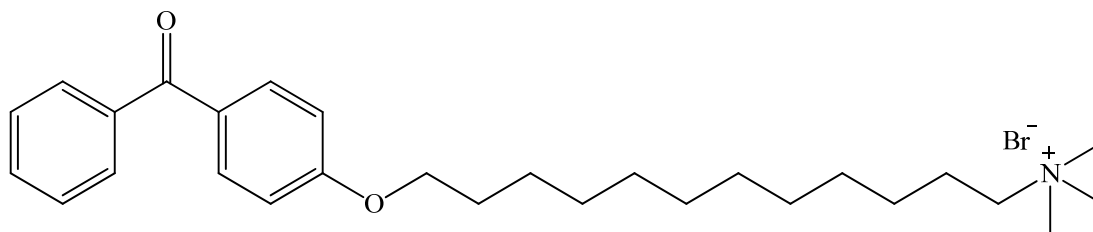
4-(12-bromododecyloxy)benzophenone⁹⁹ (**54**)



IR cm^{-1} : 1639 (C=O), 1601 (C=C), 1255, 1173 (C-O), 735 (C-Br). **¹H-NMR** (δ): 1.27-1.43 (ms, 16H, 8xCH₂), 1.78-1.88 (m, 4H, 2xCH₂), 3.34 (t, 2H, CH₂Br, J_{vic} = 6.8 Hz), 3.98 (t, 2H, OCH₂, J_{vic} = 6.5 Hz), 6.90-7.77 (ms, 9H, 9xCH_{Ar}). **¹³C-NMR** (ppm): 195.5 (C=O), 163.0 (CO), 138.4, 132.6, 131.9, 130.0, 129.8, 128.3, 114.1 (C_{Ar}), 68.3 (OCH₂), 34.1 (CH₂Br), 32.9, 29.6, 29.5, 29.5, 29.2, 28.9, 28.3, 26.1 (CH₂).

3.1.5.2 Synthesis of *N,N,N,N*-12-(4-benzoylphenoxydodecyl)trimethyl ammonium bromide (**55**)

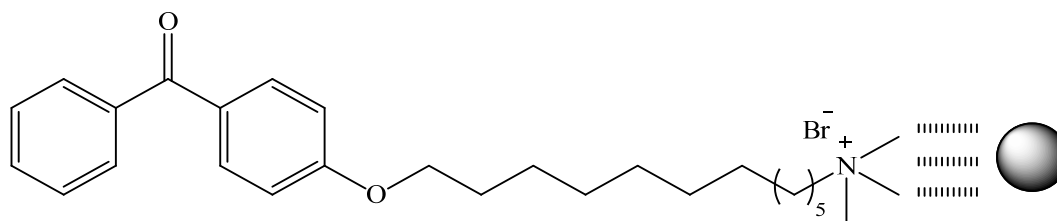
4-(12-Bromododecyloxy)benzophenone (**54**) (3.66 g, 8.20 mmol) and trimethylamine (2.53 mL, 10.66 mmol) were dissolved in a 2:1 chloroform/ether solution (30 mL) and the solution was stirred at rt for 48 h. A white precipitate formed which was filtered off and washed with diethyl ether to remove any unreacted bromide, giving the quaternary ammonium salt (**55**) as a white solid, (2.74 g, 70%), mp 178.0-179.0 °C.

***N,N,N,N*-12-(4-benzoylphenoxydodecyl)trimethyl ammonium bromide (55)**

IR (cm⁻¹): 1641 (C=O), 1604 (C=C), 1467 (C-N), 1247, 1173 (C-O). **¹H-NMR (δ):** 1.26-1.47 (m, 16H, 8xCH₂), 1.69-1.83 (m, 4H, 2xCH₂), 3.46 (s, 9H, N(CH₃)₃), 3.55-3.59 (m, 2H, CH₂N), 4.02 (t, 2H, OCH₂, *J*_{vic} = 6.5 Hz), 6.93-7.76 (ms, 9H, 9xCH_{Ar}). **¹³C-NMR (ppm):** 195.7 (C=O), 163.0 (CO), 138.4, 132.7, 132.0, 129.9, 129.8, 128.3, 114.1 (C_{Ar}), 68.3 (CH₂O), 67.1 (CH₂N), 53.5 (N(CH₃)₃), 29.54, 29.52, 29.46, 29.42, 29.35, 29.30, 29.2, 26.2, 26.0, 23.3 (CH₂). **HRMS (CI):** M+H⁺, C₂₈H₄₂NO₂; Calculated: 424.3216; Found: 424.3232.

3.1.5.3 Attachment of the quaternary ammonium salt (55) to silica

The quaternary ammonium salt (55) (2.02 g, 4.00 mmol) was dissolved in chloroform (30 mL) and silica (10.00 g), previously dried in a vacuum oven at 100 °C for 24 h, was added. The solvent was removed under atmospheric pressure (40 min, 75 °C), and following this, the solid was dried in a vacuum oven at 70 °C for 24 h giving a white powder (12.01 g) which was stored in a desiccator prior to use. Gravimetrically, **SP5 (Figure 88)** contained 0.33 mmol photomediator/g.

**Figure 88**

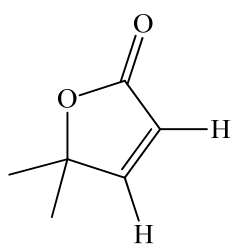
3.2 Photochemical reactions using 3-aminopropyl silica bound benzophenone SP1

3.2.1 Reactions with the monosubstituted alkyne methyl propiolate using SP1

3.2.1.1 Photochemical reaction of methyl propiolate with 2-propanol

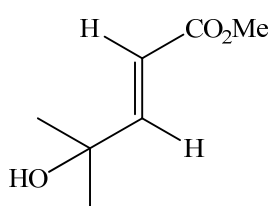
A solution of methyl propiolate (0.25 g, 3.00 mmol) and 2-propanol (3.60 g, 60.0 mmol) in acetonitrile (60 mL) containing SP1 (0.31 g, 0.50 mmol of photomediator) was placed in a cylindrical pyrex tube and degassed with nitrogen for 20 min. The solution was then irradiated, while stirring, with 350 nm mercury lamps in a Rayonet reactor for 7 h, at which time no further reaction of the alkyne was occurring (GC, 68% conversion). GC analysis indicated the presence of three products, 5,5-dimethylfuran-2(5*H*)-one (**3**), methyl (2*Z*)-4-hydroxy-4-methylpent-2-enoate (**75**) and methyl (2*E*)-4-hydroxy-4-methylpent-2-enoate (**4**) in a 25:28:47 ratio. The supported photomediator was filtered off and the solution was concentrated under reduced pressure giving a mixture of (**3**) and (**4**) as a yellow oil (0.29 g). Subsequent purification by column chromatography using ether (15-32%)/petroleum ether gave the products (**3**) (0.13 g, 39%) and (**4**) (0.12 g, 28%) with the following spectroscopic data:

5,5-Dimethylfuran-2(5*H*)-one¹⁰⁰ (**3**)



IR (cm^{-1}): 1750 (C=O), 1660 (C=C), 1277, 1132 (C-O), 699 (CH=CH_{cis}). **¹H-NMR** (δ): 1.45 (s, 6H, 2xCH₃), 5.99 (d, 1H, CH=CHC(O), $J_{cis} = 5.6$ Hz), 7.38 (d, 1H, $J_{cis} = 5.6$ Hz). **¹³C-NMR** (ppm): 172.0 (C=O), 161.6 (CH=CHC(O)), 120.0 (CH=CHC(O)), 86.9 (C(CH₃)₂), 25.4 (CH₃).

Methyl (2*E*)-4-hydroxy-4-methylpent-2-enoate¹⁰² (**4**)



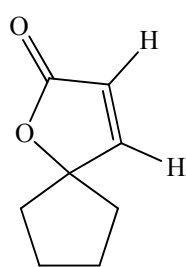
IR (cm^{-1}): 3441 (O-H), 2978 (CH), 1707 (C=O), 1660 (C=C), 1287, 1256 (C-O), 981 (CH=CH_{trans}). **¹H-NMR** (δ): 1.33 (s, 6H, 2xCH₃), 3.70 (s, 3H, OCH₃), 5.96 (d, 1H, CH=CHC(O), $J_{trans} = 15.7$ Hz), 6.98 (d, 1H, CH=CHC(O),

$J_{trans} = 15.7$ Hz). $^{13}\text{C-NMR}$: (ppm) 167.6 (C=O), 155.3 (CH=CHC(O)), 117.6 (CH=CHC(O)), 70.9 (C(CH₃)₂), 51.8 (OCH₃), 29.3 (CH₃).

3.2.1.2 Photochemical reaction of methyl propiolate with cyclopentanol

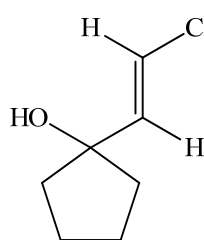
A solution of methyl propiolate (0.25 g, 3.00 mmol) and cyclopentanol (5.16 g, 60.0 mmol) in acetonitrile (60 mL) containing **SP1** (0.31 g, 0.50 mmol of photomediator) was prepared as before (Section 3.2.1.1). The solution was irradiated, while stirring, until no further reaction of the alkyne occurred (GC, 30 h, 50% conversion). GC analysis indicated the presence of two products, 1-oxaspiro[4.4]non-3-en-2-one (**56**) and methyl (2*E*)-3-(1-hydroxycyclopentyl)acrylate (**57**), in a 45:55 ratio. The supported photomediator was filtered off and the solution evaporated *in vacuo*. The excess cyclopentanol was removed using kugelrohr distillation, leaving a mixture of (**56**) and (**57**) as a yellow oil (0.26 g). Analysis of the NMR of the crude mixture confirmed the formation of (**56**) and (**57**):

1-Oxaspiro[4.4]non-3-en-2-one¹⁰³ (**56**)



IR (cm⁻¹): 1746 (C=O), 1600 (C=C). **¹H-NMR** (δ): 5.96 (d, 1H, CH=CHC(O), $J_{cis} = 5.6$ Hz), 7.35 (d, 1H, CH=CHC(O), $J_{cis} = 5.6$ Hz). **¹³C-NMR** (ppm): 170 (C=O), 159.3 (CH=CHC(O)), 120.3 (CH=CHC(O)), 97.1 (CO), 36.9, 24.0 (CH₂ ring).

Methyl (2*E*)-3-(1-hydroxycyclopentyl)-2-propenoate¹³² (**57**)

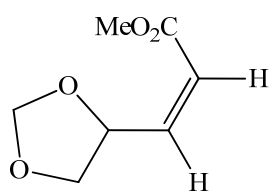


IR (cm⁻¹): 3441 (O-H), 1704 (C=O), 1654 (C=C). **¹H-NMR** (δ): 1.54 (broad s, 1H, OH), 3.72 (s, 3H, OCH₃), 6.09 (d, 1H, CH=CHC(O), $J_{trans} = 15.6$ Hz), 7.04 (d, 1H, CH=CHC(O), $J_{trans} = 15.6$ Hz). **¹³C-NMR** (ppm): 167.5 (C=O), 154.6 (CH=CHC(O)), 117.3 (CH=CHC(O)), 81.7 (COH), 51.6 (OCH₃), 40.5 (CH₂ ring), 24.8 (CH₂ ring).

3.2.1.3 Photochemical reaction of methyl propiolate with 1,3-dioxolane

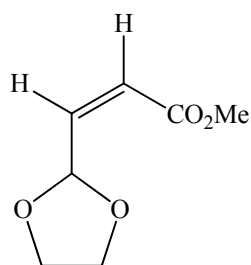
A solution of methyl propiolate (0.25 g, 3.00 mmol) and 1,3-dioxolane (4.44 g, 60.0 mmol) in acetonitrile (60 mL) containing **SP1** (0.31 g, 0.50 mmol of photomediator) was prepared as before (Section 3.2.1.1). The solution was irradiated, while stirring, until no further reaction of the alkyne was occurring (GC, 17 h, 60% conversion). GC analysis indicated the presence of four products, methyl (2*Z*)-3-(1,3-dioxan-4-yl)-2-propenoate (**58**), methyl (2*Z*)-3-(1,3-dioxan-2-yl)-2-propenoate (**59**), methyl (2*E*)-3-(1,3-dioxan-2-yl)-2-propenoate (**60**) and methyl 3,3-di(1,3-dioxolan-2-yl)propanoate (**61**), in a ratio of 6:39:49:6. The supported photomediator was filtered off and the solution was concentrated under reduced pressure affording a mixture of (**58**), (**59**), (**60**) and (**61**) as a yellow oil (0.38 g). Subsequent purification by column chromatography (diethyl ether (3-11%)/petroleum ether) gave, in order of elution, the products (**58**) (0.03 g, 6%), (**59**) (0.08 g, 17%), (**60**) (0.09 g, 19%) and (**61**) (0.02 g, 3%) with the following spectroscopic data:

Methyl (2*Z*)-3-(1,3-dioxan-4-yl)-2-propenoate¹⁰⁴ (**58**)

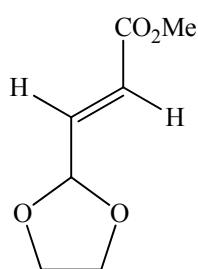


IR (cm⁻¹): 1715 (C=O), 1645 (C=C), 1207, 1186, 1085 (C-O). **¹H-NMR (δ):** 3.53 (dd, 1H, OCH(**H**)CH, $J_{gem} = 8.2$ Hz, $J_{vic} = 6.4$ Hz), 3.69 (s, 3H, OCH₃), 4.27 (t, 1H, OCH(**H**)CH, $J_{gem} = J_{vic} = 8.2$ Hz), 4.89 (s, 1H, OCH(**H**)O), 5.05 (s, 1H, OCH(**H**)O), 5.35 (m, 1H, OCH₂CH), 5.85 (dd, 1H, CHCH=CHC(O), $J_{cis} = 11.6$ Hz, $J_{LR} = 1.8$ Hz), 6.36 (dd, 1H, CHCH=CHC(O), $J_{cis} = 11.6$ Hz, $J_{vic} = 6.4$ Hz). **¹³C-NMR (ppm):** 166.2 (C=O), 149.1 (CH=CHC(O)), 120.6 (CH=CHC(O)), 95.4 (OCH₂O), 73.4 (CHCH=CHC(O)), 70.2 (OCH₂CH), 51.6 (OCH₃).

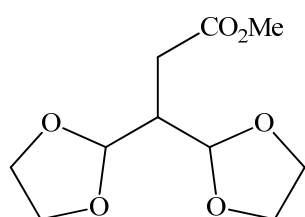
Methyl (2*Z*)-3-(1,3-dioxan-2-yl)-2-propenoate¹⁰⁴ (**59**)



IR (cm⁻¹): 1727 (C=O), 1668 (C=C), 1206, 1115, 1030 (C-O). **¹H-NMR (δ):** 3.71 (s, 3H, OCH₃), 3.92-4.03 (ms, 4H, 2xCH₂), 5.98 (d, 1H, CH=CHC(O), $J_{cis} = 11.6$ Hz), 6.06 (dd, 1H, CHCH=CHC(O), $J_{cis} = 11.6$ Hz, $J_{vic} = 6.9$ Hz), 6.23 (d, 1H, CHCH=CHC(O), $J_{vic} = 6.9$ Hz). **¹³C-NMR (ppm):** 165.6 (C=O), 143.2 (CH=CHC(O)), 124.3 (CH=CHC(O)), 97.8 (CHCH=CHC(O)), 65.9 (CH₂), 65.3 (CH₂), 51.8 (OCH₃).

Methyl (2E)-3-(1,3-dioxan-2-yl)-2-propenoate¹⁰⁴ (60)

IR (cm⁻¹): 1725 (C=O), 1664 (C=C), 1265, 1173, 1030 (C-O).
¹H-NMR (δ): 3.70 (s, 3H, OCH₃), 3.86-3.97 (ms, 4H, 2xCH₂), 5.39 (dd, 1H, CHCH=CHC(O), $J_{vic} = 4.6$ Hz, $J_{LR} = 1.0$ Hz), 6.09 (dd, 1H, CH=CHC(O), $J_{trans} = 15.8$ Hz, $J_{LR} = 1.0$ Hz), 6.72 (dd, 1H, CHCH=CHC(O), $J_{trans} = 15.8$ Hz, $J_{vic} = 4.6$ Hz). **¹³C-NMR (ppm):** 166.3 (C=O), 142.3 (CH=CHC(O)), 123.9 (CH=CHC(O)), 101.2 (CHCH=CHC(O)), 65.1 (CH₂), 51.9 (OCH₃).

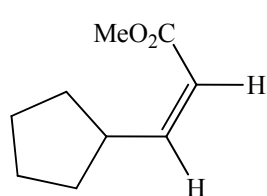
Methyl 3,3-di(1,3-dioxolan-2-yl)propanoate¹⁰⁴ (61)

IR (cm⁻¹): 1735 (C=O), 1260, 1130, 1031 (C-O). **¹H-NMR (δ):** 2.45 (d, 2H, CHCH₂C(O), $J_{vic} = 6.5$ Hz), 2.60 (m, 1H, CHCH₂C(O)), 3.60 (s, 3H, OCH₃), 3.79-3.97 (ms, 8H, 2xCH₂CH₂), 5.00 (d, 2H, OCHO, $J_{vic} = 4.2$ Hz). **¹³C-NMR (ppm):** 173.3 (C=O), 103.2 (OCHO), 65.1 (CH₂), 64.9 (CH₂), 51.6 (OCH₃), 43.3 (CHCH₂), 28.5 (CHCH₂).

3.2.1.4 Photochemical reaction of methyl propiolate with cyclopentane

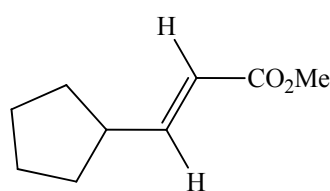
A solution of methyl propiolate (0.25 g, 3.00 mmol) and cyclopentane (4.20 g, 60.0 mmol) in acetonitrile (60 mL) containing **SP1** (0.31 g, 0.50 mmol of photomediator) was prepared as before (Section 3.2.1.1). The solution was irradiated, while stirring, until no further reaction of the alkyne was occurring (30 h, 71% conversion). GC analysis indicated the presence of two products, methyl (2*Z*)-3-cyclopentyl-2-propenoate (**5**) and methyl (2*E*)-3-cyclopentyl-2-propenoate (**6**), in a 66:34 ratio. The supported photomediator was filtered off and the solution was concentrated affording a mixture of (**5**) and (**6**) as a yellow oil (0.31 g). Analysis of the NMR of the crude mixture confirmed the formation of (**5**) and (**6**):

Methyl (2*Z*)-3-cyclopentyl-2-propenoate²¹ (**5**)



IR (cm^{-1}): 823 ($\text{CH}=\text{CH}_{\text{cis}}$). **¹H-NMR** (δ): 3.69 (s, 3H, OCH_3), 5.67 (dd, 1H, $\text{CHCH}=\text{CH}$, $J_{\text{cis}} = 11.6$ Hz, $J_{\text{LR}} = 1.2$ Hz), 6.11 (dd, 1H, $\text{CHCH}=\text{CH}$, $J_{\text{cis}} = 11.4$ Hz, $J_{\text{vic}} = 10.0$ Hz). **¹³C-NMR** (ppm): 167.6 ($\text{C}=\text{O}$), 155.8 ($\text{CHCH}=\text{CH}$), 117.6 ($\text{CHCH}=\text{CH}$), 51.0 (OCH_3), 39.2 ($\text{CHCH}=\text{CH}$), 33.5 (CH_2), 25.7 (CH_2).

Methyl (2*E*)-3-cyclopentyl-2-propenoate¹⁰⁵ (**6**)

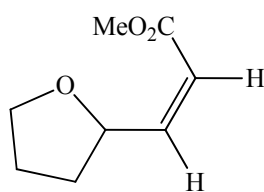


IR (cm^{-1}): 956 ($\text{CH}=\text{CH}_{\text{trans}}$). **¹H-NMR** (δ): 3.71 (s, 3H, OCH_3), 5.78 (dd, 1H, $\text{CHCH}=\text{CH}$, $J_{\text{trans}} = 15.6$ Hz, $J_{\text{LR}} = 1.2$ Hz), 6.94 (dd, 1H, $\text{CHCH}=\text{CH}$, $J_{\text{vic}} = 8.0$ Hz, $J_{\text{trans}} = 15.6$ Hz). **¹³C-NMR** (ppm): 167.1 ($\text{C}=\text{O}$), 154.0 ($\text{CHCH}=\text{CH}$), 118.9 ($\text{CHCH}=\text{CH}$), 51.5 (OCH_3), 42.9 ($\text{CHCH}=\text{CH}$), 32.4 (CH_2), 24.9 (CH_2).

3.2.1.5 Photochemical reaction of methyl propiolate with tetrahydrofuran (THF)

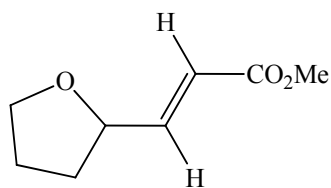
A solution of methyl propiolate (0.25 g, 3.00 mmol) in THF (20 mL, 24.7 mmol) containing **SP1** (0.31 g, 0.50 mmol of photomediator) was prepared as before (**Section 3.2.1.1**). The solution was irradiated, while stirring, until complete reaction of the alkyne had occurred (GC, 1.50 h). GC analysis indicated the presence of two products, methyl (2*Z*)-3-(tetrahydrofuran-2-yl)-2-propenoate (**62**) and methyl (2*E*)-3-(tetrahydrofuran-2-yl)-2-propenoate (**63**), in a 43:57 ratio. The supported photomediator was filtered off and the solution was concentrated under reduced pressure affording a mixture of (**62**) and (**63**) as a yellow oil (0.45 g). Subsequent purification by column chromatography gave the products (**62**) (0.21 g, 45%) and (**63**) (0.20 g, 43%) with the following spectroscopic data:

Methyl (2*Z*)-3-(tetrahydrofuran-2-yl)-2-propenoate¹⁰⁷ (**62**)



IR (cm^{-1}): 1718 (C=O), 1178, 1054 (C-O), 670 ($\text{CH}=\text{CH}_{\text{cis}}$). **¹H-NMR** (δ): 1.48-2.35 (ms, 4H, 2xCH₂), 3.69 (s, 3H, OCH₃), 3.78-3.94 (ms, 2H, OCH₂), 5.25 (m, 1H, OCH), 5.74 (dd, 1H, CHCH=CH, $J_{\text{cis}} = 11.7$ Hz, $J_{\text{LR}} = 1.6$ Hz), 6.28 (dd, 1H, CH-CH=CH, $J_{\text{cis}} = 11.7$ Hz, $J_{\text{vic}} = 7.2$ Hz). **¹³C-NMR** (ppm): 166.3 (C=O), 151.7 (CH=CHC(O)), 118.8 (CH=CHC(O)), 76.0 (OCH), 68.4 (OCH₂), 51.4 (OCH₃), 32.2 (CH₂), 26.2 (CH₂).

Methyl (2*E*)-3-(tetrahydrofuran-2-yl)-2-propenoate¹⁰⁷ (**63**)



IR (cm^{-1}): 1720 (C=O), 1161, 1035 (C-O), 980 ($\text{CH}=\text{CH}_{\text{trans}}$). **¹H-NMR** (δ): 1.62-2.13 (ms, 4H, 2xCH₂), 3.70 (s, 3H, OCH₃), 3.77-3.92 (ms, 2H, OCH₂), 4.48 (m, 1H, OCH), 5.98 (dd, 1H, CHCH=CH, $J_{\text{trans}} = 15.6$ Hz, $J_{\text{LR}} = 1.6$ Hz), 6.88 (dd, 1H, CHCH=CH, $J_{\text{trans}} = 15.6$ Hz, $J_{\text{vic}} = 4.8$ Hz). **¹³C-NMR** (ppm): 167.9 (C=O), 149.6 (CH=CHC(O)), 120.3 (CH=CHC(O)), 77.3 (OCH), 69.0 (OCH₂), 51.9 (OCH₃), 31.8 (CH₂), 25.7 (CH₂).

3.2.2 Reaction with a larger quantity of methyl propiolate using SP1

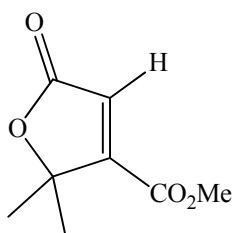
3.2.2.1 Photochemical reaction of methyl propiolate with 1,3-dioxolane

A solution of methyl propiolate (0.50 g, 6.00 mmol) and 1,3-dioxolane (4.44 g, 60.0 mmol) in acetonitrile (60 mL), containing **SP1** (0.31 g, 0.50 mmol of photomediator) was prepared as before (**Section 3.2.1.1**). The solution was irradiated, while stirring, until complete reaction of the alkyne had occurred (GC, 17 h). GC analysis indicated three products, **(59)**, **(60)** and **(61)**, in a 29:49:22 ratio. The supported photomediator was filtered off and the solution was concentrated using rotary evaporation leaving a mixture of **(59)**, **(60)** and **(61)** as a yellow oil (0.95 g). The spectroscopic data obtained for **(59)**, **(60)** and **(61)** from the mixture were identical to those obtained previously (**Section 3.2.1.3**).

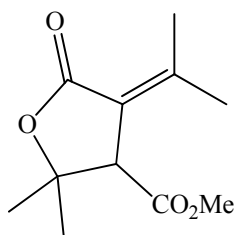
3.2.3 Reactions with the disubstituted alkyne DMAD using SP1

3.2.3.1 Photochemical reaction of DMAD with 2-propanol

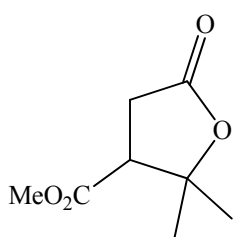
A solution of DMAD (0.43 g, 3.00 mmol) and 2-propanol (3.60 g, 60.0 mmol) in acetonitrile (60 mL) containing **SP1** (0.31 g, 0.05 mmol of photomediator) was prepared as before (**Section 3.2.1.1**). The solution was then irradiated, while stirring, for 4.5 h at which time complete reaction of the alkyne had occurred (GC). GC analysis indicated the presence of five products, methyl 2,2-dimethyl-5-oxo-2,5-dihydrofuran-3-carboxylate **(64)**, methyl 2,2-dimethyl-4-(1-methylethylidene)-5-oxotetrahydrofuran-3-carboxylate **(65)**, methyl 2,2-dimethyl-5-oxotetrahydrofuran-3-carboxylate **(66)**, dimethyl (2*Z*)-2-(1-hydroxy-1-methylethyl)but-2-enedioate **(67)** and dimethyl (2*E*)-2,3-bis(1-hydroxy-1-methylethyl)but-2-enedioate **(68)** in a 42:13:2:25:18 ratio. The supported photomediator was filtered off and the solution was concentrated *in vacuo*. The resulting mixture (0.48 g) was adsorbed onto silica (45 g) and eluted with diethyl ether (15-35%)/petroleum ether. The products **(64)** (0.06 g, 12%), **(65)** (0.04 g, 6%), **(66)** (0.01 g, 2%) and **(67)** (0.05 g, 8%) were obtained as light yellow oils. Dimethyl (2*E*)-2,3-bis(1-hydroxy-1-methylethyl)but-2-enedioate **(68)** (0.04 g, 7%) eluted last and was obtained as a white solid:

Methyl 2,2-dimethyl-5-oxo-2,5-dihydrofuran-3-carboxylate¹¹¹ (64)

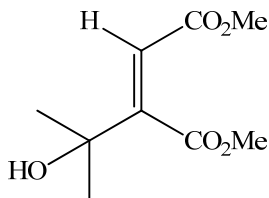
IR (cm^{-1}): 1763 (C=O), 1730 (C=O), 1635 (C=C), 1227, 1129 (C-O). **¹H-NMR** (δ): 1.60 (s, 6H, 2xCH₃), 3.86 (s, 3H, OCH₃), 6.56 (s, 1H, C=CH). **¹³C-NMR** (ppm): 169.8 (C=O), 161.2 (C=O), 160.9 (C=CH), 126.2 (C=CH), 87.2 (C(CH₃)₂), 52.6 (OCH₃), 25.1 (CH₃).

Methyl 2,2-dimethyl-4-(1-methylethylidene)-5-oxotetrahydrofuran-3-carboxylate (65)

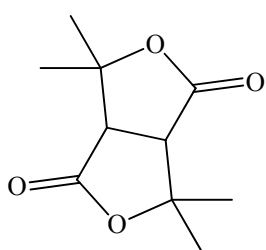
IR (cm^{-1}): 1737 (C=O), 1664 (C=C), 1247, 1169 (C-O). **¹H-NMR** (δ): 1.37 (s, 3H, CH₃), 1.40 (s, 3H, CH₃), 1.80 (s, 3H, C=CCH₃), 2.28 (s, 3H, C=CCH₃), 3.60 (s, 1H, CH), 3.69 (s, 3H, OCH₃). **¹³C-NMR** (ppm): 170.9 (C=O), 168.3 (C=O), 154.1 (C=C(CH₃)₂), 120.7 (C=C(CH₃)₂), 79.9 (C(CH₃)₂), 56.0 (OCH₃), 52.2 (CH), 30.2 (CH₃), 24.5 (CH₃), 23.9 (CH₃), 20.4 (CH₃).

Methyl 2,2-dimethyl-5-oxotetrahydrofuran-3-carboxylate¹¹² (66)

IR (cm^{-1}): 1776 (C=O), 1730 (C=O), 1250, 1168 (C-O). **¹H-NMR** (δ): 1.30 (s, 3H, CH₃), 1.60 (s, 3H, CH₃), 2.70 (dd, 1H, CHC(H)H, $J_{gem} = 17.7$ Hz, $J_{vic} = 8.6$ Hz), 3.08 (dd, 1H, CHC(H)H, $J_{gem} = 17.7$ Hz, $J_{vic} = 9.7$ Hz), 3.19 (dd, 1H, CH, $J_{vic} = 8.8$ Hz, $J_{vic} = 9.6$ Hz), 3.76 (s, 3H, OCH₃). **¹³C-NMR** (ppm): 173.9 (C=O), 170.4 (C=O), 84.4 (C(CH₃)₂), 52.5 (CH), 50.5 (OCH₃), 31.9 (CH₂), 28.6 (CH₃), 23.4 (CH₃).

Dimethyl (2Z)-2-(1-hydroxy-1-methylethyl)but-2-enedioate¹¹³ (67)

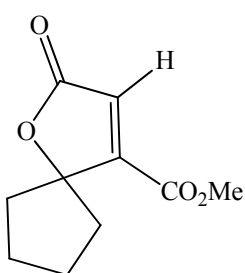
IR (cm^{-1}): 3478 (O-H), 1722 (C=O), 1648 (C=C), 1257, 1167 (C-O). **¹H-NMR** (δ): 1.41 (s, 6H, 2xCH₃), 3.68 (s, 3H, OCH₃), 3.80 (s, 3H, OCH₃), 6.06 (s, 1H, CH). **¹³C-NMR** (ppm): 168.5 (C=O), 165.6 (C=O), 157.9 (C=CH), 117.0 (C=CH), 71.9 (C(CH₃)₂), 52.5 (OCH₃), 52.0 (OCH₃), 29.0 (CH₃).

Dimethyl (2E)-2,3-bis(1-hydroxy-1-methylethyl)but-2-enedioate¹¹⁴ (68)

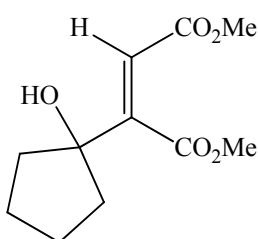
IR (cm⁻¹): 1757 (C=O), 1254, 1123 (C-O). **¹H-NMR (δ):** 1.51 (s, 6H, 2xCH₃), 1.57 (s, 6H, 2xCH₃), 3.37 (s, 2H, 2xCH). **¹³C-NMR (ppm):** 172.2 (C=O), 83.8 (C(CH₃)₂), 52.1 (CH), 31.2 (CH₃), 24.7 (CH₃).

3.2.3.2 Photochemical reaction of DMAD with cyclopentanol

A solution of DMAD (0.43 g, 3.00 mmol) and cyclopentanol (5.16 g, 60.0 mmol) in acetonitrile (60 mL) containing **SP1** (0.31 g, 0.05 mmol of photomediator) was prepared as before (**Section 3.2.1.1**). The solution was irradiated, while stirring, until no further reaction of the alkyne occurred (GC, 5 h, 25% conversion). GC analysis indicated the formation of two products, methyl 2-oxo-1-oxaspiro[4.4]non-3-ene-4-carboxylate (**69**) and dimethyl (2Z)-2-(1-hydroxycyclopentyl)but-2-enedioate (**70**), in a 54:46 ratio. The supported photomediator was filtered off and the solution was concentrated under reduced pressure. The excess cyclopentanol was removed using kugelrohr distillation, giving a mixture of (**69**) and (**70**) as a yellow oil (0.13 g). Analysis of the NMR of the crude mixture confirmed the presence of (**69**) and (**70**):

Methyl 2-oxo-1-oxaspiro[4.4]non-3-ene-4-carboxylate¹¹¹ (69)

IR (cm⁻¹): 1763 (C=O). **¹H-NMR (δ):** 3.86 (s, 3H, OCH₃), 6.62 (s, 1H, C=CH). **¹³C-NMR (ppm):** 126.9 (C=CH), 37.1 (CH₂), 25.3 (CH₂).

Dimethyl (2Z)-2-(1-hydroxycyclopentyl)but-2-enedioate¹¹⁵ (70)

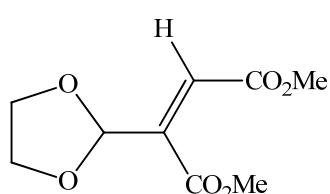
(CH₂ ring).

IR (cm⁻¹): 3323 (OH), 1727 (C=O), 1626 (C=C), 1259, 1169 (C-O). **¹H-NMR (δ):** 3.74 (s, 1H, OCH₃), 3.84 (s, 1H, OCH₃), 6.17 (s, 1H, C=CH). **¹³C-NMR (ppm):** 168.6 (C=O), 165.6 (C=O), 156.1 (C=CH), 117.5 (C=CH), 82.2 (COH), 52.6 (OCH₃), 52.0 (OCH₃), 39.8 (CH₂ ring), 23.7

3.2.3.3 Photochemical reaction of DMAD with 1,3-dioxolane

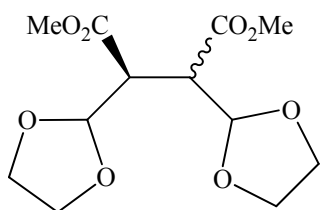
A solution of DMAD (0.43 g, 3.00 mmol) and 1,3-dioxolane (4.44 g, 60.0 mmol) in acetonitrile (60 mL) containing **SP1** (0.31 g, 0.50 mmol of photomediator) was prepared as before (Section 3.2.1.1). The solution was irradiated, while stirring, until complete reaction of the alkyne had occurred (GC, 16 h). GC analysis indicated the presence of three products, dimethyl (2*Z*)-2-(1,3-dioxany-2-yl)but-2-enedioate (**71**), and dimethyl 2,3-di(1,3-dioxolan-2-yl)butanedioate (**72**) as a mixture of diastereomers, in a 19:25:56 ratio. The supported photomediator was filtered off and the solution was concentrated under reduced pressure affording a mixture of (**71**), and (**72**) as a mixture of diastereomers, as a yellow oil (0.81 g). Analysis of the NMR of the crude mixture confirmed the presence of (**71**) and (**72**):

Dimethyl (2*Z*)-2-(1,3-dioxany-2-yl)but-2-enedioate¹⁰⁴ (**71**)



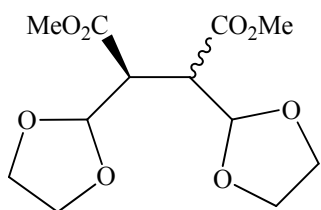
IR (cm⁻¹): 1660 (C=C). **¹H-NMR** (δ): 5.67 (s, 1H, OCHO), 6.24 (s, 1H, C=CH). **¹³C-NMR** (ppm): 166.1 (C=O), 165.2 (C=O), 144.6 (C=CHC(O)), 122.7 (C=CHC(O)), 100.6 (CHC=CH-C(O)), 52.7 (OCH₃), 52.3 (OCH₃).

Dimethyl 2,3-di(1,3-dioxolan-2-yl)butanedioate¹⁰⁴ (**72**)



¹H-NMR (δ): 5.22 (dd, 2H, 2xOCHO, $J_{vic} = 4.0$ Hz, $J_{LR} = 1.9$ Hz). **¹³C-NMR** (ppm): 170.6 (C=O), 103.1 (OCHO), 65.0 (CH₂), 48.9 (C(O)CHCHC(O)).

Dimethyl 2,3-di(1,3-dioxolan-2-yl)butanedioate¹⁰⁴ (**72**)

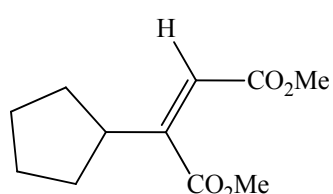


¹H-NMR (δ): 3.15-3.17 (m, 2H, C(O)CHCHC(O)), 5.36-5.38 (m, 2H, 2xOCHO). **¹³C-NMR** (ppm): 170.8 (C=O), 102.3 (OCHO), 48.1 (C(O)CHCHC(O)).

3.2.3.4 Photochemical reaction of DMAD with cyclopentane

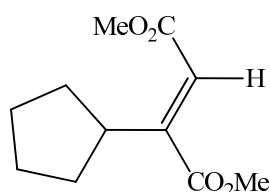
A solution of DMAD (0.43 g, 3.00 mmol) and cyclopentane (4.20 g, 60.0 mmol) in acetonitrile (60 mL) containing **SP1** (0.31 g, 0.50 mmol of photomediator) was prepared as before (Section 3.2.1.1). The solution was irradiated, while stirring, until no further reaction of the alkyne was occurring (GC, 52 h, 62% conversion). GC analysis indicated the presence of one minor product, dimethyl (2*Z*)-2-cyclopentylbut-2-enedioate (**73**), and one major product, dimethyl (2*E*)-2-cyclopentylbut-2-enedioate (**74**), in a 7:93 ratio. The supported photomediator was filtered off and the solution was concentrated leaving a mixture of (**73**) and (**74**) as a yellow oil (0.34 g). Analysis of the NMR of the crude mixture confirmed the presence of (**73**) and (**74**):

Dimethyl (2*Z*)-2-cyclopentylbut-2-enedioate²¹ (**73**)



IR (cm⁻¹): 1724 (C=O), 1646 (C=C), 1266, 1172 (C-O). **¹H-NMR** (δ): 3.68 (s, 3H, OCH₃), 3.80 (s, 3H, OCH₃), 5.79 (s, 1H, C=CH). **¹³C-NMR** (ppm): 169.0 (C=O), 165.7 (C=O), 155.0 (CHC=CH), 116.9 (CHC=CH), 52.3 (OCH₃), 51.8 (OCH₃), 44.5 (CHC=CH), 32.0 (CH₂), 24.9 (CH₂).

Dimethyl (2*E*)-2-cyclopentylbut-2-enedioate²¹ (**74**)

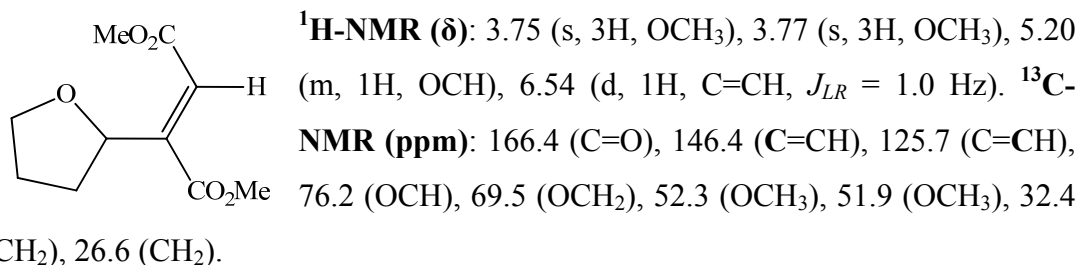


¹H-NMR (δ): 3.70 (s, 3H, OCH₃), 3.81 (s, 3H, OCH₃), 6.25 (s, 1H, C=CH).

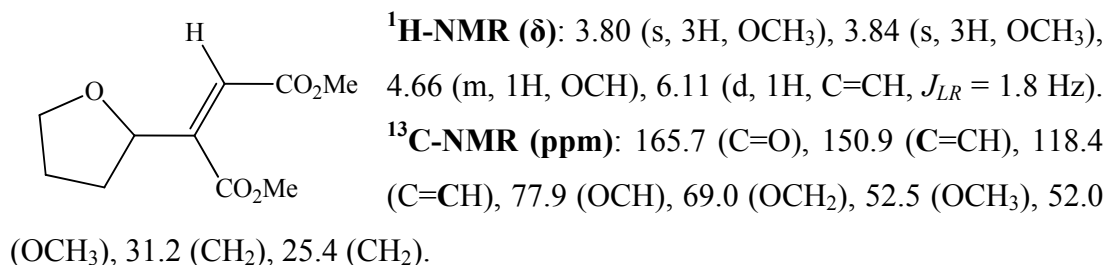
3.2.3.5 Photochemical reaction of DMAD with THF

A solution of DMAD (0.43 g, 3.00 mmol) in THF (20 mL, 24.7 mmol) containing **SP1** (0.31 g, 0.50 mmol of photomediator) was prepared as before (**Section 3.2.1.1**). The solution was irradiated, while stirring, for 3 h until no further reaction of the alkyne was occurring (GC). GC analysis indicated the presence of two products, dimethyl (2*E*)-2-(tetrahydrofuran-2-yl)but-2-enedioate (**20**) and dimethyl (2*Z*)-2-(tetrahydrofuran-2-yl)but-2-enedioate (**21**), in a 55:45 ratio. The supported photomediator was filtered off and the solution was concentrated under reduced pressure affording a mixture of (**20**) and (**21**) as a yellow oil (0.61 g). Analysis of the NMR of the crude mixture confirmed the presence of (**20**) and (**21**).

Dimethyl (2*E*)-2-(tetrahydrofuran-2-yl)but-2-enedioate⁵¹ (**20**)



Dimethyl (2*Z*)-2-(tetrahydrofuran-2-yl)but-2-enedioate⁵¹ (**21**)



3.3 Photochemical reactions using propyl linked 4-hydroxybenzophenone silica SP2

3.3.1 Reactions with the monosubstituted alkyne methyl propiolate using SP2

3.3.1.1 Photochemical reaction of methyl propiolate with 2-propanol

A solution of methyl propiolate (0.25 g, 3.00 mmol) and 2-propanol (3.60 g, 60.0 mmol) in acetonitrile (60 mL) containing **SP2** (1.20 g, 3.5 mmol of photomediator) was prepared as before (**Section 3.2.1.1**). The solution was irradiated, while stirring, for 36 h at which time complete reaction of the alkyne had occurred (GC). GC analysis indicated the presence of two products, **(3)** and **(4)**, in a 42:58 ratio. The supported photomediator was filtered off and the solution was concentrated under vacuum giving a mixture of **(3)** and **(4)**, as a yellow oil (0.38 g). The spectroscopic data of the crude product confirmed the formation of **(3)** and **(4)** (**Section 3.2.1.1**).

3.3.1.2 Photochemical reaction of methyl propiolate with cyclopentanol

A solution of methyl propiolate (0.25 g, 3.00 mmol) and cyclopentanol (5.16 g, 60.0 mmol) in acetonitrile (60 mL) containing **SP2** (1.20 g, 3.5 mmol of photomediator) was prepared as before (**Section 3.2.1.1**). The solution was irradiated, while stirring, until no further reaction of the alkyne was occurring (GC, 53 h, 88% conversion). GC analysis indicated the presence of **(56)** and **(57)** in a 35:65 ratio. The supported photomediator was filtered off and the solution was concentrated under reduced pressure. The excess cyclopentanol was removed using kugelrohr distillation, leaving a mixture of **(56)** and **(57)** as a yellow oil (0.42 g). The spectroscopic data obtained for **(56)** and **(57)** from the mixture were identical to those obtained previously (**Section 3.2.1.2**).

3.3.1.3 Photochemical reaction of methyl propiolate with 1,3-dioxolane

A solution of methyl propiolate (0.25 g, 3.00 mmol) and 1,3-dioxolane (4.44 g, 60.0 mmol) in acetonitrile (60 mL) containing **SP2** (1.20 g, 3.5 mmol of photomediator) was prepared as before (**Section 3.2.1.1**). The solution was irradiated, while stirring, until no further reaction of the alkyne was occurring (GC, 50 h, 80% conversion). GC analysis indicated the presence of four products, **(58)**, **(59)**, **(60)** and **(61)**, in a

7:34:49:10 ratio. The supported photomediator was filtered off and upon concentration of the solution, a mixture of **(58)**, **(59)**, **(60)** and **(61)** was obtained as a yellow oil (0.41 g). The spectroscopic data of the various products in the mixture were identical to those obtained previously (**Section 3.2.1.3**).

3.3.1.4 Photochemical reaction of methyl propiolate with cyclopentane

A solution of methyl propiolate (0.25 g, 3.00 mmol) and cyclopentane (4.20 g, 60.0 mmol) in acetonitrile (60 mL) containing **SP2** (1.20 g, 3.5 mmol of photomediator) was prepared as before (**Section 3.2.1.1**). The solution was irradiated, while stirring, until complete reaction of the alkyne occurred (GC, 120 h). GC analysis indicated the presence of two products, **(5)** and **(6)**, in a 35:65 ratio. The supported photomediator was filtered off and the solution was concentrated under reduced pressure affording the expected products **(5)** and **(6)** as a yellow oil (0.42 g). The spectroscopic data of the crude product confirmed the formation of **(5)** and **(6)** (**Section 3.2.1.4**).

3.3.1.5 Photochemical reaction of methyl propiolate with THF

A solution of methyl propiolate (0.25 g, 3.00 mmol) in THF (20 mL, 24.7 mmol) containing **SP2** (1.20 g, 3.5 mmol of photomediator) was prepared as before (**Section 3.2.1.1**). The solution was irradiated, while stirring, until complete reaction of the alkyne occurred (GC, 2.5 h). GC analysis indicated the presence of two products, **(62)** and **(63)**, in a 43:57 ratio. The supported photomediator was filtered off and the solution evaporated under reduced pressure affording a mixture of **(62)** and **(63)** as a yellow oil (0.46 g). The spectroscopic data obtained for **(62)** and **(63)** from the mixture were identical to those obtained previously (**Section 3.2.1.5**).

3.3.2 Reactions with the disubstituted alkyne DMAD using SP2

3.3.2.1 Photochemical reaction of DMAD with 2-propanol

A solution of DMAD (0.43 g, 3.00 mmol) and 2-propanol (3.60 g, 60.0 mmol) in acetonitrile (60 mL) containing SP2 (1.20 g, 3.5 mmol of photomediator) was prepared as before (**Section 3.2.1.1**). The solution was irradiated, while stirring, for 8.5 h at which time complete reaction of the alkyne had occurred (GC). GC analysis indicated the presence of two major and two minor products, **(64)**, **(65)**, **(66)** and **(67)**, in a 42:5:5:48 ratio. The supported photomediator was filtered off and the solution was concentrated under reduced pressure giving a mixture of the four products as a yellow oil (0.50 g). The spectroscopic data obtained for **(64)**, **(65)**, **(66)** and **(67)** in the mixture were identical to those obtained previously (**Section 3.2.3.1**).

3.3.2.2 Photochemical reaction of DMAD with cyclopentanol

A solution of DMAD (0.43 g, 3.00 mmol) and cyclopentanol (5.16 g, 60.0 mmol) in acetonitrile (60 mL) containing SP2 (1.20 g, 3.5 mmol of photomediator) was prepared as before (**Section 3.2.1.1**). The solution was irradiated, while stirring, for 21 h at which point no reaction of the alkyne had occurred (GC).

3.3.2.3 Photochemical reaction of DMAD with 1,3-dioxolane

A solution of DMAD (0.43 g, 3.00 mmol) and 1,3-dioxolane (4.44 g, 60.0 mmol) in acetonitrile (60 mL) containing SP2 (1.20 g, 3.5 mmol of photomediator) was prepared as before (**Section 3.2.1.1**). The solution was irradiated, while stirring, until complete reaction of the alkyne occurred (GC, 22 h). GC analysis showed the formation of only one product, the unsaturated diester **(71)**. The supported photomediator was filtered off and the solution was concentrated under reduced pressure affording **(71)** as a yellow oil (0.54 g). The spectroscopic data obtained for **(71)** from the crude product were identical to those obtained previously (**Section 3.2.3.3**).

3.3.2.4 Photochemical reaction of DMAD with cyclopentane

A solution of DMAD (0.43 g, 3.00 mmol) and cyclopentane (4.20 g, 60.0 mmol) in acetonitrile (60 mL) containing **SP2** (1.20 g, 3.5 mmol of photomediator) was prepared as before (**Section 3.2.1.1**). The solution was irradiated, while stirring, for 27 h at which point only 8% conversion of the alkyne had been achieved. GC analysis indicated the presence of a single product, the unsaturated diester (**73**). The supported photomediator was filtered off and the solution was concentrated using rotary evaporation. This afforded (**73**) as a yellow oil (0.03 g). The spectroscopic data of the crude product confirmed the formation of (**73**) (**Section 3.2.3.4**).

3.3.2.5 Photochemical reaction of DMAD with THF

A solution of DMAD (0.43 g, 3.00 mmol) in THF (20 mL, 24.7 mmol) containing **SP2** (1.20 g, 3.5 mmol of photomediator) was prepared as before (**Section 3.2.1.1**). The solution was irradiated, while stirring, until complete reaction of the alkyne had occurred (GC, 4.5 h). GC analysis indicated the presence of only the addition product (**21**). The supported photomediator was filtered off and the solution was concentrated under reduced pressure affording (**21**) as a yellow oil (0.60 g). The spectroscopic data of the crude product confirmed the formation of (**21**) (**Section 3.2.3.5**).

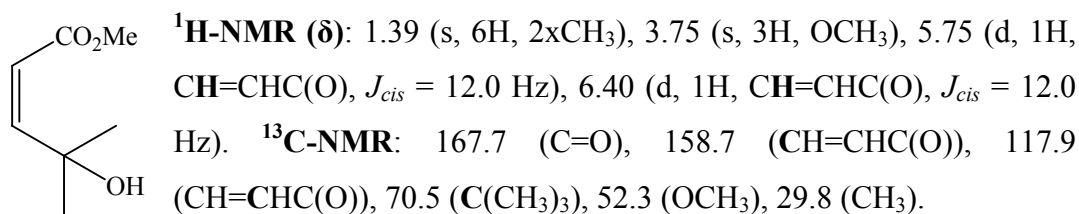
3.4 Photochemical reactions using silica supported C-5 quaternary ammonium salt SP3

3.4.1 Reactions with the monosubstituted alkyne methyl propiolate using SP3

3.4.1.1 Photochemical reaction of methyl propiolate with 2-propanol

A solution of methyl propiolate (0.25 g, 3.00 mmol) and 2-propanol (3.60 g, 60.0 mmol) in acetonitrile (60 mL) containing SP3 (1.20 g, 0.41 mmol of photomediator) was prepared as before (Section 3.2.1.1). The solution was irradiated, while stirring, for 2.75 h at which time complete reaction of the alkyne had occurred (GC). GC analysis indicated the presence of three products, (3), methyl (2*Z*)-4-hydroxy-4-methylpent-2-enoate (75) and (4), in a 22:21:57 ratio. The supported photomediator was filtered off and the solution was concentrated under reduced pressure giving a mixture of (3), (75) and (4) as a yellow oil (0.36 g). The spectroscopic data for (3) and (4) were identical to those obtained previously (Section 3.2.1.1). The NMR data for the crude mixture confirmed the presence of (75):

Methyl (2*Z*)-4-hydroxy-4-methylpent-2-enoate (75)



3.4.1.2 Photochemical reaction of methyl propiolate with cyclopentanol

A solution of methyl propiolate (0.25 g, 3.00 mmol) and cyclopentanol (5.16 g, 60.0 mmol) in acetonitrile (60 mL) containing SP3 (1.20 g, 0.41 mmol of photomediator) was prepared as before (Section 3.2.1.1). The solution was irradiated, while stirring, until complete reaction of the alkyne had occurred (GC, 9 h). GC analysis indicated the presence of two products, (56) and (57), (34:66). The supported photomediator was filtered off and the solvent was concentrated under reduced pressure. The excess cyclopentanol was removed using kugelrohr distillation, leaving a mixture of (56) and (57) as a yellow oil (0.46 g). The spectroscopic data of the crude product confirmed the formation of (56) and (57) (Section 3.2.1.2).

3.4.1.3 Photochemical reaction of methyl propiolate with 1,3-dioxolane

A solution of methyl propiolate (0.25 g, 3.00 mmol) and 1,3-dioxolane (4.44 g, 60.0 mmol) in acetonitrile (60 mL) containing **SP3** (1.20 g, 0.41 mmol of photomediator) was prepared as before (**Section 3.2.1.1**). The solution was irradiated, while stirring, until no further reaction of the alkyne was occurred (GC, 7.75 h, 80% conversion). GC analysis indicated the presence of three products, **(59)**, **(60)** and **(61)**, in a 23:39:38 ratio. The supported photomediator was filtered off and the solution was concentrated under reduced pressure affording **(59)**, **(60)** and **(61)** as a yellow oil (0.52 g). The spectroscopic data obtained for the various products in the mixture were identical to those obtained previously (**Section 3.2.1.3**).

3.4.1.4 Photochemical reaction of methyl propiolate with cyclopentane

A solution of methyl propiolate (0.25 g, 3.00 mmol) and cyclopentane (4.20 g, 60.0 mmol) in acetonitrile (60 mL) containing **SP3** (1.20 g, 0.41 mmol of photomediator) was prepared as before (**Section 3.2.1.1**). The solution was irradiated, while stirring, until no further reaction of the alkyne was occurring (GC, 11 h, 92% conversion). GC analysis indicated two products, **(5)** and **(6)**, had been formed in a 30:70 ratio. The supported photomediator was filtered off and the solution was evaporated under reduced pressure affording a mixture of **(5)** and **(6)** as a yellow oil (0.40 g). The spectroscopic data obtained for **(5)** and **(6)** from the mixture were identical to those obtained previously (**Section 3.2.1.4**).

3.4.1.5 Photochemical reaction of methyl propiolate with THF

A solution of methyl propiolate (0.25 g, 3.00 mmol) in THF (20 mL, 24.7 mmol) containing **SP3** (1.20 g, 0.41 mmol of photomediator) was prepared as before (**Section 3.2.1.1**). The solution was irradiated, while stirring, until complete reaction of the alkyne occurred (GC, 1.50 h). GC analysis indicated the presence of two products, **(62)** and **(63)**, (43:57). The supported photomediator was filtered off and the solution was concentrated affording a mixture of **(62)** and **(63)** as a yellow oil (0.45 g). The spectroscopic data of the crude product confirmed the formation of **(62)** and **(63)** (**Section 3.2.1.5**).

3.4.2 Reactions carried out using larger quantities of SP3

3.4.2.1 Photochemical reaction of methyl propiolate with 2-propanol

A solution of methyl propiolate (0.25 g, 3.00 mmol) and 2-propanol (3.60 g, 60.0 mmol) in acetonitrile (60 mL) containing SP3 (2.00 g, 0.68 mmol of photomediator) was prepared as before (Section 3.2.1.1). The solution was irradiated, while stirring, for 2.5 h at which time complete reaction of the alkyne had occurred (GC). GC analysis indicated the presence of three products, (3), (75) and (4), in a 14:21:65 ratio. The supported photomediator was filtered off and the solution was concentrated under reduced pressure giving a mixture of (3), (75) and (4) as a yellow oil (0.36 g). The spectroscopic data for the crude mixture confirmed the formation of (3), (75) and (4) (Sections 3.2.1.1 and 3.4.1.1).

3.4.2.2 Photochemical reaction of methyl propiolate with 1,3-dioxolane

A solution of methyl propiolate (0.25 g, 3.00 mmol) and 1,3-dioxolane (4.44 g, 60.0 mmol) in acetonitrile (60 mL) containing SP3 (2.00 g, 0.68 mmol of photomediator) was prepared as before (Section 3.2.1.1). The solution was irradiated, while stirring, for 4.3 h at which time complete reaction of the alkyne had occurred (GC). GC analysis indicated the presence of (58), (59) and (60) and (61), in a 16:26:9:49 ratio. The supported photomediator was filtered off and the solution was concentrated under reduced pressure giving a mixture of (58), (59), (60) and (61) as a light orange oil (0.52 g). The spectroscopic data obtained for (58), (59), (60) and (61) from the mixture were identical to those obtained previously (Section 3.2.1.3).

3.4.2.3 Photochemical reaction of methyl propiolate with THF

A solution of methyl propiolate (0.25 g, 3.00 mmol) in THF (20 mL, 24.7 mmol) containing SP3 (2.00 g, 0.68 mmol of photomediator) was prepared as before (Section 3.2.1.1). The solution was irradiated, while stirring, until complete reaction of the alkyne occurred (GC, 1 h). GC analysis indicated the presence of two products, (62) and (63), in a 43:57 ratio. The supported photomediator was filtered off and the solution was concentrated using rotary evaporation affording a mixture of (62) and (63) as a yellow oil (0.45 g). The spectroscopic data for the crude mixture confirmed the formation of (62) and (63) (Section 3.2.1.5).

3.4.3 Reaction carried out using a smaller quantity of SP3

3.4.3.1 Photochemical reaction of methyl propiolate with 2-propanol

A solution of methyl propiolate (0.25 g, 3.00 mmol) and 2-propanol (3.60 g, 60.0 mmol) in acetonitrile (60 mL) containing **SP3** (0.155 g, 0.05 mmol of photomediator) was prepared as before (**Section 3.2.1.1**). The solution was irradiated, while stirring, until no further reaction of the alkyne was occurring (GC, 5 h, 80% conversion). GC analysis indicated the presence of three products, **(3)**, **(75)** and **(4)**, in a 23:25:52 ratio. The supported photomediator was filtered off and the solution was concentrated under reduced pressure giving a mixture of **(3)** and **(4)** as a yellow oil (0.28 g). The spectroscopic data obtained for **(3)** and **(4)** from the mixture were identical to those obtained previously (**Section 3.2.1.1**).

3.4.4 Reactions with the disubstituted alkyne DMAD using SP3

3.4.4.1 Photochemical reaction of DMAD with 2-propanol

A solution of DMAD (0.43 g, 3.00 mmol) and 2-propanol (3.60 g, 60.0 mmol) in acetonitrile (60 mL) containing SP3 (1.20 g, 0.41 mmol of photomediator) was prepared as before (Section 3.2.1.1). The solution was then irradiated, while stirring, for 3.75 h at which time complete reaction of the alkyne had occurred (GC). GC analysis indicated the formation of a mixture of products, corresponding to that obtained previously (Section 3.2.3.1), containing one major product, methyl 2,2-dimethyl-5-oxo-2,5-dihydrofuran-3-carboxylate (**64**). The supported photomediator was filtered off and the solution was concentrated under reduced pressure giving a yellow oil (0.49 g). The spectroscopic data of the crude product confirmed the formation of (**64**) (Section 3.2.3.1).

3.4.4.2 Photochemical reaction of DMAD with cyclopentanol

A solution of DMAD (0.43 g, 3.00 mmol) and cyclopentanol (5.16 g, 60.0 mmol) in acetonitrile (60 mL) containing SP3 (1.20 g, 0.41 mmol of photomediator) was prepared as before (Section 3.2.1.1). The solution was irradiated, while stirring, until complete reaction of the alkyne had occurred (GC, 5 h). GC analysis indicated the presence of one product, the unsaturated ester (**70**). The supported photomediator was filtered off and the solvent was concentrated under reduced pressure. The excess cyclopentanol was removed using kugelrohr distillation, leaving (**70**) as a yellow oil (0.53 g). The spectroscopic data of the crude product confirmed the formation of (**70**) (Section 3.2.3.2).

3.4.4.3 Photochemical reaction of DMAD with 1,3-dioxolane

A solution of DMAD (0.43 g, 3.00 mmol) and 1,3-dioxolane (4.44 g, 60.0 mmol) containing SP3 (1.20 g, 0.41 mmol of photomediator) in acetonitrile (60 mL) was prepared as before (Section 3.2.1.1). The solution was irradiated, while stirring, until complete reaction of the alkyne had occurred (GC, 10 h). GC analysis indicated the formation of (**71**), and (**72**) as a mixture of diastereomers, in a 27:39:34 ratio. The supported photomediator was filtered off and the solution was concentrated *in vacuo* affording a mixture of (**71**) and (**72**), as a mixture of diastereomers, as a yellow oil

(0.74 g). The spectroscopic data of the crude product confirmed the formation of **(71)** and **(72)**, as a mixture of diastereomers (**Section 3.2.3.3**).

3.4.4.4 Photochemical reaction of DMAD with cyclopentane

A solution of DMAD (0.43 g, 3.00 mmol) and cyclopentane (4.20 g, 60.0 mmol) in acetonitrile (60 mL) containing **SP3** (1.20 g, 0.41 mmol of photomediator) was prepared as before (**Section 3.2.1.1**). The solution was irradiated, while stirring, for 26 h at which point only 28% conversion of the alkyne to a single product, **(73)**, had occurred. The reaction was stopped. The NMR data for the crude product confirmed that only **(73)** had been formed (**Section 3.2.3.4**).

3.4.4.5 Photochemical reaction of DMAD with THF

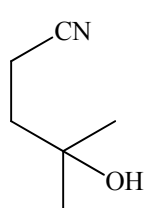
A solution of DMAD (0.43 g, 3.00 mmol) in THF (20 mL, 24.7 mmol) containing **SP3** (1.20 g, 0.41 mmol of photomediator) was prepared as before (**Section 3.2.1.1**). The solution was irradiated, while stirring, until complete reaction of the alkyne had occurred (GC, 2.5 h). GC analysis indicated the presence of two products, **(20)** and **(21)**, in a 40:60 ratio. The supported photomediator was filtered off and the solution was concentrated under reduced pressure affording a mixture of **(20)** and **(21)** as a yellow oil (0.63 g). The spectroscopic data of the crude product confirmed the formation of **(20)** and **(21)** (**Section 3.2.3.5**).

3.4.5 Reactions with monosubstituted alkenes using SP3

3.4.5.1 Photochemical reaction of acrylonitrile with 2-propanol

A solution of acrylonitrile (0.16 g, 3.00 mmol) and 2-propanol (3.60 g, 60.0 mmol) in acetonitrile (60 mL) containing **SP3** (2.00 g, 0.68 mmol of photomediator) was prepared as before (**Section 3.2.1.1**). The solution was irradiated, while stirring, for 14 h at which time complete reaction of the alkene had occurred (GC). GC analysis indicated the formation of a mixture of products. The supported photomediator was filtered off and the solution concentrated on a rotary evaporator leaving a light orange oil (0.45 g). The spectroscopic data of the crude product confirmed the formation of 4-hydroxy-4-methylpentanenitrile (**41**)¹¹⁶. The crude product was adsorbed onto silica (15 g) and eluted with ethyl acetate (2-40%)/petroleum ether. No identifiable product was isolated.

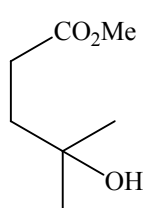
4-Hydroxy-4-methylpentanenitrile (**41**)¹¹⁶



IR (cm⁻¹): 3379 (O-H), 2252 (C≡N). **¹H-NMR (δ):** 1.25 (s, 6H, 2xCH₃), 1.83 (t, 2H, CH₂COH, *J*_{vic} = 7.6 Hz), 2.46 (t, 2H, CH₂CN, *J*_{vic} = 7.6 Hz). **¹³C-NMR (ppm):** 120.6 (CN), 69.8 (COH), 38.7 (CH₂COH), 29.2 (CH₃), 12.2 (CH₂CN).

3.4.5.2 Photochemical reaction of methyl acrylate with 2-propanol

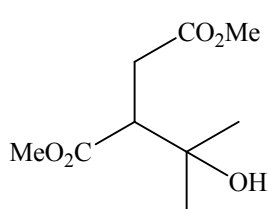
A solution of methyl acrylate (0.26 g, 3.00 mmol) and 2-propanol (3.60 g, 60.0 mmol) in acetonitrile (60 mL) containing **SP3** (2.00 g, 0.68 mmol of photomediator) was prepared as before (**Section 3.2.1.1**). The solution was irradiated, while stirring, for 4 h at which time complete reaction of the alkene had occurred (GC). GC analysis indicated the presence of two products in a 69:31 ratio. The supported photomediator was filtered off and the solution concentrated leaving a light orange oil (0.45 g). The sample degraded during column chromatography. The crude mixture did not contain any lactone (IR, NMR); on the basis of the spectroscopic data obtained, the major product formed was methyl 4-hydroxy-4-methylpentanoate (**76**):

Methyl 4-hydroxy-4-methylpentanoate (76)¹¹⁷

IR (cm^{-1}): 1730 (C=O), 1264, 1162 (C-O). **¹H-NMR** (δ): 1.22 (s, 6H, 2xCH₃), 1.81 (t, 2H, CH₂C(CH₃)₂), $J_{vic} = 7.4$ Hz), 2.44 (t, 2H, CH₂C(O), $J_{vic} = 7.4$ Hz).

3.4.6 Reactions with disubstituted alkenes using SP3**3.4.6.1 Reaction of dimethyl maleate with 2-propanol (alkene:SP3, 30:1)**

A solution of dimethyl maleate (0.43 g, 3.00 mmol) and 2-propanol (3.60 g, 60.0 mmol) in acetonitrile (60 mL) containing **SP3** (0.31 g, 0.10 mmol of photomediator) was prepared as before (**Section 3.2.1.1**). The solution was irradiated, while stirring, for 36 h at which time no further reaction of the alkene was occurring (GC, 90% conversion). Two products, methyl 2,2-dimethyl-5-oxo-tetrahydrofuran-3-carboxylate (**66**) and dimethyl 2(1-hydroxy-1-methylethyl)succinate (**77**) were present in a ratio of 17:83. The supported photomediator was filtered off and the solution was concentrated using rotary evaporation leaving a yellow oil (0.53 g). NMR data for the crude mixture confirmed the formation of (**77**) as the major product, and the formation of (**66**) in only trace amounts (¹H-NMR, IR, **Section 3.2.3.1**).

Dimethyl 2(1-hydroxy-1-methylethyl)succinate (77)¹¹⁸

IR (cm^{-1}): 3463 (O-H), 1735 (C=O), 1254, 1172 (C-O). **¹H-NMR** (δ): 1.23 (s, 3H, CH₃), 1.24 (s, 3H, CH₃), 2.57 (s, 1H, OH), 2.64-2.91 (m, 3H, CHCH₂), 3.67 (s, 3H, OCH₃), 3.74 (s, 3H, OCH₃). **¹³C-NMR**: 174.8 (C=O), 172.9 (C=O), 70.9 (C(CH₃)), 52.1 (CH), 52.0 (OCH₃), 51.6 (OCH₃), 32.5 (CH₂), 28.2 (CH₃), 27.4 (CH₃).

3.4.6.2 Reaction of dimethyl maleate with 2-propanol (alkene:SP3, 14:1)

A solution of dimethyl maleate (0.43 g, 3.00 mmol) and 2-propanol (3.60 g, 60.0 mmol) in acetonitrile (60 mL) containing **SP3** (0.61 g, 0.21 mmol of photomediator) was prepared as before (**Section 3.2.1.1**). Upon irradiating and stirring for 28.5 h, 100% conversion of the alkene occurred (GC), giving (**66**) and (**77**) in a 15:85 ratio.

The supported photomediator was filtered off and the solution was concentrated using rotary evaporation leaving a yellow oil (0.59 g). The spectroscopic data obtained for (77) from the mixture were identical to those obtained previously (Section 3.4.6.1).

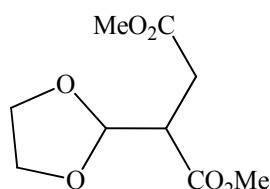
3.4.6.3 Reaction of dimethyl maleate with 2-propanol (alkene:SP3, 4:1)

A solution of dimethyl maleate (0.43 g, 3.00 mmol) and 2-propanol (3.60 g, 60.0 mmol) in acetonitrile (60 mL) containing SP3 (2.00 g, 0.68 mmol of photomediator) was prepared as before (Section 3.2.1.1). The solution was irradiated, while stirring, for 30 h, at which point 100% conversion of the alkene had occurred. The products, (66) and (77) were again present in a ratio of 15:85. The supported photomediator was filtered off and the solution was concentrated using rotary evaporation leaving a yellow oil (0.58 g). The spectroscopic data of the crude product confirmed the formation of (77) (Section 3.4.6.1).

3.4.6.4 Reaction of dimethyl maleate with 1,3-dioxolane

A solution of dimethyl maleate (0.43 g, 3.00 mmol) and 1,3-dioxolane (4.44 g, 60.0 mmol) in acetonitrile (60 mL) containing SP3 (2.00 g, 0.68 mmol of photomediator) was prepared as before (Section 3.2.1.1). The solution was irradiated, while stirring, for 7 h, at which point 100% conversion of the alkene had occurred. GC analysis indicated the formation of a single product, dimethyl 2-(1,3-dioxolan-2-yl)succinate (78). The supported photomediator was filtered off and the solution was concentrated *in vacuo* leaving (78) as a yellow oil (0.65 g).

Dimethyl 2-(1,3-dioxolan-2-yl)succinate (78)¹¹⁹

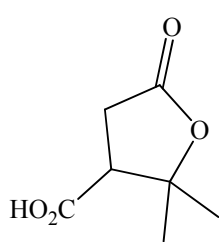


IR (cm^{-1}): 1733 (C=O), 1266, 1166 (C-O). **¹H-NMR** (δ): 2.62 (dd, 1H, CHCH(H), $J_{vic} = 4.8$ Hz, $J_{gem} = 16.9$ Hz), 2.79 (dd, 1H, CHCH(H), $J_{vic} = 9.3$ Hz, $J_{gem} = 16.9$ Hz), 3.24 (m, 1H, CHCH₂), 3.67 (s, 3H, OCH₃), 3.74 (s, 3H, OCH₃), 3.85-3.99 (ms, 4H, 2xCH₂ ring), 5.18 (d, 1H, CH ring, $J_{vic} = 4.2$ Hz). **¹³C-NMR**: 172.5 (C=O), 171.5 (C=O), 102.7 (CH), 65.4 (CH₂), 52.4 (OCH₃), 52.0 (OCH₃), 45.7 (CHCH₂), 30.1 (CHCH₂).

3.4.6.5 Synthesis of (±)-terebic acid

A solution of maleic acid (0.35 g, 3.00 mmol) in 2-propanol (11.79 g, 0.20 mol) containing **SP3** (0.09 g, 0.03 mmol of photomediator) was prepared as before (Section 3.2.1.1) and irradiated, while stirring, until complete conversion of the alkene, giving a single product, had occurred (GC, 6 h). The supported photomediator was filtered off and the solvent was concentrated giving (±)-terebic acid (2,2-dimethyl-5-oxotetrahydrofuran-3-carboxylic acid) (**37**) as an off-white solid (0.41 g, 88%). mp 170-171.5 °C, lit¹²³. 172-174 °C.

(±)-Terebic acid (2,2-Dimethyl-5-oxotetrahydrofuran-3-carboxylic acid) (**37**)¹²³



IR (cm^{-1}): 3118 (O-H), 1775 (C=O), 1728 (C=O). **¹H-NMR** (δ): 1.23 (s, 3H, CH₃), 1.43 (s, 3H, CH₃), 2.76 (dd, 1H, (CH(H)), $J_{vic} = 8.6$ Hz, $J_{gem} = 18.2$ Hz), 2.90 (dd, 1H, (CH(H)), $J_{vic} = 7.8$ Hz, $J_{gem} = 18.2$ Hz) 3.23 (dd, 1H, CH ring, $J_{vic} = 8.6$ Hz, $J_{vic} = 7.8$ Hz). **¹³C-NMR** (ppm): 178.8 (C=O), 174.4 (C=O), 87.1

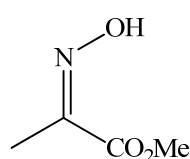
(C(CH₃)₂), 50.1 (CH), 32.2 (CH₂), 27.2 (CH₃), 22.5 (CH₃).

3.5 Synthesis of methyl (2*E*)-2-[(benzyloxy)imino]propanoate

3.5.1 Synthesis of methyl (2*Z*)-2-(hydroxyimino)propanoate

Hydroxylamine hydrochloride (0.91 g, 13.0 mmol) and pyridine (890 μ l, 11.0 mmol) were added to a solution of methyl pyruvate (1.03 g, 10.0 mmol) in methanol (18 mL). The reaction was stirred for 4 h at rt and the solvent removed under reduced pressure giving a light yellow oil which was dissolved in DCM (30 mL) and water (30 mL). The aqueous layer was separated and extracted twice more with DCM (30 mL). The combined organic layers were dried over sodium sulphate, filtered, then concentrated, and the crude product was purified by column chromatography (ethyl acetate (15%)/petroleum ether). Methyl (2*Z*)-2-(hydroxyimino)propanoate (**79**) was obtained as a colourless crystalline solid (1.00 g, 86%). mp 75.2-76.8 °C, lit¹²⁴. 74-75 °C.

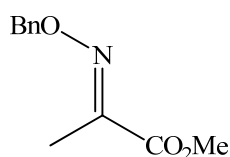
Methyl (2*Z*)-2-(hydroxyimino)propanoate¹²⁴ (**79**)



IR (cm^{-1}): 3235 (OH), 1721 (C=O). **¹H-NMR** (δ): 2.11 (s, 3H, CH₃C), 3.85 (s, 3H, OCH₃), 9.47 (s, OH). **¹³C-NMR** (ppm): 164.2 (C=O), 149.5 (C=N), 52.8 (OCH₃), 10.3 (CH₃).

3.5.2 Synthesis of methyl (2*E*)-2-[(benzyloxy)imino]propanoate

Benzyl bromide (0.86 g, 5.00 mmol) in DMF (4 mL) and methyl (2*Z*)-2-(hydroxyimino)propanoate (**79**) (0.59 g, 5.00 mmol) in DMF (6 mL) were added to a solution of sodium hydride (0.12 g, 5.00 mmol) in dry DMF (20 mL) at 0 °C, and the mixture was stirred at this temperature for 8 h. The solution was concentrated under reduced pressure, the product dissolved in DCM (15 mL) and water added (15 mL). The aqueous layer was extracted twice with DCM (2x20 mL) and the combined organic layers were dried over magnesium sulphate. The solution was filtered and the solvent removed *in vacuo* leaving a light yellow oil (1.77 g) which was adsorbed onto silica and eluted with diethyl ether (10 %)/petroleum ether. Methyl (2*E*)-2-[(benzyloxy)imino]propanoate (**80**) was obtained as a colourless oil (0.65 g, 63%).

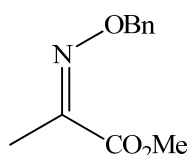
Methyl (2E)-2-[(benzyloxy)imino]propanoate¹²⁵ (80)

IR (cm⁻¹): 1725 (C=O), 1255, 1071 (C-O). **¹H-NMR (δ):** 2.09 (s, 3H, CH₃C), 3.85 (s, 3H, OCH₃), 5.30 (s, 2H, OCH₂), 7.27-7.33 (ms, 5H, 5xCH_{Ar}). **¹³C-NMR (ppm):** 164.2 (C=O), 149.5 (C=N), 136.5 (CH₂C), 128.4, 128.2 (C_{Ar}), 77.4 (OCH₂), 52.7 (OCH₃), 11.6 (CH₃).

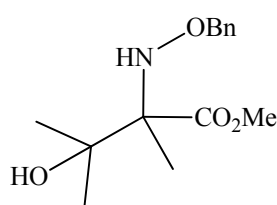
3.6 Photochemical reactions of methyl (2E)-2-[(benzyloxy)imino]propanoate using SP3

3.6.1 Photochemical reaction of benzylated oxime with 2-propanol

A solution of methyl (2E)-2-[(benzyloxy)imino]propanoate (**80**) (0.21 g, 1.00 mmol) in 2-propanol (19.7 g, 0.33 mol) containing **SP3** (2.90 g, 1.00 mmol of photomediator) was prepared as before (**Section 3.2.1.1**). The solution was irradiated, while stirring, until no further reaction of the benzyl oxime (**80**) was occurring (GC, 5.5 h, 70% conversion). GC analysis indicated the presence of one product, methyl *N*-(benzyloxy)-3-hydroxy-3-methylisovalinate (**81**). The supported photomediator was filtered off and the solution was concentrated under reduced pressure giving the crude product as a yellow oil (0.64 g). The spectroscopic data of the crude product confirmed the presence of (**81**) and both the (*E*)- and (*Z*)- isomer of methyl 2-[(benzyloxy)imino]propanoate (**80**) (1:1.5). The crude mixture was adsorbed onto silica (40 g) and eluted with ethyl acetate (2-40%)/petroleum ether. (**81**) was isolated as a yellow oil (0.06 g, 23%).

Methyl (2Z)-2-[(benzyloxy)imino]propanoate¹²⁵ (80)

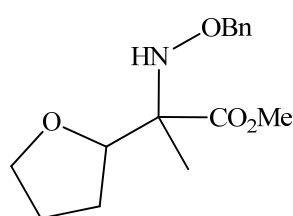
¹H-NMR (δ): 2.03 (s, 3H, CH₃C), 3.82 (s, 3H, OCH₃), 5.11 (s, 2H, OCH₂), 7.27-7.33 (ms, 5H, 5xCH_{Ar}). **¹³C-NMR (ppm):** 76.3 (OCH₂), 16.8 (CH₃).

Methyl *N*-(benzyloxy)-3-hydroxy-3-methylisovalinate¹²⁵ (81)

IR (cm^{-1}): 3442 (O-H, N-H), 1733 (C=O). **¹H-nmr** (δ): 1.15 (s, 3H, CH₃), 1.24 (s, 3H, CH₃), 1.38 (s, 3H, CH₃), 2.98 (s, 1H, OH), 3.76 (s, 3H, OCH₃), 4.68 (dd, 2H, OCH₂, $J_{gem} = 11.7$ Hz, $J_{gem} = 15.2$ Hz), 7.28-7.37 (ms, 5H, 5xCH_{Ar}). **¹³C-nmr** (ppm): 175.0 (C=O), 137.7 (OCH₂C_{Ar}), 128.7, 128.4, 127.9 (C_{Ar}), 77.3 (CH₂), 73.8 (C(CH₃)₂), 71.4 (C(CH₃)), 52.4 (OCH₃), 26.5 (CH₃), 24.3 (CH₃), 16.4 (CH₃).

3.6.2 Photochemical reaction of the benzylated oxime with THF

A solution of methyl (*2E*)-2-[(benzyloxy)imino]propanoate (**80**) (0.21 g, 1.00 mmol) in THF (27 mL, 0.33 mol) containing **SP3** (2.90 g, 1.00 mmol of photomediator) was prepared as before (**Section 3.2.1.1**). The solution was irradiated, while stirring, until no further reaction of the benzylated oxime (**80**) was occurring (GC, 22 h, 80% conversion). GC analysis indicated the presence of methyl 3,6-anhydro-2-[(benzyloxy)amino]-2,4,5-trideoxy-2-methylhexonate (**82**), as a mixture of diastereomers, in a 57:43 ratio. The supported photomediator was filtered off and the solution concentrated using rotary evaporation giving the crude product as a yellow oil (0.40 g) which was adsorbed onto silica (40 g) and eluted with ethyl acetate (2-40%)/petroleum ether. The starting material, (**80**), eluted first (0.03 g, 15%) and was followed by one diastereomer of methyl 3,6-anhydro-2-[(benzyloxy)amino]-2,4,5-trideoxy-2-methylhexonate (**82**) (0.05 g, 18%), and a mixture of diastereomers of the same material (0.13 g, 45%).

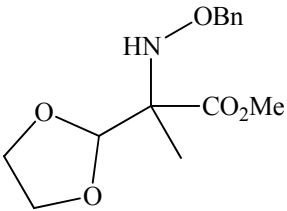
Methyl 3,6-anhydro-2-[(benzyloxy)amino]-2,4,5-trideoxy-2-methylhexonate (82)

IR (cm^{-1}): 1730 (C=O). **¹H-nmr** (δ): 1.33 (s, 3H, CH₃), 1.74-1.95 (m, 4H, CH₂CH₂), 3.72 (s, 3H, OCH₃), 3.76-3.80 (m, 2H, OCH), 3.93-3.98 (m, 2H, OCH₂CH₂), 4.60-4.69 (dd, 2H, OCH₂Ph, $J_{gem} = 11.8$ Hz, $J_{gem} = 10.0$ Hz), 7.25-7.35 (ms, 5H, 5xCH_{Ar}). **¹³C-nmr** (ppm): 173.9 (C=O), 137.9 (OCH₂C_{Ar}), 128.5, 128.4, 127.8 (C_{Ar}), 81.4 (OCH), 77.2 (OCH₂CH_{Ar}), 69.0 (OCH₂CH₂), 68.7 (CCH₃), 52.4 (OCH₃), 26.9 (CHCH₂CH₂), 25.8 (CCH₃), 16.9 (OCH₂CH₂). **HRMS** (CI): M+Na, C₁₅H₂₁NO₄; Calculated: 302.1368; Found: 302.1378.

3.6.3 Photochemical reaction of the benzylated oxime with 1,3-dioxolane

A solution of benzyl oxime (0.21 g, 1.00 mmol) in 1,3-dioxolane (24.4 g, 0.33 mol) containing **SP3** (2.90 g, 1.00 mmol of photomediator) was prepared as before (**Section 3.2.1.1**). The solution was irradiated, while stirring, until complete reaction of the benzyl oxime (**80**) had occurred (GC, 4 h). GC analysis indicated the presence of methyl 2-[(benzyloxy)amino]-2-(1,3-dioxolan-2-yl)propanoate (**83**). The supported photomediator was filtered off and the solution was concentrated leaving the crude product as a yellow oil (0.40 g) which was adsorbed onto silica (40 g) and eluted with ethyl acetate (2-40%)/petroleum ether. Methyl 2-[(benzyloxy)amino]-2-(1,3-dioxolan-2-yl)propanoate (**83**) was obtained as a yellow oil (0.12 g, 43%).

Methyl 2-[(benzyloxy)amino]-2-(1,3-dioxolan-2-yl)propanoate¹²⁵ (**83**)



IR (cm^{-1}): 3510 (N-H), 1724 (C=O), 1163, 1075 (C-O).
¹H-nmr (δ): 1.38 (s, 3H, CH₃), 3.75 (s, 3H, OCH₃), 3.83-3.93 (ms, 4H, CH₂CH₂), 4.60-4.73 (d, 2H, OCH₂Ph, $J_{gem} = 11.6$ Hz, $J_{gem} = 3.5$ Hz), 5.05 (s, 1H, OCH) 7.26-7.35 (ms, 5H, 5xCH_{Ar}). **¹³C-nmr** (ppm): 172.6 (C=O), 137.5 (OCH₂C_{Ar}), 128.5, 128.4, 127.9 (C_{Ar}), 104.1 (OCH), 68.6 (CCH₃), 65.8 (CH₂), 65.7 (CH₂), 52.7 (OCH₃), 15.3 (CH₃).

3.7 Photochemical reactions using silica supported C-8 quaternary ammonium salt SP4

3.7.1 Reactions with the monosubstituted alkyne methyl propiolate using SP4

3.7.1.1 Photochemical reaction of methyl propiolate with 2-propanol

A solution of methyl propiolate (0.25 g, 3.00 mmol) and 2-propanol (3.60 g, 60.0 mmol) in acetonitrile (60 mL) containing SP4 (1.20 g, 0.35 mmol of photomediator) was prepared as before (Section 3.2.1.1). The solution was irradiated, while stirring, for 2.5 h at which time complete reaction of the alkyne had occurred (GC). GC analysis indicated three products, (3), (75) and (4), in a 17:15:68 ratio. The supported photomediator was filtered off and the solution was concentrated under reduced pressure giving a mixture of (3), (75) and (4) as a yellow oil (0.36 g). The spectroscopic data of the crude product confirmed the formation of (3), (75) and (4) (Sections 3.2.1.1 and 3.4.1.1).

3.7.1.2 Photochemical reaction of methyl propiolate with cyclopentane

A solution of methyl propiolate (0.25 g, 3.00 mmol) and cyclopentane (4.20 g, 60.0 mmol) in acetonitrile (60 mL) containing SP4 (1.20 g, 0.35 mmol of photomediator) was prepared as before (Section 3.2.1.1). The solution was irradiated, while stirring, until complete reaction of the alkyne occurred (GC, 10.5 h). The products (5) and (6) were obtained in a 32:68 ratio. The supported photomediator was filtered off and the solution was concentrated under reduced pressure affording a mixture of (5) and (6) as a yellow oil (0.46 g). The spectroscopic data of the crude mixture confirmed the formation of (5) and (6) (Section 3.2.1.4).

3.7.1.3 Photochemical reaction of methyl propiolate with THF

A solution of methyl propiolate (0.25 g, 3.00 mmol) in THF (20 mL, 24.7 mmol) containing SP4 (1.20 g, 0.35 mmol of photomediator) was prepared as before (Section 3.2.1.1). The solution was irradiated, while stirring, until complete reaction of the alkyne occurred (GC, 1 h), giving (62) and (63) in a 43:57 ratio. The supported photomediator was filtered off and the solution was concentrated *in vacuo* affording a mixture of (62) and (63) as a yellow oil (0.46 g). The spectroscopic data

obtained for **(62)** and **(63)** from the mixture were identical to those obtained previously (**Section 3.2.1.5**).

3.7.2 Reaction with the disubstituted alkyne DMAD using SP4

3.7.2.1 Photochemical reaction of DMAD with 2-propanol

A solution of DMAD (0.43 g, 3.00 mmol) and 2-propanol (3.60 g, 60.0 mmol) in acetonitrile (60 mL) containing **SP4** (1.20 g, 0.35 mmol of photomediator) was prepared as before (**Section 3.2.1.1**). The solution was irradiated, while stirring, for 2 h at which time complete reaction of the alkyne had occurred (GC). GC analysis indicated the presence of two products, **(64)** and **(67)**, in a 28:72 ratio. The supported photomediator was filtered off and the solution was concentrated using rotary evaporation giving a mixture of **(64)** and **(67)** as a yellow oil (0.49 g). The spectroscopic data of the crude product confirmed the formation of **(64)** and **(67)** (**Section 3.2.3.1**).

3.8 Photochemical reactions using silica supported C-12 quaternary ammonium salt SP5

3.8.1 Reactions with monosubstituted alkyne methyl propiolate using SP5

3.8.1.1 Photochemical reaction of methyl propiolate with 2-propanol

A solution of methyl propiolate (0.25 g, 3.00 mmol), 2-propanol (3.60 g, 60.0 mmol) and dodecane as IS (0.0453 g, 0.267 mmol) in acetonitrile (60 mL), containing **SP5** (1.20 g, 0.39 mmol of photomediator), was prepared as before (**Section 3.2.1.1**). The solution was irradiated, while stirring, for 2.25 h at which time complete reaction of the alkyne had occurred (GC), giving **(3)** and **(4)** in a 32:68 ratio and a combined yield (GC) of 79%. The spectroscopic data obtained for **(3)** and **(4)** from the crude mixture were identical to those obtained previously (**Section 3.2.1.1**).

3.8.1.2 Photochemical reaction of methyl propiolate with 1,3-dioxolane

A solution of methyl propiolate (0.25 g, 3.00 mmol) and 1,3-dioxolane (4.44 g, 60.0 mmol) in acetonitrile (60 mL), containing **SP5** (1.20 g, 0.39 mmol of photomediator), was prepared as before (**Section 3.2.1.1**). The solution was irradiated, while stirring, for 1 h at which time no further reaction of the alkyne was taking place (GC, 75% conversion). GC analysis indicated the presence of **(60)** and **(61)** in a 22:78 ratio. The supported photomediator was filtered off and the solution was concentrated *in vacuo* leaving a mixture of **(60)** and **(61)** as a yellow oil (0.38 g). The spectroscopic data obtained for **(60)** and **(61)** from the mixture were identical to those obtained previously (**Section 3.2.1.3**).

3.8.1.3 Photochemical reaction of methyl propiolate with THF

A solution of methyl propiolate (0.25 g, 3.00 mmol) in THF (20 mL, 24.7 mmol) with dodecane (IS) (0.0821 g, 0.48 mmol) containing **SP5** (1.20 g, 0.39 mmol of photomediator) was prepared as before (**Section 3.2.1.1**). The solution was irradiated, while stirring, until complete reaction of the alkyne occurred (GC, 1 h), giving **(62)** and **(63)** in a 42:58 ratio and a combined yield (GC) of 99%. The supported photomediator was filtered off and the solution was concentrated under reduced pressure affording a mixture of **(62)** and **(63)** as a yellow oil (0.46 g). The

spectroscopic data of the crude mixture confirmed the formation of **(62)** and **(63)** (Section 3.2.1.5).

3.8.2 Reactions with the disubstituted alkene maleic acid using SP5

3.8.2.1 Synthesis of (\pm)-terebic acid

A solution of maleic acid (0.35 g, 3.00 mmol) in 2-propanol (11.79 g, 0.20 mol) containing **SP5** (0.08 g, 0.03 mmol of photomediator) was prepared as before (Section 3.2.1.1). The solution was irradiated, while stirring, for 6 h, at which point complete conversion of the alkene to a single product, **(37)**, had occurred (GC). The supported photomediator was filtered off and the solution was concentrated, giving **(37)** as an off-white solid (0.45 g, 96%). The spectroscopic data of the crude product confirmed the formation of **(37)** (Section 3.4.6.5).

3.8.3 Reaction with methyl (2*E*)-2-[(benzyloxy)imino]propanoate using SP5

3.8.3.1 Photochemical reaction of benzylated oxime with 2-propanol

A solution of methyl (2*E*)-2-[(benzyloxy)imino]propanoate **(80)** (0.21 g, 1.00 mmol) in 2-propanol (25 mL, 0.33 mol) containing **SP5** (2.90 g, 1.00 mmol of photomediator) was prepared as before (Section 3.2.1.1). The solution was irradiated, while stirring, until no further reaction of the benzylated oxime was occurring (GC, 22 h, 13% conversion). GC analysis indicated the presence of one product, methyl *N*-(benzyloxy)-3-hydroxy-3-methylisovalinate **(81)** and both the (*E*)- and (*Z*)- isomers of methyl 2-[(benzyloxy)imino]propanoate **(80)** (1:1.5). The supported photomediator was filtered off and the solution was concentrated under reduced pressure giving the crude product as a yellow oil (0.15 g). The spectroscopic data of the crude product confirmed the presence of **(81)** and both the (*E*)- and (*Z*)- isomers of methyl 2-[(benzyloxy)imino]propanoate **(80)**.

3.9 Recycling of supported photomediators

3.9.1 Photochemical reaction of methyl propiolate with 2-propanol using SP1

The reaction of methyl propiolate and 2-propanol was carried out as before (Section 3.2.1.1) using dodecane (IS). The solution was irradiated, while stirring, for 2.5 h at which point complete reaction of the alkyne had occurred (GC). The supported photomediator was filtered off and the solution was concentrated to give (3) and (4) in a 40:60 ratio (Table 32, Run 1). The spectroscopic data for the mixture were identical to those obtained previously (Section 3.2.1.1). The supported photomediator was washed with 20 mL acetonitrile and dried in a vacuum oven (70 °C, 12 h) prior to re-use. The reaction was then repeated a number of times using the recovered photomediator and the same mole ratio of reactants (Table 32), taking into account any mechanical loss of SP1.

Run	Time (h)	Conversion (GC, %)	(3):(4)	Yield (GC, %)
1	7	100	40:60	86
2	22	100	32:68	84
3	28	100	37:63	85
4	48	86	36:65	61

Table 32

3.9.2 Photochemical reaction of methyl propiolate with 2-propanol using SP3

The reaction of methyl propiolate and 2-propanol was carried out as before (Section 3.2.1.1). The solution was irradiated, while stirring, for 2.5 h at which point complete reaction of the alkyne had occurred (GC). The supported photomediator was filtered off and the solution concentrated to give (3), (75) and (4) in a 14:21:65 ratio (0.35 g) (Table 33, Run 1). The spectroscopic data for the mixture were identical to those obtained previously (Section 3.2.1.1). The supported photomediator was washed with 20 mL acetonitrile and dried in a vacuum oven (70 °C, 12 h) prior to re-use. The reaction was then repeated a number of times using the recovered photomediator, with the same mole ratio of reactants, adjusting the amounts for any mechanical loss of SP3 (Table 33).

Run	Time (h)	Conversion (GC, %)	(3):(75):(4)	Crude mass (g)
1	2.5	100	14:21:65	0.35
2	22	100	25:9:66	0.32
3	29	100	29:15:56	0.32
4	32	100	25:17:58	0.29
5	44	100	39:7:54	0.28
6	57	71	51:0:49	0.26

Table 33

3.9.3 Photochemical reaction of methyl propiolate with 2-propanol using SP5

The reaction of methyl propiolate and 2-propanol was carried out as before (**Section 3.2.1.1**) using dodecane (IS). The solution was irradiated, while stirring, for 2.5 h at which point complete reaction of the alkyne had occurred (GC). The supported photomediator was filtered off and the solution concentrated *in vacuo* to give **(3)** and **(4)** in a 40:60 ratio (**Table 34, Run 1**). The spectroscopic data for the mixture were identical to those obtained previously (**Section 3.2.1.1**). The supported photomediator was washed with 20 mL acetonitrile and dried in a vacuum oven (70 °C, 12 h) prior to use. The reaction was then repeated a number of times using the recovered photomediator, with the same mole ratio of reactants, adjusting the amounts for any mechanical loss of **SP5** (**Table 34**).

Run	Time (h)	Conversion (GC, %)	(3):(4)	Yield (GC, %)
1	2	100	34:66	84
2	2.25	100	41:59	85
3	3.25	100	40:60	84
4	4	100	38:62	76
5	8	40	37:63	24

Table 34

3.10 Optimisation of the methyl propiolate/2-propanol reaction using SP3

3.10.1 Effect of varying the quantity of photomediator

a A solution of methyl propiolate (0.25 g, 3.00 mmol), 2-propanol (3.60 g, 60.0 mmol) and dodecane (IS) (0.0518 g, 0.305 mmol) in acetonitrile (60 mL), containing **SP3** (2.00 g, 0.68 mmol of photomediator), was prepared as before (**Section 3.2.1.1**). The solution was then irradiated, while stirring, for 2.5 h at which time complete reaction of the alkyne had occurred (GC). GC analysis indicated the formation of **(3)** and **(4)** in a 36:64 ratio and a combined yield (GC) of 89%.

b The reaction was prepared as before (**Section 3.2.1.1**) using **SP3** (1.00 g, 0.34 mmol of photomediator) and dodecane (IS) (0.0475 g, 0.279 mmol). The solution was irradiated, while stirring, for 3 h at which time complete reaction of the alkyne had occurred (GC). GC analysis indicated the formation of **(3)** and **(4)** in a 37:63 ratio, and a combined yield (GC) of 91%.

c The reaction was prepared as before (**Section 3.2.1.1**) using **SP3** (0.50 g, 0.17 mmol of photomediator) and dodecane (IS) (0.0503 g, 0.294 mmol). The solution was irradiated, while stirring, for 9.5 h at which time complete reaction of the alkyne had occurred (GC). GC analysis indicated the presence of **(3)** and **(4)** in a 28:72 ratio and a combined yield (GC) of 91%.

Rxn	MP^a	2-PrOH^a	SP3^b	CH₃CN^c	Time^d (h)	(3):(4)^e	Yield^f (%)
a	3	60	2.00/0.68	60	2.5	36:64	89
b*	3	60	1.00/0.34	60	3	37:63	91
c	3	60	0.50/0.17	60	9.5	28:72	91

^a mmol, ^b mass (g) and mmol of photomediator, ^c mL of solvent, ^d reaction went to completion (GC) unless otherwise stated, ^e GC ratio, ^f combined yield of (3) and (4) (GC), * reaction involving the optimum quantity of photomediator

Table 13: Effect of varying the quantity of photomediator

3.10.2 Effect of varying the quantity of solvent

Rxn b, Table 13 (Section 3.10.1) represented the optimum conditions for the methyl propiolate/2-propanol reactions in terms of the amount of photomediator. The conditions used in this experiment were taken as a starting point for the investigation of the effect of changing the volume of the solvent, acetonitrile.

d The reaction of methyl propiolate and 2-propanol was prepared as before (**Section 3.2.1.1**) using dodecane (IS) (0.0479 g, 0.282 mmol) in acetonitrile (30 mL). The solution was irradiated, while stirring, for 3.5 h at which time complete reaction of the alkyne had occurred (GC). GC analysis indicated the presence of **(3)** and **(4)** in a 36:64 ratio and a combined yield (GC) of 75%.

e The reaction of methyl propiolate and 2-propanol was prepared as before (**Section 3.2.1.1**) using dodecane (IS) (0.0460 g, 0.271 mmol) in acetonitrile (30 mL). The solution was irradiated, while stirring, for 4.5 h at which time complete reaction of the alkyne had occurred (GC). GC analysis indicated the presence of **(3)** and **(4)** in a 36:64 ratio and a combined yield (GC) of 71%.

f The reaction was prepared as before (**Section 3.2.1.1**) using dodecane (IS) (0.0453 g, 0.266 mmol) in acetonitrile (15 mL). The solution was irradiated, while stirring, for 4.5 h at which time complete reaction of the alkyne had occurred (GC). GC analysis indicated the presence of **(3)** and **(4)** in a 36:64 ratio and a combined yield (GC) of 90%.

Rxn	MP ^a	2-PrOH ^a	SP3 ^b	CH ₃ CN ^c	Time ^d (h)	(3):(4) ^e	Yield ^f (%)
b	3	60	1.00/0.34	60	3	37:63	91
d	3	60	1.00/0.34	30	3.5	36:64	75
e	3	60	1.00/0.34	30	4.5	36:64	71
f*	3	60	1.00/0.34	15	4.5	36:64	90

^a mmol, ^b mass (g) and mmol of photomediator, ^c mL of solvent, ^d reaction went to completion (GC) unless otherwise stated, ^e GC ratio, ^f combined yield of (3) and (4) (GC), * reaction involving the optimum volume of solvent

Table 14: Effect of varying the quantity of solvent

3.10.3 Effect of varying the amount of alkyne

Rxn f, Table 14 (Section 3.10.2) represented the optimum conditions in terms of the quantity of photomediator and the amount of solvent for the methyl propiolate/2-propanol reaction. It was used as a baseline for any consideration of the effect of varying the amount of the alkyne.

g The reaction was prepared as before (Section 3.2.1.1) using methyl propiolate (0.50 g, 6.00 mmol) and dodecane (IS) (0.0871 g, 0.512 mmol) in acetonitrile (15 mL). The solution was irradiated, while stirring, for 25 h at which time complete reaction of the alkyne had occurred (GC). GC analysis indicated the presence of **(3)** and **(4)** in a 37:63 ratio and a combined yield (GC) of 80%.

h The reaction was prepared as before (Section 3.2.1.1) using dodecane (IS) (0.0703 g, 0.414 mmol) in acetonitrile (30 mL). The solution was irradiated, while stirring, for 11 h at which time complete reaction of the alkyne had occurred (GC). GC analysis indicated the presence of **(3)** and **(4)** in a 38:62 ratio and a combined yield (GC) of 95%.

Rxn	MP ^a	2-PrOH ^a	SP3 ^b	CH ₃ CN ^c	Time ^d (h)	(3):(4) ^e	Yield ^f (%)
f*	3	60	1.00/0.34	15	4.5	36:64	90
g	6	60	1.00/0.34	15	25	37:63	80
h	6	60	1.00/0.34	30	11	38:62	95

^a mmol, ^b mass (g) and mmol of photomediator, ^c mL of solvent, ^d reaction went to completion (GC) unless otherwise stated, ^e GC ratio, ^f combined yield of **(3)** and **(4)** (GC), * reaction involving the optimum quantity of alkyne

Table 15: Effect of varying the quantity of alkyne

3.10.4 Effect of varying the amount of H-donor

Rxn f, **Table 14 (Section 3.10.2)** represented the optimum conditions for the methyl propiolate/2-propanol reaction in terms of the quantity of photomediator, the amount of solvent and the quantity of alkyne. It was used as a standard for the investigation of the effect of varying the amount of the H-donor.

i A solution of methyl propiolate and 2-propanol (1.80 g, 30 mmol) was prepared as before (**Section 3.2.1.1**) using dodecane (IS) (0.0501 g, 0.29 mmol). The solution was irradiated, while stirring, for 30 h at which time complete reaction of the alkyne had occurred (GC). GC analysis indicated the presence of **(3)** and **(4)** in a 38:62 ratio and a combined yield (GC) of 80%.

Rxn	MP^a	2-PrOH^a	SP3^b	CH₃CN^c	Time^d (h)	(3):(4)^e	Yield^f (%)
f*	3	60	1.00/0.34	15	4.5	36:64	90
i	3	30	1.00/0.34	15	30	38:62	80

^a mmol, ^b mass (g) and mmol of photomediator, ^c mL of solvent, ^d reaction went to completion (GC) unless otherwise stated, ^e GC ratio, ^f combined yield of **(3)** and **(4)** (GC), * reaction involving the optimum quantity of hydrogen donor

Table 16: Effect of varying the quantity of H-donor

3.11 Optimisation of the methyl propiolate/THF reaction using SP3

3.11.1 Effect of varying the quantity of photomediator

a A solution of methyl propiolate (0.25 g, 3.00 mmol), THF (4.85 mL, 60.0 mmol) and dodecane (IS) (0.0758 g, 0.446 mmol) in acetonitrile (60 mL) containing SP3 (2.00 g, 0.68 mmol of photomediator) was prepared as before (Section 3.2.1.1). The solution was irradiated, while stirring, for 1.5 h at which time complete reaction of the alkyne had occurred (GC). GC analysis indicated the presence of (62) and (63) in a 44:56 ratio and a combined yield (GC) of 81%.

b The reaction was prepared as before (Section 3.2.1.1) using SP3 (1.00 g, 0.34 mmol of photomediator) and dodecane (IS) (0.0715 g, 0.421 mmol). The solution was irradiated as before for 1.5 h at which time complete reaction of the alkyne had occurred (GC). GC analysis indicated the presence of (62) and (63) in a 44:56 ratio and a combined yield (GC) of 77%.

c The reaction was prepared as before (Section 3.2.1.1) using SP3 (0.50 g, 0.17 mmol of photomediator) and dodecane (IS) (0.0746 g, 0.0439 mmol). The solution was irradiated, while stirring, for 7 h at which time complete reaction of the alkyne had occurred (GC). GC analysis indicated the presence of (62) and (63) in a 46:54 ratio and a combined yield (GC) of 58%.

Rxn	MP ^a	THF ^a	SP3 ^b	CH ₃ CN ^c	Time ^d (h)	(62):(63) ^e	Yield ^f (%)
a	3	60	2.00/0.68	60	1.5	44:56	81
b*	3	60	1.00/0.34	60	1.5	44:56	77
c	3	60	0.50/0.17	60	7	46:54	58

^a mmol, ^b mass (g) and mmol of photomediator, ^c mL of solvent, ^d reaction went to completion (GC) unless otherwise stated, ^e GC ratio, ^f combined yield of (62) and (63) (GC), * reaction involving the optimum quantity of photomediator

Table 17: Effect of varying the quantity of photomediator

3.11.2 Effect of varying the quantity of solvent

Rxn b, Table 17 (Section 3.11.1) represented the optimum conditions for the methyl propiolate/THF reaction in terms of the quantity of photomediator. It was used as a standard for the investigation of the effect of varying the quantity of solvent.

d The reaction was prepared as before (Section 3.2.1.1) using dodecane (IS) (0.0807 g, 0.475 mmol) in acetonitrile (30 mL). The solution was irradiated, while stirring, for 3.75 h at which time complete reaction of the alkyne had occurred (GC). GC analysis indicated the presence of **(62)** and **(63)** in a 47:53 ratio and a combined yield (GC) of 45%.

e The reaction was prepared as before (Section 3.2.1.1) using dodecane (IS) (0.0762 g, 0.448 mmol) and acetonitrile (15 mL). The solution was irradiated, while stirring, for 4.25 h at which time complete reaction of the alkyne had occurred (GC). GC analysis indicated the presence of **(62)** and **(63)** in a 47:53 ratio and a combined yield (GC) of 44%.

Rxn	MP ^a	THF ^a	SP3 ^b	CH ₃ CN ^c	Time ^d (h)	(62):(63) ^e	Yield ^f (%)
b*	3	60	1.00/0.34	60	1.5	44:56	77
d	3	60	1.00/0.34	30	3.8	47:53	45
e	3	60	1.00/0.34	15	4.25	47:53	44

^a mmol, ^b mass (g) and mmol of photomediator, ^c mL of solvent, ^d reaction went to completion (GC) unless otherwise stated, ^e GC ratio, ^f combined yield of **(62)** and **(63)** (GC), * reaction involving the optimum volume of solvent

Table 18: Effect of varying the quantity of solvent

3.11.3 Effect of varying the quantity of photomediator using a very large excess of THF

f A solution of methyl propiolate (0.25 g, 3.00 mmol), THF (20 mL, 247 mmol) and dodecane (IS) (0.076 g, 0.447 mmol) in acetonitrile (60 mL) containing **SP3** (2.00 g, 0.68 mmol of photomediator) was prepared as before (**Section 3.2.1.1**). The solution was irradiated, while stirring, for 1.66 h at which time complete reaction of the alkyne had occurred (GC). GC analysis indicated the formation of **(62)** and **(63)** in a 44:56 ratio and a combined yield (GC) of 60%.

g The reaction was prepared as before (**Section 3.2.1.1**) using **SP3** (1.00 g, 0.34 mmol of photomediator) and dodecane (IS) (0.081 g, 0.476 mmol). The solution was then irradiated, while stirring, for 1.83 h at which time complete reaction of the alkyne had occurred (GC). GC analysis indicated the formation of **(62)** and **(63)** in a 45:55 ratio and a combined yield (GC) of 70%.

h The reaction was prepared as before (**Section 3.2.1.1**) using **SP3** (0.50 g, 0.17 mmol of photomediator) and dodecane (IS) (0.0891 g, 0.524 mmol). The solution was irradiated, while stirring, for 1.66 h at which time complete reaction of the alkyne had occurred (GC). GC analysis indicated the formation of **(62)** and **(63)** in a 46:54 ratio and a combined yield (GC) of 81%.

i The reaction was prepared as before (**Section 3.2.1.1**) using **SP3** (0.25 g, 0.09 mmol of photomediator) and dodecane (IS) (0.0766 g, 0.451 mmol). The solution was irradiated, while stirring, for 2.5 h at which time complete reaction of the alkyne had occurred (GC). GC analysis indicated the formation of **(62)** and **(63)** in a 47:53 ratio and a combined yield (GC) of 71%.

Rxn	MP ^a	THF ^a	SP3 ^b	CH ₃ CN ^c	Time ^d (h)	(62):(63) ^e	Yield ^f (%)
f	3	247	2.00/0.68	60	1.66	44:56	60
g	3	247	1.00/0.34	60	1.83	45:55	70
h*	3	247	0.50/0.17	60	1.66	46:54	81
i	3	247	0.25/0.09	60	2.5	47:53	71

^a mmol, ^b mass (g) and mmol of photomediator, ^c mL of solvent, ^d reaction went to completion (GC) unless otherwise stated, ^e GC ratio, ^f combined yield of **(62)** and **(63)** (GC), * reaction involving the optimum quantity of photomediator

Table 19: Effect of varying the quantity of photomediator using a very large excess of THF

3.12 Photochemical reactions using benzophenone

3.12.1 Photochemical reaction of methyl propiolate with 2-propanol

A solution of methyl propiolate (0.25 g, 3.00 mmol) and 2-propanol (3.60 g, 60.0 mmol) in acetonitrile (60 mL) containing benzophenone (0.12 g, 0.68 mmol) was prepared as before (**Section 3.2.1.1**). The solution was irradiated until complete reaction of the alkyne occurred (GC, 1.25 h). GC analysis indicated the presence of two products, **(3)** and **(4)**, in a 54:36 ratio. The solvent was removed under reduced pressure affording the expected products **(3)** and **(4)** as a yellow oil (0.50 g). The spectroscopic data of the crude product confirmed the formation of **(3)** and **(4)** (**Section 3.2.1.1**).

3.12.2 Photochemical reaction of methyl propiolate with THF

A solution of methyl propiolate (0.25 g, 3.00 mmol) and THF (20 ml) containing benzophenone (0.12 g, 0.68 mmol) was prepared as before (**Section 3.2.1.1**). The solution was irradiated until complete reaction of the alkyne occurred (GC, 1 h). GC analysis indicated the presence of two products, **(62)** and **(63)**, in a 38:62 ratio. The solvent was concentrated under reduced pressure affording the expected products **(62)** and **(63)** as a yellow oil (0.55 g). The spectroscopic data of the crude product confirmed the formation of **(62)** and **(63)** (**Section 3.2.1.5**).

3.12.3 Photochemical reaction of DMAD with 2-propanol

A solution of DMAD (0.25 g, 3.00 mmol) and 2-propanol (3.60 g, 60.0 mmol) in acetonitrile (60 mL) containing benzophenone (0.12 g, 0.68 mmol) was prepared as before (**Section 3.2.1.1**). The solution was irradiated, while stirring, until complete reaction of the alkyne occurred (GC, 0.75 h). GC analysis indicated the presence of two products, **(64)** and **(67)**, in a 45:55 ratio. The supported photomediator was filtered off and the solution was concentrated under reduced pressure affording the expected products **(64)** and **(67)** as a yellow oil (0.52 g). The spectroscopic data of the crude product confirmed the formation of **(64)** and **(67)** (**Section 3.2.3.1**).

3.13 Conformational searching

A Monte Carlo based conformational search was carried out for each of the supported photomediators to determine the lowest energy conformations. The starting point for each search involved the photomediator and its linking chain approximately orthogonal to the silica surface. The results of the molecular modelling study (**Tables 34-38**) are discussed above (**Section 2.12**).

Conformer	Relative E (kJ mol ⁻¹)	Conformer	Relative E (kJ mol ⁻¹)
M0001	0.00	M0021	150.04
M0002	22.06	M0022	153.86
M0003	59.57	M0023	155.32
M0004	60.72	M0024	175.02
M0005	61.90	M0025	176.40
M0006	68.02	M0026	176.92
M0007	77.15	M0027	177.69
M0008	77.15	M0028	180.63
M0009	81.60	M0029	181.80
M0010	82.84	M0030	182.70
M0011	83.37	M0031	184.38
M0012	88.40	M0032	185.49
M0013	92.16	M0033	187.88
M0014	94.91	M0034	189.80
M0015	113.85	M0035	190.65
M0016	116.80	M0036	196.90
M0017	117.91	M0037	206.06
M0018	121.35	M0038	206.07
M0019	122.87	M0039	207.47
M0020	125.56	M0040	207.62

Conformer	Relative E (kJ mol ⁻¹)	Conformer	Relative E (kJ mol ⁻¹)
M0041	214.82	M0066	303.13
M0042	218.96	M0067	307.92
M0043	226.21	M0068	319.74
M0044	233.18	M0069	324.12
M0045	234.14	M0070	331.44
M0046	234.34	M0071	332.66
M0047	235.86	M0072	335.24
M0048	251.15	M0073	337.64
M0049	253.53	M0074	337.99
M0050	254.73	M0075	338.92
M0051	259.25	M0076	341.13
M0052	262.36	M0077	343.79
M0053	273.22	M0078	347.81
M0054	274.84	M0079	348.19
M0055	277.41	M0080	348.43
M0056	279.29	M0081	351.48
M0057	281.78	M0082	361.35
M0058	282.66	M0083	365.23
M0059	290.67	M0084	366.64
M0060	292.69	M0085	366.99
M0061	296.15	M0086	367.56
M0062	301.04	M0087	375.15
M0063	301.06	M0088	376.79
M0064	301.17	M0089	377.64
M0065	302.88	M0090	380.74

Conformer	Relative E (kJ mol ⁻¹)	Conformer	Relative E (kJ mol ⁻¹)
M0091	387.84	M0093	398.00
M0092	390.54	M0094	398.77

Table 35: Relative energies of SP1 conformations within 400 kJ mol⁻¹ of the lowest energy conformation

Conformer	Relative E (kJ mol ⁻¹)	Conformer	Relative E (kJ mol ⁻¹)
M0001	0.00	M0027	162.68
M0002	3.28	M0028	166.93
M0003	21.73	M0029	168.59
M0004	31.41	M0030	176.33
M0005	41.52	M0031	185.68
M0006	41.59	M0032	190.63
M0007	48.26	M0033	197.96
M0008	57.28	M0034	201.75
M0009	59.58	M0035	251.36
M0010	59.81	M0036	259.18
M0011	63.38	M0037	261.86
M0012	89.80	M0038	266.65
M0013	96.77	M0039	269.04
M0014	101.38	M0040	274.27
M0015	105.42	M0041	276.28
M0016	108.03	M0042	284.5
M0017	128.36	M0043	284.78
M0018	139.73	M0044	286.52
M0019	141.83	M0045	294.79
M0020	143.36	M0046	294.97
M0021	144.24	M0047	295.89
M0022	144.44	M0048	296.98
M0023	154.97	M0049	299.32
M0024	156.20	M0050	299.83
M0025	160.92	M0051	299.84
M0026	161.46	M0052	301.2

Conformer	Relative E (kJ mol ⁻¹)	Conformer	Relative E (kJ mol ⁻¹)
M0053	303.08	M0075	338.78
M0054	305.87	M0076	338.95
M0055	305.90	M0077	338.98
M0056	306.45	M0078	339.2
M0057	312.32	M0079	342.56
M0058	312.99	M0080	343.54
M0059	314.94	M0081	344.61
M0060	317.03	M0082	349.87
M0061	317.68	M0083	350.64
M0062	317.73	M0084	351.64
M0063	318.76	M0085	351.8
M0064	319.37	M0086	352.58
M0065	321.08	M0087	358.88
M0066	323.92	M0088	358.99
M0067	325.66	M0089	362.79
M0068	330.15	M0090	364.78
M0069	331.66	M0091	365.73
M0070	331.98	M0092	367.42
M0071	332.44	M0093	367.51
M0072	332.65	M0094	383.16
M0073	334.83	M0095	386.38
M0074	336.15	M0096	397.46

Table 36: Relative energies of SP2 conformations within 400 kJ mol⁻¹ of the lowest energy conformation

Conformer	Relative E (kJ mol ⁻¹)	Conformer	Relative E (kJ mol ⁻¹)
M0001	0.00	M0027	218.56
M0002	21.66	M0028	220.01
M0003	33.69	M0029	224.84
M0004	36.51	M0030	226.58
M0005	64.93	M0031	237.26
M0006	68.41	M0032	246.73
M0007	84.51	M0033	247.4
M0008	102.20	M0034	249.87
M0009	122.38	M0035	251.38
M0010	139.83	M0036	252.68
M0011	157.62	M0037	253.06
M0012	159.25	M0038	253.8
M0013	159.61	M0039	256.94
M0014	160.91	M0040	257.7
M0015	172.12	M0041	263.8
M0016	174.96	M0042	279.66
M0017	185.04	M0043	281.38
M0018	192.68	M0044	281.85
M0019	194.96	M0045	286.7
M0020	195.63	M0046	290.45
M0021	195.83	M0047	291.3
M0022	197.32	M0048	291.56
M0023	200.90	M0049	296.17
M0024	205.16	M0050	296.2
M0025	208.58	M0051	297.16
M0026	214.31	M0052	298.9

Conformer	Relative E (kJ mol ⁻¹)	Conformer	Relative E (kJ mol ⁻¹)
M0053	301.14	M0074	345.00
M0054	302.67	M0075	349.26
M0055	303.52	M0076	349.42
M0056	306.60	M0077	349.78
M0057	307.07	M0078	352.24
M0058	310.17	M0079	352.55
M0059	310.79	M0080	355.2
M0060	314.56	M0081	355.45
M0061	315.25	M0082	357.72
M0062	315.44	M0083	357.78
M0063	320.54	M0084	361.67
M0064	321.51	M0085	361.98
M0065	322.27	M0086	364.63
M0066	323.78	M0087	369.4
M0067	324.40	M0088	376.29
M0068	325.54	M0089	383.87
M0069	332.28	M0090	384.21
M0070	334.87	M0091	386.14
M0071	338.75	M0092	394.14
M0072	341.21	M0093	397.01
M0073	344.27		

Table 37: Relative energies of SP3 conformations within 400 kJ mol⁻¹ of the lowest energy conformation

Conformer	Relative E (kJ mol ⁻¹)	Conformer	Relative E (kJ mol ⁻¹)
M0001	0.00	M0028	201.70
M0002	2.89	M0029	203.40
M0003	10.92	M0030	205.05
M0004	48.84	M0031	207.68
M0005	50.85	M0032	211.43
M0006	71.63	M0033	215.43
M0007	73.02	M0034	218.21
M0008	94.39	M0035	227.01
M0009	98.27	M0036	227.59
M0010	99.43	M0037	230.01
M0011	107.37	M0038	237.35
M0012	110.23	M0039	243.15
M0013	116.50	M0040	250.25
M0014	122.86	M0041	161.41
M0015	129.05	M0042	169.16
M0016	130.02	M0043	178.57
M0017	132.47	M0044	255.27
M0018	133.50	M0045	258.18
M0019	148.45	M0046	260.84
M0020	158.28	M0047	263.05
M0021	161.41	M0048	266.65
M0022	169.16	M0049	268.82
M0023	178.57	M0050	269.94
M0024	181.82	M0051	270.03
M0025	183.30	M0052	275.40
M0026	189.76	M0053	288.24
M0027	192.55	M0054	290.56

Conformer	Relative E (kJ mol ⁻¹)	Conformer	Relative E (kJ mol ⁻¹)
M0055	293.59	M0075	338.35
M0056	295.63	M0076	341.31
M0057	296.10	M0077	352.54
M0058	302.54	M0078	356.44
M0059	303.27	M0079	361.54
M0060	303.74	M0080	362.26
M0061	303.90	M0081	362.58
M0062	304.80	M0082	369.63
M0063	310.89	M0083	370.40
M0064	312.65	M0084	374.51
M0065	314.90	M0085	380.79
M0066	322.95	M0086	381.58
M0067	323.21	M0087	381.70
M0068	325.11	M0088	391.49
M0069	326.88	M0089	392.67
M0070	327.81	M0090	392.85
M0072	336.48	M0091	392.92
M0073	336.54	M0092	393.04
M0074	338.17	M0093	395.12

Table 38: Relative energies of SP4 conformations within 400 kJ mol⁻¹ of the lowest energy conformation

Conformer	Relative E (kJ mol ⁻¹)	Conformer	Relative E (kJ mol ⁻¹)
M0001	0.00	M0027	246.78
M0002	32.18	M0028	247.08
M0003	87.00	M0029	249.43
M0004	118.16	M0030	258.85
M0005	139.26	M0031	259.66
M0006	174.54	M0032	262.65
M0007	196.14	M0033	265.08
M0008	200.62	M0034	265.70
M0009	208.64	M0035	267.53
M0010	213.41	M0036	270.44
M0011	215.95	M0037	270.84
M0012	222.78	M0038	276.17
M0013	223.62	M0039	277.35
M0014	229.06	M0040	277.81
M0015	229.90	M0041	278.58
M0016	231.85	M0042	287.39
M0017	231.93	M0043	291.05
M0018	232.04	M0044	296.33
M0019	234.58	M0045	297.66
M0020	235.47	M0046	299.33
M0021	236.62	M0047	301.27
M0022	237.23	M0048	302.48
M0023	239.52	M0050	310.02
M0024	243.29	M0051	311.68
M0025	243.87	M0052	314.31
M0026	244.79	M0053	318.88

Conformer	Relative E (kJ mol ⁻¹)	Conformer	Relative E (kJ mol ⁻¹)
M0054	322.10	M0074	363.95
M0055	322.70	M0075	372.04
M0056	323.30	M0076	372.10
M0057	328.16	M0077	372.11
M0058	330.32	M0078	372.40
M0059	331.37	M0079	375.81
M0060	333.44	M0080	376.81
M0061	338.77	M0081	378.01
M0062	341.12	M0082	380.21
M0063	343.72	M0083	380.67
M0064	346.01	M0084	380.73
M0065	346.41	M0085	381.14
M0066	347.20	M0086	383.49
M0067	350.10	M0087	383.70
M0068	351.43	M0088	384.10
M0069	352.31	M0089	384.55
M0070	352.81	M0090	385.92
M0071	355.28	M0091	387.46
M0072	355.32	M0092	388.38
M0073	357.93	M0093	400.05

Table 39: Relative energies of SP5 conformations within 400 kJ mol⁻¹ of the lowest energy conformation

Bibliography

- (1) Clayden, J.; Greeves, N.; Warren, S.; Wothers, P. *Organic Chemistry*; Oxford University Press, **2000**.
- (2) Rowlands, G. J. *Tetrahedron* **2009**, *65*, 8603.
- (3) Gansäuer, A. *Radicals in Synthesis I: Methods and Mechanisms*; Springer-Verlag: Berlin, **2006**; Vol. 263.
- (4) Reinhard Brückner, P. W. *Organic Mechanisms: Reactions, Stereochemistry and Synthesis*, **2010**, p1.
- (5) Nonhebel, D. C.; Walton, J. C. *Free-Radical Chemistry. Structure and Mechanism*; Cambridge Univ. Press, **1974**, p37.
- (6) Ashby, E. C. *Acc. Chem. Res.* **1988**, *21*, 414.
- (7) Blanksby, S. J.; Ellison, G. B. *Acc. Chem. Res.* **2003**, *36*, 255.
- (8) Fossey, J.; Lefort, D.; Sorba, J. *Free Radicals in Organic Chemistry*; Wiley: Chichester, **1995**, p50.
- (9) Parsons, A. F. *An Introduction to Free Radical Chemistry*; Blackwell Science, **2000**, p77.
- (10) Fox, M. A.; Whitesell, J. K. *Organic Chemistry*; Third ed.; Jones & Bartlett Publishers, **2004**, p117.
- (11) Johnson, A. W. *Invitation to Organic Chemistry*; Jones & Bartlett Learning, **1999**, p333.
- (12) Geraghty, N. W. A.; Hernon, E. M. *Tetrahedron Lett.* **2009**, *50*, 570.
- (13) Miller, A.; Solomon, P. H. *Writing Reaction Mechanisms in Organic Chemistry, 2nd Ed.*; Academic Press, **1999**, p285.

- (14) Denisov, E. T. *Handbook of Free Radical Initiators*; John Wiley & Sons, **2003**, p30.
- (15) Dobbs, A. *J. Org. Chem.* **2000**, *66*, 638.
- (16) Bryans, J. S.; Large, J. M.; Parsons, A. F. *J. Chem. Soc., Perkin Trans. 1* **1999**, 2897.
- (17) Fagnoni, M.; Dondi, D.; Ravelli, D.; Albini, A. *Chem. Rev.* **2007**, *107*, 2725.
- (18) Forkan, D. J. *Ph.D Thesis, National University of Ireland, Galway*, **2005**.
- (19) Geraghty, N. W. A.; Hannan, J. J. *Tetrahedron Lett.* **2001**, *42*, 3211.
- (20) Doohan, R. A.; Geraghty, N. W. A. *Green Chem.* **2005**, *7*, 91.
- (21) Doohan, R. A.; Hannan, J. J.; Geraghty, N. W. A. *Org. Biomol. Chem.* **2006**, *4*, 942.
- (22) Luo, Y.-R. *Handbook of Bond Dissociation Energies in Organic Compounds*; CRC Press, **2002**, p164.
- (23) Ciamician, G.; Silber, P. *Chem. Ber.* **1900**, 2911.
- (24) Wells, C. H. J. *Introduction to Molecular Photochemistry (Chapman and Hall Chemistry Textbook Series)*; Chapman and Hall, **1972**, p18.
- (25) Padwa, A. *Tetrahedron Lett.* **1964**, *5*, 3465.
- (26) Horspool, W. M.; Song, P. S. *Handbook of Organic Photochemistry and Photobiology*; CRC Press, **1995**, Volume 1, Chapter 58.
- (27) Evans, M. G.; Polanyi, M. *Trans. Faraday Soc.* **1938**, *34*, 11.
- (28) Ueda, M.; Kondoh, E.; Ito, Y.; Shono, H.; Kakiuchi, M.; Ichii, Y.; Kimura, T.; Miyoshi, T.; Naito, T.; Miyata, O. *Org. Biomol. Chem.* **2011**, *9*, 2062.
- (29) Montanaro, S.; Ravelli, D.; Merli, D.; Fagnoni, M.; Albini, A. *Org. Lett.* **2012**, *14*, 4218.

- (30) Yamada, K.; Nakano, M.; Maekawa, M.; Akindele, T.; Tomioka, K. *Org. Lett.* **2008**, *10*, 3805.
- (31) Griller, D.; Howard, J. A.; Marriott, P. R.; Scaiano, J. C. *J. Am. Chem. Soc.* **1981**, *103*, 619.
- (32) Malatesta, V.; Ingold, K. U. *J. Am. Chem. Soc.* **1981**, *103*, 609.
- (33) Coyle, J. D. *Introduction to Organic Photochemistry*; Wiley, **1986**, p117.
- (34) Ryu, I.; Tani, A.; Fukuyama, T.; Ravelli, D.; Fagnoni, M.; Albini, A. *Angew. Chem. Int. Ed.* **2011**, *50*, 1869.
- (35) Esposti, S.; Dondi, D.; Fagnoni, M.; Albini, A. *Angew. Chem. Int. Ed.* **2007**, *46*, 2531.
- (36) Geraghty, N. W. A.; Lally, A. J. *Chem. Commun.* **2006**, 4300.
- (37) Wedegaertner, D. K.; Kopchik, R. M.; Kampmeier, J. A. *J. Am. Chem. Soc.* **1971**, *93*, 6890.
- (38) Ravelli, D.; Albini, A.; Fagnoni, M. *Chem. Eur. J.* **2011**, *17*, 572.
- (39) Dondi, D.; Ravelli, D.; Fagnoni, M.; Mella, M.; Molinari, A.; Maldotti, A.; Albini, A. *Chem. Eur. J.* **2009**, *15*, 7949.
- (40) Grovenstein Jr., E.; Campbell, T. C.; Shibata, T. *J. Org. Chem.* **1969**, *34*, 2418.
- (41) Büchi, G.; Fearheller, S. H. *J. Org. Chem.* **1969**, *34*, 609.
- (42) Schwack, W.; Walker, F.; Bourgeois, B. *J. Agric. Food. Chem.* **1995**, *43*, 3088.
- (43) Cardarelli, A. M.; Fagnoni, M.; Mella, M.; Albini, A. *J. Org. Chem.* **2001**, *66*, 7320.
- (44) Dondi, D.; Cardarelli, A. M.; Fagnoni, M.; Albini, A. *Tetrahedron* **2006**, *62*, 5527.

- (45) Hill, C. L. *Synlett* **1995**, 127.
- (46) Dondi, D.; Fagnoni, M.; Molinari, A.; Maldotti, A.; Albini, A. *Chem. Eur. J.* **2004**, *10*, 142.
- (47) Dondi, D.; Fagnoni, M.; Albini, A. *Chem. Eur. J.* **2006**, *12*, 4153.
- (48) Zheng, Z.; Hill, C. L. *Chem. Commun.* **1998**, 2467.
- (49) Rosenthal, I.; Elad, D. *Tetrahedron* **1967**, *23*, 3193.
- (50) Kemmler, M.; Herdtweck, E.; Bach, T. *Eur. J. Org. Chem.* **2004**, 4582.
- (51) Singh, P. *J. Org. Chem.* **1972**, *37*, 836.
- (52) Shetlar, M. D. *J. Chem. Soc., Chem. Commun.* **1975**, 653.
- (53) Reineke, N.; Zaidi, N. A.; Mitra, M.; O'Hagan, D.; Batsanov, A. S.; Howard, J. A. K.; Naumov, D. Y. *J. Chem. Soc., Perkin Trans. 1* **1996**, 147.
- (54) Paleta, O.; Církva, V.; Kvicala, J. *J. Fluorine Chem.* **1996**, *80*, 125.
- (55) Chambers, R. D.; Grievson, B. *J. Chem. Soc., Perkin Trans. 1* **1985**, 2215.
- (56) Malatesta, V.; Scaiano, J. C. *J. Org. Chem.* **1982**, *42*, 1455.
- (57) Nishio, T.; Omote, Y. *J. Chem. Soc., Perkin Trans. 1* **1988**, 957.
- (58) Miyake, A.; Oka, Y.; Yurugi, S. *Chem. Pharm. Bull.* **1975**, *23*, 1500.
- (59) Rosenthal, I.; Elad, D. *J. Org. Chem.* **1968**, *33*, 805.
- (60) Mosca, R.; Fagnoni, M.; Mella, M.; Albini, A. *Tetrahedron* **2001**, *57*, 10319.
- (61) Dondi, D.; Caprioli, I.; Fagnoni, M.; Mella, M.; Albini, A. *Tetrahedron* **2003**, *59*, 947.
- (62) Manfrotto, C.; Mella, M.; Freccero, M.; Fagnoni, M.; Albini, A. *J. Org. Chem.* **1999**, *64*, 5024.
- (63) Yang, N. C.; Yang, D.-D. H. *J. Am. Chem. Soc.* **1958**, *80*, 2913.
- (64) Fernández, M.; Alonso, R. *Org. Lett.* **2003**, *5*, 2461.
- (65) Parsons, P. J.; Cowell, J. K. *Synlett* **2000**, 107.

- (66) Ghosh, A. K.; Leshchenko, S.; Noetzel, M. *J. Org. Chem.* **2004**, *69*, 7822.
- (67) Urry, W. H.; Stacey, F. W.; Huyser, E. S.; Juveland, O. O. *J. Am. Chem. Soc.* **1954**, *76*, 450.
- (68) Schenck, G. O.; Koltzenburg, G.; Grossmann, H. *Angew. Chem. Int. Ed.* **1957**, *69*, 177.
- (69) Kato, T.; Sato, M.; Kitagawa, Y.; Sato, R. *Chem. Pharm. Bull.* **1981**, *29*, 1624.
- (70) Benko, Z.; Fraser-Reid, B.; Mariano, P. S.; Beckwith, A. L. J. *J. Org. Chem.* **1988**, *53*, 2066.
- (71) Al-Amoudi, M. A. S.; Vernon, J. M. *J. Chem. Soc., Perkin Trans. 2* **1999**, 2667.
- (72) Bown, D. H.; Bradshaw, J. S. *J. Org. Chem.* **1980**, *45*, 2320.
- (73) Ma, S.; Shi, Z.; Yu, Z. *Tetrahedron Lett.* **1999**, *40*, 2393.
- (74) Taylor, E. C.; Maki, Y.; Evans, B. E. *J. Am. Chem. Soc.* **1969**, *91*, 5181.
- (75) Ono, I.; Hata, N. *Bull. Chem. Soc. Jpn.* **1987**, *60*, 2891.
- (76) Murgida, D. H.; Aramendía, P. F.; Erra-Balsells, R. *Photochem. Photobiol.* **1998**, *67*, 487.
- (77) Ley, S. V.; Baxendale, I. R.; Bream, R. N.; Jackson, P. S.; Leach, A. G.; Longbottom, D. A.; Nesi, M.; Scott, J. S.; Storer, R. I.; Taylor, S. J. *J. Chem. Soc., Perkin Trans. 1* **2000**, 3815.
- (78) Fenniri, H. *Combinatorial Chemistry: A Practical Approach*; Oxford University Press, **2000**.
- (79) Merrifield, R. B. *J. Am. Chem. Soc.* **1963**, *85*, 2149.
- (80) Blossey, E. C.; Neckers, D. C. *Tetrahedron Lett.* **1974**, *15*, 323.
- (81) Ayadim, M.; Soumillion, J. P. *Tetrahedron Lett.* **1995**, *36*, 4615.

- (82) Ayadim, M.; Soumillion, J. P. *Tetrahedron Lett.* **1996**, 37, 381.
- (83) De Chadarevian, S.; Hopwood, N. *Models: The Third Dimension of Science*; Writing Science, **2004**, p250.
- (84) Vlachakis, D. *An Introduction to Molecular Modelling, from Theory to Application*, **2007**.
- (85) Hehre, W. J. *A Guide to Molecular Mechanics and Quantum Chemical Calculations*; Wavefunction, **2003**, Chapter 4.
- (86) Jensen, J. H. *Molecular Modeling Basics*; CRC Press, **2010**.
- (87) Goodman, J. M. *Chemical Applications of Molecular Modelling*; Royal Society of Chemistry, **1998**, p23.
- (88) Hehre, W. J. *A Guide to Molecular Mechanics and Quantum Chemical Calculations*; Wavefunction, **2003**, Chapter 14.
- (89) Hehre, W. J. *A Guide to Molecular Mechanics and Quantum Chemical Calculations*; Wavefunction, **2003**, p19.
- (90) Hehre, W. J. *A Guide to Molecular Mechanics and Quantum Chemical Calculations*; Wavefunction, **2003**, Chapter 2.
- (91) Lewars, E. *Computational Chemistry: Introduction to the Theory and Applications of Molecular and Quantum Mechanics*; First ed.; Springer, **2003**, p232.
- (92) Hohenberg, P.; Kohn, W. *Phys. Rev.* **1964**, 136, B864.
- (93) Kohn, W.; Sham, L. J. *Phys. Rev.* **1965**, 140, A1133.
- (94) Prucker, O.; Naumann, C. A.; Ruhe, J.; Knoll, W.; Frank, C. W. *J. Am. Chem. Soc.* **1999**, 121, 8766.
- (95) Schvartzapel, A. J.; Zhong, L.; Docampo, R.; Rodriguez, J. B.; Gros, E. G. *J. Med. Chem.* **1997**, 40, 2314.

- (96) Sakamoto, M.; Kim, S. S.; Fujitsuka, M.; Majima, T. *J. Phys. Chem. C* **2007**, *111*, 6917.
- (97) Hassoon, S.; Sarker, A.; Polykarpov, A. Y.; Rodgers, M. A. J.; Neckers, D. *C. J. Phys. Chem.* **1996**, *100*, 12386.
- (98) Tanimoto, Y.; Okada, N.; Takamatsu, S.; Itoh, M. *Bull. Chem. Soc. Jpn.* **1990**, *63*, 1342.
- (99) Nakagaki, R.; Yamaoka, M.; Mutai, K. *Bull. Chem. Soc. Jpn.* **1999**, *72*, 347.
- (100) Ohe, K.; Takahashi, H.; Uemura, S.; Sugita, N. *J. Org. Chem.* **1987**, *52*, 4859.
- (101) Williams, D. H.; Fleming, I. *Spectroscopic Methods in Organic Chemistry. 4th Ed*; Hirokawa Publishing Co., **1990**, p40.
- (102) van Haard, P. M. M.; Thijs, L.; Zwanenburg, B. *Tetrahedron Lett.* **1975**, *16*, 803.
- (103) Albrecht, U.; Langer, P. *Tetrahedron* **2007**, *63*, 4648.
- (104) Lally, A. J. *Ph.D Thesis, National University of Ireland, Galway*, **2006**.
- (105) Stiller, J.; Marqués-López, E.; Herrera, R. P.; Fröhlich, R.; Strohmam, C.; Christmann, M. *Org. Lett.* **2011**, *13*, 70.
- (106) Silverstein, R. M.; Webster, F. X.; Kiemie, D. *Spectrometric Identification of Organic Compounds, 7th Ed.*; Wiley, **2002**, p120.
- (107) Pak, C. S.; Lee, E.; Lee, G. H. *J. Org. Chem.* **1993**, *58*, 1523.
- (108) Larson, G. L.; Fernandez de Kaifer, C.; Seda, R.; Torres, L. E.; Ramirez, J. *R. J. Org. Chem.* **1984**, *49*, 3385.
- (109) Blackburn, L.; Wei, X.; J. K. Taylor, R. *Chem. Commun.* **1999**, 1337.
- (110) Wei, X.; Taylor, R. J. K. *Tetrahedron Lett.* **1998**, *39*, 3815.
- (111) Patel, R. M.; Argade, N. P. *Synthesis* **2010**, 1188.

- (112) Jacobine, A. M.; Lin, W.; Walls, B.; Zercher, C. K. *J. Org. Chem.* **2008**, *73*, 7409.
- (113) Gabriele, B.; Salerno, G.; De Pascali, F.; Costa, M.; Paolo Chiusoli, G. *J. Chem. Soc., Perkin Trans. I* **1997**, 147.
- (114) Brownbridge, P.; Chan, T.-H. *Tetrahedron Lett.* **1980**, *21*, 3427.
- (115) Oka, R.; Nakayama, M.; Sakaguchi, S.; Ishii, Y. *Chem. Lett.* **2006**, *35*, 1104.
- (116) Torneiro, M.; Fall, Y.; Castedo, L.; Mouriño, A. *Tetrahedron* **1997**, *53*, 10851.
- (117) Ward, D. E.; Gai, Y.; Lazny, R.; Pedras, M. S. C. *J. Org. Chem.* **2001**, *66*, 7832.
- (118) Sato, T.; Yoshiie, S.; Imamura, T.; Hasegawa, K.; Miyahara, M.; Yamamura, S.; Ito, O. *Bull. Chem. Soc. Jpn.* **1977**, *50*, 2714.
- (119) Jung, J. C.; Kim, Y. H.; Lee, K. *Tetrahedron Lett.* **2011**, *52*, 4662.
- (120) M. Gielen, R. W., H. Dalil, D. de Vos, C. M. Kuiper, and G. J. Peters *Metal Based Drugs* **1998**, *5*, 83.
- (121) Schenck, G. O.; Koltzenburg, G.; Grossmann, H. *Angew. Chem.* **1957**, *69*, 177.
- (122) Dondi, D.; Protti, S.; Albini, A.; Carpio, S. M.; Fagnoni, M. *Green Chem.* **2009**, *11*, 1653.
- (123) Kawazu, K.; Inaba, M.; Mitsui, T. *Agr. Biol. Chem.*, **1967**, *31*, 498.
- (124) Mirjafari, A.; Mobarrez, N.; O'Brien, R. A.; Davis Jr, J. H.; Noei, J. C. *R. Chim.* **2011**, *14*, 1065.
- (125) Torrente, S.; Alonso, R. *Org. Lett.* **2001**, *3*, 1985.
- (126) Rimola, A.; Sodupe, M.; Tosoni, S.; Civalleri, B.; Ugliengo, P. *Langmuir* **2006**, *22*, 6593.

- (127) Tosaka, R.; Yamamoto, H.; Ohdomari, I.; Watanabe, T. *Langmuir* **2010**, *26*, 9950.
- (128) Tielens, F.; Gervais, C.; Lambert, J. F.; Mauri, F.; Costa, D. *Chem. Mater.* **2008**, *20*, 3336.
- (129) Garofalini, S. H. *J. Non-Cryst. Solids* **1990**, *120*, 1.
- (130) Folliet, N.; Roiland, C.; Begu, S.; Aubert, A.; Mineva, T.; Goursot, A.; Selvaraj, K.; Duma, L.; Tielens, F.; Mauri, F.; Laurent, G.; Bonhomme, C.; Gervais, C.; Babonneau, F.; Azais, T. *J. Am. Chem. Soc.* **2011**, *133*, 16815.
- (131) Baur, W. H. *Acta Crystallogr., Sect. B* **1977**, *B33*, 2615.
- (132) Hernon, E. M. *Ph.D Thesis, National University of Ireland, Galway*, **2008**.
- (133) Luo, Y.-R. *Comprehensive Handbook of Chemical Bond Energies*; CRC Press, **2007**.
- (134) Reichardt, C.; Welton, T. In *Solvents and Solvent Effects in Organic Chemistry*; Wiley-VCH Verlag GmbH & Co. KGaA: **2010**, p472-474.
- (135) Armarego, W. L. F.; Perrin, D. D. *Purification of Laboratory Chemicals, 4th Ed.*; Pergamon, **1997**.